Unified Model Predictive Control of Complex Powertrains

Rachid Amari

UNIVERSITE DE GRENOBLE
INSTITUT POLYTECHNIQUE DE GRENOBLE

N° attribué par la bibliothèque
|__|__|__|__|__|__|__|__|__|__|__|

T H E S E

pour obtenir le grade de

DOCTEUR DE L'Université de Grenoble
délivré par l'Institut polytechnique de Grenoble

Spécialité : *« Automatique Productique »*

préparée au laboratoire Grenoble Image Parole Signal Automatique

dans le cadre de **l'Ecole Doctorale** ***« Electronique, Electrotechnique, Automatique, Télécommunications, Signal (EEATS)»***

présentée et soutenue publiquement

par

Rachid AMARI

le 22 Juin 2010

TITRE

Commande Prédictive Unifiée de Groupes Motopropulseurs Complexes

DIRECTEUR DE THESE
Mazen ALAMIR

CO-DIRECTEUR(S) DE THESE
Paolino TONA

JURY

M.	Olivier SENAME	, Président
M.	Francesco VASCA	, Rapporteur
M.	Yann CHAMAILLARD	, Rapporteur
M.	Mazen ALAMIR	, Directeur de thèse
M.	Paolino TONA	, Co-encadrant
M.	Patrick BOUCHER	, Examinateur
M.	Nicolas LANGLOIS	, Examinateur

To my family,
and every one who contributed to this work,

Contents

Résumé de la thèse

A/ Introduction

Depuis quelques années, la mise en oeuvre des unités de contrôle embarqué dans les véhicules a permis d'assurer une percée majeure dans la technologie automobile. Plus particulièrement, les unités de contrôle moteur (ECU) ont permis de réaliser des progrès substantiels dans l'optimisation de l'efficacité des moteurs, la réduction de la consommation de carburant, la réduction des émissions de polluants, et l'augmentation de la fiabilité des véhicules en général.

Aujourd'hui, la plupart des développements technologiques en cours ont tendance à augmenter la complexité du groupe motopropulseur. Les transmissions de base ont évolué en introduisant de nouveaux concepts, tels que les transmissions manuelles automatisées, transmissions à double embrayage ou les transmissions continûment variables. L'industrialisation de ce type de transmissions est devenue de plus en plus courante dans les véhicules de série. Cette évolution est accompagnée par l'introduction de nouveaux composants actifs et passifs servo-commandés (embrayage, boîte, différentiel). Avec cette augmentation du nombre d'actionneurs et de contrôleurs, de plus en plus de dynamiques doivent être prises en compte lors de la gestion des phases de fonctionnement et particulièrement lors de transition d'une phase à l'autre. D'autre part, même pour les motorisations équipées d'une transmission manuelle standard, l'adoption de nouveaux concepts conduit souvent à une augmentation de la complexité du contrôle. C'est par exemple le cas des moteurs thermiques de taille réduite dont l'agrément de conduite est substantiellement impacté.

Pour gérer l'augmentation de la complexité, en respectant des spécifications devenues plus sévères, le groupe propulseur moderne doit être optimisé et contrôlé dans son ensemble. Pour cela nous devons étendre la commande du moteur thermique seul vers une commande intégrale dédiée au groupe motopropulseur complet.

D'un point de vue automatique, cela nécessite :

- Une prise en compte de la nature hybride (ce qui revient à mélanger les dynamiques à temps continu et discret) du système de contrôle;
- Un traitement efficace du couplage entre les états du système, ce qui implique le recours à des stratégies de contrôle multivariable;
- Une génération des trajectoires de référence qui correspondent à la volonté du conducteur dans chaque mode de fonctionnement;
- Une définition des spécifications qui imposent des contraintes d'agrément de conduite et de consommation de carburant.

A partir de ces considérations, au cours de mes recherches de doctorat, j'ai proposé des solutions originales à deux problèmes différents liés au contrôle de groupe motopropulseur. Le premier problème concerne le contrôle d'un groupe propulseur relativement complexe, caractérisé par une transmission manuelle automatisée (AMT) et une hybridation légère, comme celle de la Figure 1. Dans ce type de transmission (AMT), l'embrayage et la boîte de vitesses ne sont pas contrôlés par le conducteur. Les actionneurs de la transmission sont pilotés par une unité de contrôle embarqué afin d'assurer un engagement en douceur de l'embrayage et des changements de vitesses.

Ce type de groupe motopropulseur fait l'objet d'un démonstrateur IFP intitulé VEHGAN [1] (Tona et al. (2006)), mis au point dans le cadre d'investigation des avantages de combiner, dans une petite citadine (`smart`), un moteur de taille réduite (660 cm3) fonctionnant au gaz naturel, avec un alterno-démarreur réversible en utilisant des ultra-capacités pour le stockage électrique. Ce groupe motopropulseur AMT hybride léger offre un excellent cadre de travail pour illustrer les problèmes découlant de la présence de plusieurs producteurs et consommateurs de couple, et met en évidence les avantages de l'adoption des stratégies de contrôle avancé au lieu des approches de contrôle conventionnel en boucle ouverte basées sur des cartographies.

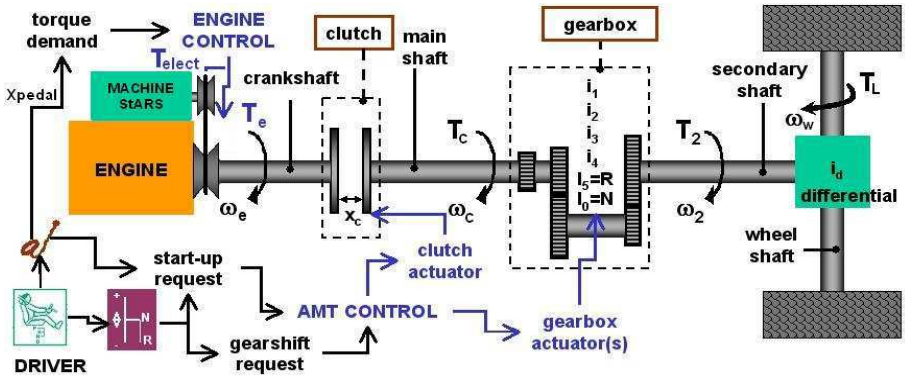

Figure 1: Architecture d'un groupe motopropulseur léger équipé d'une transmission manuelle robotisée (AMT).

Le deuxième problème à investiguer concerne l'assistance au décollage d'un groupe motopropulseur composé d'une transmission manuelle et d'un moteur à essence de taille réduite. Ce concept de "motorisation taille réduite" consiste à réduire la cylindrée du moteur et de compenser la perte de puissance par un turbocompresseur dans le but de réduire la consommation de carburant. Dans un tel véhicule, la manoeuvre de décollage, qui est en principe entièrement contrôlée par le conducteur, requiert une compétence appropriée en raison de l'insuffisance du couple moteur à bas régime. Afin d'améliorer l'agrément de conduite, on peut mettre en oeuvre un système de contrôle embarqué qui agit sur la dynamique du moteur pour aider le conducteur afin d'éviter le décrochage du moteur et/ou les oscillations de la transmission. Le cadre expérimental est prévu dans ce cas par un autre démonstrateur IFP, développé dans le cadre projet Ecosural (Le Solliec et al. (2006)): une Renault VelSatis, dont le moteur standard a une cylindrée de 3.0 litres et à allumage commandé, a été remplacé par un moteur de 1.8 litres avec un calage variable VVT, et un turbocompresseur. Bien que le gain de consommation de carburant soit important (environ 20%), avec un tel véhicule lourd, la qualité de l'agrément de conduite est particulièrement affectée au décollage du véhicule. Une stratégie efficace d'aide au décollage du véhicule conduirait à une plus grande acceptation de cette technologie.

Pour les deux problèmes, les solutions proposées sont basées sur une commande prédictive en utilisant des modèles de contrôle hybride en tenant compte des différentes configurations du groupe motopropulseur. Notamment une paramétrisation du contrôle a été adoptée permettant ainsi une optimisation en ligne et le respect des contraintes via un algorithme de recherche dichotomique qui permet une mise en oeuvre en temps réel. En outre, grâce à l'utilisation d'estimateurs de couple en ligne, ces stratégies ne nécessitent pas de capteurs supplémentaires hormis ceux déjà implémentés dans les véhicules de série.

[1] VEhicule Hybride au GAz Naturel

En dehors du cadre commun des deux problématiques, chaque problème a besoin d'une solution spécifique.

B/ Résumé

Dans le problème du contrôle de la transmission manuelle automatisée (AMT), la dynamique du groupe motopropulseur est totalement pilotable via le contrôle embarqué, avec deux entrées : le couple moteur et le couple d'embrayage. Les deux sorties sont la vitesse du moteur et la vitesse de l'arbre primaire (ou vitesse de glissement de l'embrayage). Du point de vue contrôle, trois modes de fonctionnement sont à considérer : le contrôle du ralenti, le démarrage du véhicule et les changements de vitesses. Le but du système de contrôle est d'assurer un traitement unifié des trois modes de fonctionnement. Une particularité de la stratégie proposée est le fait que, dans les deux cas de décollage du véhicule et passage de vitesses, les solutions sous optimales sont directement liées à la position de la pédale accélérateur afin de promouvoir une sorte de transparence vis-à-vis la demande du conducteur.

Dans le second problème concernant le contrôle de la transmission manuelle (MT), la dynamique du régime moteur est commandée via un contrôleur MPC unifié impliquant : le contrôle du ralenti, le démarrage du véhicule, et la régulation entraînée du véhicule. Du point de vue fonctionnel, une transmission manuelle opère comme une transmission robotisée (ouverture et engagement d'un nouveau rapport), excepté que dans le cas de la transmission manuelle (MT), seulement le couple thermique peut être manipulé par le contrôle embarqué, tandis que l'action de la pédale d'embrayage est vue comme une perturbation. Dans ce contexte, une estimation plus précise du couple d'embrayage est nécessaire. Pour subvenir à ce besoin, un modèle phénoménologique de la transmissibilité du couple lors de l'engagement de l'embrayage a été développé. Le modèle est fondé sur une identification d'une caractéristique non linéaire qui concerne la transmissibilité du couple moteur à l'arbre primaire en prenant en compte la position de l'actionneur de la pédale d'embrayage et la vitesse de glissement. Intégrés dans une commande prédictive non linéaire, ce modèle améliore considérablement les performances de l'assistance au décollage par rapport aux stratégies fondées sur un contrôle feedforward avec des modèles simplistes vis-à-vis de la transmissibilité du couple via l'embrayage.

La thèse est organisée comme suit :

✠ Partie I : **Contrôle du Groupe Motopropulseur et Agrément de Conduite**

– Chapitre 1 : **Contrôle Avancé d'un Groupe Motopropulseur pour Agrément de Conduite**

1.1 Introduction

Pour introduire la problématique générale du contrôle moteur, nous commençons par rappeler ce qu'est un groupe motopropulseur et ses principales composantes, en se concentrant sur le cas particulier des moteurs à combustion interne et des transmissions manuelles et manuelles robotisées. Nous décrivons les fonctionnements et les caractéristiques pertinentes de chaque composant (moteur, embrayage, boîte de vitesses) qui constituent le groupe motopropulseur, ainsi que la structure des systèmes de contrôle correspondants.

1.2 Le Groupe Motopropulseur et ses Constituants

1. **Moteur**
   Les moteurs à combustion interne sont les plus largement utilisés pour la production de l'énergie mécanique. Ces moteurs sont alimentés par un carburant à haute densité énergétique (provenant généralement de combustibles fossiles) qui offrent un excellent rapport

puissance - poids. Les moteurs à combustion interne peuvent être classés comme alternatif ou rotatif, à allumage commandé ou allumage par compression, et à deux ou à quatre temps. Pour les applications automobiles, les moteurs alternatifs à quatre temps à allumage commandé et à allumage par compression sont les choix les plus courants. En ce qui concerne la production de couple, en raison de son comportement alternatif et de la nature discrète des événements de combustion, le moteur peut être considéré comme un système échantillonné variable dans le domaine temporel et constant dans le domaine angulaire. Dans ces moteurs, l'injection et l'allumage doivent être synchronisés à l'égard de chaque PMH[2] de combustion. Le temps d'injection et l'avance à l'allumage sont les principales variables manipulées pour contrôler la production du couple thermique. La fonction principale du moteur dans un véhicule est de fournir un couple au vilebrequin, et sa transmission aux roues via la chaîne de transmission. Pour réaliser ce couple, plusieurs actionneurs doivent être coordonnés afin d'obtenir la production requise du niveau de couple, tout en maintenant des conditions de fonctionnement optimales de bonnes performances en termes de consommation de carburant et d'émission de polluants. Cette coordination est réalisée dans un module de contrôle embarqué appelé ECU[3].

2. **Transmissions**
   La recherche d'un bon couplage du moteur thermique aux roues, en assurant un bon compromis entre rendement, confort et coût, a conduit au développement de plusieurs architectures de transmission (Wagner (2001)) :

   (a) Transmission Manuelle (*Manual Transmission*, MT).
   Elles sont constituées d'un embrayage et d'une boîte de vitesses dont les rapports sont discrets. Cet ensemble est piloté manuellement par le conducteur. Chaque changement de rapport nécessite l'ouverture effective de la chaîne de transmission, entraînant une discontinuité dans la transmission du couple. Mis à part cet inconvénient, ce type de transmission reste intéressant : bon rendement, faible coût, facilité d'entretien et faible consommation de carburant.

   (b) Transmission Automatique (*Automatic Transmission*, AT).
   Ce type de transmission est constitué d'un convertisseur de couple hydraulique et d'un train épicycloïdal. Le passage des rapports se fait d'une manière continue et sans interruption de la transmission du couple. Cela conduit à un confort de conduite très appréciable. Les défauts majeurs sont la complexité technologique qui engendre une augmentation du coût et du poids et la réduction du rendement global du groupe motopropulseur.

   (c) Transmission Continûment Variable (*Continuously Variable Transmission*, CVT).
   Dans ce type de transmission la modulation du couple se fait via un système de courroies métalliques qui s'adaptent aux caractéristiques de combustion du moteur thermique. Une partie du gain d'optimisation de la combustion est perdue dans les courroies qui ont des frottements importants. Un autre aspect désagréable est le bruit occasionné par les courroies. Cependant, l'agrément de conduite est assez comparable à ce celui d'une transmission automatique.

   (d) Transmission Robotisée (*Automated Manual Transmission*, AMT).
   Les organes mécaniques de base sont ceux d'une transmission manuelle. Les actionneurs pour l'asservissement de l'embrayage et de la boîte sont directement pilotés par une couche de contrôle qui doit répondre aux demandes du conducteur en assurant un bon agrément de conduite. Le coût et le poids des composants d'automatisation

[2]Point Mort Haut
[3]Engine Control Unit

restent relativement faibles par rapport aux transmissions AT et CVT. Le développement de l'électronique et du contrôle demande un investissement supplémentaire par rapport aux transmissions purement manuelles. Une couche de contrôle supplémentaire permet de réaliser un choix automatique des rapports à passer (*Automated Shift Transmission*, AST), qui permet de se rapprocher du fonctionnement des transmissions AT et CVT, sans toutefois pouvoir assurer le même confort. Le confort peut être amélioré en rajoutant un deuxième embrayage qui permet d'assurer une transmission de couple continue durant les passages de rapports. Ces transmissions à double embrayage (*Dual-clutch transmission*) sont naturellement plus coûteuses.

Dans le cas des transmissions manuelles et manuelles robotisées, étudiées dans cette thèse, la propulsion du véhicule provient des actions combinées sur :

- le moteur, qui fournit le couple nécessaire;
- l'embrayage, qui couple le moteur à l'arbre de transmission et ainsi transmet le couple thermique progressivement qui est produit selon le besoin;
- et la boîte de vitesses qui transmet le couple d'embrayage aux roues avec un rapport approprié choisi par le conducteur ou par le contrôle embarqué.

3. **Embrayage**
Conceptuellement, le mécanisme de l'embrayage est conçu comme un dispositif de contrôle inversé. Autrement dit, lorsque l'entrée de commande est nulle, l'embrayage est en position fermée. Une entrée de contrôle non nulle est nécessaire pour ouvrir l'embrayage (pour lutter contre le ressort du diaphragme). Ce concept de fonctionnement permet de minimiser l'effort de contrôle sur la position de l'embrayage qui est censé être fermé en position permanente (fermée). En position fermée, l'embrayage transmet totalement le couple net du moteur thermique à la transmission. Il est à noter que l'embrayage a un effet protecteur sur la transmission qui filtre les pics importants du couple moteur. Si cette situation apparaît, les disques d'embrayage doivent glisser afin de dissiper cet excès de couple sous forme de chaleur. Chaque embrayage a son couple maximum admissible qui est garanti par le constructeur. En supposant que le couple appliqué sur l'arbre du moteur ne dépasse pas le couple maximum admissible, trois modes de fonctionnement principaux peuvent être définis pour l'embrayage : ouvert, fermé, et en glissement. Lorsque l'embrayage est (entièrement) ouvert il n'y a pas de couple transmis et les vitesses des deux disques évoluent indépendamment. Quand il est (entièrement) fermé, le couple moteur est transmis totalement, et les deux disques évoluent à la même vitesse. Lorsque les deux disques sont en contact, durant le mode glissement, seulement une fraction du couple moteur est transmise.

1.3 Contrôle du Groupe Motopropulseur

Dans cette section, nous introduisons la commande du groupe motopropulseur, qui est basée sur une structure de commande en couple développée pour les véhicules équipés d'une transmission manuelle, puis nous présentons une extension possible de cette structure pour le cas de transmission manuelle robotisée.

1. **Contrôle du Groupe Motopropulseur Equipés d'une Transmission Manuelle**
Même dans un groupe motopropulseur à transmission manuelle standard, tel que celui illustré sur la figure 1, le rôle d'un système de contrôle moteur va au-delà d'une simple commande de la composante moteur. En fait, la tâche principale est de rendre le moteur capable de produire du couple et de le livrer à la transmission afin d'assurer la propulsion du véhicule:

(a) en répondant aux demandes du conducteur;

(b) et en respectant plusieurs contraintes (agrément de conduite, consommation, émission de polluants).

Une structure hiérarchique typique de contrôle/commande en couple pour un groupe motopropulseur équipé d'une transmission manuelle et d'un moteur à allumage commandé est illustrée sur la figure 2. Une telle structure a été proposée dès le début des années 90 (Streib et Leonhard (1992)) et devenue maintenant standard (Livshiz et al. (2004)). Dans les conditions nominales de conduite, la demande de propulsion exprimée par le conducteur via la pédale d'accélérateur est généralement traduite en un couple de consigne (ou puissance) à réaliser au niveau des roues. Cette consigne sera exprimée en couple moteur en prenant en compte le rapport de boîte engagé. En plus de cette consigne de couple, le système de contrôle moteur (ECU) doit assurer la compensation des frottements internes, les pertes de pompage, et la consommation du réseau électrique de bord (phares, vitres électriques, radio, climatisation, etc.). Par ailleurs, au niveau du contrôle bas-niveau, la consigne de couple se traduit en plusieurs consignes pour des actionneurs bas-niveau (position du papillon, temps d'injection, avance à l'allumage, ainsi de suite). Il y a lieu de noter que le couple moteur demandé est essentiellement réalisé en contrôlant la position du papillon, les autres boucles de contrôle sont configurées en esclave comme le temps d'injection et le rapport air-carburant (généralement autour de 1). En raison de la dynamique du collecteur d'air, le moteur ne fournit le couple demandé qu'après un certain retard. Une réalisation relativement rapide du couple peut être obtenue via une dégradation de l'avance à l'allumage, mais cela seulement pour un temps limité et avec une variation de couple limitée. Remarquons aussi que, pour des raisons de coût, dans la plupart des véhicules il n'y a pas de mesure de couple réel fourni par le moteur ni celui transmis aux roues. Il est très important de souligner que même dans le plus simple des groupes motopropulseurs, le système de contrôle moteur doit générer les consignes de couple en tenant compte de la façon dont le couple moteur est transmis aux roues, en prenant en compte :

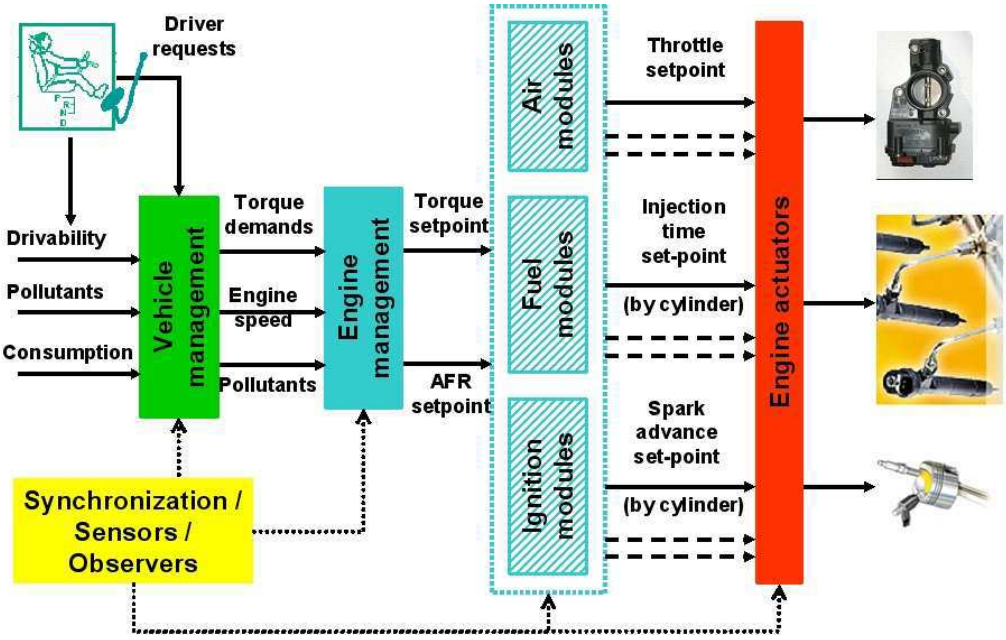

Figure 2: Structure hiérarchisée d'un système de contrôle/commande d'un groupe motopropulseur équipé d'une boîte manuelle et d'un moteur à allumage commandé.

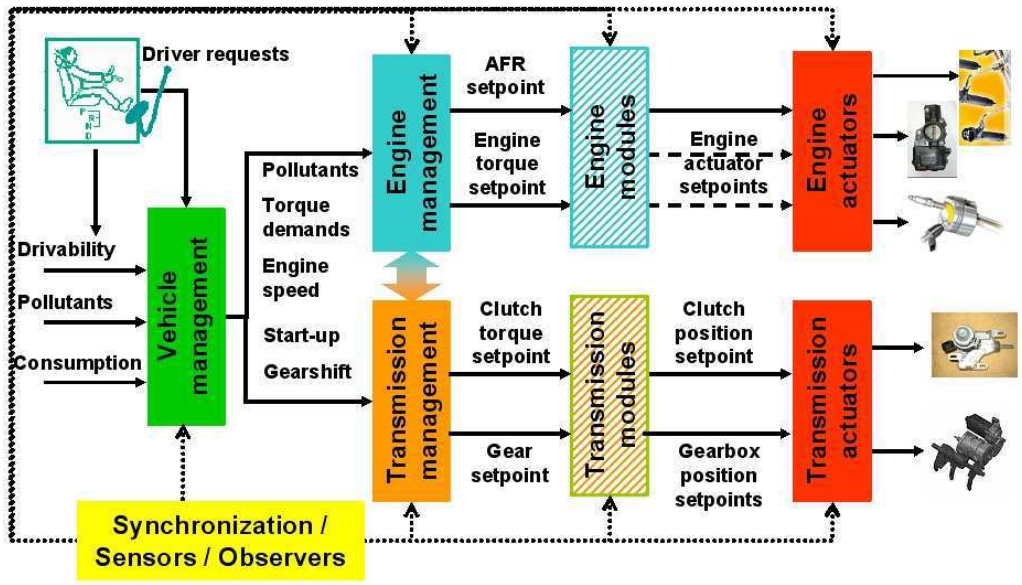

Figure 3: Structure hiérarchisée d'un système de contrôle/commande d'un groupe motopropulseur équipé d'une boîte manuelle robotisée et d'un moteur à allumage commandé.

- L'état de la transmission défini par
  - l'embrayage (ouvert, fermé ou glissement)
  - et la boîte de vitesses (synchronisation, rapport engagé, neutre);
- La dynamique de la transmission, en particulier:
  - l'inertie, les torsions, l'amortissement des composants;
  - le problème du *Backlash*;
  - le frottement dans l'embrayage, la synchronisation, et le couple de la chaussée.

2. **Contrôle du Groupe Motopropulseur des Véhicules Equipés d'une Transmission Manuelle Robotisée**
   Dans un véhicule équipé d'une transmission manuelle robotisée (voir Figure 3), le pilotage des actionneurs de la transmission est décidé et exécuté par des stratégies de contrôle embarqué. Ce module de contrôle embarqué, doit contrôler le comportement de l'embrayage et de la boîte de vitesses, et doit interagir avec l'unité de contrôle moteur avec une bonne coordination, particulièrement durant les phases de décollage du véhicule et les passages de vitesses. Ces manœuvres sont effectuées à la demande du conducteur : le décollage du véhicule est lancé en appuyant sur la pédale d'accélérateur, lorsque le levier de vitesses se trouve dans une position engagée, et de changements de vitesses qui sont effectués sur le levier de vitesses (ou bouton). Toutefois, il existe d'autres actions possibles qui ne dépendent pas de la demande explicite du conducteur, comme un pilotage complètement automatique des passages de vitesses, l'ouverture de l'embrayage et de rétrogradage au premier rapport lorsque le véhicule est arrêté. Concernant le développement du contrôle, il n'y a pas encore de normes établies structurant le logiciel de pilotage des groupes motopropulseurs équipés d'AMT. Une structure possible est celle de la Figure 3, qui peut être obtenue par l'extension de la structure de contrôle en couple des moteurs standards. La mise en œuvre effective de cette structure dépend de la configuration de l'unité de contrôle embarqué. Les différentes fonctionnalités peuvent être réparties sur plusieurs calculateurs.

1.4 Modèle de Contrôle du Groupe Motopropulseur

La phase de glissement de l'embrayage durant le décollage du véhicule et le passage de vitesses est la plus complexe du système groupe motopropulseur. Le modèle de contrôle peut être représenté par un système d'équation d'ordre trois (Glielmo et al. (2006)) lié aux dynamiques régissant les variables suivantes:

- Le régime moteur ω_e;
- la vitesse arbre primaire ω_c;
- et la vitesse véhicule ω_w;

Le modèle utilisé exprime des relations entre les accélérations des inerties en rotation et des couples disponibles sur les axes. Ce modèle est obtenu par application du principe de Lagrange-d'Alembert. Ce modèle est bien adapté à une structure de contrôle en couple, il est adopté tout au long de la thèse vu qu'il traite la dynamique longitudinale du véhicule d'une façon macroscopique. Ce modèle est utilisé pour formaliser les objectifs de la commande liés aux problèmes de contrôle des groupes motopropulseurs équipés d'une transmission manuelle ou d'une transmission manuelle robotisée.

1.5 Contrôle du Système Groupe Motopropulseur

D'une façon générale, les problèmes de contrôle du groupe motopropulseur doivent être représentés/résolus dans le cadre commun décrit par la figure 4. Que nous nous référions à une transmission manuelle, ou à une transmission manuelle robotisée, le conducteur est toujours le maître de l'application, dans laquelle le contrôle embarqué est soumis aux requêtes et actions du conducteur. Du point de vue contrôle, c'est la nature de la transmission qui détermine la façon dont le contrôle embarqué interagit avec le conducteur. Dans les transmissions manuelles, le conducteur contrôle totalement la transmission moyennant la pédale d'embrayage, le levier de boîte de vitesses et la pédale de frein. La pédale d'accélérateur est utilisée pour contrôler la dynamique du moteur. Dans ce contexte, les stratégies de contrôle embarqué ne peuvent corriger les actions du conducteur sur la transmission pour améliorer l'agrément de conduite. Dans le cas des transmissions manuelles robotisées, il y n'a que l'action de freinage qui est appliquée directement à la transmission, tandis que la pédale d'accélérateur et le levier de vitesses sont seulement des requêtes aux stratégies de contrôle embarqué. Dans ce cas, l'agrément de conduite dépend totalement des stratégies de contrôle embarqué qui doivent garantir l'agrément de conduite en assurant une certaine transparence entre les exigences du conducteur et la dynamique du véhicule. Pour traiter ces problèmes en faisant face à des cahiers des charges de plus en plus strictes, les bureaux d'études et de conception sont contraints de formaliser ces exigences en faisant appel à des méthodologies de conception efficaces et industrialisables. Dans ce contexte, le cadre de la commande prédictive semble être le candidat le plus naturel à condition qu'elle soit compatible avec le calcul en ligne et les limites de stockage (mémoire).

1.6 Commande prédictive pour les applications automobiles

La commande prédictive (MPC) est une méthodologie de contrôle avancée de conception de loi de commande qui a acquis une grande importance au cours des trois dernières décennies. L'idée de base de cette commande est de résoudre, à chaque instant de contrôle, un problème de contrôle optimal en boucle ouverte défini en fonction de l'état actuel du système et d'une prédiction de l'évolution du système le long de l'horizon de prédiction. La solution du problème est une séquence optimale d'actions de contrôle à venir. La première action de cette séquence est ensuite appliquée au système. Au prochain instant d'échantillonnage, l'état est mis à jour (par mesure

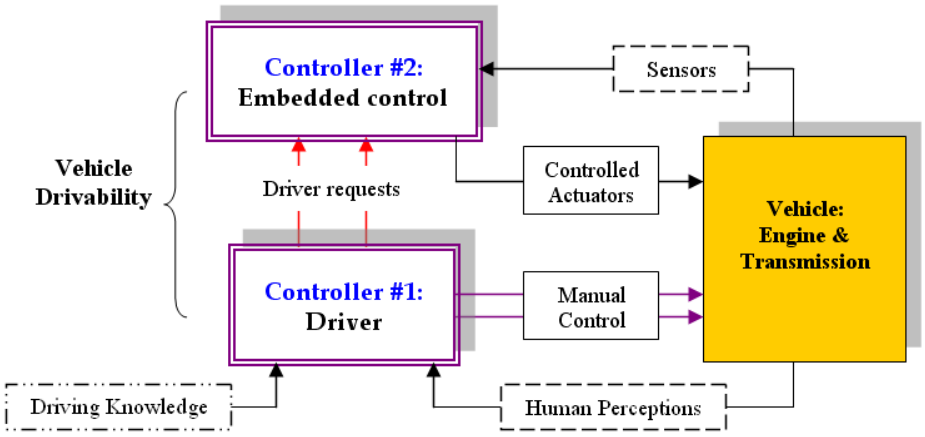

Figure 4: Structure hiérarchisée de contrôle liée à la dynamique longitudinale du véhicule.

ou par observateur d'état) et un nouveau problème en boucle ouverte est résolu pour obtenir une nouvelle séquence de contrôle.

Les travaux de recherche sur la commande MPC au cours des 90 ont mis l'accent sur les problèmes de stabilité. Une énorme quantité de travail a été consacrée à l'approfondissement de la compréhension des conditions suffisantes de la stabilité de la boucle fermée résultants. Ces conditions impliquent tous les ingrédients utilisés dans la définition du problème de contrôle optimal, à savoir la fonction de coût, les contraintes qui peuvent être ajoutées à la formulation de manière à assurer la faisabilité et la stabilité de la boucle fermée (Mayne et al. (2000)).

L'utilisation de la commande MPC dans l'automobile est un sujet de recherche assez prometteur. En effet, les problèmes de contrôle comportent nécessairement des contraintes telles que la saturation des actionneurs, la sécurité opérationnelle, les points de fonctionnement optimaux et ainsi de suite. En outre, il devient indispensable que le contrôle du véhicule prenne en compte des contraintes typiques de l'automobiles telle que la consommation de carburant, et la minimisation de la pollution, pour n'en citer que ces quelques exemples.

Dans ce travail, une approche de contrôle paramétrique (CPA[4]) (Alamir (2006a)) est adoptée. La philosophie de cette approche se trouve dans les idées suivantes :

1. Le mise à jour du calcul de la séquence optimale de commandes futures permettent d'obtenir un comportement très riche en boucle fermée même si le profil temporel en boucle ouverte est assez simple (Alamir et Marchand (2003));

2. Il vaut mieux tenter de résoudre correctement un problème d'optimisation bien condition même si elle conduit à une solution sous optimale plutôt que de tenter de résoudre le problème d'origine sans succès. Cette idée intuitive est schématiquement représentée sur la figure 5;

3. La paramétrisation classique, dans laquelle toutes les valeurs de contrôle sont des degrés de liberté augmente inutilement la dimension du problème d'optimisation. Ceci est d'autant plus vrai dans le cas où la trajectoire de l'état du système (trajectoires futures) est prise comme un degré de liberté. Il est vrai que le problème résultant est hautement structuré et

[4]Control Prametrization Approach

peut être résolu au moyen de logiciels dédiés permettant de manipuler les matrices creuses. Il n'en demeure pas moins vrai que les codes correspondant sont délicats à utiliser et s'apprêtent difficilement à être embarqués sur puce. Le problème de la mémoire nécessaire à leur mise en œuvre reste posé dans le cadre d'une implémentation sur véhicule sans parler de la difficulté associée à leur certification.

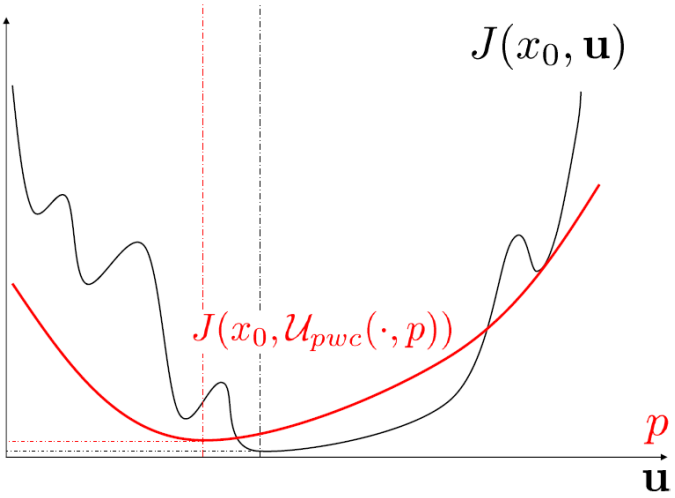

Figure 5: Illustration schématique de l'idée intuitive selon laquelle il est préférable d'obtenir une bonne solution sous optimale plutôt de résoudre le problème exact d'origine qui est complexe. Ici, la ligne noire représente la fonction coût lors d'une paramétrisation triviale classique. Sur cette courbe il existe de nombreux minimaux locaux à cause de la paramétrisation trop riche. En rouge, la fonction coût correspondant à une paramétrisation à dimension réduite pour laquelle le problème est beaucoup mieux conditionné au prix d'une légère augmentation de la fonction coût.

✠ Partie II : **Commande Prédictive Unifiée d'une Transmission Manuelle Robotisée**

– Chapitre 2 : **Contrôle des groupes motopropulseurs équipés d'AMT**

2.1 Introduction

La technologie des transmissions manuelles robotisées (AMTs) essaie de combiner l'efficacité des transmissions manuelles avec l'agrément des transmissions automatiques. Une transmission AMT opère comme une transmission manuelle, sauf qu'il ne nécessite pas de pilotage de l'embrayage et de la boîte de vitesses par le conducteur. Les actionneurs de la transmission sont contrôlés par le contrôle embarqué. Dans les véhicules à transmission manuelle, l'agrément de conduite dépend directement de la coordination des actions du conducteur sur le moteur, l'embrayage et le levier de vitesses. Un conducteur inexpérimenté, aura du mal à assurer un pilotage sans oscillations ou sans décrochage du moteur. Le besoin de stratégies efficaces explique pourquoi la recherche de solutions nouvelles aux problèmes de contrôle groupe motopropulseur a attiré une attention considérable ces dernières années, tant dans l'industrie que dans les milieux universitaires.

Dans ce chapitre, nous introduisons une commande innovante que nous avons développée pour contrôler un groupe motopropulseur équipé d'une transmission AMT. Ce contrôle est applicable d'une façon unifiée dans différents modes de fonctionnement. Dans la section 2.2, nous présentons les principes généraux de fonctionnement d'une transmission AMT. Ensuite, nous examinerons les principales approches reportées dans la littérature pour résoudre les problèmes de contrôle AMT (section 2.3). Dans la section 2.4, nous décrivons les caractéristiques du problème de contrôle AMT que nous étudions dans cette thèse. Enfin, la méthodologie et le contexte de la commande prédictive proposée sont développés dans la section 2.5.

2.2 Principe de Fonctionnement d'une Transmission AMT

Les transmissions manuelles robotisées ont été conçues par les constructeurs automobiles pour améliorer l'agrément de conduite, surtout dans les cycles urbains où le trafic entraîne souvent des arrêts fréquents. Une transmission manuelle robotisée est essentiellement une transmission manuelle exploitée par un système de contrôle embarqué, de telle sorte que le véhicule puisse être conduit sans pédale d'embrayage, aussi facilement qu'avec une transmission automatique conventionnelle. Bien sûr, une transmission AMT avec un simple embrayage ne peut pas fournir une transmission continue du couple lors des passages de vitesses, parce que le flux de couple du moteur aux roues est interrompu lorsque l'embrayage est ouvert. Néanmoins, étant donné que les transmissions AMT conservent la haute efficacité (95%) des transmissions manuelles leurs coûts restent relativement élevés. Elles sont considérées comme une solution intéressante tant pour les voitures de petites cylindrées que les véhicules utilitaires lourds, qui offrent un bon compromis entre la consommation de carburant et l'agrément de conduite.

2.3 Etat de l'Art du Contrôle de l'AMT

Il y a plusieurs contributions dans la littérature qui proposent des solutions au problème de contrôle de la transmission manuelle automatisée (AMT). Pour plus de détails à ce sujet, le lecteur peut se référer à la section 2.3 de la version complète du manuscrit.

2.4 Contrôle Hybride du Groupe Motopropulseur

Le pilotage d'une transmission AMT est toujours effectué dans une structure hiérarchisée qui va de l'interprétation de la demande du conducteur à des systèmes de contrôle bas niveaux liés aux actionneurs. Même si la structure réelle dépend de la configuration matérielle et de la façon dont le logiciel est distribué entre les différents calculateurs, il est possible d'identifier trois niveaux:

- Une couche de coordination entre le module moteur et les modules de la transmission. Généralement cette couche représente le superviseur véhicule;
- Une couche intermédiaire, ou couche fonctionnelle qui est responsable de l'exécution des fonctions de contrôle/commande liées au moteur et à la transmission;
- Une couche bas niveau, ou couche actionneur qui assure le pilotage des actionneurs.

La couche intermédiaire doit être supervisée par la couche de coordination (superviseur) qui gère les transitions entre les différents modes de fonctionnement du groupe motopropulseur, en réponse aux demandes du conducteur et aux conditions opératoires de conduite. Ainsi, par exemple un superviseur de groupe motopropulseur, illustré sur la figure 6, devrait inclure des modes dédiés à la maîtrise des manœuvres AMT, à savoir les démarrages du véhicule et le passage des vitesses. D'autres modes conventionnels sont à prendre en compte comme les modes stand-by et roulage.

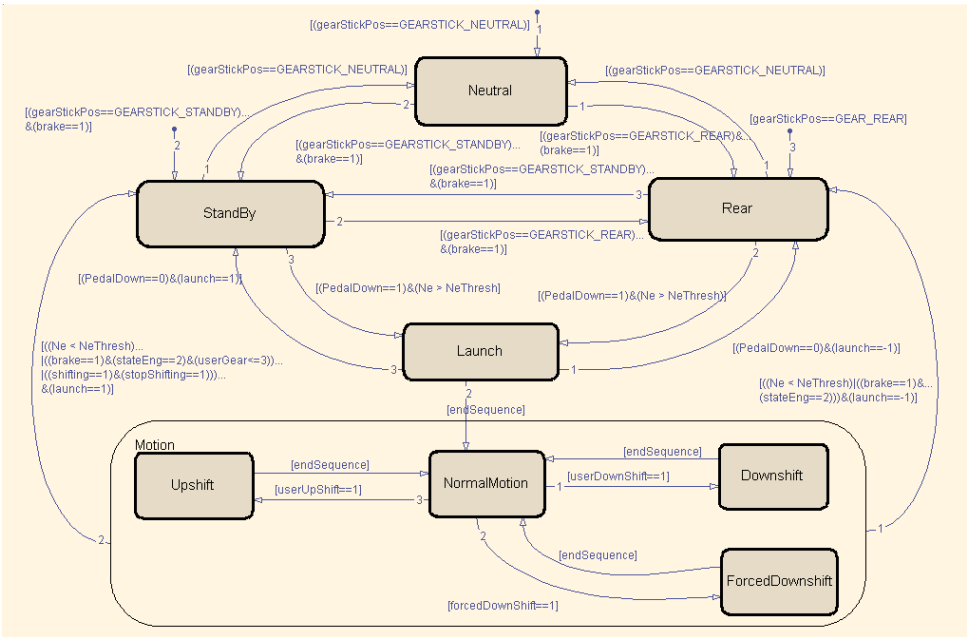

Figure 6: Superviseur typique d'un groupe motopropulseur équipé d'une transmission manuelle robotisée (AMT).

2.5 Commande Prédictive Unifiée pour Groupe Motopropulseur Equipé d'une AMT

La figure 7 résume le contexte du contrôle AMT. Le système de contrôle manipule deux consignes "haut niveau" : le couple moteur T_e^{SP} et le couple de l'embrayage T_c^{SP}. Une consigne supplémentaire liée à l'efficacité du couple thermique ($\eta_{T_e}^{SP}$) pourra être considérée, qui fait intervenir l'avance à l'allumage. Une autre consigne haut niveau est le rapport de boîte qui pourra être choisi par le conducteur ou par un superviseur dans le cas des passages de vitesses complètement automatisés.

La partie la plus à droite de la figure 7 montre une représentation du système physique. Parmi les variables qui influencent la dynamique du système, T_e et T_c qui sont des entrées de commande non mesurées, tandis que les autres peuvent être considérées comme facteurs de perturbation, (T_{elect}, le couple appliqué par un alternateur ou un moteur électrique, et T_L le couple de charge). Les variables à contrôler sont la vitesse du moteur ω_e et la vitesse de l'arbre primaire ω_c qui sont mesurables. La vitesse véhicule est également mesurable.

La solution que nous présentons dans cette thèse tente de répondre à plusieurs exigences :

1. Prendre en compte la nature hybride et multivariable du groupe motopropulseur, en gardant le couplage entre les dynamiques du système et en assurant des transissions douces entre les modes de fonctionnement;

2. Exploiter le potentiel du groupe motopropulseur pendant les manoeuvres AMT de façon optimale, en respectant des spécifications d'agrément de conduite et de contraintes opérationnelles;

3. Capturer la demande du conducteur de façon transparente dans les spécifications de contrôle;

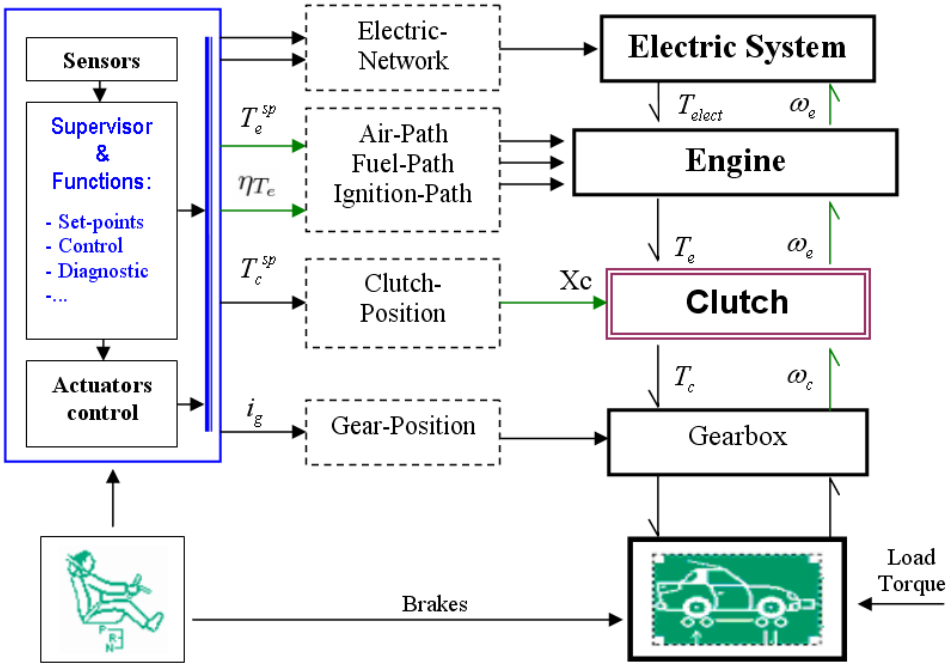

Figure 7: Topologie d'une structure de contrôle en couple appliquée à un groupe motopropulseur équipé d'une transmission manuelle robotisée (AMT).

4. Faire face à des incertitudes sur des variables inconnues, tout en n'utilisant que les mesures disponibles sur les véhicules de série afin d'éviter les surcoûts des capteurs supplémentaires;

5. Respecter les contraintes de mise en œuvre en temps réel, particulièrement les limitations des calculateurs embarqués.

Le premier point fait appel à des modèles appropriés de chaque phase de l'AMT en utilisant une approche unifiée, en gardant une correspondance directe entre l'évolution de la dynamique du groupe motopropulseur et le modèle de contrôle associé. Le contrôleur unique proposé dans cette thèse intègre toutes les phases qui peuvent être formalisées en boucle fermée : contrôle de ralenti, contrôle du moteur et du glissement de l'embrayage pendant les phases de démarrage du véhicule, et passages de vitesses (montants et descendants). Le deuxième point stipule que la loi de contrôle/commande doit assurer un pilotage optimale du groupe motopropulseur en intégrant directement les spécifications du cahier de charge, en particulier la gestion des contraintes liées aux couples : la commande prédictive est appropriée à ce type de problématique. Les exigences de transparence peuvent être satisfaites en reliant la consigne de la vitesse de l'arbre primaire, ou la vitesse de glissement, à la position pédale accélérateur qui est une demande en couple (couple pédale). En ce qui concerne le quatrième point, il sous-entend la capacité de surmonter les imperfections des modèles de contrôle et de l'estimation des variables non mesurées. L'utilisation des observateurs nous semble le moyen le plus naturel d'y arriver. Enfin, pour répondre aux fortes contraintes liées au calcul en temps réel, une formulation alternative doit remplacer la commande prédictive standard : dans cette thèse nous avons adopté l'approche de la commande prédictive paramétrique.

– Chapitre 3 : **Application et Validation de la Commande AMT sur un Démonstrateur**

Ce chapitre illustre l'application et la validation de la commande prédictive proposée. Dans la première partie, nous illustrons le contexte de l'application, et plus particulièrement un démonstrateur VEHGAN, un véhicule hybride léger doté d'une plateforme de prototypage rapide pour le contrôle embarqué. Dans ce chapitre, nous expliquons l'implémentation de la commande prédictive dans la structure de contrôle "prototypage rapide".

Le reste du chapitre est consacré à la validation. Trois environnements différents de validation sont utilisés :

- sous Simulink, en simulant le contrôleur basé sur la commande prédictive avec un modèle simplifié du groupe motopropulseur;
- en Co-simulation, en simulant un système de contrôle complet du groupe motopropulseur (sous Simulink), avec un modèle détaillé du groupe motopropulseur (sous AMESim);
- sur démonstrateur, le logiciel de contrôle est exporté sur l'unité de prototypage rapide en utilisant (Simulink-xPCTarget), faisant d'état d'une validation en temps réel.

La première phase de la validation permet de valider le principe fonctionnel de la commande développée pour obtenir les performances nominales. Le modèle de simulation, d'ordre réduit, est mis en œuvre sous Simulink dans lequel la complexité est maîtrisée et les perturbations sont bien connues. Ainsi, cet environnement permet également d'évaluer les performances nominales des estimateurs.

La deuxième phase de validation a été réalisée dans un environnement de co-simulation. Du point de vue contrôle, le logiciel de contrôle/commande a été utilisé avec des modifications minimes nécessaires pour mettre en œuvre la commande avec la plateforme de co-simulation. Du point de vue modélisation, qui est codé sous AMESim, nous avons bénéficié de différentes versions développées dans le cadre du projet VEHGAN, permettant ainsi des évolutions séparées du contrôle et des modèles de simulation .

Le modèle de référence de base est le 0-D à haute fréquence, construits avec des composants de la bibliothèque AMESim IFP Engine, qui permet de reproduire le comportement complet de la dynamique du moteur jusqu'à 0,1 degré vilebrequin. Toutefois, le cycle de combustion moteur suffit pour saisir la dynamique longitudinale de décollage du véhicule et de changement de rapport, donc un modèle moyen de combustion (MVEM [5]) a été utilisé pour la plupart des tests de co-simulation. La boîte de vitesses et l'embrayage sont modélisés par des éléments appartenant aux bibliothèques IFP-Drive et IFP-powertrain, respectivement.

La phase ultime de validation de la commande prédictive unifiée a été effectuée sur le véhicule réel, avec la configuration matérielle et logicielle décrite précédemment. Les performances du contrôle proposé sont à comparer avec ceux du contrôle déjà implémenté sur le démonstrateur, d'une part, et de montrer la compatibilité du contrôle proposé avec les contraintes d'implémentation en temps réel, d'autre part.

✠ Partie III: **Commande Prédictive Unifiée d'Assistance au Décollage**

– Chapitre 4 : **Modélisation du Couple Embrayage**

[5] Mean Value Engine Model

4.1 Introduction

La caractérisation du couple d'embrayage durant la phase de glissement permet d'assurer un contrôle efficace du groupe motopropulseur : cette caractérisation permet de mettre en phase la production du couple thermique et sa transmissibilité via l'embrayage. La quantification du couple transmis est particulièrement importante dans le contexte du contrôle du groupe motopropulseur, car elle est le noyau du problème d'agrément de conduite. Dans les véhicules équipés d'une transmission manuelle robotisée, le couple d'embrayage est une entrée de commande, qui peut être utilisée pour contrôler à la fois le régime moteur et la vitesse de l'arbre primaire. Une connaissance exacte de la commande réalisée est souhaitable mais pas indispensable pour un bon contrôle, à condition que la loi de commande soit conçue pour surmonter les incertitudes. Dans les véhicules équipés d'une transmission manuelle, le problème de contrôle est plus contraignant car le couple d'embrayage est une perturbation importante, et de plus, c'est une inconnue qui agit directement sur l'arbre moteur. Dans ce cas, l'information sur le couple d'embrayage serait utile pour contrôler la production du couple thermique. Cela devient particulièrement visible, lorsqu'il s'agit des véhicules équipés d'une transmission manuelle et d'un moteur thermique fortement de taille réduite, où la production du couple thermique est plus contraignante par rapport aux véhicules conventionnels.

Ce chapitre est organisé comme suit. La transmissibilité du couple d'embrayage dépend des forces de frottement induites entre les disques d'embrayage, la section 4.2 donne un bref aperçu sur la modélisation de ces forces de frottement : cela à partir de modèle plus simple jusqu'aux plus récents et plus complexes. En effet, dans les applications automobiles, l'embrayage en question, est monté entre le moteur thermique et la boîte de vitesses, il est conçu pour être exploité comme un système de connexion qui transmet le couple moteur à la boîte de vitesses. Ce mode de fonctionnement nous incite à introduire dans la section 4.3, un modèle décrivant la façon dont le couple moteur est transmis. Les paramètres et les caractéristiques d'un tel modèle sont alors identifiés sur deux motorisations différentes, utilisant des données expérimentales provenant de deux démonstrateurs : le démonstrateur VEHGAN équipé d'une AMT, étudié dans le chapitre précédent, et un démonstrateur à motorisation de taille réduite (VelSatis EcoSural) équipé d'une transmission manuelle, qui fera l'objet du chapitre 6. Outre les applications de contrôle, qui seront étudiées dans les chapitres suivants, le modèle phénoménologique du couple d'embrayage pourra être utilisé pour analyser les oscillations de la transmission à engagement de l'embrayage, comme expliqué dans la section 4.5.

4.2 Quelques commentaires sur les forces de frottement

Tout contact mécanique entre deux corps en mouvement génère une force de frottement qui dépend directement de la nature de la surface et de la vitesse de glissement entre les deux corps. Ce phénomène a été étudié de façon approfondie au fil des ans, ainsi de nombreux modèles ont été proposés pour capturer le comportement des dynamiques en vertu du frottement. La plupart de ces modèles dépendent de la vitesse de glissement (Armstrong (1991)). Pour avoir un aperçu de ces modèles, le lecteur peut se référer à la version complète de la thèse (voir Section 4.2).

4.3 Modèle du couple d'embrayage

En général, les embrayages sont utilisés pour joindre facilement deux inerties tournant à différentes vitesses. Le contact entre les deux corps permet l'écoulement de la puissance d'une inertie à une autre selon le signe de la vitesse relative (vitesse de glissement). Dans les embrayages à sec, la transmission du couple se fait par un phénomène de frottement entre les deux

surfaces ou disques : un matériau à forte adhérence est ajouté à une surface afin de maximiser le coefficient de frottement. Dans les applications automobiles, les embrayages sont utilisés pour coupler ou désaccoupler la transmission du moteur. Lorsque l'embrayage est ouvert, aucun couple n'est transmis. Lorsque l'embrayage est en glissement (vitesse relative non nulle), seule une fraction du couple moteur est transmise, l'autre partie est perdue sous forme de chaleur. Par ailleurs, lorsque l'embrayage est complètement fermé, le couple moteur est intégralement transmis, à moins qu'il ne dépasse un certain seuil défini par le couple maximum de l'embrayage, qui est garanti par les fabricants afin de protéger la transmission d'un excès de couple. Dans ce cas, l'embrayage doit glisser pour dissiper l'excès de couple sous forme de chaleur.

① Pressure plat
② Clutch disk
③ Pilot shaft
④ Throw-out bearing
⑤ Pilot pushing

Figure 8: Embrayage à frottement à sec

La quantité du couple d'embrayage peut être directement contrôlée par la position de la pédale d'embrayage qui actionne un vérin électrique ou hydro-électrique. En effet, dans la plupart des stratégies de contrôle proposées pour le contrôle des transmissions manuelles robotisées et d'assistance au décollage, une caractéristique statique (non-linéaire) permet de renseigner la quantité du couple transmise (voir par exemple Glielmo et al. (2004), Dolcini et al. (2005), Tona et al. (2007), Van Der Heijden et al. (2007)). Cependant, le couple transmis dépend de nombreux autres facteurs, tels que la vitesse de glissement et l'accélération, l'usure, la température et l'état des différentes ressorts présents dans l'embrayage (diaphragme, et ressorts de torsion). Les performances de contrôle peuvent être considérablement affectées par ces facteurs si on les néglige, même si un observateur est inclus dans le système de contrôle. Ceci est dû au fait qu'il est difficile d'implémenter des modèles relativement complexes avec un minimum de mesure sur véhicule.

Dans cet ordre d'idée, nous avons développé un modèle phénoménologique lié à la transmissibilité du couple moteur à la transmission durant la phase de glissement de l'embrayage. Ce modèle utilise des mesures disponibles sur les véhicules de série permettant sa mise œuvre pratique. Ces entrées sont : la position de l'actionneur d'embrayage, la vitesse de glissement, et le couple moteur de consigne car le couple moteur effectif n'est pas mesurable.

Fondamentalement, l'embrayage permet au groupe motopropulseur d'être déplacé d'un point de fonctionnement 'A' défini par $[\omega_e := \omega_e^{idle},\ \omega_c := 0]$ à un nouveau point de fonctionnement 'B' défini par $(\omega_c := \omega_e)$. L'effort nécessaire pour ce déplacement est transmis via les deux commandes T_e et $T_c(\cdot,\cdot)$. Lorsque l'embrayage se rapproche de la position fermée (groupe motopropulseur se rapproche du point 'B'), il peut être pensé comme un interrupteur fermé pour lequel le couple net du moteur est totalement disponible sur l'arbre primaire permettant ainsi de noter : $T_c(\cdot,\cdot) := T_e$. Cela signifie que le couple de l'embrayage est très proche du couple moteur

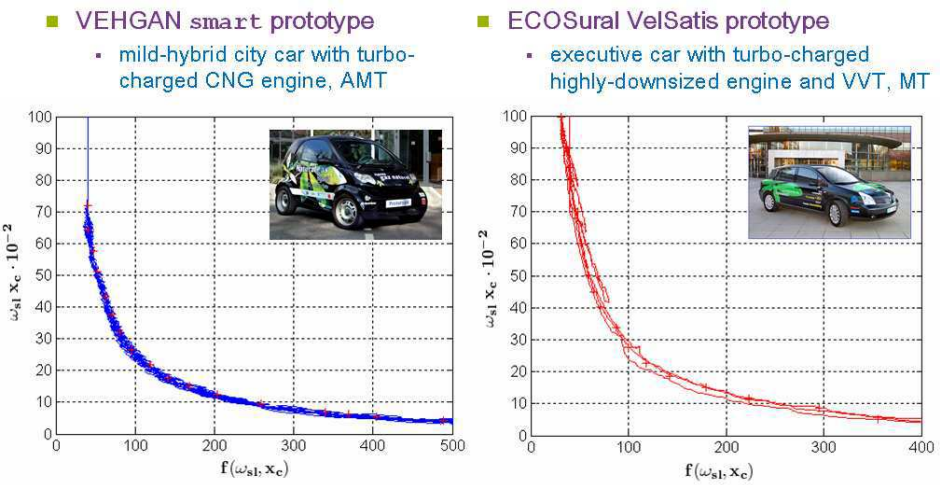

Figure 9: Identification de caractéristique de transmissibilité du couple d'embrayage sur deux démonstrateurs.

(valeur net), et explique notre motivation d'introduire une dépendance fonctionnelle en T_e tout le long de la phase de glissement.

Nous prévoyons que l'insertion du couple moteur dans le modèle aurait un effet de lissage sur les variations de la transmissibilité du couple de frottement, qui ne sont pas directement liées à la position de l'embrayage x_c et à la vitesse de glissement ω_{sl}.
Parmi plusieurs structures possibles, évaluées de façon expérimentale, nous avons sélectionné la suivante :

$$T_c(\cdot,\cdot) := T_e \cdot \omega_{sl} \cdot f(x_c, \omega_{sl})$$

où $f(.)$ est une fonction non linéaire inconnue, à identifier, qui dépend de la position de l'embrayage et de la vitesse de glissement. Cette caractéristique $f(\cdot)$ doit être reconstruite expérimentalement.

4.4 Validation

Le modèle a été identifié et validé sur deux prototypes de véhicules avec des caractéristiques très différentes : une petite citadine avec une transmission manuelle robotisée pilotée par le contrôle embarqué, et une grosse voiture avec une transmission manuelle pilotée par le conducteur. Cette diversité suggère un certain degré de généricité du modèle dans deux contextes différents. La figure 9 représente les caractéristiques obtenues sur les deux véhicules.

4.5 Application : Condition de non Oscillation de la Transmission

Au-delà de l'utilité du modèle dans le calcul du contrôleur, un exemple d'application est donné pour montrer une utilité du modèle pour analyser/expliquer le phénomène qui fait apparaître des oscillations dans la transmission à la fermeture de l'embrayage. Cette analyse est basée sur un calcul de puissance, en amont et en aval de l'embrayage, en utilisant le modèle phénoménologique du couple d'embrayage.

Dans le chapitre suivant, le modèle présenté ci-dessus sera utilisé dans une formulation d'assistance au décollage pour un véhicule à motorisation taille réduite équipé d'une transmission

manuelle. Plus particulièrement, il s'agit d'une commande prédictive non linéaire qui implémente le modèle phénoménologique proposé.

– Chapitre 5 : **Contrôle d'Assistance au Décollage du Véhicule**

5.1 Introduction

Dans la plupart des véhicules équipés de transmissions manuelles, la qualité de l'agrément de conduite dépend entièrement du talent du conducteur. En particulier, pendant les phases de démarrage du véhicule, où le conducteur doit contrôler à la fois la production du couple thermique via la pédale d'accélérateur et sa transmission via la pédale d'embrayage. Le confort qui en résulte dépend de la capacité du conducteur à synchroniser ces deux tâches. Cet objectif est encore plus difficile à réaliser dans le cas des véhicules à motorisation taille réduite puisque le moteur thermique fait toujours face à des charges relativement élevées avec peu de puissance disponible à bas régime. Dans ce contexte, certaines stratégies de contrôle avancé peuvent être mises en place afin d'améliorer l'agrément de conduite en appliquant quelques corrections sur les actions du conducteur. Plus clairement, les stratégies d'assistance peuvent modifier la demande de couple exprimée via la pédale d'accélérateur ou le couple d'embrayage. Ce dernier point d'action, n'est possible que dans certaines applications spécifiques qui sont dotées d'un mécanisme de by-pass sur l'embrayage.

5.2 Le Concept de "motorisation taille réduite"

Le concept de "motorisation taille réduite" consiste à diminuer la cylindrée du moteur thermique, afin de réduire les frottements internes dans le moteur et les pertes par pompage et cela dans le but d'améliorer l'efficacité de combustion. Du fait que ce procédé permet de réduire la consommation, il est largement adopté dans les véhicules de série. De l'autre côté, pour compenser la diminution de la cylindrée un système de suralimentation est ajouté afin d'augmenter la densité de l'air entrant dans le moteur. Des systèmes de turbocompression sont utilisés pour comprimer l'air d'admission en utilisant une fraction des gaz d'échappement. D'autre part, moyennant les technologies utilisées, il est difficile de faire fonctionner les turbocompresseurs à bas régime à cause de l'énergie des gaz d'échappement qui est faible à bas régime.

La suralimentation est souvent associée à une ou plusieurs technologies avancées, comme le calage variable des soupapes (VVT), la recirculation des gaz d'échappement (EGR), et l'injection directe (DI). Moyennant ces solutions, les émissions de polluants sont considérablement réduites. Néanmoins, comme les contraintes environnementales deviennent plus en plus strictes, de nouvelles solutions sont constamment recherchées (voir par exemple le lac et al. (2004), dans lequel les auteurs présentent cinq approches alternatives de suralimentation pour des moteurs à essence à injection directe).

Dans le véhicule à motorisation taille réduite, l'aide au décollage ne dépend pas du concept "motorisation taille réduite" : elle dépend de la couche de contrôle haut niveau liée à la demande de couple, alors que le concept de "motorisation taille réduite" est directement lié à la couche bas niveau associée aux actionneurs (réalisation de la demande de couple).

5.3 Commande Hybride d'un Groupe Motopropulseur Equipé d'une Transmission Manuelle (MT)

Dans les applications automobiles, il est bien connu que la phase de décollage du véhicule est la plus contraignante à cause des forces de frottement dans les disques d'embrayage qui sont très importantes. Cela est dû au fait que le véhicule commence le mouvement d'une vitesse nulle pour laquelle la composante du couple statique est importante. Dans ce contexte, les informations sur le couple de charge et/ou le couple d'embrayage seraient utiles pour contrôler la production du couple thermique. En outre, dans les véhicules à motorisation taille réduite, les informations sur les couples résistants sont très utiles puisque les points de fonctionnement des moteurs de taille réduite sont différents de ceux des moteurs conventionnels.

Dans les véhicules conventionnels équipés de transmission manuelle, le conducteur pilote à la fois les pédales d'accélérateur et d'embrayage pour déplacer le véhicule. Conceptuellement, la commande de l'embrayage est appliquée directement au mécanisme de l'embrayage, qui permet de transmettre le couple moteur à l'arbre primaire. Quant à la position de la pédale d'accélérateur, elle est indirectement liée à la production du couple thermique à travers les stratégies de contrôle embarqué et quelques actionneurs bas niveau, comme le montre la figure 10. Dans cette architecture, il est possible d'identifier trois niveaux communs :

- Un contrôleur haut niveau (contrôleur maître) qui représente le conducteur, qui a un contrôle total sur toutes les composantes de la transmission (embrayage, boîte de vitesses et freins) et fournit des consignes (requêtes) au contrôle embarqué;
- Des contrôleurs secondaires qui assurent des conditions de fonctionnement nominales liées à : la demande du conducteur, l'état de la chaîne cinématique, la combustion, et la consommation du réseau de bord. La gestion de la pédale d'accélérateur est traitée par ce module;
- Des contrôleurs d'actionneurs bas niveau, ayant pour but d'asservir les consignes de références calculées à partir des couches de contrôleurs secondaires.

En considérant le système groupe motopropulseur, présenté sur la figure 10, l'agrément de conduite peut être amélioré en remplaçant le contrôle classique en boucle ouverte (demande de couple) par un contrôle avancé en assurant un bon pilotage du moteur thermique. Rappelons que, la demande de couple exprimée par le conducteur est calculée à partir d'une cartographie statique (couple pédale) ayant pour entrée la position de la pédale d'accélérateur et le régime moteur.

Dans le cadre de l'assistance au décollage, un contrôle spécifique en boucle fermée peut être mis en œuvre pour aider le conducteur durant la manœuvre de décollage. Par exemple, le contrôleur de ralenti peut être étendu à la phase de décollage en corrigeant/réajustant le couple pédale qui est calculé en boucle ouverte.

5.4 Modèle Phénoménologique du Couple Embrayage pour l'Assistance au Décollage

Afin de garantir une bonne assistance, il est fondamental d'avoir une bonne caractérisation du couple d'embrayage, car ce couple est une perturbation importante qui peut causer des oscillations un niveau de la transmission et peut même provoquer le décrochage du moteur thermique. Dans le chapitre précédent, nous avons proposé un modèle phénoménologique lié à la transmissibilité du couple via l'embrayage pendant la phase de décollage du véhicule. Ce modèle utilise le

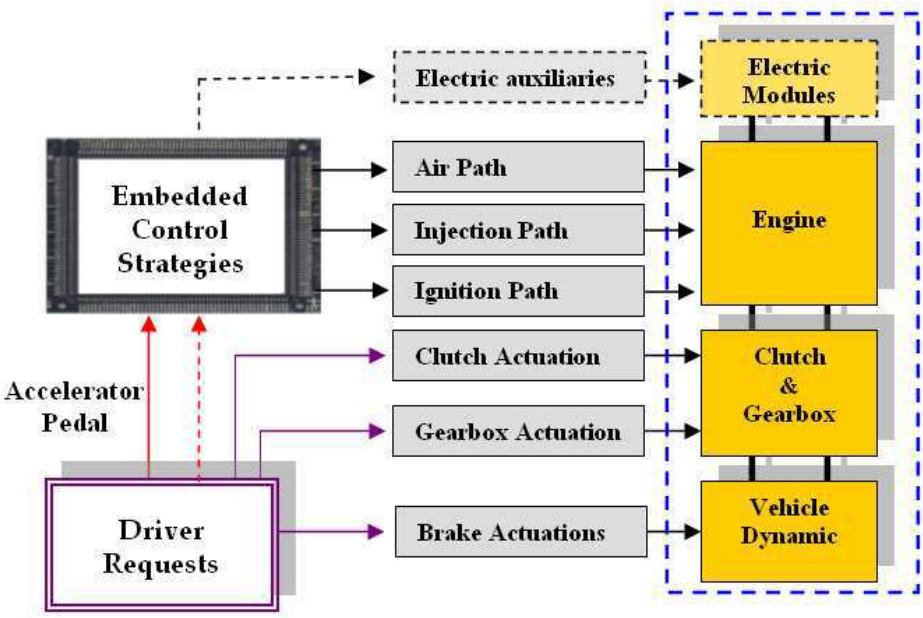

Figure 10: Architecture de contrôle d'un groupe motopropulseur équipé d'une transmission manuelle.

couple moteur de consigne, la vitesse de glissement de l'embrayage, et une caractéristique non linéaire. Cette caractéristique dépend de la position de la pédale d'embrayage et de la vitesse de glissement, elle est à identifier expérimentalement.

5.5 Commande Prédictive (MPC) Unifiée pour un Groupe Motopropulseur Equipé d'une Transmission Manuelle

Dans l'approche de contrôle unifié proposée, la formulation comporte trois phases de fonctionnement qui sont : le contrôle de ralenti, l'assistance au décollage, et la régulation entraînée. Au cours de ces phases, la stratégie MPC a pour but de réguler et d'asservir le régime moteur autour d'une trajectoire de référence, en utilisant seulement le couple moteur comme une entrée de commande.

Pour rester proche de la structure initiale de contrôle (boucle ouverte), un sélecteur est utilisé pour appliquer soit la commande en boucle ouverte (couple pédale), soit celle de la boucle fermée (MPC). En gros, ce module sélectionne et applique le plus important des deux couples. Cela permet de maintenir une certaine sensibilité sur la pédale d'accélérateur quand le conducteur sollicite des couples importants. Notez que, dans la structure de contrôle proposée, les frottements internes du moteur sont compensés en aval afin de limiter la complexité de la commande MPC, d'une part, et de rester proche d'une topologie de contrôle conventionnelle, d'autre part.

Une contribution majeure de ce chapitre est l'implémentation du modèle phénoménologique lié à la transmissibilité du couple via l'embrayage, développé dans le chapitre précédent, dans un cadre d'une commande prédictive d'assistance au décollage. La mise en œuvre de cette stratégie est réalisée via une approche de contrôle paramétrique (CPA), qui permet de prendre en compte les contraintes d'implémentation en temps réel. Il en résulte, un problème d'optimisation scalaire simple qui peut être résolu par dichotomie dans laquelle le calcul de la fonction coût est obtenu en résolvant un système linéaire de taille modérée.

En outre, le contrôle proposé utilise des mesures disponibles sur les véhicules de série, à l'exception du capteur position de l'embrayage qui peut être absent dans certains véhicules. Le coût relativement faible de ce capteur et les avantages de l'assistance au décollage peut facilement mettre en avant la généralisation de ce capteur.

Le chapitre suivant présente une validation de la commande prédictive non linéaire proposée via son implémentation sur un démonstrateur à motorisation taille réduite équipé d'une transmission manuelle.

– Chapitre 6 : **Application et Validation de la Modélisation du Couple d'Embrayage et du Contrôle d'Assistance au Décollage dans un Démonstrateur Muni d'une Transmission Manuelle (MT)**

Ce chapitre illustre l'application et la validation des contributions développées dans les deux chapitres précédents (4 et 5) : il s'agit d'une commande prédictive d'assistance au décollage pour des véhicules équipés d'une transmission manuelle.

Dans la première partie du chapitre, nous présentons le contexte de l'application, et plus particulièrement, le démonstrateur IFP VelSatis -EcoSural, un véhicule à motorisation taille réduite équipé d'un turbo compresseur et d'une transmission manuelle. Ensuite, nous expliquons en détail le contrôle d'assistance au décollage dans une structure de contrôle standard. Nous décrivons également la plateforme de co-simulation utilisée pour la validation du contrôle.

Le reste du chapitre est consacré à la validation. Nous présentons les premiers pas de validation du modèle phénoménologique lié au couple d'embrayage. Plus exactement il s'agit d'une version simplifiée du modèle proposé, implémenté en feedforward pour assister le contrôleur standard de ralenti. Ce module de contrôle est initialement assisté par une cartographie statique liée au couple d'embrayage qui dépend uniquement de la position de l'actionneur d'embrayage. L'implémentation du modèle simplifié conduit à une nette amélioration des performances de contrôle.

La deuxième partie de la validation est consacrée à la validation du contrôle d'assistance au décollage en implémentant la forme complète du modèle phénoménologique du couple d'embrayage, moyennant une commande prédictive non linéaire compatible avec les contraintes temps réel. Les performances de cette stratégie sont illustrées par des résultats de co-simulation.

C/ Conclusion et perspectives

Avec l'augmentation de la complexité des systèmes mécatroniques utilisés dans les véhicules modernes, les systèmes de contrôle jouent aujourd'hui un rôle fondamental dans le monde de l'automobile. En réponse à des contraintes de plus en plus strictes d'environnement, d'économie de carburant, et d'exigences de performance, les constructeurs automobiles sont contraints de développer et de perfectionner de nouveaux moteurs et groupes motopropulseurs. Les concepteurs des systèmes de contrôle doivent, à leur tour, fournir des solutions pour aider à la maîtrise de la complexité qui en résulte.

Des solutions viables sont celles qui traitent de manière appropriée les problèmes de conception et d'implémentation en prenant en compte :

- Les modes de fonctionnement hybride, avec un mélange des dynamiques à temps discret et à temps continu;
- Les contraintes sur les variables manipulées;
- La rareté des capteurs disponibles;
- L'intégration standard, distribuée, des architectures de contrôle;
- Le calcul et les limites de stockage de données;
- La facilité de calibration.

Lors de notre investigation nous avons pris en compte l'ensemble de ces considérations lorsque nous avons abordé les deux problématiques de contrôle qui font l'objet de cette thèse :

- Le contrôle d'un groupe motopropulseur hybride léger équipé d'une transmission manuelle automatisée;
- L'assistance au décollage d'un groupe motopropulseur fortement à motorisation taille réduite équipé d'une transmission manuelle.

Bien que ces problèmes soient différents, nous les avons étudié dans un cadre commun. Le conducteur agit en tant que contrôleur principal pour fournir des références à un contrôleur esclave, ou d'appliquer directement ses commandes à la transmission. Dans ce cadre, nous avons développé une approche de contrôle structurée, basée sur un seul contrôleur qui interagit directement avec le conducteur dans les différents modes de fonctionnement moyennant une stratégie de commande prédictive. Pour répondre aux exigences serrées en temps réel déclinées par le contrôle automobile, nous avons eu recours à une approche de contrôle paramétrique.

Concernant l'architecture de contrôle, nous estimons que la contribution de notre travail de thèse est double :

1. La définition d'un schéma de commande unifié basé sur un modèle simplifié. La simplification utilise de façon extensive des observateurs dynamiques afin de récupérer des quantités non mesurées et non modélisées comme : le couple de charge, l'imperfection des boucles de contrôle bas niveau liées aux couples moteur et d'embrayage. Une grande partie du succès de la mise en oeuvre est due à la simplification ci-dessus;
2. L'implémentation des schémas itératifs permettant la résolution des problèmes quadratiques contraints moyennant une résolution d'une série de problèmes quadratiques sans contraintes. Sans un tel schéma itératif, la stratégie de commande prédictive ne peut être appliquée en temps réel.

Dans l'architecture proposée, les spécifications liées au problème, comme la transparence vis-à-vis de la pédale d'accélérateur et la douceur de l'engagement de l'embrayage, sont pris en compte par la définition des trajectoires de référence du régime moteur et la vitesse de glissement. Le principe de l'horizon fuyant permet une mise à jour périodique de ces trajectoires de référence, conformément à l'action du conducteur.

Les validations expérimentales sur le prototype ont montré les performances de la stratégie proposée et le respect du temps de calcul qui ne prend qu'une petite fraction du calcul global. Une fonctionnalité intéressante de la solution proposée réside dans la mémoire de stockage qui est relativement faible par rapport aux solutions basées sur une optimisation hors-ligne. En outre, la stratégie proposée peut être facilement étendue à des contextes potentiellement différents (nouveaux actionneurs, nouveaux signaux exogènes, etc.), alors que l'on sait que les solutions calculées hors-ligne doivent être entièrement recalculées (avec une augmentation rapide de la complexité) lorsqu'il y a un changement, même léger, dans la définition du problème.

Nous avons montré que pour résoudre le problème d'assistance au décollage, une connaissance plus précise du couple transmis par l'embrayage est nécessaire. À cette fin, nous avons développé un modèle phénoménologique original caractérisant le couple d'embrayage, fondé uniquement sur des mesures standard disponibles sur les véhicules de série. Ce modèle a été utilisé pour concevoir une loi de commande prédictive non linéaire (NMPC) d'assistance au décollage.

Contrairement au cas de contrôle de la transmission manuelle automatisée (AMT), abordés dans la première partie de la thèse, l'évolution de l'assistance au décollage n'a pas été validée sur le véhicule. En effet, une validation expérimentale de la commande NMPC sur le démonstrateur serait une suite naturelle de ce travail. En outre, il serait intéressant d'évaluer le modèle phénoménologique du couple d'embrayage dans le cas de la transmission manuelle automatisée, en vue d'une amélioration des performances durant les changements de vitesses.

Introduction

In the recent past, the implementation of embedded electronic control units in vehicles represented a major breakthrough in automotive technology. More particularly, engine control has enabled manufacturers to make substantial progress in the optimization of engine efficiency, the reduction of fuel consumption, the abatement of pollutant emission, the improvement of drivability and the increase of general reliability of vehicles.

Nowadays, most technological developments under way in the automotive field tend to increase powertrain complexity. Basic transmission types have evolved into new concepts, such as automated manual, dual-clutch or continuously variable transmissions, which become more and more common in production vehicles. This evolution is accompanied by the introduction of new active and passive servo-actuated transmission components (clutch, gearbox, differential). Moreover, because of the growing interest in the development of hybrid powertrains, systems with several torque producers and consumers are now commonplace. With the increase in the number of components and actuators, more and more complex dynamics must be taken into account while the management of the transitions between operating modes and configurations becomes a challenging problem. On the other hand, even for powertrains equipped with standard manual transmission, the adoption of a particular advanced engine concept often leads to an increase of control complexity at vehicle level. This is for instance the case of extreme engine downsizing which has a direct impact on vehicle drivability.

To manage a greatly increased complexity, and to comply with more and more severe specifications, modern powertrain must be optimized and controlled as a whole. We have to move from engine control to *integrated powertrain control*.

From an automatic control point of view, this requires:

- taking into account the *hybrid* nature (that is, mixing continuous-time and discrete-time dynamics) of the controlled system;
- dealing effectively with couplings, which implies having recourse to multi-variable control strategies;
- generating reference trajectories which correspond to driver's will in each operating mode;
- defining specifications which enforce drivability and fuel consumption constraints.

Starting from these considerations, during my PhD research I have tried to find an original solution to two different but related powertrain control problems. The first problem involves the control of a relatively complex powertrain, characterized by an automated manual transmission and mild hybridization, such as the one shown in Figure 11. In an automated manual transmission (AMT) system, the clutch and the gearbox are not directly controlled by the driver.

Transmission actuators are computer controlled instead, and embedded control strategies are in charge of ensuring smooth clutch engagement and gear shifting. This kind of powertrain actually equips a demo car, VEHGAN[6] (Tona et al. (2006)), developed for a project investigating the benefits of combining, in a small city car (a MCC `smart`), a dedicated downsized engine (660 cm3) fueled with compressed natural gas, with a starter-alternator reversible system based on ultra-capacitors, providing mild-hybrid capabilities. This mild-hybrid AMT powertrain provides an excellent framework to illustrate the problems arising from the presence of several torque producers and consumers, and the benefits stemming from the adoption of an advanced control strategy instead of the standard open-loop control approach, based on look-up tables.

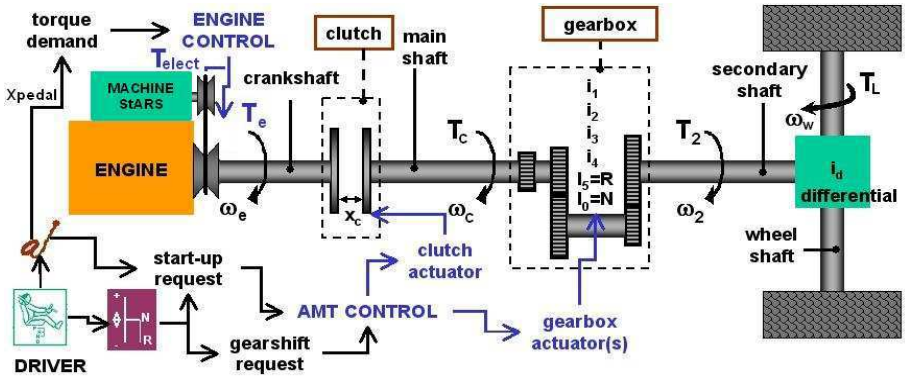

Figure 11: Conventional powertrain architecture of a mild-hybrid vehicle equipped with an automated manual transmission (AMT)

The second problem I have investigated is driver assistance during vehicle start-up with a powertrain composed of a manual transmission and a highly *downsized* gasoline engine. Downsizing means reducing engine displacement and compensating the loss of power by turbocharging, with the aim of lowering fuel consumption. In such a vehicle, the start-up maneuver, which could be in principle entirely carried out by the driver, often requires above-average driving skills due to insufficient engine torque availability at low speed. To improve drivability, one can implement a control system which acts on engine dynamics to assist the driver in order to avoid engine stall or transmission oscillations. The experimental framework is provided in this case by another demo car, developed for the Ecosural project (Le Solliec et al. (2006)): a Renault Velsatis, whose standard naturally aspirated 3.0-liter spark-ignition engine has been replaced by a turbocharged 1.8-liter engine with twin variable camshaft timing. Though downsizing provides a significant fuel saving (about 20%), with such a heavy vehicle, it also affects driving comfort at start-up. An effective driver assistance control strategy would lead to greater acceptance of this technology.

For both problems, the solutions proposed here are based on constrained model predictive control laws using a hybrid control model taking into account the different powertrain configurations. Particular control parametrizations enable online optimization and respect of the constraints, via a simple dichotomic search algorithm which permits real-time implementation with an embedded control system. Moreover, thanks to the use of on-line torque estimators, those strategies do not require any additional sensors than those normally available in commercial powertrain or further test bench calibrations.

Aside from this common framework, each problem has required a specific solution.

[6] VEhicule Hybride au GAz Naturel

In the AMT control problem, the system to be controlled is fully actuated, with two inputs, engine torque and clutch torque, and two outputs, engine speed and mainshaft speed (or clutch slip speed). Three powertrain modes are considered: idle speed control, vehicle start-up and gear shifting. The control scheme enables a unified treatment of the three modes. A remarkable feature of the proposed control strategy is the fact that, in both start-up and gear shifting modes, the sub-optimal solutions are directly linked to the accelerator pedal position in order to promote a sort of *constrained transparency* to the driver.

In the driver assistance control problem, the idle speed control, the vehicle start-up, and vehicle coasting are considered. The system to be controlled has the same inputs and outputs as in the AMT case, but only engine torque can be manipulated (correcting the torque demanded by the driver), while clutch torque acts as a disturbance. In this context, a more precise estimation of clutch torque is needed with respect to the former problem. For this reason, a phenomenological model for torque transmissibility during clutch engagement has been developed. The model is based on the identification of a nonlinear characteristic that relates the transmissibility of engine torque to the mainshaft to the clutch actuator position and the clutch slip speed. Incorporated in a truly nonlinear model predictive control law, this model greatly improves the performance of driver assistance with respect to strategies based on feed-forward control and simplistic clutch torque transmissibility models.

The thesis is organized as follows:

- Part I: **Powertrain Control and Drivability**
  - Chapter 1: **Advanced Powertrain Control for Drivability**
    The first chapter explain what a powertrain is, addresses the general issues of powertrain control, puts into perspective the set of drivability-related problems that are the focus of this thesis, and introduces the advanced control methodology adopted to solve those problems: Model Predictive Control. The chapter ends with a description of the Control Parametrization Approach, adopted in the following to comply with the hard implementation constraints that any viable control solution must meet.
- Part II: **Unified Predictive Control of an Automated Manual Transmission**
  - Chapter 2: **Control of Powertrains Equipped with AMT**
    This chapter presents a model predictive control strategy developed for handling the different operating modes of an automated manual transmission in a unified way. First, the general operating principles of automatic manual transmissions are introduced. Then, after an examination of the main approaches reported in the literature to solve AMT control problems, the characteristics of the AMT control which is the focus of the first part of the thesis are outlined. Finally, the methodology and the framework the unified model predictive control strategy are presented.
  - Chapter 3: **Application and Validation of AMT Control on a Demo Car**

    This chapter illustrates the application and validation of the unified MPC strategy for AMT control. In the first part, the application context is introduced: the VEHGAN demo-car, a mild-hybrid vehicle equipped with a rapid prototyping powertrain control system. Then, the implementation of the unified model predictive control strategy in the integrated powertrain control structure of the demo-car is explained. Nominal control performances are first validated in a simplified simulation environment. Then, the AMT control module is validated and pre-calibrated in a co-simulation

environment which includes a detailed powertrain model. Finally, results of real-time experiments carried out on the demo car are presented.

- Part III: **Unified Predictive Control for Vehicle Start-Up Assistance**
  - Chapter 4: **Clutch Torque Modeling**
    After a brief overview of friction force modeling, this chapter presents an original phenomenological clutch model to characterize the transmissibility of the engine torque to the mainshaft during the clutch engagement phase of vehicle start-up. Its parameters and characteristics are identified for two different powertrains, using experimental data from two demo cars: the AMT demo car VEHGAN, introduced before, and the downsized-engine MT demo car EcoSural, which is the focus of the second application presented in this thesis.
  - Chapter 5: **Control Assistance During Vehicle Start-Up**
    In this chapter a model predictive control design is proposed for the start-up assistance for vehicles equipped with a manual transmission. The specific context of start-up assistance in the presence of engine downsizing is recalled, then the features of the proposed strategy are introduced. The model predictive control strategy uses the phenomenological clutch model developed before to perform precise prediction of the system behavior over the prediction horizon. Again, the problem of real-time implementation of the proposed MPC strategy is addressed thanks to a suitable parametrization.
  - Chapter 6: **Application and Validation of Clutch Torque Modeling and Vehicle Start-Up Assistance on a MT Demo-Car**
    The last chapter illustrates the application and validation of the the phenomenological clutch torque transmissibility model and of the model predictive control design proposed for start-up assistance, based upon it. First, the application context is introduced : the EcoSural demo-car, a manual transmission vehicle equipped with a highly-downsized turbo-charged engine, the role of a start-up assistance controller and its with the standard engine control modes. After a description of the control and co-simulation layout used for validation, simulation and experimental results are presented and discussed.

At the end of the thesis, some general conclusions are drawn and perspectives for future work are outlined.

Part I

Powertrain Control and Drivability

Chapter 1

Advanced Powertrain Control for Drivability

1.1 Introduction

Drivability is the quality of being easy or pleasant to drive. For a vehicle, drivability essentially means the smooth delivery of power, as demanded by the driver. The part of vehicle which is responsible for producing power, via an internal combustion engine (in most cases), and delivering it the wheels, via a transmission, is referred to as the powertrain.

Contrary to early vehicles, where fuel injection, air flow, ignition timing and other parameters influencing engine combustion were directly controlled by mechanical and pneumatic devices, the operation of internal combustion engines nowadays is mostly determined by electronic devices called engine control units. The introduction of electronics in automotive systems has improved dramatically vehicle performance in terms of drivability, safety, fuel consumption and pollutant emissions. At the same time, vehicle performance depends less and less on direct actions by the driver on the powetrain: more often than not, interaction with the powertrain is screened and monitored by embedded control systems, which translate driver's requests and are responsible of the overall performance. This is particularly true when considering vehicles equipped with more advanced transmission concepts, such as automated manual, dual-clutch or continuously variable transmissions, or hybrid electric vehicles.

As a matter of fact, the rise in complexity of powertrains has been consistently accompanied by the need for more effective control systems, capable to comply with increasingly stringent specifications on drivability, fuel consumption and pollutant emissions. In this thesis, we focus on two drivability-related powertrain control problems: control of a mild-hybrid powertrain with an automated manual transmission and driver assistance for vehicle start-up with a powertrain composed of a manual transmission and a highly downsized gasoline engine. These problems are challenging because of the the hybrid nature of powertrain operation and the complexity of the control objectives to attain. This has motivated us to develop a structured control approach, based on a single controller which interacts directly with the driving. We have chosen to solve these two problems in the framework of Model Predictive Control (MPC), an advanced control design methodology capable to handle nonlinearities, uncertainties, coupling and constraints on both the control and the state of the system. However, since computation of conventional MPC is time consuming, we have resorted to the so-called Control Parametrization Approach (CPA) to meet the tight real-time requirements of automotive control.

To introduce the general issues of powertrain control, we start by recalling what is a powertrain (1.2) and what are its main components, focusing on the particular case of internal combustion engines (1.2.1) and manual and automated manual transmissions (1.2.3). We describe the operation and the relevant characteristics of each component (engine, clutch, gearbox), as well as the structure of the corresponding control systems. In section (1.3), we introduce the standard torque-based powertrain control structure for vehicles equipped with manual transmissions, then we present a possible extension of this structure to the automatic manual transmission case. The recognition of the hybrid nature of powertrain control leads to the modeling approach described in section 1.4. Section 1.5 describes the common framework for the drivability-related control problems addressed in this thesis, and list the set of hard implementation constraints that any viable solution must meet. The general background and the relevance of model predictive control for automotive applications is given in section 1.6, as well as a description of the control parametrization approach, adopted to solve the problems addressed in the thesis.

1.2 The powertrain and its components

The *powertrain* is the group of components that makes vehicle propulsion possible. In wheeled land vehicles, it includes at least one prime mover, or *motor*, which is the source of power for propulsion, and a *transmission*, which delivers the power to the wheels and, thus, to the road surface. The most widespread motor nowadays is still the *internal combustion engine* (ICE), even though other types of engine can be used and *electric motors* are becoming increasingly common. The transmission does not only provide the mechanical link to deliver power to wheels, but also adapts the torque and speed requirements of the vehicle to the torque–speed characteristics of the engine. In fact, the operating speed of an internal combustion engine is usually comprised between 600 and 6000rpm, whereas the typical wheel speed range is 0–1800rpm. Moreover, vehicle propulsion requires high torque at low speed, whereas internal combustion engines provides high torque only at relatively high speed, and cannot provide any torque at all at zero speed. Thus, the transmission must contain components to transmit progressively engine torque to wheels at low speed and to transform speed and torque with a ratio adapted to driving conditions (generally, a reduction ratio to increase torque while reducing speed). In manual transmissions, the most common transmission type, these roles are played respectively by a dry clutch and a gearbox.

1.2.1 Internal-Combustion Engine

An internal-combustion engine (ICE) is an engine in which combustion of the fuel occurs with an oxidizer (usually air) and takes place in a confined space, the *combustion chamber*, producing expanding gases that are used directly to provide mechanical power.

Internal-combustion engines are the most broadly applied and widely used power-generating devices currently in existence. Indeed, powered by an energy-dense fuel (nearly always liquid, derived from fossil fuels) the ICE delivers an excellent power-to-weight ratio. Internal-combustion engines are classified as reciprocating or rotary, spark ignition or compression ignition, and two-stroke or four-stroke. For automotive applications, reciprocating four-stroke spark-ignition and compressed-ignition engines are the most common choices. Compression-ignition engines (diesel engines), where the heat from compression alone ignites the mixture, are generally used in heavy-duty and medium-duty vehicles worldwide, and in roughly half of the passenger cars registered in Europe nowadays. Spark-ignition engines, where the fuel-air mixture is ignited with a spark,

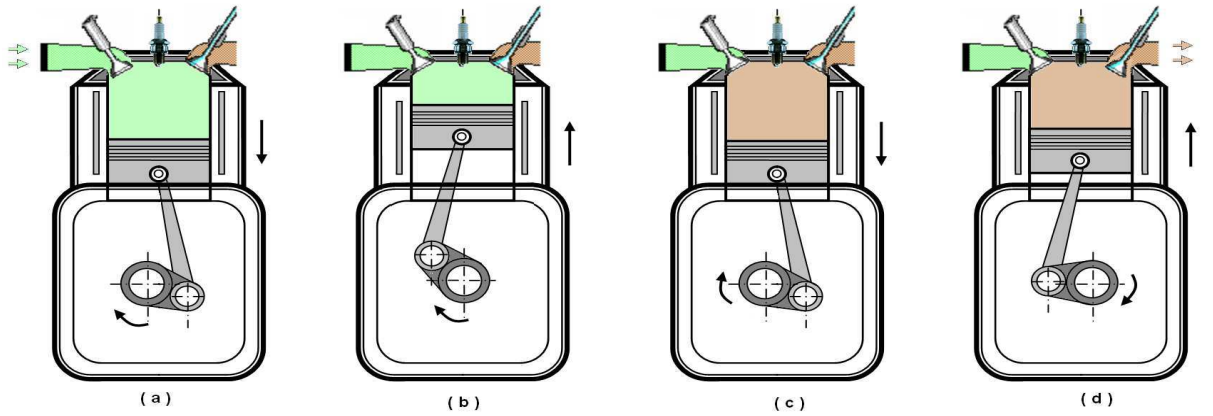

Figure 1.1: Cycles of internal combustion gasoline engine. (a) : Intake stroke; (b) : Compression stroke; (c) : Power Stroke; (d) : Exhaust Stroke;

are mostly used in light-duty vehicles.

In the following we will restrain our discussion to spark-ignition engines, since the application context of this thesis concerns only them.

Spark-ignition (SI) engines use an air-fuel mixture to provide heating energy, which is then transformed into mechanical energy. The air-fuel mixture, generally kept at a stoichiometric ratio, is aspirated into a cylinder, then ignited by a spark-plug. Pressure generated by expansion of hot gases is converted into a rotating motion transmitted to the crankshaft via a *reciprocating* piston. SI engines may have from 1 to 6 cylinders in-line or from 2 to 16 cylinders in V-formation.

The Otto or four-stroke cycle consists of adiabatic compression, heat addition at constant volume, adiabatic expansion and rejection of heat at constant volume. A working cycle consists of two crankshaft rotations during which four strokes occurs, namely the intake, compression, combustion (power), and exhaust strokes. Figure 1.1 represents the position of one particular engine cylinder during one cycle, with the four strokes:

- **Intake Stroke**
  In the first stroke, the piston descends from the position in which it is farthest from the crankshaft, called Top Dead Center (TDC), the intake valve is maintained opened while the piston is still going down, and this enables the mixed fuel to be aspirated inside the cylinder. When, the piston reaches the nearest position to the crankshaft (Bottom Dead Center, BDC), the volume becomes maximum. The amount of the heating energy is directly depending on the amount of fuel included in this fixed maximum volume.

- **Compression Stroke**
  During this phase, the intake and the exhaust valves are completely closed, and the mixed fuel is being compressed while the piston is going up from the BDC position to the TDC position. The ratio between the nominal and maximum volumes is denoted by *volumetric ratio*, and it is a physical limitation of the engine. To transcend the performances of naturally-aspirated engines, turbocharging and supercharging may be used, which enable to increase the density of air entering the engine to create more power.

- **Power Stroke**
  When the piston approaches TDC again, the mixed fuel is ignited through an electric spark.

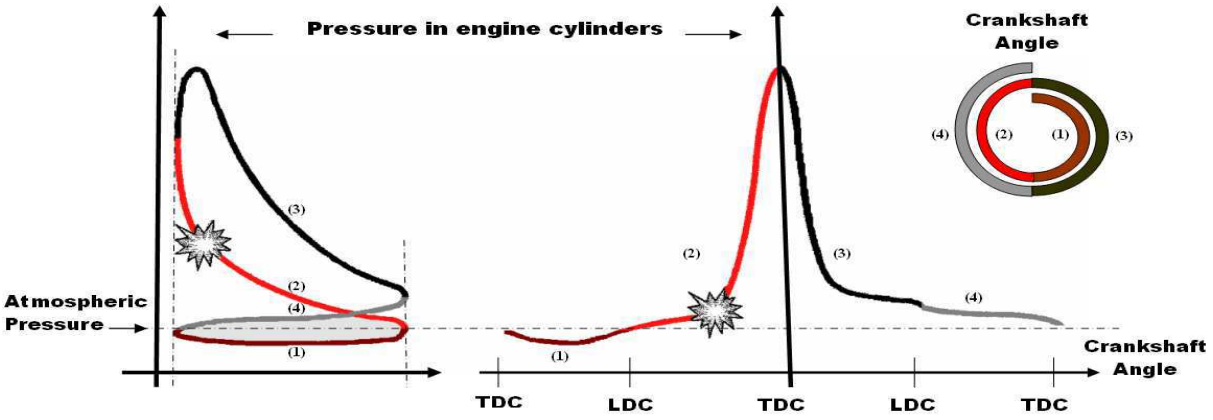

Figure 1.2: Typical profiles of pressure in engine cylinders. TDC: Top Dead Center; BDC: Bottom Dead Center

The temperature and the pressure rise significantly, so the piston is pushed back to the BDC position. This is the only only part of the cycle where mechanical energy is produced in the engine. At the end of this phase, the exhaust valve is opened, and exhaust gases are expelled from the cylinder with an exhaust puff. Thus, the pressure decreases to values close to the atmospheric one.

- **Exhaust Stroke**
  During the exhaust phase the cylinder moves from the BDC position to the TDC position, and push the residual exhaust gases still maintained inside the cylinder. Before the piston reaches the TDC position the intake valve is opened, and a bit after the TDC the exhaust valve is closed. Thus, the system is ready to start a new cycle with the intake stroke.

Figure 1.2 represents a typical profile of the pressure acting on a piston during a cycle, composed of two crankshaft revolutions. Pressure profiles are approximately the same for each cylinder in the engine (assuming correct operation). Therefore, in an engine with n cylinders there will be n combustion events, and the overall torque transmitted to the crankshaft during a cycle will result from the superposition of n pressure profiles like the one of Figure 1.2 each shifted of one n-th of the cycle time, or of $4\pi/n$ rad if an angular basis is taken. This period, called *segment time*, is thus given by $t_{seg} = 2 \cdot (60/N_e)/n$, where N_e is the engine speed in rpm. Since the resulting periodic torque peaks cause unpleasant oscillations of crankshaft speed (and of the whole engine), a flywheel with significant inertia is designed to rotate with the engine in order to smooth engine speed dynamics. The surface of the flywheel is designed to be connected to the clutch friction disk and thus to the rest of the transmission.

With respect to torque generation, because of its reciprocating behavior and the discrete nature of combustion events, engine can be considered as a sampled system, with variable sampling in the time domain and constant sampling in the angular domain. Injection and ignition and commands must be synchronized with respect to each combustion TDC. For injections, the duration of each injection must be defined (*injection time*) as well as its phasing with respect to TDC (*injection advance*). For ignitions, the most important parameter is the *spark advance*, the angular position of the crankshaft relative to combustion TDC at which spark ignition occurs, usually ranging between -40 and $+10$ crankshaft degrees. Injection time and (to a lesser extent) spark advance are the main manipulated variables to control the production of engine torque.

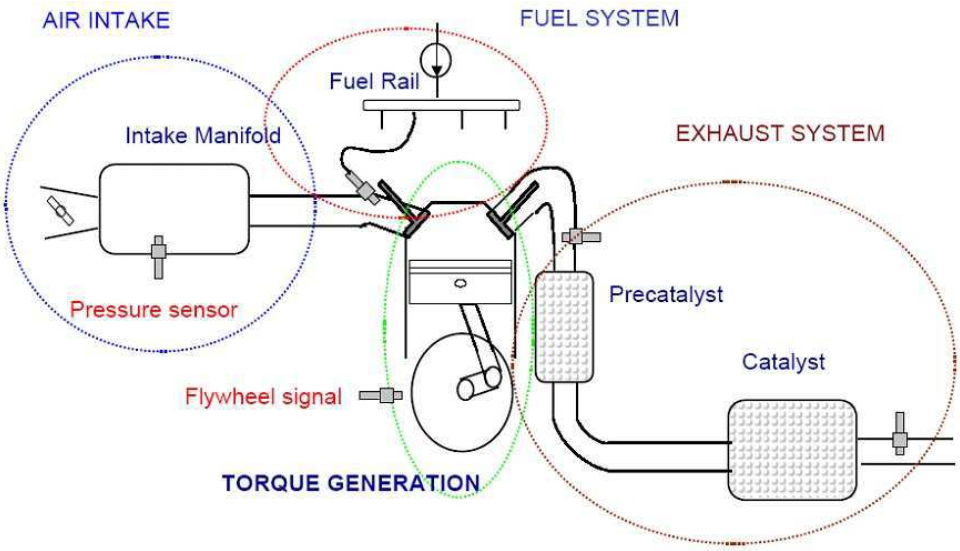

Figure 1.3: Engine subsystems

As shown in Figure 1.3, there are other subsystems to be taken into account to make the engine work. The intake manifold is in charge of evenly distributing the air-mixture (or just air in a direct injection engine) to each intake port in the cylinder heads. An air throttle is used to control the quantity of air in the mixture. The air-fuel ratio (AFR), denoted by λ, must be controlled to a value equal or close to the stoichiometric ratio to have a uniform combustion and to let the gas exhaust after-treatment system reduce pollutant emissions. When gasoline is used, this means that the fuel system must inject $1g$ of fuel for $14.6g$ of air. An air-fuel ratio control system is needed, which uses a measurement at engine exhaust via a *lambda sensor* to calculate the correct amount of fuel corresponding to the quantity of air being aspirated into the engine. Since air and fuel quantities are not independent, engine torque output can be directly related to the air flowing through the engine or the pressure built in the manifold. Notice that the dynamics of these subsystems does not share the reciprocating and discrete-event driven nature of torque generation via the Otto cycle.

In modern engines, a number of additional actuators may be present depending on the technological solutions implemented to improve performance: turbo-charging, exhaust-gas recirculation (EGR), variable valve timing (VVT), and so on. Moreover, some advanced concepts impose radically different operating modes (for instance, *lean-burn* combustion zones, that is, with an excess of air).

1.2.2 Engine Control

The main function of the engine in a vehicle is to provide torque to the crankshaft, and, through the transmission, to the wheels. Several actuators must be coordinated to obtain the production of the required level of torque, while maintaining safe operating conditions and good performances in terms of fuel consumption and pollutant emissions. This coordination is realized in a software module called Engine Management System, embedded in a dedicated electronic control unit (often called Engine Control Unit, ECU).

For engine control, and simple simulation purposes, it is customary to adopt a *mean-value* approach and consider the torque constant (and equal to its mean value) over a cycle or a segment time. On the basis of a desired torque set-point, set-points for low-level actuators controlling

the cycle (injectors, spark plugs) are updated at each segment time, thus at a variable sampling period, comprised between $5ms$ and $50ms$ (respectively for $N_e = 6000rpm$ and $N_e = 600rpm$) for a four-cylinders engine. Other set-points, as those for the *air-path* (throttle position, turbine wastegate position, etc.) may be synchronized to the cycle or updated at a different, fixed sampling period (typically $10ms$). Notice that low-level control of engine actuators (throttle servo, injector control) will require specific modules at faster sampling rates that may be hosted in dedicated control units.

Engine control is in charge of translating high-level setpoints (torque setpoints, but also AFR set-point) into actuator setpoints (throttle position, spark advance, injection time, etc.). Till the nineties, engine control was almost entirely based on *engine mapping*, which consists in finding *static* relationships, identified on a part (a set of points) of the engine operating domain, linking engine *outputs* Y_{eng} (torque, air-fuel ratio, exhaust gas pollutants) to engine *inputs* U_{eng} (throttle position, spark advance, injection time, etc.) and engine *states* X_{eng} (engine speed, pressures, temperatures), under fuel consumption and pollutant emissions constraints:

$$Y_{eng} = f(U_{eng}, X_{eng}) \text{ with } \begin{cases} C_s = C_{s_{min}} \\ CO, HC, NO_x \leq S \end{cases}$$

where C_s and $C_{s_{min}}$ are the specific fuel consumption and its target minimum, and CO, HC, NO_x are the emission rates of the regulated pollutants, that have to be lower than a legal threshold S.

The experimental identification of these static maps (look-up tables), sampled on a part of the engine operating domain, takes into account not only the aforementioned explicit constraints, but also other implicit criteria, such as engine stability and knock protection.

"Traditional" engine control consisted essentially in inverting those maps to find the engine inputs (the setpoints of engine actuators) corresponding to the desired engine outputs at a given engine operating point:

$$U_{eng} = g(Y_{eng}, X_{eng}) \text{ with } \begin{cases} C_s = C_{s_{min}} \\ CO, HC, NO_x \leq S \end{cases}$$

The actuator setpoints thus calculated are "optimal" for the operating conditions at which the engine maps entries were identified, and had to be corrected with respect to current engine operating conditions, represented by intake manifold temperature and pressure measurements. Beside this static correction, PI or PID controllers had to used to compensate for having neglected dynamic behavior in the relationship linking U_{eng} and X_{eng} to Y_{eng}. An example of this approach is given in Figure 1.4, where the "traditional" way of controlling injection time is shown.

The former engine control structures offered limited possibilities for optimization of engine operation, were difficult to calibrate and inherently non-modular. In modern engine control, a hierarchical torque structure is adopted instead, which heavily relies on knowledge-based or black-box dynamic models, observers and intermediate feedback controllers to correct errors with respect to available measurements. Though look-up tables are still used, most of them are related to physical characteristics of the system: volumetric efficiency, effective throttle area, and so on. An example, of how injection time is controlled in a modern spark-ignition engine management system is given in Figure 1.5

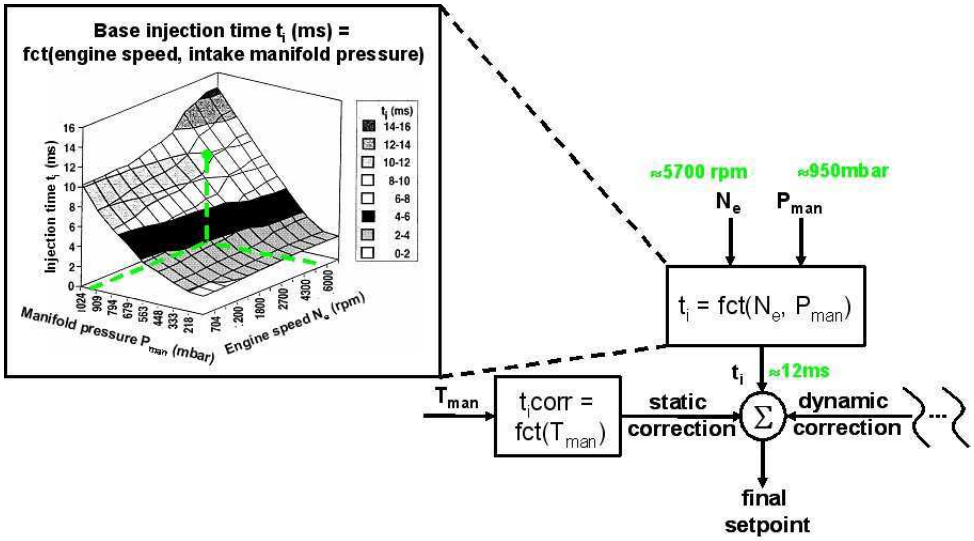

Figure 1.4: Control of injection time in early engine management systems

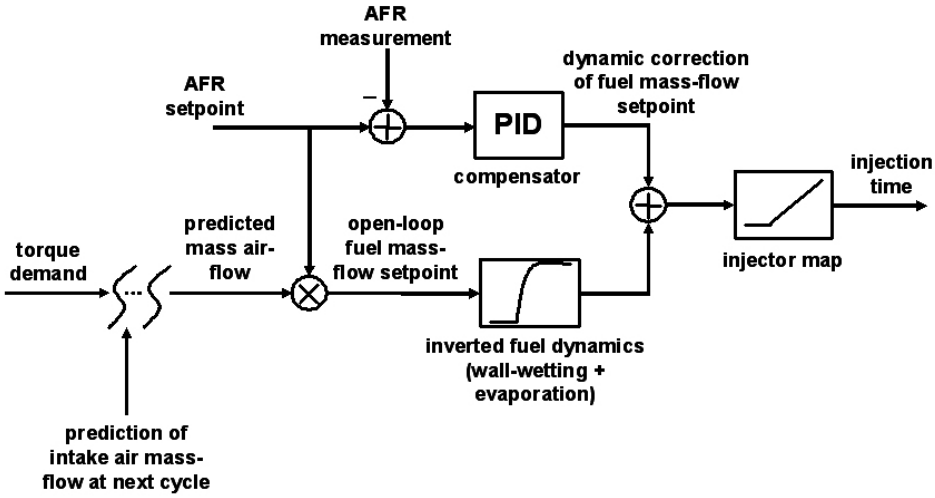

Figure 1.5: Control of injection time in modern engine management systems

The success of the hierarchical structure is also strongly related to the possibility of ensuring torque coordination between engine and powertrain subsystems. This possibility is very important, as it is clarified further in section 1.3.

1.2.3 Transmission

Over the years, several types of transmissions have been developed and proposed in automotive industry. The main challenge in the development has been to ensure high efficiency in the transmission engine torque to wheels. Other important aspects to be taken into consideration are manufacturing costs and complexity. The most commonly used transmissions are (adapted from Wagner (2001)):

Manual Transmission, MT.
The earliest development and the most common transmission for light-duty vehicles outside the United States, popular for its high efficiency, low weight and low cost. A dry clutch is used to couple and decouple progressively the engine to and from the rest of the transmission, and a gearbox with a finite number of gear ratios is used to transform speeds and torques. The driver controls directly the clutch and gearbox actuators, through a clutch pedal and a gearshift stick. Any gear shifting requires a total opening of the transmission: first, the clutch must be opened and then a new gear can be engaged. This operating mode generates a discomfort because of the discontinuity in torque transmission.

Automatic Transmission, AT.
This transmission, which has equipped most cars sold in the United States since the 1950s, consists of a hydraulic torque converter and a planetary gear train. The gear shifting is done automatically without interruption of engine torque transmission, thus leading to cars that are easier to drive and with a higher level of comfort (compared to MT cars). Its major drawbacks from an industrial point of view are technological complexity, weight increase and manufacturing costs. Moreover, an automatic transmission is not as efficient as a manual transmission, which, in comparison, can provide a significant fuel economy when properly operated.

Continuously Variable Transmission, CVT.
In this transmission, the coupling system consists of rubber belt/variable pulley or chains, which enable to get an infinite number of effective gear ratios. This system allows the engine to be operated at the most efficient operating points, thus yielding lesser fuel consumption than AT. Its driving comfort is comparable to the comfort of automatic transmissions. Its main drawbacks are: the generated noises and the dependency on the strength between the torque source and the transmission medium. The latter point is a limiting factor in low-powered cars and more generally in light-duty applications.

Automated Manual Transmission, AMT.
Conceptually, an automated manual transmission is just an advanced *drive-by-wire* manual transmission, in which the embedded control strategies control clutch and gearbox actuators to perform maneuvers such as vehicle start-up from still and gear shifting. Vehicles equipped with AMT are easier to drive than conventional MT vehicles: there is no clutch pedal and in some models the gear shifting decision can be also automated (in this case, the term *Automated Shift Transmission*, AST, applies). However, there still is a torque discontinuity during gear shifting resulting in a lower level of comfort compared to conventional AT. Despite this limitation, this transmission is competitive since its cost and hardware

complexity are comparable to those of traditional manual transmission. Moreover, if the embedded control strategies are efficient enough, it can also provide significant fuel savings.

Dual-Clutch Transmission, DCT.
Dual-clutch (or twin-clutch) transmission is an old technology (patented in 1939 by Adolphe Kégresse) being rediscovered nowadays, as it potentially combines the efficiency and the limited cost of an AMT, with the comfort of a conventional AT. This transmission is basically an AMT with two clutches and two separate sets of gears (odd/even) available. When a gearshift request arrives, torque transmission with the new (preselected) gear ratio is obtained by progressively disengaging one clutch and engaging the other one at the same time. Gearshifts can be carried out without torque interruption, provided that efficient control strategies have been implemented.

Table1.1, adapted from (Matias et al. (2001)) and updated, compares the different transmissions presented so far, using the manual transmission as a reference. Dual-clutch AMT seems to offer the best trade-off and can be considered as the most promising transmission concept nowadays. Notice that with computer-controlled transmissions, fuel consumption, performances and comfort strongly depend on the quality of the embedded control strategies.

	Cost	**Weight**	**Fuel consumption**	**Performances**	**Comfort**
MT	0	0	0	0	0
AT	- - -	- - -	-	-	+++
CVT	- - -	- - -	0	0	+++
AMT	-	-	+	0	0
AST	-	-	0 to +	0 to +	0 to +
DCT	- -	- -	0 to +	0 to +	++ to +++

Table 1.1: An exhaustive comparaison between different types of transmissions referring to the manual transmission as a reference.

With manual and automated manual transmission systems, studied in this thesis, vehicle propulsion stems from combined actions on the engine, which provides the necessary torque, on the clutch, which decouples the engine from the rest of the driveline and transmits its couple progressively when required, and the gearbox which maps engine torque into the appropriate wheel torque. A closer look at these transmission components is then required.

1.2.3a Clutch

A clutch is a mechanical device for transmitting rotational movement. In general, it enables to connect two bodies or shafts rotating at different speeds. In vehicular systems, it is used to connect or disconnect the transmission from the engine. During the connecting process, known as *clutch engagement*, engine torque is progressively transmitted to the transmission through the friction forces applied to the rotating surfaces of the clutch (clutch disks or plates). The amount of the transmitted torque is controlled through the clutch bearing position (see Figure 1.6). In manual transmission, this position is set by the driver via the clutch pedal, directly or via an electric or electro-hydraulic servomechanism, whereas in automated manual transmissions the servo-actuated position is set by the embedded control strategies.

Though many clutch designs are available, the most common are based on one or more friction disks pressed against the flywheel using springs. Thus, the first half of the clutch rotates with the crankshaft, at engine speed, and the second half rotates with the main-shaft or primary

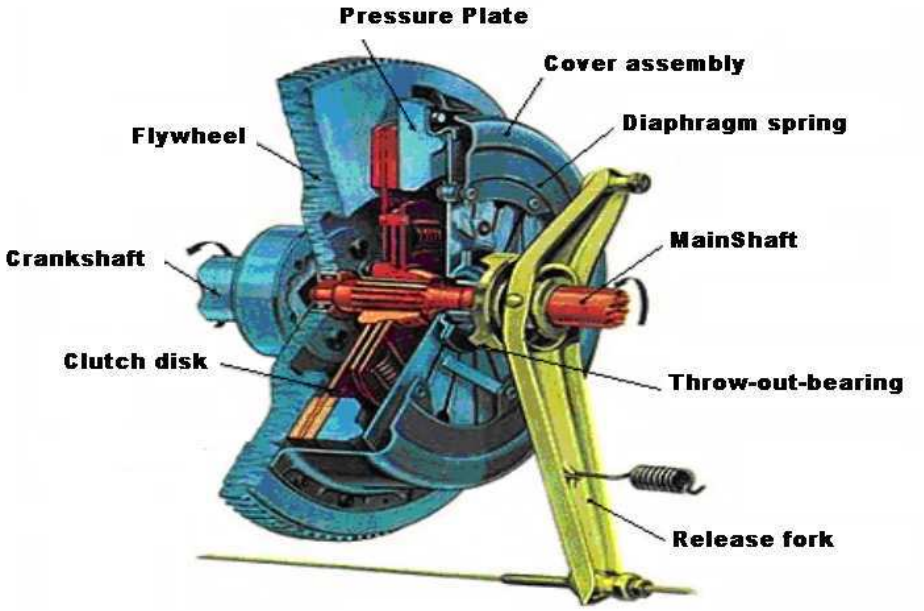

Figure 1.6: Dry clutch system: typical architecture with the main components.

shaft entering the gearbox. Since transmissibility of engine torque is obtained through friction, one clutch disk is covered with a high-friction material. During the engagement process, the clutch bearing position enables to control the contact surface included between the clutch disks and thus the transmitted torque. At the end of the engagement process, the two shafts will be locked together and spin at the same speed, while the friction forces will be null. The control strategies or the driver should manage to limit the duration of the engagement, to avoid clutch wear while trying to get a smooth clutch engagement, to avoid oscillations. Chattering is in part limited by design, via the inclusion of damper springs.

Conceptually, the clutch mechanism is designed as an *inverted controlled device*. That is, when the control input is null, the clutch is in a closed position. A non null control input is required to open the clutch (to counteract the diaphragm spring). This operating concept enables to minimize the control effort since the closed position is supposed to be the standard clutch position. In this case, the clutch transmits totally the net engine torque available on the engine shaft to the transmission. It is noticeable to say that the clutch has a protecting effect on the transmission when there is important peak on the engine torque. If this case appears, the clutch disks should slip to dissipate this torque excess as heat. Each clutch has its maximum admissible torque which is guaranteed by the producing factory.

Clutch operating modes. Assuming that the torque being applied on the engine shaft does not exceed the maximum admissible torque, three main states can be defined for the clutch: *opened*, *closed*, *slipping*. When the clutch is (fully) opened no torque is transmitted and the speeds of the two parts (shafts) evolve independently. When it is (fully) closed, the whole engine torque is transmitted and the two speeds are equal. When the two disks are in contact and slip, only a fraction of engine torque is transmitted.

When considering a servo-actuated clutch, it is convenient, from a (driver's or automatic) control point of view, to distinguish the slipping phase during clutch opening from the slipping

phase during clutch closing. Indeed, the former is generally much faster than the latter, and definitely less problematic. It is important to consider separately the phase at the beginning of clutch closing when the two disks are approaching but not in contact yet. This phase ends when the clutch bearing is positioned at the *torque transmitting point*, corresponding to the first contact between the two clutch disks.

To summarize, for control purposes we should consider five clutch operating phases (or modes), the closed position being naturally the first state since, as noted before, the clutch is an *inverted controlled device*:

- **Closed**
  Engine torque is fully transmitted from the engine shaft to the main-shaft, rotating at the same speed.
- **Slipping opening**
  Clutch disengagement disconnects the engine shaft from the main-shaft. This is generally a fast manoeuver.
- **Opened**
  Engine shaft is completely disconnected from the main-shaft and no engine torque is transmitted.
- **Prepositioning**
  The throw-out bearing is set from the position corresponding to a fully open clutch to the limit at which the clutch disks start to be in contact. No torque is transmitted yet.
- **Slipping closing**
  In this mode, the engine torque begins to be transmitted progressively to the transmission. Torque transmission is controlled via the throw-out bearing position, but depends on many other factors, and in particular on the slip speed (i.e. the difference between engine speed and main-shaft speed. When this speed becomes null, all engine torque is transmitted and the clutch goes again to the closed position. This is the most delicate clutch operating phase.

Notice that the dynamic behavior of the powertrain during each phase will depend on the state of the gearbox downstream in the driveline.

1.2.3b Gearbox

As explained before, when the motor of a powertrain is an internal combustion engine, a gearbox is needed to adapt its narrow speed range to the much wider range of wheel (and vehicle) speed. The total (reduction) ratio from engine to wheels cannot be a fixed one because of the torque-speed characteristics of the engine and of the torque-speed requirements at wheels. Most manual transmissions and automated manual transmissions provide five or six discrete ratios for forward propulsion in their gearboxes, called *gear ratios* or *gear numbers*, plus one rear gear. The first gear ratio has the largest value, to obtain high wheel torque at low speed and to enable moving heavy loads. The last gear ratio has the smallest value, which might even be lesser than unity (not a *reduction* ratio anymore, then), to cover the high speed range where smaller torque is required.

Figure 1.7 shows a typical configuration of manual transmission gearbox. The gear selector fork enables to combine pinions available on the main-shaft (layshaft) with the suitable one available on the secondary shaft, and this according to the selected gear number. Modern gearboxes

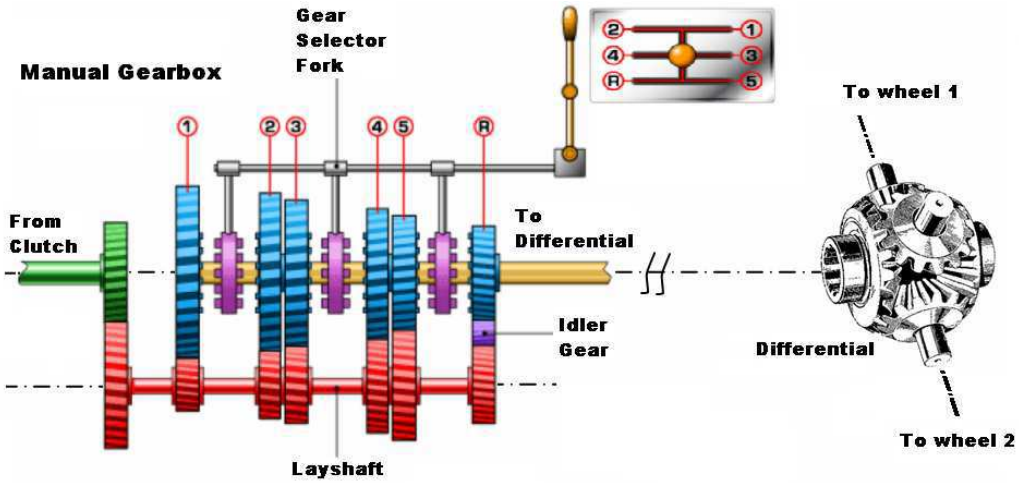

Figure 1.7: Manual Transmission: five gear gearbox

are equipped with synchronizers, which are protecting devices that smoothen the disengagement of the old gear and the engagement of the new one and prevent gear-shifting when the difference between the rotating speeds is too high. They operate similarly to dry clutches, generally over a shorter time horizon.

Gearbox operating modes. Similarly to the clutch case, gearbox operating modes define the connection between the two rotating shafts:

- i^{th} **gear engaged**
  The main-shaft is connected to the secondary shaft, which rotates at speed $\omega_g = \omega_c/i_g$, where ω_c is the main-shaft speed and i_g the gear-ratio corresponding to gear i. Assuming 100% efficiency (95% is a more realistic figure) the torque on the secondary shaft side will be $T_g = T_c \cdot i_g$, where T_g is the torque on the main-shaft side.

- **Neutral gear engaged**
  The main-shaft is disconnected to the secondary shaft and no torque is transmitted.

- **Synchronization**
  This phase corresponds to the passage from the current gear to the new one. It is controlled by the gear selector and the synchronizer actuators.

Notice that there is one important transmission component yet between the gearbox and the wheels: the differential. The differential is mechanical device which ensures a split of the mechanical power that comes from the gearbox into two paths leading to the left and right (front or rear) wheels. Drive-shafts realize the mechanical links. In rear traction, the differential is situated between the two rear wheels, and is linked to the secondary shaft through a long drive-shaft (assuming the engine is frontal position). Whereas in front traction, the differential is directly connected to the gearbox. In four-wheel propulsion, the left and the right part of the differential are related to two other differentials which ensure front and rear propulsion. Conceptually, the differential consists on an epicycloidal train that enables the engine torque to be divided beside the differential. Generally, the left and the right shafts are rotating at two different speeds. In some situation, the transmitted torque on one shaft can be null, and this leads to an unsuitable null torque on the other shaft. In this case, a braking mechanism is supposed to block the differential. In this context three main technologies have been developed in automotive industry. The first concept uses friction disks to dissipate the power, whereas the second concept assumes

viscous dissipation. The third concept is the Torsen differential, which dissipates power just on the less efficient side.

The differential is not actively controlled by the driver nor by AMT control strategies. Its reduction ratio, the differential ratio i_d is constant for a given powertrain. Multiplied by the current gear ratio i_g, it will give the total transmission ratio between the main-shaft (and the crankshaft, when the clutch is closed) and the wheels.

1.2.4 Transmission Control

1.2.4a Clutch Control

In traditional manual transmissions, the throw-out bearing, which ultimately determines the state of the clutch and torque transmission through it, is directly linked to the clutch pedal (through a wire, as shown in Figure 1.6). In modern vehicles, the general trend toward "X-by-wire" leads to a system where the clutch pedal is just an input device (a "joystick") whose position is interpreted as a set-point for a low level servo controlling the throw-out bearing position. The throw-out bearing actuator is generally a piston connected to an electro-hydraulic circuit. In some cases, for small vehicles where the maximum admissible torque is not very high, a simple DC/DC motor can be used instead.

Automated manual transmissions also rely on a servo-actuated clutch. However, in this case there is no clutch pedal at all, and the throw-out bearing position set-point is manipulated by higher level control strategies. These strategies are hosted directly in the Engine Control Unit, or in a special Transmission Control Unit (TCU), while the clutch servo code is usually embedded in a dedicated control unit.

1.2.4b Gearbox Control

In traditional manual transmissions, the gear selector fork is mechanically linked to the gear stick. Analogously to the "clutching-by-wire" case, modern vehicles often offer a "gear-shifting-by-wire" systems where both gear selection and gear engagement and disengagement are servo-actuated with trajectories determined by the gear stick position. In most pieces of design, there is a separate actuator for gear selection and for synchronization. Both electric actuation and electro-hydraulic actuation are possible.

Needless to say, automated manual transmissions rely on a servo-actuated gearbox. There still is a gear stick, used in this case to inform the control system of the driver's will to perform a whole gear shifting process, which involves operations on both the clutch and the gearbox. The gearbox servo code is usually embedded in a dedicated control unit, while the gear shifting strategies are hosted directly in a special module of the Engine Control Unit, or in a full-fledged Transmission Control Unit.

1.3 Powertrain Control

1.3.1 Automotive Control Standards

The first attempt at an industry standard for distributed control units in vehicles was OSEK, founded in 1993 by a German automotive company consortium (BMW, Robert Bosch GmbH,

DaimlerChrysler, Opel, Siemens, and Volkswagen Group) and the University of Karlsruhe. OSEK is an abbreviation for "*Offene Systeme und deren Schnittstellen für die Elektronik im Kraftfahrzeug*" (Open Systems and the Corresponding Interfaces for Automotive Electronics). In 1994, OSEK was merged with VDX (Vehicle Distributed eXecutive), a similar projet carried out by The French car manufacturers PSA and Renault, thus creating the joined standard OSEK/VDK.

The open architecture introduced by OSEK/VDX comprises three application-independent areas (Abou et al. (2002)):

- Communication (data exchange within and between control units);
- Operating System (real-time execution of ECU software and base for the other OSEK/VDX modules);
- Network Management (Configuration determination and monitoring).

In principle, OSEK/VDX system should allow to easily integrate pieces of software or hardware that come from different manufacturers. This system manages the synchronization between different tasks which are implemented in different separated processors (modules) independently on the media and protocols. Under OSEK/VDX, an Engine Control Unit (ECU) developed by an OEM, should be able, for instance, to interact with a Transmission Control Unit (TCU) developed by another OEM.

The OSEK/VDK effort has been superseded by AUTOSAR (Automotive Open System Architecture), an open and standardized automotive software architecture, developed since 2003 by a larger consortium of automobile manufacturers, suppliers and tool developers. The professed goals are modularity, scalability, transferability and re-usability of functions to provide a standardized platform for automotive systems. This should enable system wide configuration and optimization to meet runtime requirements of automotive devices. Many of the low-level components of AUTOSAR (the real time operating system and communications layer) are derived from OSEK work.

AUTOSAR is meant to be an enabling technology to manage the growing automotive electronics complexity and to facilitate the exchange and update of software and hardware over the service life of the vehicle. AUTOSAR software architecture supports a component-based design model, in the attempt to create a paradigm shift in automotive software development from an ECU-based approach to a function-based approach.

Unfortunately, AUTOSAR is still far from being an universally adopted standard, since it raises concerns on various issues. Efficiency, for instance: the more complete the AUTOSAR implementation is, the higher the ECU resource demands are, especially in terms memory footprint and computing power. Timing is also an issue, as its meta-model lacks information about timing requirements, to deal with problems such as buffer-overflow or missed deadlines.

The result is that software "plug-and-play" compatibility seems to be as unrealistic as ever, and that automobile manufacturers, suppliers and tool developers mostly still follow their own standards for control software development.

To conclude this brief overview on automotive control standards, let us recall that there exist several communication protocols designed to allow microcontrollers and devices to communicate with each other within a vehicle. The most popular is certainly the message-based CAN (Controller Area Network) protocol, designed by Bosch and available since the end of the '80s. In

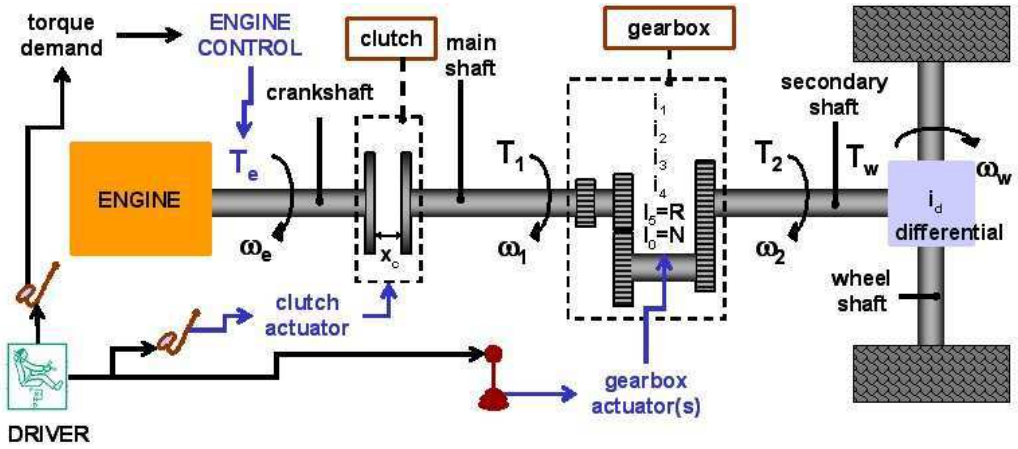

Figure 1.8: A manual transmission powertrain

particular, one of the CAN physical layer standards, the ISO 11898-2, is the most used physical layer in car powertrain applications. In a future, it could be widely replaced by FlexRay, a new automotive network communications protocol, designed to be faster and more reliable than CAN. At the moment, since it is also more expensive, only few high-end series production vehicles utilize FlexRay.

1.3.2 Powertrain Control for MT Vehicles

Even in a standard manual transmission powertrain, such as the one shown in Figure 1.8, the role of an engine management systems goes beyond the simple control of the engine component.

In fact, its main task is to make the engine produce torque to be delivered to the transmission in order to enable vehicle propulsion:

- in response to driver's requests;
- under several constraints (drivability, consumption, emissions).

A typical hierarchical torque control structure of an engine management system for a manual-transmission powertrain equipped with a spark-ignition engine is shown in Figure 1.9. Such structure has been investigated since the early nineties (Streib & Leonhard (1992)) and is now standard (Livshiz et al. (2004)).

In normal driving conditions, the propulsion demand expressed by the driver via the accelerator pedal position is usually translated into a torque (or power) setpoint at wheel level, then in a net engine torque setpoint depending on the gear ratio engaged, transmitted by the *Vehicle manager*, to the lower *Engine manager* layer. The latter computes the actual torque that is to be realized by the engine to compensate for internal friction and pumping loss on one hand, and to supply power to the auxiliaries (car lights, electric windows, radio, air conditioning, and so on) on the other hand. The torque setpoint is translated into low level actuator setpoints (throttle position, injection time, spark advance, an so on) by specific modules for the *air path*, the *injection path* and the *ignition path*. Let us recall that the requested engine torque is essentially realized by controlling the throttle position, with the injection time being controlled by a slave control system which regulates the air-fuel ratio at its setpoint (generally around 1). Because of the intake manifold dynamics, engine provides the requested torque only after a certain lag when acting on the air throttle. Faster torque actuation for transients can be obtained via a

degradation of the spark advance, but only for a limited time and limited torque variations. Let us also notice that, for cost reasons, in most vehicles, there is no feedback on the actual torque provided by the engine to the mainshaft or the wheels.

It is very important to underline that even in the simplest of powertrains, the engine management system must generate engine torque setpoints taking into account how engine torque is transmitted to wheels, considering:

- the state of the transmission defined by
  - the clutch (open, closed or slipping) and
  - the gearbox (synchronizing, gear engaged, neutral);
- the driveline dynamics:
  - inertia, torsion, damping of components;
  - backlash
  - frictions clutch, synchronizers, tire-road).

In a standard engine management system, the *engine manager* is a finite state machine which defines the current engine state and generates the engine torque setpoint according to it. Engine states are usually defined as follows:

- **Engine stopped**:
  The engine is stopped.
- **Engine start-up**:
  When the driver turns the key, the crankshaft shaft is driven from rest to a nominal speed value (generally $Ne \leq 400rpm$. Then, after a synchronization to TDC, torque setpoints are applied in open-loop to start the combustion and rise engine speed to values suitable for idle mode.

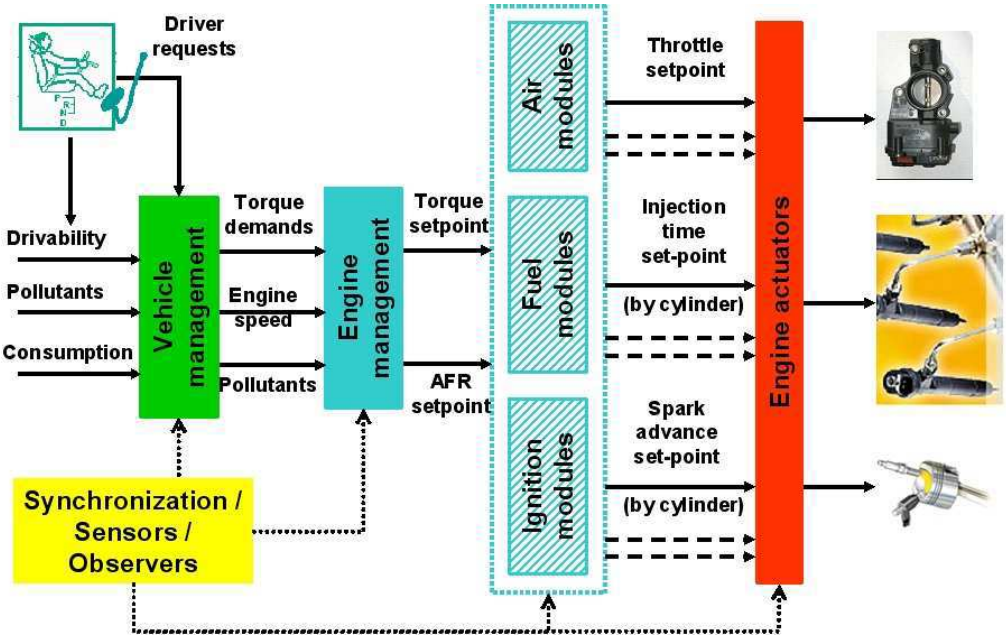

Figure 1.9: Hierarchical torque control structure of an engine management system for a manual-transmission powertrain equipped with a spark-ignition engine

- **Idle mode**:
  Engine speed is regulated in closed-loop around a given setpoint. When the transmission is open, the engine produces just enough torque to match friction and pumping losses plus the power required by the auxiliaries. Assuming that the vehicle is at rest and the driver has opened the clutch and engages the first gear this is the mode in which a vehicle start-up begins. Notice that, if the clutch only is used to start the vehicle, the engine remains in idle mode. However a slightly different idle mode should be defined for the transmission-closed configuration. In this case the idle mode must supply additional torque to provide a minimal vehicle propulsion (not defined by the driver).

- **Pedal mode**:
  The natural mode for vehicle propulsion, activated whenever the driver presses the accelerator pedal. With the clutch is completely closed and a gear engaged, the engine is controlled in open-loop mode, using a torque setpoint generated by some defined look-up table according to the accelerator pedal position and powertrain conditions (for instance, engine speed and/or engaged gear number).

- **Cut-off mode**:
  Fuel injection is stopped when the driver releases the accelerator pedal. The engine goes to idle mode.

The more advanced the manual transmission vehicle is, the more complex the engine manager becomes, in order to implement more sophisticated powertrain control functions such as cruise control or anti-jerk control.

An example of such an engine manager is given in Figure 1.10. The "Force Tracking" state correspond to a static pedal mode, while the "Force Transient" states take care of fast pedal

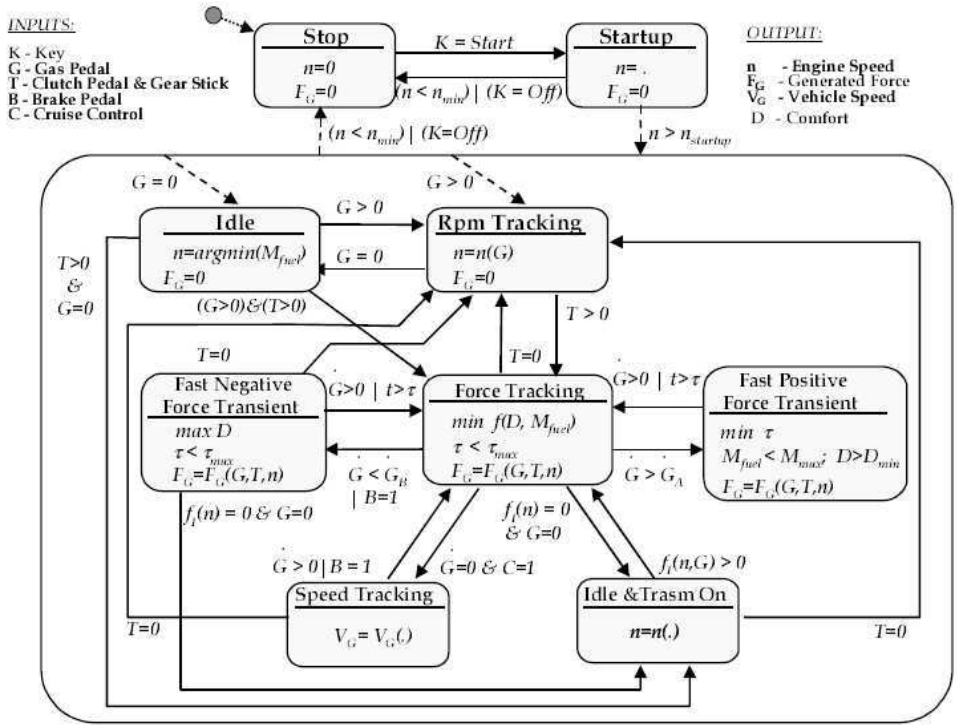

Figure 1.10: An advanced engine manager for a manual transmission vehicle (from Antoniotti et al. (1998))

actions (*tip-ins* and *tip-outs*). A "Speed Tracking" state is added to implement cruise control.

Furthermore, when the vehicle hosts technologies like ABS (*Anti-lock Braking System*) or ESP (*Electronic Stability Program*), a *dynamic coordination* module is required at the vehicle manager layer to ensure that the control of longitudinal dynamics interacts correctly with the other vehicle dynamics. It can be concluded that modern manual transmission vehicles need a true *powertrain* manager in their engine management system.

1.3.3 Powertrain Control for AMT Vehicles

In a vehicle equipped with an automatic manual transmission (see Figure 1.11), actions on transmission actuators are decided and performed by embedded control strategies.

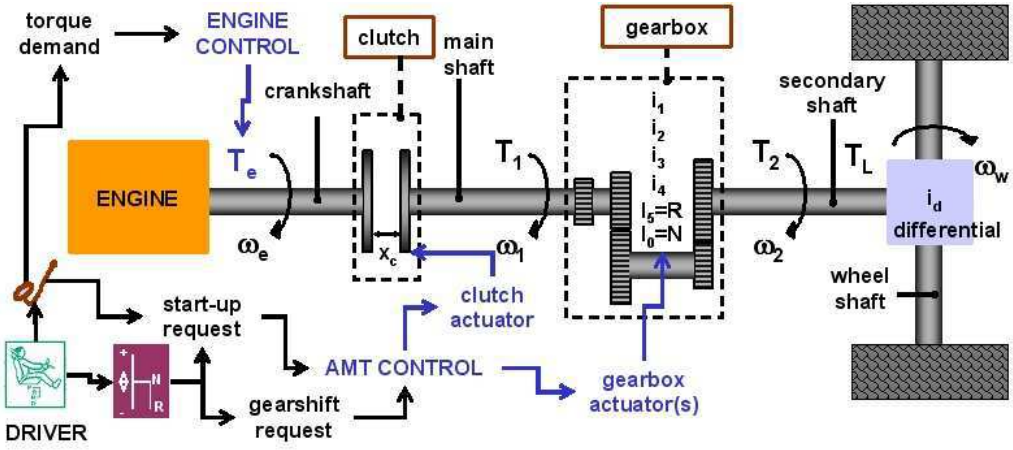

Figure 1.11: An AMT powertrain

A transmission management module, controlling the behavior of the clutch and the gearbox, must interact with the engine manager to coordinate engine and transmission actions in maneuvers such as vehicle start-up and gearshifts. Those maneuvers are performed on driver's request: vehicle start-up is initiated by pressing the accelerator pedal, when the gearshift lever is in a specific position (*standby*), and gearshifts are performed by tipping the gearshift lever. Notice that there are other possible actions which do not depend on an explicit driver's request, such as opening the clutch and downshift to first gear when the vehicle is halted. There are no standards yet for designing control software for a vehicle with an AMT powertrain. A possible structure, shown in Figure 1.12, can be obtained extending the standard engine torque control structure. The actual implementation of this structure depends on the electronic control unit configuration. The different modules could be distributed across several ECUs.

The coordination between transmission and engine control modules is best performed by a *powertrain manager*, at the vehicle manager level. For this thesis, we have considered a powertrain manager structured as shown in Figure 1.13. Beside the states we usually find in an engine manager, it includes two states dedicated to the control of AMT manoeuvres:

- **Vehicle start-up** (*Vehicle_StartUp*):
  When the driver presses the accelerator pedal (start-up request), the transmission is progressively closed by controlling the engine torque and the torque transmitted by the clutch.
- **Gearshift** (*Gearshift*):
  This phase is activated by a request to engage a new gear from the driver, via the gearshift

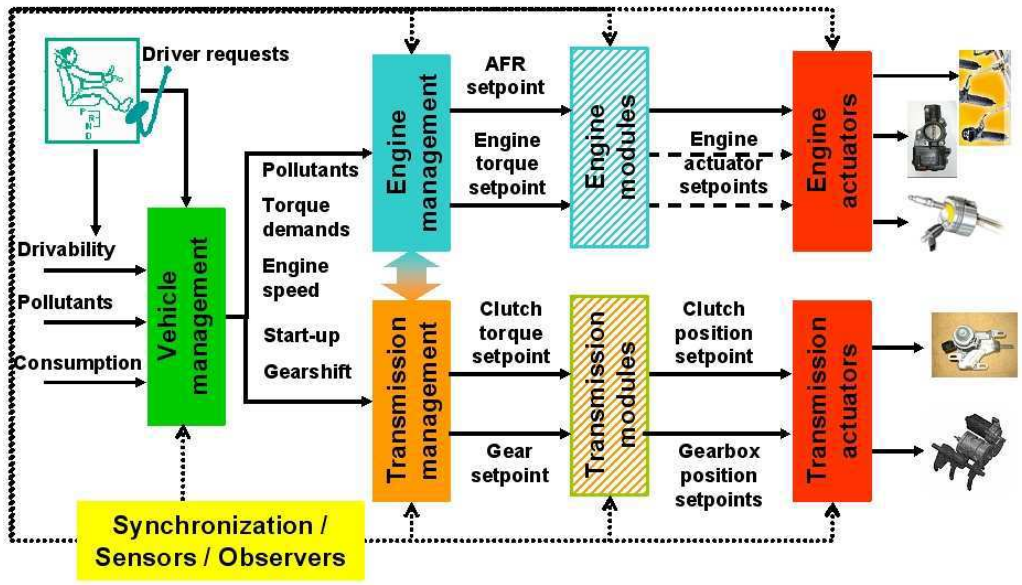

Figure 1.12: Possible hierarchical torque control structure of a *powertrain* management system for an AMT powertrain equipped with a spark-ignition engine

lever, or from the detection of particular powertrain conditions requiring a forced downshift. The gearshift mode includes sub-states to handle upshifts and downshifts separately (and also passages to neutral gear). Those sub-states further include the execution of the following steps:

- complete opening of the clutch;
- engagement of a new gear (synchronization);
- control of engine speed and of the clutch engagement.

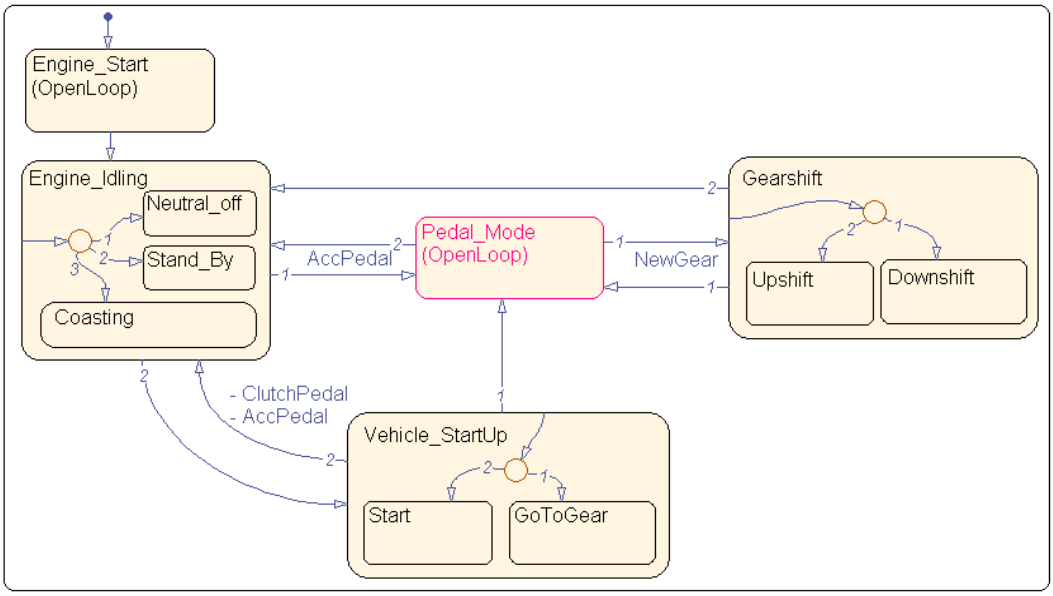

Figure 1.13: Powertrain manager for an AMT vehicle

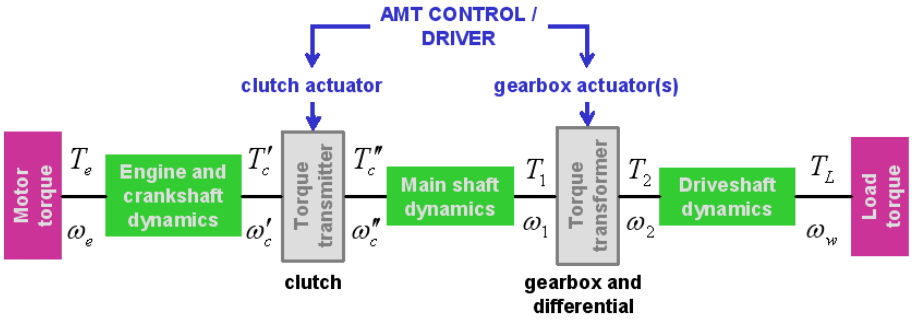

Figure 1.14: Conceptual sketch of the powertrain under investigation

The actual structure of the finite state machine corresponding to these two states depends on the characteristics of the control strategy chosen for each manoeuvre.

1.4 Powertrain Modeling for Control

A conceptual sketch of the class of powertrains we consider in this thesis is represented in Figure1.14. The motor torque is produced by an internal combustion engine, which can be assisted, to consider a more general case, by an electric motor in parallel. The (dry) clutch smoothly connects the flywheel to the main shaft, rotating at different speeds, thus allowing the transmission of (net) motor torque to the wheels. The role of the gearbox is to extend secondary shaft (and wheel shaft) speed range from the limited range of engine speeds to the larger range of possible vehicle speeds, transforming speed and torque through gear ratios.

The configuration of this kind of powertrain depends on direct drivers' actions on it or on driver's requests to the embedded control systems. Depending on inputs such as the accelerator pedal position, the clutch bearing position, and the gear lever position, the powertrain will reconfigure in one of a set of possible operating modes. It is quite natural to assimilate its operation to that of a hybrid system, that is a system mixing discrete-event dynamics and continuous-time dynamics, as suggested in (Garofalo et al. (2001), Glielmo et al. (2004, 2006)) or (Bemporad et al. (2001)), for the particular case of AMT powertrains. The discrete-event part is associated to the different states the clutch and the gearbox can be in. As explained in section 1.2.3a, the clutch can be disengaged (or fully open), with zero torque transmitted to the main shaft, engaged (or fully closed), with the engine torque completely transmitted to the main shaft, or in an intermediate state, with the clutch disk slipping before complete engagement or disengagement. As to the gearbox, different states correspond to different gear ratios (including neutral). A further state corresponds to the synchronization phase before the engagement of a new gear ratio. The continuous-time part takes in rotational dynamics of the different shafts.

A sensible approach consists in lumping driveline parts that rotate together when the clutch and the gearbox interrupt torque transmission. With respect to Figure 1.14, we can distinguish, from engine (plus motor eventually) to wheels: engine and flywheel dynamics, main shaft dynamics including the parts of clutch and gearbox rotating with it, and the dynamics of the rotating parts comprised between the gearbox parts on the secondary (or transmission) shaft side and the wheels. The next issue is how to characterize each dynamics in terms of moment of inertia, torsion, damping. It can be interesting to take into account flexibility in both the main shaft and the drive shaft (Glielmo et al. (2004)), at least for simulation purposes, or to introduce modeling terms for tire friction forces (Dolcini et al. (2005)) or backlash effects in the gearbox.

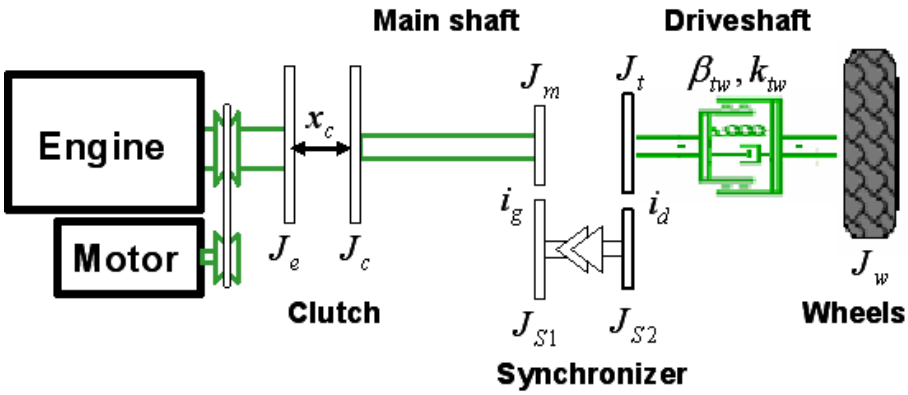

Figure 1.15: Main components of the powertrain system.

However, since too complex models are seldom suitable for control design, the most common choice encountered in the literature for powertrain control consists in simplifying the system by considering the mainshaft rigid (Glielmo et al. (2006)).

Hereafter, we present a torque-based modeling of the powertrain according to the hybrid operating phases and the simplifications on dynamics described above, represented in Figure 1.15

1.4.0a Clutch Slipping Mode Model

The clutch slipping phase is the most complex of powertrain operating modes, and the most important for control purposes both for vehicle start-up and gear shifting. The model presented here expresses relations between the accelerations of the rotating bodies and the available torques on the rotating shafts obtained by applying Lagrange–d'Alembert principle and the simplification suggested in (Glielmo et al. (2006)), with an equivalent shaft between the clutch and the wheels. This enables to derive the following fourth order model for the powertrain system, valid for the clutch slipping phases vehicle start-up and gearshifts:

$$J_e\dot{\omega}_e = T_{comb} - T_{frict}(\omega_e, .) + T_{elect} - sign(\omega_{sl}) \cdot T_c\,(x_c, .) \tag{1.1a}$$

$$\left[J_c + J_{eq}\,(i_g, i_d)\right]\dot{\omega}_c = sign(\omega_{sl}) \cdot T_c\,(x_c, .) - \frac{1}{i_g\ i_d}\left[k_{tw}\,\theta_{cw} + \beta_{tw}\left(\frac{\omega_c}{i_g\ i_d} - \omega_w\right)\right] \tag{1.1b}$$

$$J_w\dot{\omega}_w = k_{tw}\theta_{cw} + \beta_{tw}\left(\frac{\omega_c}{i_g\ i_d} - \omega_w\right) - T_L\,(\omega_w, .) \tag{1.1c}$$

$$\dot{\theta}_{cw} = \frac{\omega_c}{i_g\ i_d} - \omega_w \tag{1.1d}$$

where :

- J are inertia, T torques, ω and θ angular speeds and positions;
- the subscripts e, c, m, t, w, $comb$, $frict$, $elect$ denote engine, clutch, main-shaft, transmission, wheels, combustion, friction, and electric respectively;
- x_c is the position of the clutch (throw-out bearing);
- k and β are elasticity and friction coefficients, respectively;

- i_g is the gear ratio and i_d is the differential ratio;
- J_{eq} is the equivalent inertia of the transmission (main-shaft, synchronizer and driveshaft) given by:
$$J_{eq}(i_g, i_d) = J_m + \frac{1}{i_g^2}\left(J_{S_1} + J_{S_2} + \frac{J_t}{i_d^2}\right)$$
- $\omega_{sl} = \omega_e - \omega_c$ is a slipping speed between the engine and the clutch;
- $\theta_{cw} = \theta_c - \theta_w$;
- T_L is the load torque which depends on aerodynamic resistance, tire–road frictions, and road grade.

The combustion torque T_{comb} represents the main manipulated (control) variable in this system. Following a MVEM (mean-engine value modeling) approach we are only interested in its mean value during a cycle (or a segment), since in-cycle variations have little relevance for the control problems studied in this thesis. Assuming a spark-ignition engine and stoichiometric operation, T_{comb} is directly linked to the quantity of air injected in the engine at each cycle, as a consequence of the pressure attained in the manifold or the air flowing through the throttle valve. Through the throttle valve opening and other air-path actuators, the manifold pressure and/or the mass-air flow are regulated to some prescribed set-points calculated by the engine management system to satisfy driver's torque demands. In principle, T_{comb} should thus be equal to the engine torque set-point value generated at each cycle (or segment) by the engine management system. However, the response of the engine is not instantaneous (mainly because of the manifold dynamics), and the error between expected torque and produced torque cannot be compensated by feedback control (torque or in-cylinder pressure sensors are very rare in mass produced cars). These aspects must be taken into account for control design.

Engine friction torque T_{frict} acts as disturbance on the system. It can be estimated with some uncertainties via look-up tables, generally function of engine speed, manifold pressure and coolant temperature, characterized off line on an engine test bench. The electric torque T_{elect} is a manipulated variable in the case of a mild-hybrid (or a full parallel hybrid) powertrain were a starter-alternator or a full-fledged motor is available to provide traction or resistant torque. In the case of a conventional powertrain, T_{elect} is a disturbance variable corresponding to the resistant torque applied by the alternator to power vehicle auxiliaries. In both cases, if current measures are available its effective value can be estimated with less uncertainties than in the previous cases.

Concerning the clutch torque T_c, it represents a manipulated variable or a disturbance variable depending on the powertrain we focus on. T_c depends directly on x_c, the clutch bearing position, which is the true actuator, controlled by the driver or the AMT control system. But it also depends on many other variables and parameters in a very complex way. Some form of off-line characterization or on-line estimation is needed for control.

The load torque depends on the aerodynamic resistance and on the nature and conditions of the road. Though some form of estimation is possible, we will consider it as an unknown disturbance in the following.

1.4.0b Idle Mode Model

In this mode, a closed-loop control system regulates the engine speed, while the transmission is assumed to be completely opened or completely closed. The former situation occurs before every

vehicle start-up, while the latter may follow after a vehicle start-up or a gear-shift if the driver does not press the accelerator pedal and the engine speed is low.

The transmission-open case, where no engine torque is transmitted to the wheels, includes two different situations depending on whether the main shaft is rotating with the engine or not. When the clutch is completely opened, the engine rotates alone (with the flywheel, total inertia J_e), facing the friction and electric torques, namely:

$$J_e\dot{\omega}_e = T_{comb} - T_{frict}(\omega_e, .) + T_{elect} \tag{1.2}$$

When the clutch is completely closed and no gear is engaged (neutral position), the main shaft rotates together with the engine. In this case, the rotating system will have a new inertia J_{ec}, which is the total equivalent inertia of the coupled system engine–clutch–main shaft:

$$J_{ec}\dot{\omega}_e = T_{comb} - T_{frict}(\omega_e, .) + T_{elect} \tag{1.3}$$

Notice that, for idle speed control in a SI engine, fast variations of T_{elec} can be compensated by acting on spark advance, though at the expense of an increase in fuel consumption.

When both the clutch and the gearbox are engaged, the vehicle is in coasting mode. In this case, it is assumed that there is no actions on the accelerator pedal position, and the embedded control drives the engine to face the load torque:

$$J_e\dot{\omega}_e = T_{comb} - T_{frict}(\omega_e, .) + T_{elect} - \frac{1}{i_g\ i_d}\left[k_{tw}\,\theta_{ew} + \beta_{tw}\left(\frac{\omega_e}{i_g\ i_d} - \omega_w\right)\right] \tag{1.4a}$$

$$J_w\dot{\omega}_w = k_{tw}\theta_{ew} + \beta_{tw}\left(\frac{\omega_e}{i_g\ i_d} - \omega_w\right) - T_L\left(\omega_w, .\right) \tag{1.4b}$$

$$\dot{\theta}_{ew} = \frac{\omega_e}{i_g\ i_d} - \omega_w \tag{1.4c}$$

Remark 1.4.1.

A simplification of equation (1.4) can be considered by reporting the load torque to the engine shaft equation:

$$J_e\dot{\omega}_e = T_{comb} - T_{frict}(\omega_e, .) + T_{elect} - \tilde{T}_L(\omega_w, i_d, i_d, ..)$$

where: $\tilde{T}_L(.)$ is an equivalent load torque on the engine shaft.

1.4.0c Pedal Mode Model

This is the standard powertrain operating mode. To let the the driver control vehicle dynamics, the accelerator pedal position is converted to a torque demand that is to be realized by the engine (and eventually by the motor, in a hybrid vehicle):

$$J_{ew}\dot{\omega}_e = T^{OL}_{comb} - T_{frict}(\omega_e, .) + T_{elect} - T_L(\omega_w, i_d, i_d, ..) \tag{1.5}$$

This mode occurs naturally after vehicle start-up, and before and after gearshifts, provided that the drives presses the accelerator pedal.

1.4.0d Cut-off Mode Model

When the driver releases the accelerator pedal, the engine control system switches either to the idle mode, if the engine speed is close to the idle speed set-point or to cut-off mode otherwise. In the latter case, fuel injection is cut-off mode and combustion torque is null.

1.5 Drivability-related Powertrain Control Problems

In this thesis, we examine a set of drivability-related powertrain control problems involving vehicle longitudinal dynamics. Examples of such problems, extensively studied in automotive control, literature are cruise control and *anti-jerk control* (damping of powertrain oscillations generated by gas pedal tip-in and tip-out). We focus instead on vehicle start-up and gearshift control for an AMT powertrain and driver assistance during vehicle start-up for a manual transmission powertrain.

These problems are drivability related since an incorrect handling of the start-up and gearshift phases will directly impact driving comfort, together with fuel consumption and pollutant emissions, to a lesser extent. Driving comfort is defined via quantitative and qualitative evaluations. For a start-up, the main criteria to take into account are the engagement time (the time required for mainshaft speed to reach engine speed), the amplitude of the overshoot at engagement and of the oscillations of vehicle acceleration (*jerk*) after engagement. A target engagement time is to be obtained, while limiting the overshoot and avoiding oscillations, fulfilling the so-called *no-lurch* conditions on the powertrain. Engine must be also protected, avoiding stall (*no-kill* condition) and over-revolution, by keeping its speed inside acceptable limits. Since reference values for these criteria are application-dependent, to evaluate the performances of the strategies presented in this thesis we will try to make comparisons with pre-existing strategies, whenever possible. Similar consideration apply to the gearshift control problem, where the performance criteria are related to the engine speed overshoot at clutch disengagement, to the vehicle acceleration undershoot at clutch engagement, and to the duration of the gearshift and more particularly of the clutch engagement phase.

These problems have to be solved in the common framework described by Figure 1.16. Whether we refer to a manual transmission or to an automated manual transmission, the driver is always the master and the purpose is to ensure vehicle drivability subject to driver's requests. The nature of the transmission determines how the embedded control interacts with the driver. In manual transmissions, the driver controls completely the transmission and the driveline using the clutch pedal, the gearbox lever and the brake pedal and uses the accelerator pedal to control engine dynamics. In this context, the embedded control strategies can only *correct* driver actions to improve drivability. In automated manual transmissions, only the brake action is directly applied to the transmission, while the accelerator pedal and gearbox lever are only a mean of transmitting requests to the embedded control strategies. In this case, driving comfort depends much less on driving skills and must be guaranteed by the embedded control strategies, while ensuring a certain *transparency* between driver demands and vehicle dynamics. To resume, referring to Figure 1.16, and with respect to vehicle dynamics, the driver acts as master controller providing references to a slave controller (the embedded control strategies) or applying commands directly to the transmission.

It is important to stress that a viable solution to the above formulated problem (as to most drivability-related powertrain control problems) must meet a set of quite hard implementation constraints:

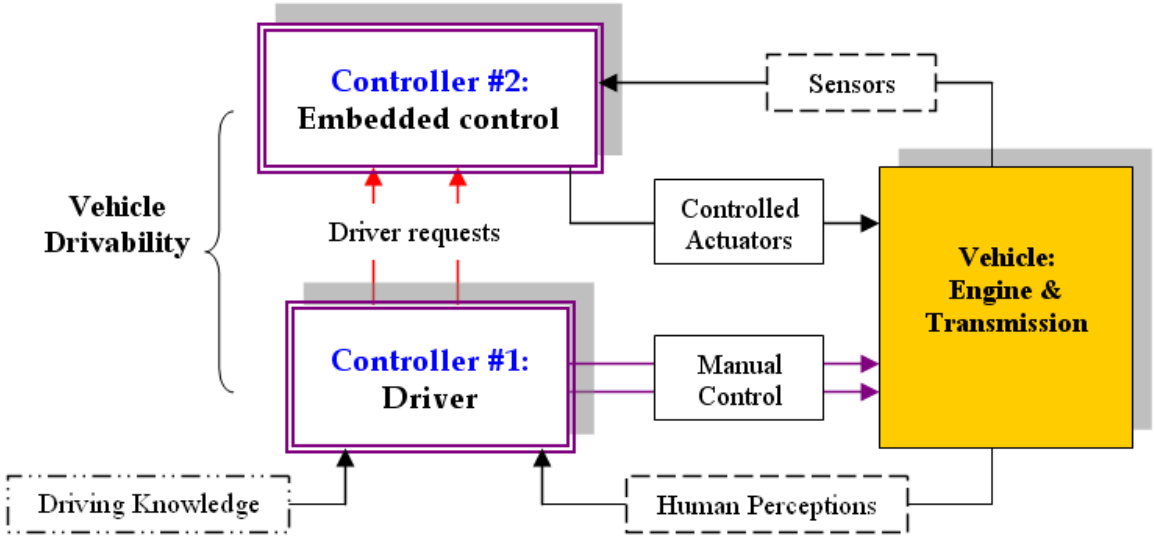

Figure 1.16: Hierarchical structure in control of vehicle longitudinal dynamics

- The dynamics to be controlled are (relatively) fast but the computation time is limited
- Engine torque is not measured
- Engine torque production is delayed and limited (at a given engine speed)
- Engine friction torque is assumed known through test bench mapping
- Engine control sample time is variable with speed
- Transmitted clutch torque is unknown
- Clutch characteristic is nonlinear, depends on many parameters (temperature, wear, ...)
- Torsional torques through transmission shafts are unknown
- The load torque is unknown (aerodynamic resistance, road grade)

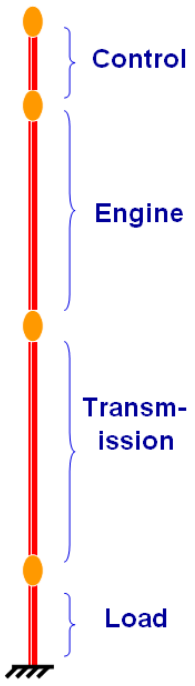

Demanding specifications and stringent constraints call for an effective and industrial–relevant control design methodology. For its ability to fine tune the trade-off between performance level and performance cost, the framework of model predictive control, that we introduce in the following section, seems to be the more natural answer, provided that an appropriate formulation, compatible with the computational and memory storage limitations of embedded electronic on-board systems, is found.

1.6 Predictive Control for Automotive Applications

1.6.1 Relevance of Model Predictive Control in Automotive Applications

Model Predictive Control (MPC) is an advanced control design methodology that gained a huge deal of interest over the three last decades. The basic idea of MPC is to solve, at each decision instant, an open-loop optimal control problem defined according to the current state of the system in order to come out with an optimal sequence of control actions. The first action of this optimal sequence is then applied to the system over the next sampling period. At the next decision instant, the state is updated (by measurement or using a state observer fed with the last measurements) and a new open-loop optimal control problem is solved to yield the new sequence of optimal actions. The first action in this new optimal sequence is applied to the system and the process continues leading to a state feedback. Indeed, the feedback nature of this strategy comes from the fact that the optimal control problem to be solved is defined with respect to the current state. Therefore the resulting sequence of optimal action does depend on the state, since the action to be applied to the system is exactly the first one in this optimal sequence, one clearly has a state feedback.

MPC control strategy has gained tremendous popularity during the last three decades. The reason for such a success lies in the ability of MPC to handle nonlinearities, coupling and constraints on both the control and the state of the system. Moreover, MPC offers a natural framework to specify *controlled* trade-off between the level of performance and the *price* involved to achieve it. This explains why this strategy has been first adopted in the chemical industry because of the security and specification related constraints that apply but also because of the huge gain one may obtain by achieving even few percentage of better performance.

There is however another reason that facilitates the use of MPC in chemical industry. Indeed, the computation of the optimal sequence at each decision instant is generally a quite involved task that needs an incompressible amount of computation time. The generally very high characteristic time of chemical processes made it possible to incorporate MPC-like strategy since quite a long time. Unlike chemical processes, electromechanical systems show characteristic times that may prevent the use of MPC strategies, at least in its nominal and standard form.

The research works on MPC during the 90's focused on the stability issues. A tremendous amount of works have been dedicated to get deeper understanding of the sufficient conditions an MPC formulation has to meet in order to guarantee the closed loop stability. These conditions involve all the *ingredients* used in the definition of the underlying optimal control problem, namely, the cost function, the constraints that may be added to the formulation in order to enforce feasibility and stability. All the related contributions have been put in a rather unified form in the seminal paper by Mayne et al. (2000) that practically closed this phase of theoretical investigations.

Since the beginning of the 21st century, researchers recognized that the theoretical formulations that have been proposed so far, while ensuring stability are rarely compatible with real-time requirements when electromechanical systems are considered. New formulations and implementation algorithms began to emerge that explicitly take into consideration the unavoidable fact according to which, optimization can scarcely be finished in within the sampling period.

The use of MPC in automotive control application falls in the very heart of this hot research topic. Indeed, automotive control problems necessarily involve constraints such as those related

to actuator saturations, safety operational regions, optimal operational regions and so on. Moreover, nowadays concerns about fuel consumption, pollution minimization to mention but a few examples put the concept of optimality in the center of the overall controlled systems evaluation and certification. If one adds the fact that optimal operation modes are more likely to be on the boundary of the admissible sets, it comes clearly that Model Predictive Control is not less than the *future of control design in the automotive industry*.

In the remainder of this chapter, the principle of Model Predictive Control is first recalled (section 1.6.2) together with a brief statement of the sufficient conditions of optimality (section 1.6.3) as unified by Mayne et al. (2000). Then more attention is focused on recent advances in MPC formulations for use on systems showing fast dynamics. In all the following presentation, the notations of Alamir (2006) are used since the solutions adopted in the present work are based on the control parametrization approach as suggested by Alamir (2006).

1.6.2 Definition of Model Predictive Control

Let us consider the following general nonlinear model of a time-invariant dynamical system:

$$x(t) = X(t, x_0, \mathbf{u}) \quad x \in \mathbb{R}^n \quad \mathbf{u} \in \mathbb{U}^{[0,T]} \quad t \leq T \tag{1.6}$$

where $x(t)$ is the state at instant t starting from the initial conditions $x(0) = x_0$ and under the control profile $\mathbf{u}$ that is defined on $[0, T]$ with values in the compact admissible set $\mathbb{U} \subset \mathbb{R}^m$.

Let $\tau > 0$ be some sampling period and take $T = N\tau$. Any map

$$\mathcal{U}_{pwc} : \mathbb{P} \rightarrow \mathbb{U}^N$$

defines on $[0, T]$ a piecewise constant control profile with parameters belonging to the admissible set of parameters $\mathbb{P} \subset \mathbb{R}^{n_p}$ by

$$\begin{array}{rcl} \mathbf{u}(t) & = & u^{(k)}(p) \quad ; \quad t \in [t_{k-1}, t_k] \quad ; \quad t_k = k\tau \\ \mathcal{U}_{pwc}(p) & := & \big(u^{(1)}(p) \quad \ldots \quad u^{(N)}(p)\big) \in \mathbb{U}^N \end{array}$$

Once such a parametrization is defined, the corresponding state evolution under the resulting control profile $\mathcal{U}_{pwc}(p)$ will be denotes hereafter by $X(t, x_0, p)$ Therefore, at each sampling instant $t_j = j\tau$ ($j \in \mathbb{N}$), $X(t, x(t_j), p)$ refers to the value of the state at instant $t_j + t$ under the control profile $\mathcal{U}_{pwc}(p)$ that is defined by the parameter vector p.

The Model Predictive Control amounts to solve at each sampling instant t_j the following optimization problem:

$$\hat{p}(x(t_j)) := \arg\min_{p \in \mathbb{P}} \Big[J(x(t_j), p) \Big] \quad \text{under} \quad C(x(t_j), p) \leq 0$$

then to apply the first control in the optimal sequence $\mathcal{U}_{pwc}(\hat{p}(x(t_j)))$, namely

$$K(x(t_j)) := \big[u^{(1)} \circ \hat{p}\big](x(t_j))$$

during the sampling period $[t_j, t_{j+1}]$.

Note that $J(x, p)$ represents a cost function that involves the future evolution that would take place if the control sequence defined by the parameter p is applied to the system. Moreover, the inequality

$$C(x, p) \leq 0$$

gathers all the constraints that have to be satisfied either at some specific instants (in particular final instant) or over the whole future time interval of length T referred to hereafter as the *prediction horizon*.

At the next sampling instant, the new optimization problem is defined based on the new values (or estimated value) of the state vector $x(t_{j+1})$ and the control

$$K(x(t_{j+1})) := \left[u^{(1)} \circ \hat{p}\right](x(t_{j+1}))$$

is applied during the time interval $[t_{j+1}, t_{j+2}]$ and so on.

Consequently, the Model Predictive Control is nothing but the implicit control law given by:

$$K := u^{(1)} \circ \hat{p} : \mathbb{R}^n \to \mathbb{U}$$

This law simply apply what everybody is doing in his own life:

> *find the best strategy given the current data, apply the first part of it, as soon as a new situation arises, update the strategy by re-considering the new situation, apply the first part of it etc.*

1.6.3 Sufficient Conditions of Stability

Although the very basic idea of MPC is rather intuitive, the resulting closed-loop system may become instable if the underlying optimal control problem is not carefully defined. More precisely, we are concerned here with the stability of the origin of the state space of the closed-loop system given by:

$$x^+ = X(\tau, x, u^{(1)} \circ \hat{p}(x))$$

that is supposed here to be an equilibrium point under vanishing control $u^{(1)} \circ \hat{p}(0) = 0$ that is also assumed to be an admissible solution of the optimization problem when defined at $x = 0$.

Since the early results on the stability proposed by (Keerthi & Gilbert (1988)), a huge literature on the stability issue emerged during the 90's containing either new formulations or different proofs for existing results. Almost all these results have been then unified in a general form by Mayne et al. (2000). Note however that this unified results hold for the following particular trivial piecewise control parametrization (see section 1.6.2) referred to hereafter as the standard instantiation of control parametrization:

Standard Instantiation of control parametrization

- The trivial parametrization of control:

$$\mathbb{P} := \mathbb{U}^N \quad ; \quad \mathcal{U}_{pwc} = \mathbb{I}_{\mathbb{P}} \quad \text{(Identity in } \mathbb{P}) \tag{1.7}$$

- The cost function $J(x, p)$:

$$J(x, p) = F(x(N)) + \sum_{i=0}^{N-1} L(x(i), u(i)) \tag{1.8}$$

  where $x(i) = X(i, x, p)$ and $u(i) = u^{(i+1)}(p)$. Moreover, F and L in (1.8) are supposed to be continuous and such that

$$L(x, u) \geq c \cdot \|(x, u)\|^2 \quad \text{for} \quad c > 0$$

- The constraint $C(x,p) \leq 0$ is defined by:

$$\forall i \in \{0,\ldots,N\}\ x(i) \in \mathbb{X} \subset \mathbb{R}^n \quad ; \quad x(N) \in X_f \subset \mathbb{X}$$

  where $\mathbb{X}$ and X_f are closed with $0 \in X_f$.

In addition to the above assumptions, the general results of Mayne et al. (2000) are based on the following assumptions:

Assumption 1.6.1. *There exists a control law $\kappa_f : X_f \to \mathbb{U}$ for which the terminal set X_f is positively invariant. Moreover, the final weighting map $F(\cdot)$ is a Lyapunov function under the control law κ_f. More precisely, for all $\xi \in X_f$, the following inequality is satified*

$$\Big[\Delta F + L\Big]\big(\xi, \kappa_f(\xi)\big) \leq 0 \tag{1.9}$$

where $\Delta F(x,u) := F(X(\tau,x,u)) - F(x)$.

The general stability result can then be stated as follows:

Proposition 1.6.1. *If the standard instantiation of control parametrization is used and if assumption 1.6.1 holds then the predictive control is well defined and the origin is asymptotically stable in the Lyapunov sense. Moreover, the set defined by*

$$X_N := \Big\{x \in \mathbb{R}^n \mid \exists \mathbf{u} \in \mathbb{U}^N \text{ s.t. } X(N\tau, x, \mathbf{u}) \in X_f\Big\}$$

is a region of attraction. That is, the set of initial states that can be steered to the origin using an admissible control profile. Finally, the Lyapunov function is nothing but the optimal value of the cost function, namely $J(x, \hat{p}(x))$. ♡

It is worth underlying that the knowledge of the control law κ_f invoked in proposition 1.6.1 is not necessary for the MPC law to be implemented. The existence of κ_f is used in the proof of closed-loop stability. Let us also emphasize the fact that the above general result is valid only for the trivial instantiation of control parametrization (1.7). The existence of slightly modified result for a wider class of control parametrization has been shown in (Alamir (2006)) under the following technical requirement:

1. The terminal set is $X_f = \{0\}$.
2. The control parametrization meets the following property *referred to as the translatability property* (see Alamir (2006)):

$$(\forall p \in \mathbb{P}), \exists p^+ \mid \left\{ \begin{array}{ll} u^i(p^+) = u^{i+1}(p) & \forall i < N \\ u^N(p^+) = 0 & \end{array} \right. \tag{1.10}$$

Note that the first restriction 1) imposes the use of final equality constraint on the state at the end of the prediction horizon. This final constraint has been widely viewed as a source of numerical difficulties in terms of on-line feasibility of the corresponding on-line optimization. However, when considering robotic and electromechanical systems, one often deal with highly structured model for which such a final constraint might be easily imposed by the control parametrization itself. Many examples of such parametrization have been proposed by Alamir (2006) (see also

Problem	n_p	Computation time (s)
Minimum interception time problem	1	18×10^{-3}
Stabilization of chained systems	1	$< 10^{-3}$
Stabilization of PVTOL	2	$< 10^{-3}$
Stabilization of a double pendulum on a cart	2	< 0.25
Stabilization of satellite in failure mode	2	< 0.01

Table 1.2: Some examples illustrating the efficiency of the control parametrization approach (Alamir (2006)) when dealing with highly structured robotic and electromechanical systems. The computation times needed to solve the optimization problem in the decision variable p are given for a PC-Pentium III 1.3 GHz. n_p represents the number of parameters (the dimension of the decision variable).

table 1.2).

As for the translatability condition (1.10), it simply ensures that once the prediction horizon is shifted, the remaining part of the preceding control profile can be used to construct a candidate profile for the new problem by just adding 0 as last control inputs. The need for such condition comes from the generalization of stability arguments that is used in the proof of the standard instantiation case.

1.6.4 Real-Time Model Predictive Control for Fast Systems

The last decade witnessed an increasingly rich literature concerning the way NMPC schemes have to be adapted to fit the real-time requirements when applied to fast systems. Among many possible classifications, a straightforward one consists in splitting the approaches into two main categories: The first amounts to bringing the problem into the *linearly hybrid world* while the second keeps handling the *nonlinear* representation of the systems.

Many approaches fall in the first category such as the explicit off-line feedback computation approach based on the Piece-Wise Affine (PWA) approximation (Bemporad et al. (2001, 2002), Borrelli et al. (2003) and the reference therein), the Linear Parameter Varying (LPV) approach (Falcone et al. (2008)) using dynamic linearization and the recently developed active set approach for on-line solution of MPC for PWA models (Ferreau et al. (2006, 2007)). Roughly speaking, these approaches address the real-time requirement by replacing the original problem by a new *and generally different* one which possesses a highly structured form that lends itself to efficient computations.

The off-line explicit computation of the feedback law or the on-line active method approach are both based on the fact that the optimal feedback of the underlying problem is affine in the state. The only difference is that in the explicit method, all the region and the feedback gains are already computed off-line and saved in the central unit while in the active set approach, the subset of active constraints is discovered iteratively.

Even when the original problem is linear, the basic drawback of the explicit strategy is the explosion of the problem dimension in both the dimension of the parameters and the length of the prediction horizon. This can make the only search for the active set beyond the available computation time. Moreover, the embedded allowable memory may not be sufficient to include all the storage needed to the strategy. As for active search algorithm, it involves large scale matrix operation and need a potentially high number of iteration to converge to the problem

solution.

Although these *linearization*-like approaches attempt to solve a modified problem that can be quite different from the original one, they encountered and still have a huge *popularity*. This is based on the belief that the *complete solution* of the original nonlinear constrained problem would be intractable anyway within the available computation time. This difficulty, for a long time considered as insuperable, inspired the idea of *distributing the optimization process over the system lifetime* (Alamir (2001)).

The idea of distributed in time optimization can be shortly explained as follows: When a system with fast dynamic is considered however, only a finite number $q \in \mathbb{N}$ of iterations of some optimization process $\mathcal{S}$ can be performed during the sampling period $[t_{j-1}, t_j]$. This lead to the following extended dynamic closed-loop system:

$$x(t_{j+1}) = X(\tau, x(t_j), p(t_j)) \quad (1.11)$$

$$p(t_{j+1}) = \mathcal{S}^q\big(p^+(t_j), x(t_j)\big) \quad (1.12)$$

where $\mathcal{S}^q$ denotes q successive iterations of $\mathcal{S}$ starting from the initial guess $p^+(t_j)$ which is related to $p(t_j)$ to guarantee (if possible) the translatability property (see Alamir (2006) for more details). The stability of the extended system (1.11)-(1.12) heavily depends on the performance of the optimizer $\mathcal{S}$, the number of iterations q and the quality of the model (see Alamir (2008) for more details).

Several approaches emerged that implement this simple idea. Among these approaches, the real-time iteration (Diehl et al. (2005)) is very promising. In this approach, the problem is transformed into a huge but highly structured Nonlinear Programming Problem that is then solved using multiple shooting algorithm. In this Nonlinear Programming Problem, the values of both the state and the control at sampling instants are the components of the decision variable. The resulting problem is split into two parts: the first part does not depend on the state and can therefor be computed before the next measurement is available. The other part needs the last measurement to be available. Consequently a preparation step can be done as a parallel task during the sampling period reducing the computation task to be performed using the updated state.
Another approach that shares the distributed in time optimization idea is the Continuation/GMRES (Generalize Minimum Residual) based differential approach proposed by Ohtsuka (2004). In this approach, a dynamic state feedback is proposed in which the internal state of the controller is nothing but the sequence of future control inputs to be applied to the system, say U. The differential equation describing the evolution of U is obtained by imposing that $\dot{U}$ be a descent direction towards the satisfaction of the set of first order necessary conditions for optimality.

In this work, the Control Parametrization Approach (CPA) (Alamir (2006)) is adopted. The *philosophy* that underlines the CPA lies in the following ideas:

1) Open-loop control profiles showing very simple time structures, when used in a receding-horizon framework, generally lead to very rich closed-loop control profiles that correspond to a small drop in the overall resulting optimality (Alamir & Marchand (2003)).

2) Although the global optimum of the NMPC cost function corresponding to a low dimensional parametrization is necessarily higher than that of a classical trivial piecewise constant parametrization, for a well designed parametrization however, it is more likely that the former would be easier to achieve than the latter due to the difference in the problem complexity. More

clearly, in a constrained computational context, the suboptimal solution of a simple optimization problem may be better than the suboptimal solution of a far more complex one. This intuitive idea is schematically depicted on Figure 1.17.

3) Classical piece-wise constant control parametrization in which all the control values are degrees of freedom result in unnecessarily high dimensional optimization problems. This is *a fortiori* true in the case where even the state values along the future system's trajectory are taken as degrees of freedom. Although these high dimensional problems are highly structured and can therefore be quite efficiently handled by dedicated algorithms, they still need incompressible high demanding preparation steps. Moreover, the dedicated softwares and memory storage needed for such problems are generally incompatible with embedded capacities. This is particularly true in the automotive applications.

There are many other advantages of the CPA such as its ability to explicitly exploit the model structure that is generally strong in electromechanical systems and the possibility to use control parametrization that takes into account the constraints of the problem at the very definition of the parametrization. For a more detailed presentation of these issues, the reader can refer to Alamir (2006) and the related references.

1.7 Conclusion

Nowadays automotive applications are becoming more and more demanding in terms of safety, performance and fulfillment of constraints and of course, cost. This context makes the use of advanced control more and more appealing. Advanced powertrain control and drivability is not an exception.

Among advanced control design methodologies, MPC seems to be a privileged answer. Indeed, the ability of MPC to handle both constraints, nonlinearities, coupling in the multivariable case and the natural way it offers to express control requirements as trade-off between several, often contradictory requirements, makes it a natural choice to be undertaken.

It is a fact however that the computational requirements of MPC and sometimes, the memory storage it may involve (in the explicit versions) can make it incompatible with the embedded electronic on-board systems that can be used in large market context.

This chapter underlined the conceptually appealing nature of MPC as a solution of choice for automotive control problems but also tried to draw the barriers that still to be overcome before MPC becomes a standard embedded technologies in the automotive industry solutions. Several emerging approaches intend to overcome these difficulties have been shortly mentioned. In particular, the potential advantages of Control Parametrization Approach that is used in the present work have been underlined.

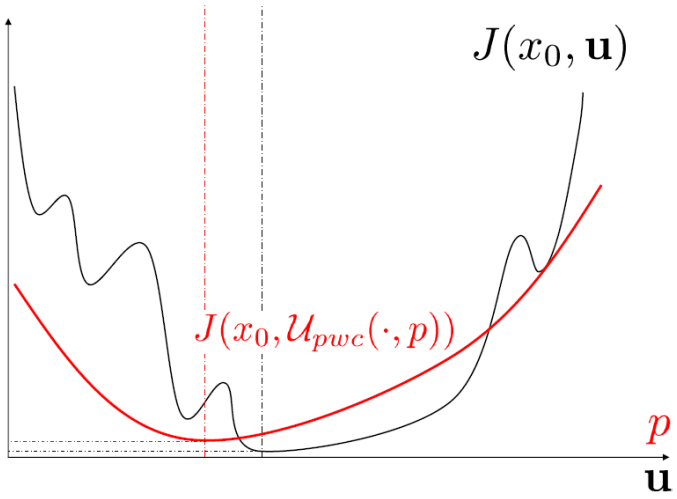

Figure 1.17: Schematic illustration of the intuitive idea according to which it is worth obtain a good solution of a suboptimal formulation rather than loosely solve the exact original problem. Here, the black line represents the variation of the cost function when classical trivial parametrization is used. many local minima exist because of the overly rich parametrization. In red, the cost function corresponding to a smart reduced dimensional parametrization for which the problem is much better conditioned at the price of a slight increase of the cost function.

Part II

Unified Predictive Control of an Automated Manual Transmission

Chapter 2

Control of Powertrains Equipped with AMT

2.1 Introduction

Automatic Manual Transmission (AMT) technology tries to combine the fuel efficiency of manual transmissions with the smooth operation of an automatic transmission. It operates similarly to a manual transmission except that it does not require direct clutch actuation or gear engaging by the driver. Transmission actuators are computer controlled, and embedded control strategies are in charge of ensuring smooth clutch engagement and gear shifting. As with a manual transmission car driven by an unexperienced driver, if clutch and engine actions are wrongly coordinated, maneuvers such as vehicle start-up and gear shifting may result in driveline oscillations or engine stall. The need for efficient control strategies is clearly paramount in this context, and explains why the search for new solutions to AMT control problems has attracted considerable attention in recent years, both in industry and in academia.

In this chapter, we introduce the innovative model predictive control strategy that we have developed for handling the different operating modes of an automated manual transmission in a unified way. In section 2.2, we present the general operating principles of automatic manual transmissions. Then, we examine the main approaches reported in the literature to solve AMT control problems (section 2.3). In section 2.4, we outline the characteristics of the AMT control problem we focus on in this thesis. Finally, the methodology and the framework of our model predictive control strategy are presented in section 2.5.

2.2 AMT operating principles

Automated manual transmissions have been designed by automobile manufacturers to provide a better driving experience, especially in cities where congestion frequently causes stop-and-go traffic patterns. An automated manual transmission is basically a manual transmission being operated by an automatic control system, in such a way that the vehicle can be driven without a clutch pedal, as easily as with a conventional automatic transmission. Of course, single-clutch AMTs cannot provide the seamless shifting of automatic transmissions, because the power flow from engine to wheels is interrupted whenever the clutch is open. Nevertheless, since they retain the high efficiency (95%) of manual transmissions and are only marginally more expensive[1], AMTs are considered an interesting solution both for passenger cars and heavy-duty vehicles,

[1] Essentially because of the increased complexity of the actuator layer and of the control electronics and software

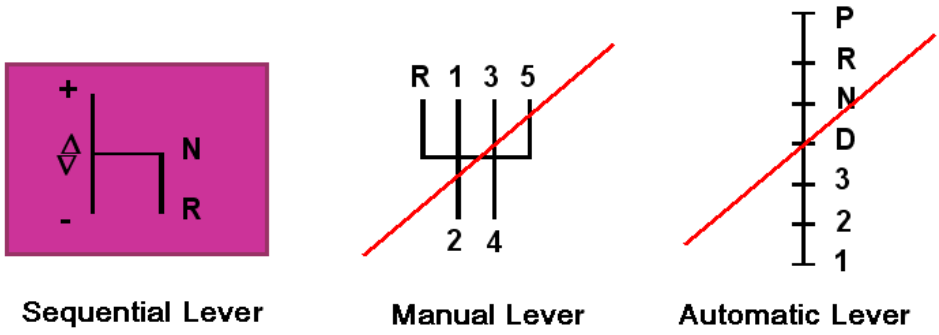

Figure 2.1: Layout gearshift levers for different transmissions

one that offers a good trade-off between fuel consumption and driving comfort.

Examples of commercial systems available on the market nowadays, are Selespeed (Magneti Marelli for Alfa Romeo and Fiat), Quickshift (Renault) and SensoDrive (PSA Peugeot Citroën) for passenger cars, I-drive (Volvo Powertrains) and AS Tronic (ZF) for heavy-duty vehicles. Interestingly, the first AMT systems have actually been developed for race cars, and more particularly for Formula One (where they have been the dominant technology since the 1990s), to obtain quicker gearshifts, with no particular concern for driving comfort or fuel consumption.

Most AMTs offer a fully automatic drive mode (AST, as automatic shift transmission), along with a manual shift mode. When in manual mode, the driver uses a plus/minus gate on the gearshift lever – or, in some models, paddles on the wheel – to shift up or down. Figure 2.1 shows the layout of the sequential gearshift lever, typical of AMTs, as opposed to the levers commonly found in vehicles equipped with manual transmissions and with automatic transmissions. With a manual transmission, if the driver wants to shift up (from second to third gear, for instance), he or she has to:

- open (disengage) the clutch, by pressing the clutch pedal;
- disengage the old gear and engage the new one, with the help of the mechanical synchronization of the pinions, by shifting the lever from the "2" position to the "3" position, via the neutral position in the middle;
- close the clutch, by releasing the clutch pedal, progressively to avoid oscillations at lock-up but as fast as possible to recover swiftly control of vehicle propulsion;
- control the engine speed throughout the gearshift via the accelerator pedal and adapt it to the new gear ratio (the "ordinary driver" would release the accelerator pedal completely then presse it again, if an acceleration is needed).

Notice also that, in this context, nothing prevents the driver from selecting an erroneous gear.

With an automated manual transmission, in manual-shift mode (see figure 2.2), if the driver wants to shift up of one gear, he "informs" the embedded control system by briefly pushing (or pulling) the gearshift lever to the `(+)` position. Then, if the control system accepts the upshift request, it will perform automatically all the steps described above, controlling directly the clutch position and the torque produced by the engine, and monitoring powertrain conditions (engine speed, mainshaft speed, vehicle speed and acceleration) and driver intentions (actions on accelerator and brake pedals). Downshifts are operated similarly, with some differences in engine speed

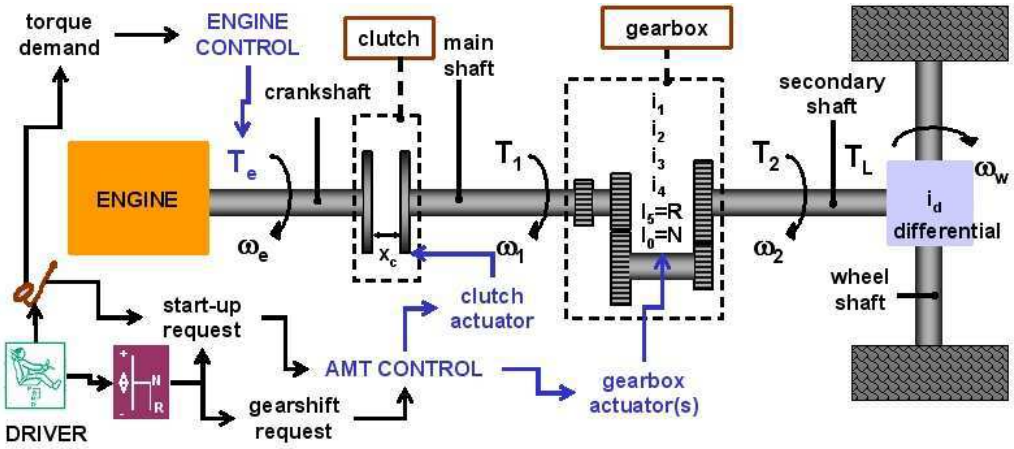

Figure 2.2: An AMT powertrain in manual-shift mode

control (engine speed must usually be increased, unless the driver wants to halt the vehicle). The AMT control unit may decide to reject a gearshift request but also to force automatically a gear change at any moment, typically to protect the engine from stall or redlining (over-revolution).

Starting up the vehicle from standstill with a manual transmission, assuming that the engine is already running and idling, requires:

- opening the clutch, by pressing the clutch pedal;
- engaging the first gear, by shifting the lever from the neutral position to the "1" position;
- closing the clutch, by releasing the clutch pedal, while increasing engine torque production via the accelerator pedal.

The last phase consists of three parts, with the driver acting on the clutch and the accelerator in a different way:

- at the beginning, the driver releases the clutch pedal quickly until he or she assesses that the clutch disks have come into contact;
- just before the torque transmitting point, the driver starts pressing the accelerator pedal and releases the clutch pedal more slowly, in order to transmit engine torque smoothly to wheels;
- when the driver assesses that clutch disks have locked up, he or she releases the clutch pedal completely and adjusts the accelerator pedal position to obtain the desired vehicle propulsion.

There are lots of things that can go wrong during a vehicle start-up maneuver: at the beginning engine may stall if the clutch is released too quickly and/or engine torque production is not increased enough, or, contrarily, its speed may increase to unnecessarily high values; clutch slipping may last too long, causing high thermal wear; powertrain oscillations may stem from a wrong coordination of clutch and accelerator actions close to clutch lock-up. To avoid all these problems, a skilled driver will use a mix of feedback and feed-forward control. Some situations can be detected through observation, such as the proximity of the torque transmitting point via the effects on engine speed and vehicle speed, but a certain degree of look-ahead is required to control vehicle start-up with good performances. Thus, a training and learning phase is always

necessary when driving a manual-transmission vehicle for the first time.

To start-up an AMT vehicle, assuming the engine already running, the driver first has to move the gearshift lever from the neutral position to the *stand-by* or gearing position (usually, the brake pedal must be kept pressed to validate this action). This makes the AMT control unit prepare the powertrain for start-up, by opening the clutch and engaging the first gear. Then, it suffices to press the accelerator pedal to get the vehicle moving. The AMT control unit will have to figure out what the driver's intentions are (a natural guess is that the more the driver presses the accelerator pedal, the faster the start-up must be), then to coordinate the actions of clutch and engine accordingly to start-up the vehicle as smoothly as possible. The same steps described before are required, from positioning the clutch at torque transmitting point to closing the clutch completely after lock-up. Speed measurements can be used for feedback control and at least a rough knowledge of clutch torque transmissibility characteristics is required for feed-forward control.

In summary, AMTs relieve the driver from the burden of controlling the clutch and synchronizing its action with engine torque production (controlled via the accelerator pedal) during complex maneuvers such as vehicle start-up and gearshifts. To obtain short engagement and shifting times, while avoiding engine stall or oscillations at clutch lock-up, the underlying control software must prove at least as "smart" as a skilled driver of manual transmission vehicles.

It turns out that up to now, in most production cars, these functions have been implemented via look-up tables, mostly in open-loop or with implicit feedback loops. For instance, a typical approach consists in generating directly engine torque and clutch torque reference trajectories, from the accelerator pedal position, via look-up tables. These setpoints are applied in open-loop at the beginning and the end of start-up. During clutch slipping, they are modulated (via other maps or static dependencies) by the engine speed and the slip speed, thus providing a sort of feedback. This approach usually require a good deal of calibration to achieve satisfying performances.

Only in recent times, model-based closed-loop strategies have started to draw the attention of car manufacturers and suppliers. And, of course, of several automatic control research groups all over the world, which explains the rather large number of papers that have been published on this subject.

2.3 State of the art of AMT control

The study presented in (Florencio et al. (2004)) states clearly that the automatization of the manual transmission, leads to a net improvement of driving comfort, and this, over a wide range of load torques. However, only dual-clutch AMTs (Ferriera & Leal (2006), Wheals et al. (2002)), where gear shifting can be achieved without torque interruption, can match the comfort of conventional automatic transmission, while preserving the efficient architecture of manual transmissions.

In the case of AMT with a single clutch, the configurations of the powertrain system are directly related to the states of the clutch (opened, slipping, and closed), and to the states of the gearbox (engaged, synchronizing, and neutral). These configurations define hybrid operating modes: for driving comfort, the correct handling of the transitions between modes is as important as the control of each single phase. The most critical phase, largely affecting driving comfort, is the clutch slipping phase, both during vehicle start-up and gear shifting. During the clutch slipping phase engine speed and mainshaft speed converge, and engine torque can be transmitted progressively to the wheels. The hybrid nature of AMT operation and the key role of the slipping

phase is largely investigated in (Garofalo et al. (2001)), in which the authors present an optimal tracking control strategy for the vehicle start-up phase, which takes directly into account the energy dissipated during the clutch engagement.

In (Glielmo et al. (2006)), a hierarchical approach is proposed by considering five AMT operating phases, defined according to clutch position (*engaged*, *slipping opening*, *go-to-slipping* and *slipping closing*) and gearbox operation (*synchronization*). During the closed-loop phases (idle speed control, start-up, and gear shifting), the strategy uses decoupled PI controllers, to control engine and clutch speeds. Additionally, a feed-forward controller is used for the engine control loop. The authors assume that the speed reference trajectories are well known, and do not address the issue of their generation in terms of driver expectations or comfort. Control performances strongly depend on the quality of the decoupling terms, which in turn requires a precise estimation not only of clutch torque, for which the authors propose an on-line observer, but also of engine torque, the latter being seldom available in the case of standard engine control systems. Notice that the complexity of the clutch model is a peculiar characteristic of (automated) manual transmission systems (Serrarense et al. (2004), Cameron et al. (2005), Gianluca et al. (2006)), and this complexity actually limits the performances of the decoupled controllers.

Linear Quadratic Control is suggested in (James & Narasimhamurthi (2006)) to control the slip speed. This optimal control takes into account the slip time, the dissipated power, and the slip acceleration in a performance index. To select a particular start-up profile, a look-up table is used. The strategy is applied to transmissions equipped with medium duty-wet clutches in which the dynamic of clutch torsional spring dumping coefficients can be neglected. The possibilities to apply this control to dry clutches seem to be limited since clutches models are very complex. The Linear Quadratic approach for clutch engagement in (Glielmo & Vasca (2000)) introduces weighting factors for the slipping speed and the control inputs. Direct real-time implementation of this strategy is difficult because of the high computation time required by the on-line solution of a Riccati differential equation. To cope with this problem, authors assert that it is possible to compute off-line the feedback gains and to find the coefficients of polynomials approximating their time evolution.

In (Bemporad et al. (2001)), authors present an explicit hybrid control formulation for the dry clutch engagement problem during vehicle start-up, via a piecewise-linear model predictive controller. To explicitly handle the input and state constraints, and cope with limitations in available computation time, the associated open-loop optimization problem is solved off-line by multi-parametric programming. The piecewise-linear feedback solution takes into consideration the duration of the engagement, the friction losses and the smoothness of engagement. The simulation results given in the paper underline the good performances of this MPC control strategy. However, on-line calibration may take a long time, since the partitions must be recomputed off line whenever the tuning parameters change. Moreover, real-time implementation may still be a major hurdle for this approach, when the number of state partitions increases, along with the size of the corresponding n-dimensional look-up tables. A recent study Van Der Heijden et al. (2007) evaluates in simulation the performances of an explicit model predictive controller for dry clutch engagement and draws the conclusion that, because of its large computational cost, explicit MPC is not suitable yet for these type of problems.

An interesting control strategy based on a finite-horizon optimal control of dry clutch engagement that has made its way to actual implementation, overcoming the computational complexity, has been proposed in (Dolcini et al. (2007)). As in conventional AMT control systems, the clutch

engagement starts with an open loop phase, which is based on look-up tables specifying a reference value for the engine and clutch torque and driven by the accelerator pedal position. Then, just before clutch lock-up, the optimization is turned on by controlling the clutch position while assuming the engine torque as a known input disturbance. Thereby, the control enables to limit the oscillations of the transmission, thus increasing the comfort level. Since the optimization is still computationally demanding and only short prediction horizons (no longer than 0.6 seconds) can be used, closed-loop control cannot be applied from the beginning of vehicle start-up. This two-phase approach does not offer a solution to avoid the long and cumbersome calibration of the look-up tables and the inherent lack of robustness of open-loop control with respect to uncertain or varying components and parameters in the system, such as the clutch torque characteristics.

Simpler and easily implementable closed-loop strategies have been presented to improve robustness and reduce calibration time, such the piecewise quadratic linear controller investigated in Van Der Heijden et al. (2007) or the PI-based approach presented in Tona et al. (2007). In the latter, for instance, a single PI controller is used to regulate the engine speed using the clutch bearing position, extending an approach suggested in Zanasi et al. (2001). However, these simple strategies are unable to explicitly handle constraints, which is a major handicap in the context of dry clutch engagement control.

2.4 Hybrid Control of the Powertrain System

2.4.1 Framework

Before presenting our approach in the next section, let us describe the framework we are assuming to work in. Control of AMT operation is always carried out within a hierarchical structure which goes from the interpretation of drivers' request to low-level actuator control systems. Even though the actual structure depends on the hardware configuration and on how the software is distributed between the different ECUs, it is possible to identify three common layers:

- the coordination between transmission and engine control modules or functions is generally dealt with in the top-most, supervisory layer;
- an intermediate, *functional* layer, is usually in charge of implementing the unitary control operations corresponding to specific engine and transmission functions;
- the lower level of the structure, the *actuator* layer, implement engine and transmission actuator servos.

Interesting control problems may arise at the *actuator* layer, when dealing with some particular transmission actuators (especially electro-hydraulic ones), but they are out of the focus of the present work: we will consider that transmission servos are well designed and respond appropriately to setpoint changes coming from the higher layers.

We will concentrate on control strategies coordinating actions on the engine and the transmission to perform AMT manoeuvres. As discussed in section 1.3.3, those strategies should be supervised by a *powertrain manager*, in the top-most vehicle manager layer, which is to handle the transitions between different powertrain modes, in response to driver's requests and driving conditions. Thus, such a powertrain manager, depicted in Figure 2.3, should include some modes dedicated to the control of AMT maneuvers, namely vehicle start-up and gearshifts. Other relevant modes are for instance vehicle *stand-by* or vehicle *normal motion*. In the former, which

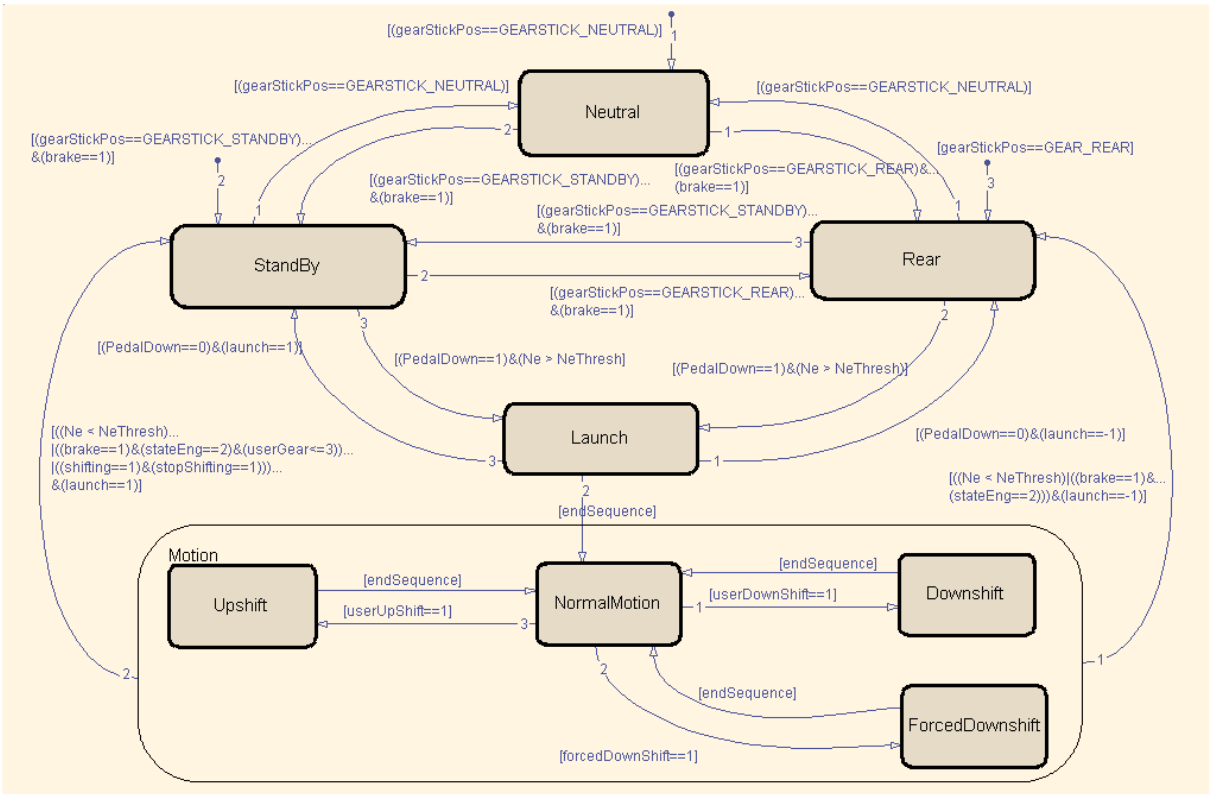

Figure 2.3: Powertrain manager

usually precedes vehicle start-up, the engine will eventually be in *idle mode* with its speed regulated around a specified value (600–900 *rpm* is the common range for SI engines), the clutch open and the first gear engaged. In the latter, the transmission is completely closed (that is, with the clutch closed and a gear ratio engaged) and the engine is running, so it can be considered as the natural mode for vehicle propulsion, provided that the driver presses the accelerator pedal (engine in *pedal mode*). Notice that AMT modes are *transient*, that is, are supposed to have a limited and short duration, as opposed to *permanent* modes, like vehicle stand-by or vehicle normal motion, which can last indefinitely. Figure 2.4 shows a typical concatenation of AMT phases.

Each AMT mode in the powertrain manager corresponds to a finite state machine controlling several powertrain configurations, defined by the states of the engine, the clutch and the gearbox, which compose a maneuver. Some of the control operations triggered by the powertrain manager are trivial or can be performed directly by the actuator servos. Other operations, and more particularly those ones where the clutch slips while transmitting engine torque to wheels, must be handled carefully by dedicated control strategies. The design of those strategies is precisely the focus of this part of the thesis.

2.4.2 Manipulated and controlled variables

For control purposes, we assume that measurements of engine and mainshaft speeds are available. As far as we know, this is indeed the case in all commercial AMT vehicles. The manipulated variables for control are the engine torque setpoint, to be translated into engine actuator setpoints by the engine control module, and the clutch torque setpoint or directly the clutch position setpoint, going to the clutch servo.

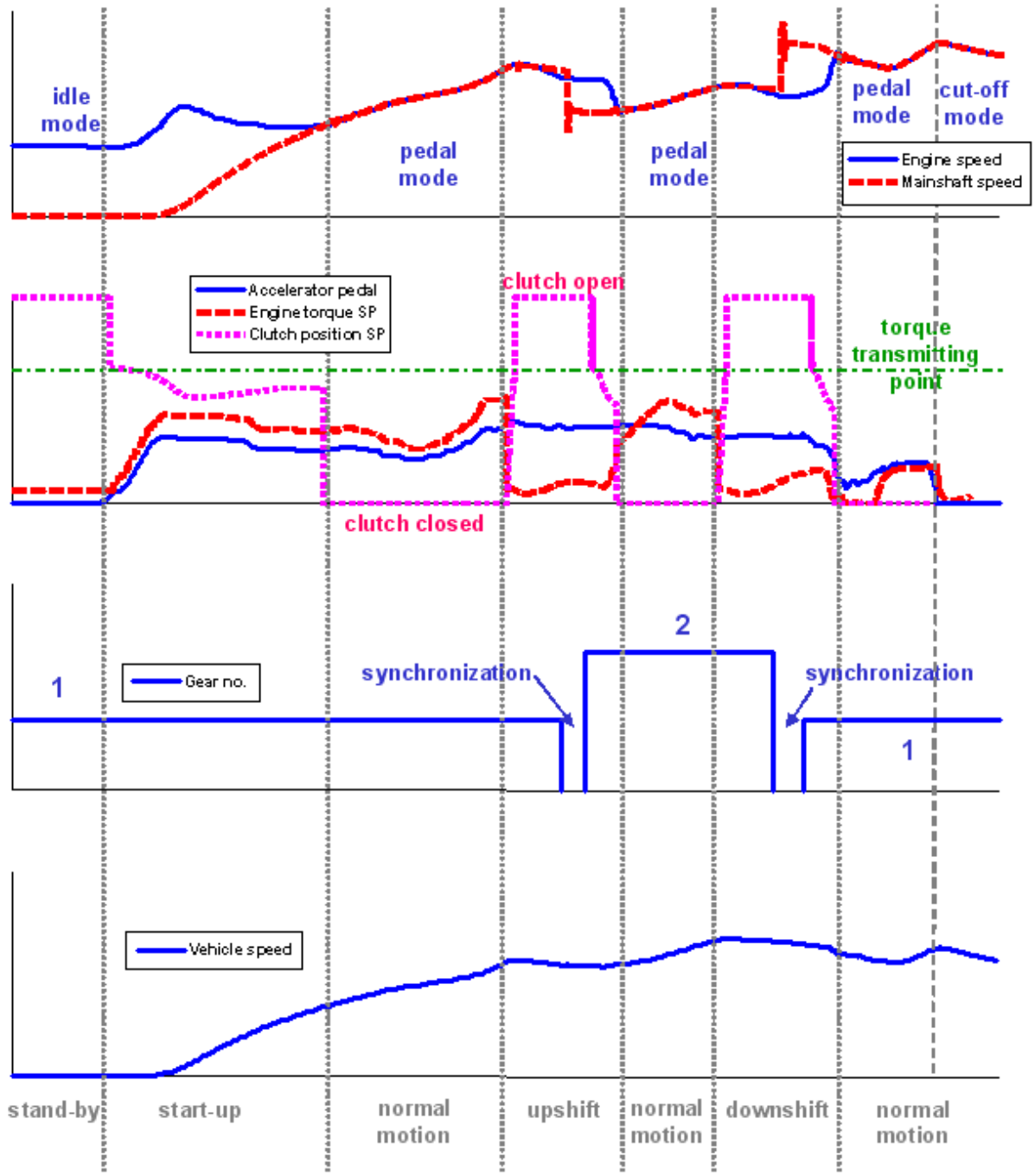

Figure 2.4: Concatenation of AMT phases

More particularly, the engine control module translate the engine torque setpoint into an air throttle position setpoint (and into position setpoints for the additional air path actuators, should they exist). The torque actually produced in response by the engine will be hopefully be close to the torque setpoint (after a certain delay and lag), if the engine control system is well calibrated ; but this cannot be verified, since no torque sensor is available in standard AMT vehicles. In a SI engine, it is possible in principle to act also on spark advance, as it is customary during idle-speed regulation to reject fast disturbances, via the high-level setpoint known as *torque efficiency* setpoint (or *fast torque* setpoint). This solution would allow more control authority on engine torque, though with a limited amount of "fast torque" available, at the expense of fuel consumption. We chose not to delve into this approach and to consider only actions on engine torque via the air path actuators.

As to the clutch control, the low-level clutch servo (generally based on a DC motor or a pump setting the pressure of a hydraulic circuit) receives a position setpoint from the higher control layers. Since, in a torque oriented framework, the high-level setpoint is more conveniently expressed as a clutch torque, a conversion block from torque to position is generally inserted before the servo. As shown in Figure 2.5, a static map is generally assumed between the desired clutch torque and the corresponding clutch position. This approach is overly simplistic, because transmitted clutch torque depends also on other variables, as it will be discussed in chapter 4. However, it is commonly found in conventional control structures. The most important part of the characteristic is the *torque-transmitting point*, that is the position of the clutch actuator starting from which torque can be transmitted (corresponding to disk surfaces coming into contact). For control purposes, it is important to have at disposal an estimate of this position, even though this position changes with temperature and, over a longer time scale, with wear, and the estimate would be, as a consequence, even imprecise and conservative. In fact, once again, no torque sensor is available to measure how much torque is actually transmitted by the clutch.

Gear ratio selection can be also considered as a manipulated variable for the powertrain system, to be translated into low-level gearbox servo setpoint(s), depending on the nature of the underlying actuator(s). In this work, we do not address the problem of how to select the gear ratio setpoint when the vehicle is in automatic shift mode. Nor we will study how to perform the actual gear change and the synchronization, problems for which closed loop solutions are seldom viable, because of the lack of appropriate feedback measurements (secondary shaft speed and/or torque sensors). We just assume the gearbox state (engaged gear, neutral, synchroniza-

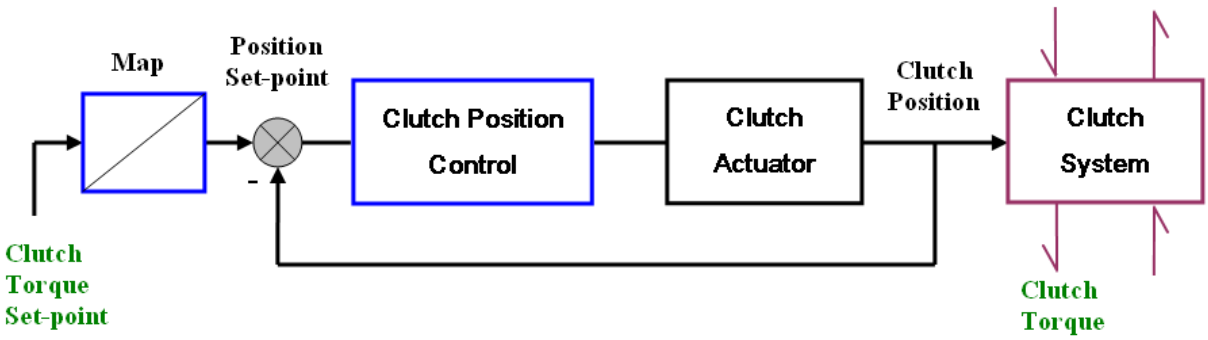

Figure 2.5: Closed loop control for the clutch actuator; a static map is assumed between the desired clutch torque and the corresponding clutch position.

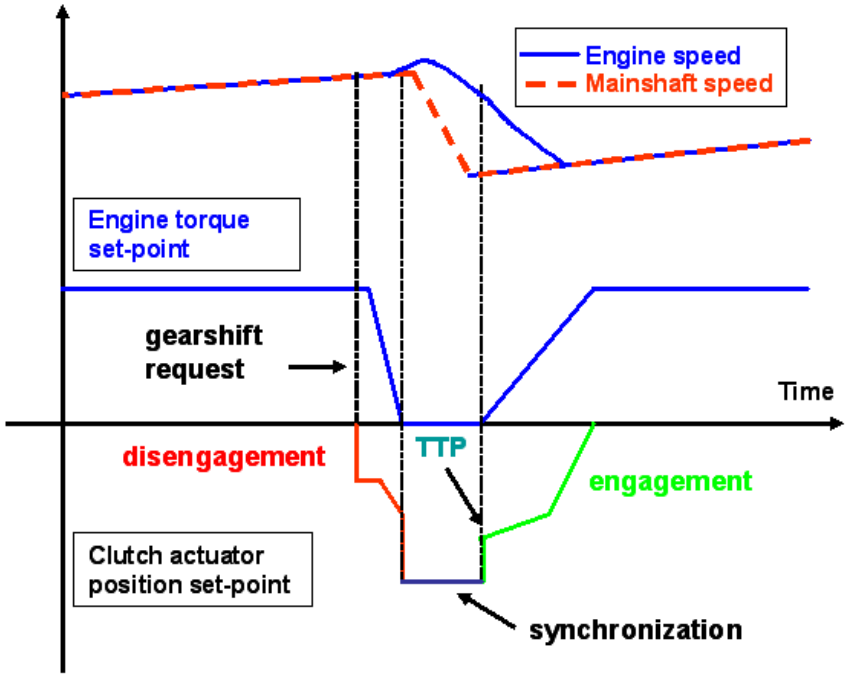

Figure 2.6: Open loop control of an upshift maneuver

tion) known.

2.4.3 Conventional AMT control

In standard AMT control system, control of vehicle start-up is generally performed by letting the engine torque be equal to the torque being requested via the accelerator pedal (set by a look-up table, function of the accelerator pedal position and the engine speed) and letting the torque transmitted by the clutch increase slowly. This is usually achieved by applying to the clutch torque set-point a fast ramp-like (or a step) profile to bring the clutch at the torque transmitting point, then a slow ramp-like profile to make engine speed and mainshaft speed converge gradually. When the slip speed is close to zero, the clutch can be closed completely.

This approach have several drawbacks, both in terms of performance and of calibration. The resulting start-ups are usually very slow, in order to avoid abrupt variations of vehicle acceleration (*jerks*), in particular at lock-up, and there is no control over engine speed. In terms of calibration, parameters such as ramp slopes and speed thresholds must be carefully adjusted to the actual acceleration pedal position profile chosen by the driver. Also, since torque measurements are not available in standard AMT vehicles, open-loop manipulation of engine torque and clutch torque does not bode well for robustness.

The gearshift maneuver includes a synchronization phase, which is dealt with by the gearbox servo, where the mainshaft speed is shifted to a different value, more suitable to the current or future vehicle speed, via a new gear ratio. As shown in Figure 2.4, gearing up implies a reduction of mainshaft speed, whereas gearing down usually implies an increase instead. The synchronization has to take place when torque on the primary side is zero or close to zero, a condition normally achieved by disengaging the clutch. When the engine "torque actuator" is faster than the clutch torque actuator, it is possible to carry out a "clutch-less" gear change,

by zeroing engine torque without opening the clutch. This approach, often adopted in heavy-duty vehicles, will not be investigated here. The last part of the gearshift manoeuver consists in matching the engine speed to the new value of mainshaft speed, by closing progressively the clutch. A fundamental difference with manual transmission operation is that the driver is not obliged to release the accelerator pedal during the gearshift; however his or her torque demand cannot be fulfilled completely before the gearshift maneuver is over.

Figure 2.6 shows how an upshift manoeuver can be controlled with an open-loop approach. After the upshift command has been received (from the driver, when in manual-shift mode, or from a gearshift supervisor, when in automatic-shift mode), the clutch is brought very close to the position where slipping is supposed to begin (condition detected by measuring the difference between engine and mainshaft speed), then a ramp profile, not too steep to avoid engine speed surges, is used to separate progressively the disks, and finally, when a certain slip speed threshold has been reached, the clutch is disengaged completely. Meanwhile, engine torque has to be reduced (not necessarily to zero). After synchronization, clutch control can be carried out similarly to the vehicle start-up case: a fast ramp-like (or a step) profile is applied to the clutch torque set-point to bring the clutch at the torque transmitting point, then a slow ramp-like profile is applied to make engine speed and mainshaft speed converge gradually, and finally, when the slip speed is close to zero, the clutch can be closed completely. Meanwhile, the engine torque set-point is progressively increased to the desired *pedal* torque.

The drawback are analogous to those described above for vehicle start-up: to avoid jerks and to keep engine speed within reasonable limits, the clutch slipping (closing) phase has to be very long. Calibration will be even more difficult, especially considering that each gearshift (from first to second gear, from second to third gear, and so on) will require its own set of parameters and look-up tables.

2.4.4 Towards viable closed-loop control strategies

The potential benefits of adopting closed-loop control strategies to implement AMT functions can be easily foreseen:

- improved robustness with respect to uncertain or varying components and parameters in the system (i.e. clutch torque characteristics);
- more accurate control of factors influencing the quality of the implemented functions, such as clutch engagement time and driveline oscillations;
- reduced calibration time, provided that the behavior of the closed-loop system can be related to few high-level tuning parameters.

Furthermore, it must be underlined that closed-loop strategies do not need additional measurements than those required by conventional AMT control: clutch actuator position, and main shaft and/or secondary shaft speed. On the other hand, a higher investment in control design and modeling is to be expected.

The phases for which closed-loop control is viable and potentially very beneficial are those where the clutch is slipping and an engine speed tracking is necessary. For those phases, the general structure shown in figure 2.7, can encompass most of the solutions proposed in the literature: SISO controllers, as in (Zanasi et al. (2001)) and (Tona et al. (2007)), decoupled MIMO controllers as in (Glielmo et al. (2006)) and (Tona et al. (2007)), full-fledged MIMO controllers

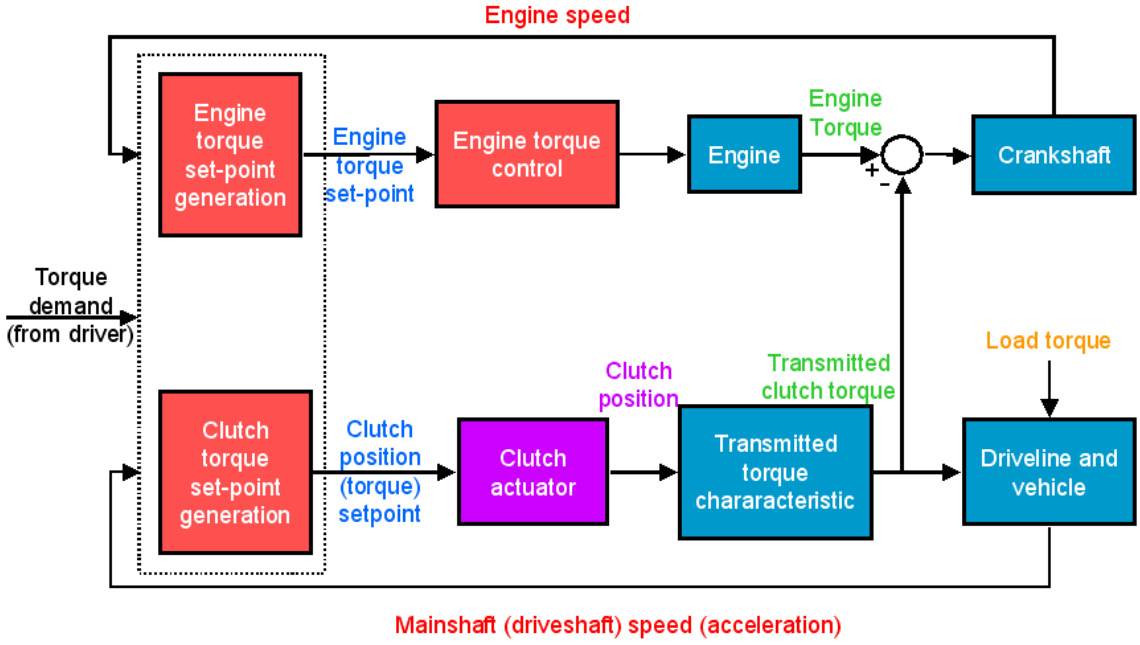

Figure 2.7: Generic control structure for the clutch slipping phase

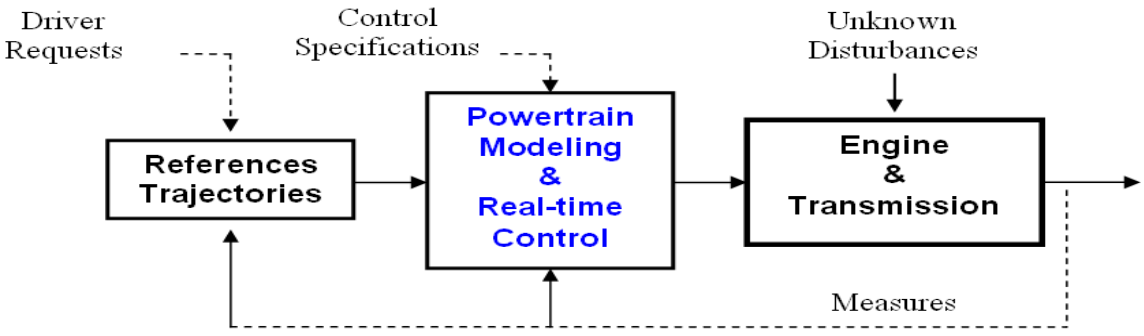

Figure 2.8: "Holistic" vision of the powertrain control problem for AMT applications.

as in (Bemporad et al. (2001)) and (Dolcini et al. (2007)).

Irrespective of the approach chosen to design the underlying control system, which obviously have an impact on how control specifications can be taken into account and on the resulting performance, we think that AMT control problems cannot be solved properly and convincingly without setting them in a realistic framework. More often than not, several aspects of the problem that should be taken into account in order to provide viable solutions are neglected in the literature: the integration in the hierarchical torque control structure, the generation of reference trajectories for the underlying control system, the constraints of real-time implementation, the uncertainties in the functional and actuator layers and the lack of on-board measurements (see Figure 2.8).

Generation of reference trajectories from driver requests for the control systems controlling start-ups and gearshifts is a problem seldom studied, or studied in a different perspective (as in Morselli et al. (2002) where open-loop operation is assumed). For instance, engine speed trajectories during vehicle start-up cannot be chosen arbitrarily, since they may not allow the engine

to deliver all the torque requested by the driver, and, on the other side, they have a "price" in terms of fuel consumption. As for mainshaft speed, it cannot imposed externally unless we are considering special cases where vehicle speed is imposed: this is the case for instance for a vehicle being driven on roll test bench to evaluate fuel consumption and pollutant emission on a normalized driving cycle such as the NEDC[2] or the FTP[3]). In normal situation, it would be sensible to relate mainshaft speed or slip speed to driver's requests. Similar considerations concerning mainshaft and/or slip speed during the clutch slipping phase, apply to gearshift control.

Another aspect it is important to insist on, in our opinion, is the fact that the manipulated variables for the AMT control systems are engine torque setpoint and clutch torque setpoint, whereas the variables acting on the powertrain system are the effective torque produced by the engine and the torque actually transmitted by the clutch, plus several disturbances one of which is load torque. None of those variables can be measured on board. We believe that mismatch, neglected dynamics and unknown variables must be dealt with explicitly in the control law to provide a viable solution.

All these concerns have influenced the design of the control strategy we present in the next section.

2.5 Unified Model Predictive Control for AMT

2.5.1 Framework, motivation, and methodology

Figure 2.9 summarizes the framework we have introduced in the previous section. The control system manipulates two "high-level" actuators, the engine torque setpoint T_e^{SP} and the clutch torque setpoint T_c^{SP}. Engine torque efficiency setpoint $\eta_{T_e}^{SP}$, a possible additional manipulated variable, will be kept set to 1, which means that fast action on engine torque via the spark advance is not considered in this part of the thesis. The gear ratio setpoint i_g^{SP} will not be considered as a manipulated variable, as it is chosen by the driver or by an automatic shift supervisor, but as a reconfiguration variable instead, used to select the correct model parameters, and consequently the appropriate control law.

All the high-level setpoints are translated, by the functional and actuator layers of the hierarchical torque-control structure, into low-level actuator setpoints controlling the operation of the powertrain system. Concerning the clutch servo, we assume to have the same structure as in Figure 2.5 and only a coarse knowledge about the $T_c(x_c)$ map or its inverse (basically, the minimum torque transmitting position and the maximum transmissible torque).

The rightmost part of Figure 2.9 shows a representation of the underlying physical system, using the Bond Graph formalism to illustrate power transfers and causality. Of the variables influencing system dynamics, T_e and T_c are the *unmeasured* control inputs, while the others can be considered as disturbance variables, measured (T_{elect}, the torque applied by an alternator or a more sophisticated electrical motor) or unmeasured (T_L, the load torque). The controlled (measured) variables are the engine speed ω_e and the mainshaft speed ω_c. Vehicle speed is also measured.

The solution we present in the following tries to fulfil several requirements:

[2]New European Driving Cycle
[3]Federal Test Procedure

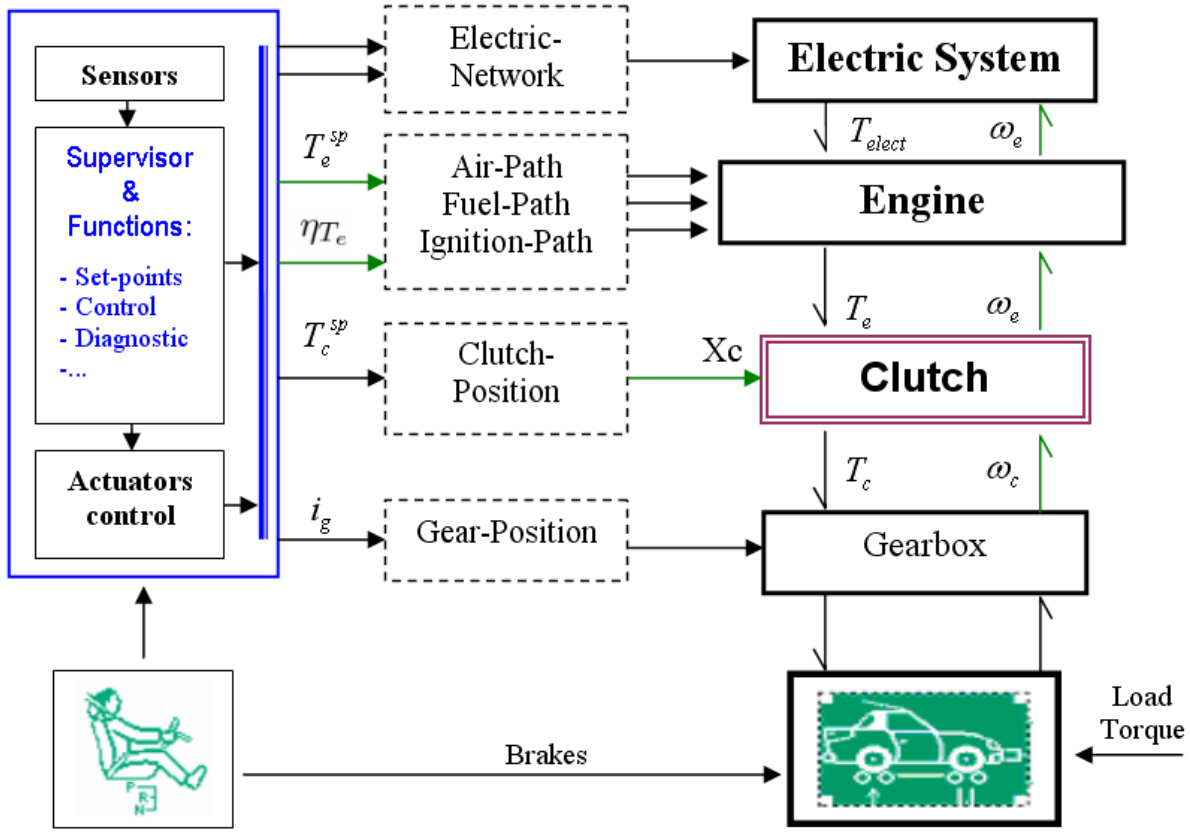

Figure 2.9: Topology of a torque-based control applied to a powertrain equipped with an Automated Manual Transmission.

1. Taking into account the multivariable and hybrid nature of powertrain control for AMT maneuvers, to handle couplings and to guarantee smooth transitions between the operating modes while avoiding as much as possible any specific initialization and filtering;

2. Exploiting the potential of the powertrain during AMT maneuvers in an optimal way, respecting drivability specifications and operating constraints;

3. Mapping driver's requests transparently into control specifications;

4. Dealing with uncertainties and unknown variables, while using only measurements normally available on standard AMT vehicles to avoid the cost of additional sensors;

5. Respecting real-time implementation constraints and more particularly limitations on available computation time in embedded ECUs.

The first point calls for adequate models of each AMT phases and for a unified approach ensuring, as far as possible, a direct correspondence between the evolution of powertrain dynamics and of the associated control model, and a natural handling of the transitions. The unified controller that we present in this thesis incorporates all the phases that can be profitably controlled in closed-loop in an AMT powertrain: engine idle mode during vehicle stand-by, and clutch slipping and engine speed tracking phases during vehicle start-up, upshifts and downshifts. The second point requires that the control law ensure the *optimal drive* integrating drivability specifications into an optimal control problem explicitly handling operating constraints, and in particular saturation constraints on torque actuators: model predictive control is capable to do

that. The *transparency* requirements can be fulfilled by linking mainshaft speed or slip speed to the accelerator pedal position or to the requested *pedal* torque. As to the fourth point, the capacity to deal with neglected dynamics and unknown variables, the use of observers seems to us the most natural way to go. Finally, to meet the severe computational constraints of real-time implementation on automotive ECU, an alternative formulation to standard MPC implementation must be found: the control parametrization approach is the solution we chose.

The following sections describe the ingredients our unified model predictive controller involves, from system model to control formulation.

2.5.2 Torque-Based Submodel During Clutch engagement

The dynamics of the key variables of the problem can be described by the following set of ordinary differential equations in which the symbols J, T, ω and θ refer to moment of inertia, torque, angular speed and position respectively:

$$J_e\dot{\omega}_e = \mathbf{T_{comb}} - T_{frict}(\omega_e, .) + T_{elect} - \mathbf{sign}(\omega_{\mathbf{sl}}) \cdot T_c\left(\mathbf{x_c}, .\right) \tag{2.1a}$$

$$\left[J_c + J_{eq}\left(\mathbf{i_g}, i_d\right)\right]\dot{\omega}_c = \mathbf{sign}(\omega_{\mathbf{sl}}) \cdot T_c\left(\mathbf{x_c}, .\right) - \frac{1}{\mathbf{i_g}\ i_d}\left[k_{tw}\,\theta_{cw} + \beta_{tw}\left(\frac{\omega_c}{\mathbf{i_g}\ i_d} - \omega_w\right)\right] \tag{2.1b}$$

$$J_w\dot{\omega}_w = k_{tw}\theta_{cw} + \beta_{tw}\left(\frac{\omega_c}{\mathbf{i_g}\ i_d} - \omega_w\right) - T_L\left(\omega_w, .\right) \tag{2.1c}$$

$$\dot{\theta}_{cw} = \frac{\omega_c}{\mathbf{i_g}\ i_d} - \omega_w \tag{2.1d}$$

The subscripts e, c, m, t, w, $comb$, $frict$, $elect$ are related to engine, clutch, main-shaft, transmission, wheels, combustion, friction, and electric related quantities. x_c is the position of the clutch. k and β denote elasticity and friction coefficients respectively. i_g is the gear ratio and i_d is the differential ratio. J_{eq} denotes the equivalent inertia of the transmission (main-shaft, synchronizer, etc.). $\omega_{sl} = \omega_e - \omega_c$ is the slipping speed between the engine and the clutch. $\theta_{cw} = \theta_c - \theta_w$ while T_L is the load torque which is commonly considered as an unknown disturbance due to aerodynamic resistance, tire–road frictions, and road grade.

2.5.3 Control Specifications

As we are looking for a control design that explicitly handles the operational constraints, these constraints need to be clearly described.

2.5.3a Constraints on torques variations and dynamics

The engine torque T_e and the clutch torque T_c are saturated by minimum and maximum values for evident reasons. Moreover, the rate of change of these variables need also to be limited. This is because the effectively produced torque are obtained thanks to local loops that possess their own and necessarily limited bandwidth. These constraints can therefore be written as follows:

$$T_e \in [T_e^{min}, T_e^{max}(\omega_e)] \tag{2.2}$$

$$T_c \in [T_c^{min}, T_c^{max}(\omega_e)] \tag{2.3}$$

$$\dot{T}_e \in \dot{T}_e^{min}, \dot{T}_e^{max}] \tag{2.4}$$

$$\dot{T}_c \in [\dot{T}_c^{min}, \dot{T}_c^{max}] \tag{2.5}$$

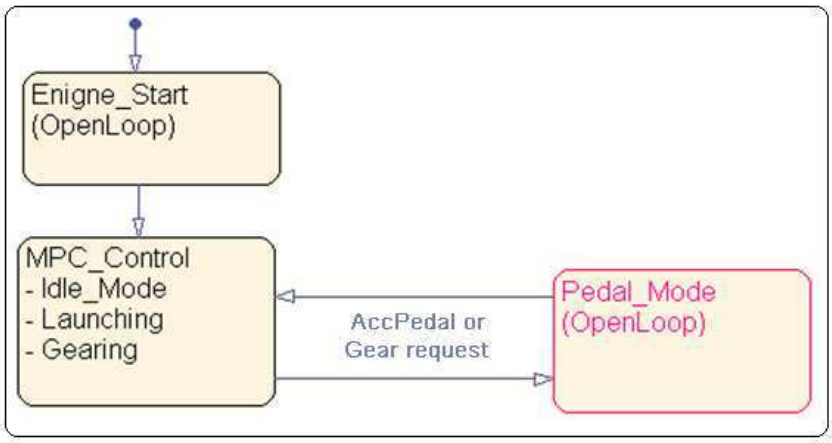

Figure 2.10: Unified model predictive control for the control of a powertrain equipped with an automated manual transmission. The unified approach includes the following modes: the idle speed control, the vehicle launching, gear up-shifting and down-shifting.

2.5.3b Constraints on the Engine Speed

The engine combustion system is designed to operate at relatively high speeds ($> 600rpm$). The main reason is that the engine cannot offer a stable combustion and low vibration level at low engine speeds. Therefore, the control design needs to monitor the engine speed in order to meet the *« no-kill condition »*, otherwise, the combustion does not occur and the engine is turned off. On the other hand, the engine is designed to operate with speeds that do not exceed some upper bound. In the common engines, this maximum limit is fixed to 6000rpm. Consequently, the following constraint has to be considered in the control design.

$$\omega_e^{min} \leq \omega_e \leq \omega_e^{max} \tag{2.6}$$

where ω_e^{min} and ω_e^{max} are the minimum and the maximum engine speeds that can be tolerated.

2.5.3c *No-lurch* Conditions

The quality of the transmission is strongly conditioned by the absence of oscillations that may take place after the clutch is completely closed. The ideal conditions that lead to no oscillation involve the dynamic of the slipping speed according to the following inequalities (Garofalo et al. (2002)):

$$\omega_{sl}^{ec}(t_f) = 0 \tag{2.7}$$
$$\omega_{sl}^{cw}(t_f) = 0 \tag{2.8}$$
$$\dot{\omega}_{sl}^{ec} = 0 \tag{2.9}$$
$$\dot{\omega}_{sl}^{cw} = 0 \tag{2.10}$$

where ω_{sl}^{ec} and ω_{sl}^{cw} are the slipping speeds between the engine and the clutch, and between the clutch and the wheels, respectively. It is needless to say that there is no control design that can guarantee the strict equalities mentioned above. Nevertheless, the control design has to take into consideration these constraints in a rather soft way.

2.5.3d Engine Torque Discontinuity

Another additional terminal constraint has to be specified on the control input T_e in order to enforce the continuity of the control during the transition from the clutch slipping phases

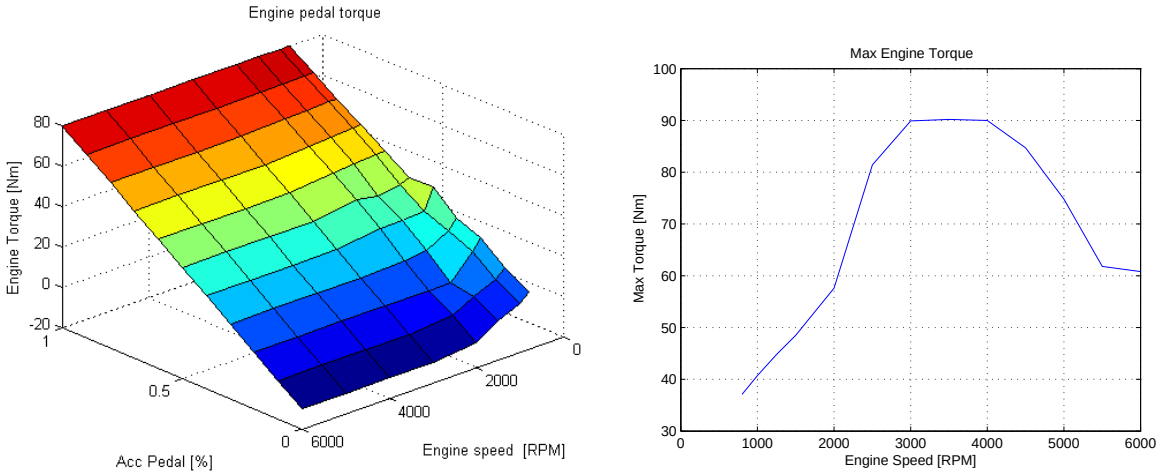

(a) Pedal torque T_e^d

(b) Engine maximum torque $\mathcal{T}$

Figure 2.11: Typical maps assumed for engine open-loop control and limitation of the engine production. The presented maps concern an IFP demo-car *Smart* 660cc (naturel gas).

(launching and gear shifting) to the pedal mode. This constraint can be written as follows:

$$T_e(t_f) = T_e^d(t_f) \tag{2.11}$$

where: $T_e^d(.)$ is the pedal torque.

In general, the oscillations induced by a potential discontinuity of the applied torque are denoted by jerks. For instance, it could be possible that the control achieves a smooth engagement, but the discontinuity of the control T_e may generate oscillations. Further analysis of the relevance of this constraints is proposed when considering the validation of the proposed NMPC control (see chapter3).

2.5.3e Fuel-Consumption and Limited Engine Torque

Recall that the purpose of the clutch engagement is to steer the slipping speed ω_{sl} from an initial value ω_{sl}^0 to 0. This has to be done while respecting the control specifications and constraints. Among these specifications, the minimization of fuel consumption is a crucial issue.

During vehicle start-up, the natural way to achieve minimum fuel consumption is to

- maintain the engine speed constant and equal to the idle speed set-point,
- and bring the main shaft speed to the engine speed.

Moreover, a by product of the achievement of this requirement is the limitation of the unpleasant noise related to the increase of the engine speed.

However, it is important to change the engine operating point wherever the engine torque goes near to its limits. These situations arise under high loads or rapid vehicle's lunching. Figure (2.11.b) shows a typical curve of the engine torque limitation as a function of the engine speed. For example, if the engine speed is regulated at `1000rpm`, the maximum torque that can be obtained through the fuel combustion is physically limited to `40Nm`. If the driver's interpreted torque according to the engine pedal torque (see Figure (2.11.a)) goes beyond this limit, the control should change the engine operating point to get more combustion torque at relatively high values of the engine speed. Note that the engine maximum torque decreases whenever the engine speed goes beyond some threshold (`4000rpm`).

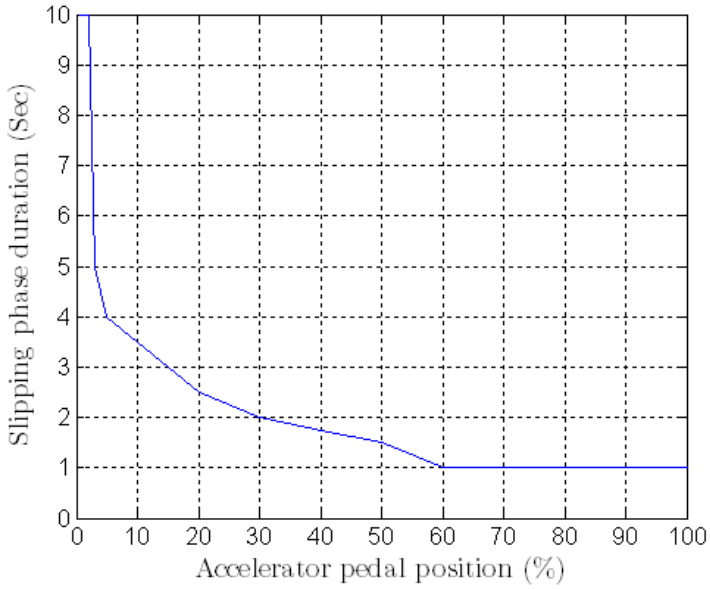

Figure 2.12: Typical map that can be assumed for expressing relation between driver demand and the time duration of clutch slipping phase.

2.5.3f Generation of the Reference Trajectories

The generation of the speeds reference trajectories is still an open issue in the automotive community. This concerns particulary the clutch engagement phases, including the vehicle start-up and the gear shifting.

Conceptually, the high level set-point is coming from the driver, and it is expressed through the accelerator pedal position [%]. The latter is then translated through a static map, according to the engine operating point, to a torque demand (see Figure 2.11.a). Generally, this torque demand is achieved in an open-loop mode, by applying directly the pedal torque to the low level actuators.

During the closed-loop phases (start-up and gear shifting), we propose here to define a different static map which converts the accelerator pedal position X_{pedal} into a desired slipping time duration, denoted hereafter by $t_f(X_{pedal})$. This time represents the duration of the clutch engagement that the control loop will try to achieve while meeting the above mentioned constraints. Doing this enhances a kind of reactivity (transparency) to the driver demand by affecting the way the closed-loop behaves for a given position of the accelerator pedal. Note however that the corresponding map is amended by feasibility constraints in order to end up with realistic set-points (response times). More precisely, if the time duration associated to the look-up table $t_f(X_{pedal})$ is achievable under the constraints, then a reference trajectory $\omega_{sl}^{ref}(t, t_f^*)$ on the slipping speed is defined that is compatible with the clutch duration $t_f^* = t_f(X_{pedal})$ otherwise, the clutch engagement duration t_f^* is increased in order to meet the constraints and the corresponding reference trajectory is considered. This clearly leads to an optimization problem in the decision variable $p = t_f^*$ that is used in a Model Predictive Control Scheme.

These issues are more detailed in the forthcoming sections. For the time being, a reduced model is needed in order to be able to perform the computation associated to the above formulation.

2.5.4 Reduced model

Recall that the model given by (2.1) involves the achieved torques. In practice, the achieved torques are generally unknown. For example, the engine combustion torque depends on many operating conditions that are related to many low level actuation issues, which are included in the air-path, the fuel-path, and the ignition-path. Moreover, in addition to the nonlinearity of the actuators, the combustion phenomenon is very complex, and depends on many parameters like the fuel properties and operating conditions. As for the clutch torque, the nonlinearity is principally involved in the clutch bearing position, and it includes many uncertainties/hysteresis related to the complexity of the friction phenomenon between the clutch disks.

In order to overcome this difficulties and to use realistic model, it is decided here that the manipulated inputs are the torque set-points

$$u := \begin{pmatrix} T_e^{SP} \\ T_c^{SP} \end{pmatrix}$$

Moreover, the differences between the achieved torques and their set-points are recovered via additional terms $\delta_e(.)$ and $\delta_c(.)$ that are obtained by dynamic observers. This leads to the following reduced-order model:

$$J_e \dot{\omega}_e = T_e^{SP} + T_c^{SP}(x_c) + \delta_e \tag{2.12a}$$

$$\left[J_c + J_{eq}(i_g, i_d)\right] \dot{\omega}_c = sign(\omega_{sl}) \cdot T_c^{SP}(x_c) - \delta_c \tag{2.12b}$$

where:

- T_c^{SP} and T_c^{SP} are the computed control inputs (the reference torque set-points)
- δ_e and δ_c are the unmeasured and non modeled quantities, which are used to gather all model mismatches and/or tracking errors including the electric torque T_{elect} and the load torque T_L.

The observation scheme needed to recover the unmeasured quantities δ_e and δ_c is described in the next section.

2.5.5 Powertrain's Observers

The reduced model enables to reconstruct the dynamics of the controlled shafts provided that an accurate estimation of the unknown torques δ_e and δ_c is obtained. This requirement can be achieved by means of a dynamic observers. Recall that a dynamic observer uses the available measurement in order to reconstruct the non measured quantities. Here, only the measurements that are available on serial vehicles are fed to the observer, namely, the speed measurements and the control set-point values T_e^{SP} and T_c^{SP}.

Note that for obvious reasons, the sampling time for the observation loop must be smaller than the sampling period of the control loop. Generally, in automotive softwares, the low level actuators are controlled at 1 kHz while the engine sampling frequency depends on the Top Dead Center (TDC) positions related to the engine cylinders. Consequently, the range of the control sampling period depends on the engine speed and on the number of the engine's cylinders. Therefore, a conventional engine with four cylinders have variable sampling period ranging from `4ms` and `50ms`. On the other hand, There are no constraints on the sampling period of the clutch actuator.

In the forthcoming development, it is assumed that the MPC strategy is updated at a constant sampling period, which is taken to be the nearest to the upper value ($\simeq$ `50ms`). As for the observation loop, a sampling frequency of 1 kHz is chosen in order to guarantee good performance even for a very low control sampling periods such as ($\simeq$ `4ms`).

The design of the observer is based on the classical technique of state extension. More precisely, δ_e and δ_c are considered to be two additional states with 0 dynamics (constant evolution). By doing so, an extended system is obtain that is observable. Moreover, decoupled observers can be used to recover δ_e and δ_c. That is to say, a first observer is used to estimate the unknown dynamic δ_e using the measurements ω_e, T_e^{SP}, and T_c^{SP} as inputs while a second observer is used to estimate δ_c using ω_c, and T_c^{SP} as inputs.

The mathematical models of the observers are given by the following equations:

Obs$_1$:

$$\dot{\hat{X}}_1 = A_1\hat{X}_1 + B_1 u - {S_1}^{-1} \cdot (C_1\hat{X}_1 - y_1) \tag{2.13}$$

$$\dot{S}_1 = -\theta_1 S_1 - {A_1}^T S_1 - S_1 A_1 + C_1^T C_1 \tag{2.14}$$

where:

$$\hat{X}_1^T = [\hat{\omega}_e \quad \hat{\delta}_e]; \quad y_1 = \omega_e; \quad u^T = [T_e \quad T_c]; \quad A_1 = \begin{bmatrix} 0 & J_e^{-1} \\ 0 & 0 \end{bmatrix};$$
$$B_1 = \begin{bmatrix} J_e^{-1} & -J_e^{-1} \\ 0 & 0 \end{bmatrix}; \quad C_1 = [1 \quad 0];$$

Obs$_2$:

$$\dot{\hat{X}}_2 = A_2\hat{X}_2 + B_2 u - {S_2}^{-1} \cdot (C_2\hat{X}_2 - y_2) \tag{2.15}$$

$$\dot{S}_2 = -\theta_2 S_2 - {A_2}^T S_2 - S_2 A_2 + C_2^T C_2 \tag{2.16}$$

where:

$$\hat{X}_2^T = [\hat{\omega}_c \quad \hat{\delta}_c]; \quad y_2 = \omega_c; \quad b = [J_c + J_{eq}\,(i_g, i_d)]^{-1}; \quad A_2 = \begin{bmatrix} 0 & -b \\ 0 & 0 \end{bmatrix};$$
$$B_2 = \begin{bmatrix} 0 & b \\ 0 & 0 \end{bmatrix}; \quad C_2 = [1 \quad 0];$$

2.5.6 The proposed NMPC design

In this section, the Model Predictive Control design is explained. One major feature in the proposed design is the way the degrees of freedom are specified in order to derive a tractable optimization problem under tight real-time requirements. Model Predictive Control is now a widely used control design methodology because of its ability to handle problem constraints and nonlinearities in the process model. MPC design need the system to be written in the following general form:

$$x(k+1) \quad = \quad f(x(k), u(k)) \tag{2.17}$$

where $x \in \mathbb{R}^n$, $u \in \mathbb{R}^m$ are the state and the input respectively. $x(k)$ denote the value of the state vector at the sampling instant k.

The definition of an MPC need a cost function to be chosen that reflects the control objective. This cost function defines a sort of desired behavior by defining weighting functions that

penalize, for each choice of the sequence of future actions, the deviation from the desired behavior. The cost function is defined over a time horizon N_p that is referred to as the prediction horizon. Therefore, at each instant k, the cost function takes the following form:

$$J(x(k), \mathbf{u}(k), \mathbf{r}(k), \nu(k)) \tag{2.18}$$

where

- $\mathbf{u}(k) = \left(u^T(k), u^T(k+1), \ldots, u^T(k+N-1)\right) \in \mathbb{R}^{Nm}$ is the candidate sequence of future control actions.
- $x(k)$ is the current state at instant k.
- $\mathbf{r}(k)$ is some desired trajectories that may be defined on the regulated variables. Here, reference trajectories $\omega_{sl}^{ref}(\cdot)$ and $\omega_e^{ref}(\cdot)$ on both the slipping speed ω_{sl} and the engine speed ω_e are used. This is explained in deeper details in the sequel.
- ν is an exogenous input vector that describes some key quantities of the context at instant k that may influence the definition of the cost function. In our case, this vector is given by:

$$\nu := \begin{pmatrix} \hat{\delta} \\ t_f \\ X_{pedal} \end{pmatrix} \in \mathbb{R}^2 \times \mathbb{R} \times \mathbb{R} \tag{2.19}$$

  where :

  $\hat{\delta} := (\hat{\delta}_e, \hat{\delta}_c)$ are the estimations delivered by the observers.

  t_f is the slipping-time duration for the clutch engagement. This is used later to define the reference trajectory on the slipping speed $\omega_c^{ref}(\cdot)$.

  $Xpedal$ is the accelerator pedal position. Here again, this information is used to generate the reference trajectory $\omega_e^{ref}(\cdot)$ on the engine velocity in order to enhance a kind of transparency w.r.t the driver demands.

The cost function has then to be minimized in the decision variable $\mathbf{u}(k) \in \mathcal{U}(k) \subset \mathbb{R}^{Nm}$ unless a low dimensional parametrization is adopted following the lines explained in the previous section. Note also that the minimization has to be performed over the admissible set $\mathcal{U}(k)$ of decision variables. This is defined through a set of operational constraints that have to be respected in closed-loop. The constrained set $\mathcal{U}(k)$ gathers all the limitations that are partially described by (2.2)-(2.5). Note that the admissible set $\mathcal{U}(k)$ can be implicity state dependent through the time index k.

In order to complete the description of the cost function, the reference trajectories $\mathbf{r}(k)$ need now to be defined on the engine speed and the slipping speed.

2.5.6a Reference Trajectories during Clutch Engagement

A. Slipping Speed Reference Trajectory

As mentioned above, the slipping speed reference trajectory ω_{sl}^{ref} is directly linked to the accelerator pedal position X_{pedal}. To do so, the accelerator pedal position is first translated into an engagement duration, through a static map. Then an analytical expression is used to define the slipping speed profile over the engagement duration, while taken into consideration the terminal

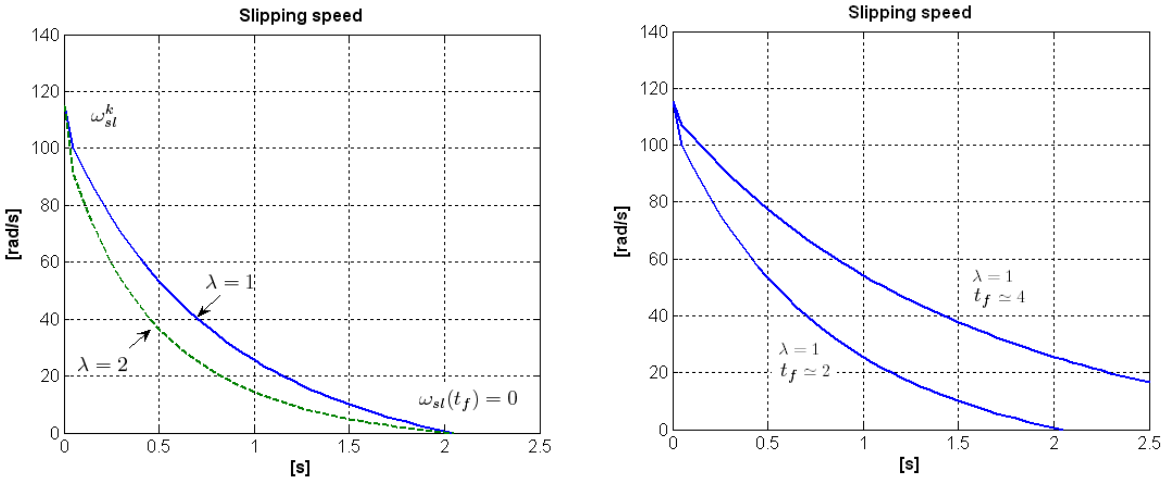

(a) Variation of the slipping speed according to the tuning parameter λ.

(b) Variation of the slipping speed according to the slipping time duration.

Figure 2.13: Typical variations of the desired reference trajectories according of the tuning parameter λ and to the slipping time duration t_f.

constraint related to the *no-lurch* condition, expressed before in the equations (2.7)-(2.10).

This can be formally summarized as follows:

$$\begin{array}{ccccc} [0 \quad 100] & \rightarrow & [t_f^{min} \quad +\infty] & \rightarrow & \mathbb{R}^{[k,\infty]} \\ X_{pedal} & \mapsto & t_f = f_1(X_{pedal}) & \rightarrow & \omega_{sl}^{ref}(k+\cdot, t_f) \end{array}$$

where $f_1(.)$ is a static map while for each $i \in \mathbb{N}$, the reference trajectory value $\omega_{sl}^{ref}(k+i, t_f)$ is given by:

$$\omega_{sl}^{ref}(k+i, t_f) = \frac{1 - i/N_f}{(1 + \lambda \cdot i/N_f)^2} \cdot \omega_{sl}(k) \quad ; \quad t_f = N_f \cdot \tau_s \tag{2.20}$$

Note that at the future instant $k + t_f$, the desired value of the slipping speed is 0 in accordance with the constraints (2.7)-(2.8). The constraints on the accelerations, given by (2.9)-(2.10) are taken into consideration through the parameter λ. This parameter plays the role of a weighting factor for the terminal slipping speed. Relatively high values of λ enables to guarantee very limited slipping accelerations at the final time $k + t_f$. Figure 2.13.a shows the resulting reference trajectories on the slipping velocity for two different values of λ. Figure 2.13.b shows how the reference trajectories are affected by different choices of the engagement duration ($t_f = 2$ *sec* and $t_f = 4$ *sec*).

It is worth noting that since the reference trajectory on the slipping speed depends on both X_{pedal} and t_f, the cost function does also depend on those quantities. This explains why the context vector ν is used as an argument in the definition of the cost function (5.18).

B. Engine Speed Reference Trajectory

The reference trajectory of the engine speed is defined according to the following argumentation:

- First, a desired torque is defined based on the knowledge of the accelerator pedal position X_{pedal} and the current value of the engine speed. This is done using the static map depicted

on Figure 2.11.(a) This value is denoted hereafter by:

$$T_e^d(X_{pedal}, \omega_e)$$

Note however that this map does not take into account the feasible torque that can be achieved given the value of the engine speed ω_e.

- Indeed, Figure 2.11.(b) gives the engine maximum achievable torque as a function of the engine speed. This enables a corresponding minimum speed to be defined. This is denoted hereafter by the following notation:

$$\mathcal{T}^{-1}(T_e^d(X_{pedal}, \omega_e))$$

Based on the above arguments, at each instant k, the reference trajectory of the engine speed over the prediction horizon $[k, k+N_p]$ is given by:

$$\omega_e^{ref}(k+i, X_{pedal}(k)) = \max\{\omega_e^0, \mathcal{T}^{-1}(T_e^d(X_{pedal}(k), \omega_e(k)))\} \tag{2.21}$$

Namely, if the minimum engine speed that is necessary to produce the desired torque is greater than ω_e^0, then the reference is taken equal to $\mathcal{T}^{-1}(T_e^d(X_{pedal}, \omega_e))$. Otherwise, the reference value of the engine speed is precisely ω_e^0.

2.5.6b Control Structure and Parametrization

The predictive control formulation is based on the simplified model (2.12) in which the manipulated variables are the set-point of the engine torque $u_1 := T_e^{SP}$ and the set-point on the clutch torque $u_2 := T_c^{SP}$. Ideally, in the absence of real-time implementation constraint, the decision variable at sampling instant k would be the piece-wise profile of these two decision variables over the prediction horizon $[k, k+N_p]$, namely:

$$\mathbf{u}(k) = \big(u^T(k), \ldots, u^T(k+N_p-1)\big)^T \in \mathbb{R}^{2N_p} \tag{2.22}$$

Note also that the constraints on the actuators given by (2.2)-(2.5) can be expressed by a system of linear inequalities in the decision variable $\mathbf{u}(k)$ in a straightforward way. This system can be shortly written as follows:

$$A_c \cdot \mathbf{u}(k) \leq b_c \tag{2.23}$$

Therefore, ideally, given the value of the exogenous vector

$$\nu(k) = \begin{pmatrix} \hat{\delta}^T(k) & t_f(k) & X_{pedal}(k) \end{pmatrix}^T$$

the predictive control formulation would be given by the following constrained optimization problem:

$$\min_{\mathbf{u}} \Omega(\mathbf{u}, \omega(k), \nu(k)) \quad \text{under } A_c\mathbf{u} \leq b_c \tag{2.24}$$

where

$$\Omega(\mathbf{u}, \omega(k), \nu(k)) := \sum_{i=1}^{N_p} \left\| \begin{pmatrix} \omega_{sl}(k+i) - \omega_{sl}^{ref}(k+i, t_f(k)) \\ \omega_e(k+i) - \omega_e^{ref}(k+i, X_{pedal}(k)) \end{pmatrix} \right\|_Q^2 \tag{2.25}$$

in which $\omega_{sl}(k+i)$ and $\omega_e(k+i)$ are given by the solution of the reduced model starting from the initial conditions $\omega(k)$ under the control profile defined by $\mathbf{u}$ and using the estimations $\hat{\delta}_e(k)$ and $\hat{\delta}_c(k)$ contained in the context vector $\nu(k)$ while the reference trajectories $\omega_{sl}^{ref}(\cdot)$ and $\omega_e^{ref}(\cdot)$ are defined as described above given $t_f(k)$ and $X_{pedal}(k)$.

It is a fact however that solving the constrained quadratic problem (2.24) would be impossible in the available computation time and given the available on-board computational facilities. That is the reason why a sub-optimal formulation is proposed hereafter that is tractable in real-time.

The idea is to consider the following unconstrained optimization problem given by:

$$\min_{\mathbf{u}} \Omega^{unc}(\mathbf{u}, \omega(k), \nu(k), p) \tag{2.26}$$

in which

$$\Omega^{unc}(\mathbf{u}, \omega(k), \nu(k), p) := \sum_{i=1}^{N_p} \left\| \begin{pmatrix} \omega_{sl}(k+i) - \omega_{sl}^{ref}(k+i, p)) \\ \omega_e(k+i) - \omega_e^{ref}(k+i, X_{pedal}(k)) \end{pmatrix} \right\|_Q^2 \tag{2.27}$$

where the parameter p a candidate engagement duration. The intuition behind the parametrization is that by taking p sufficiently large, the constraints (2.23) can be fulfilled. Let us denote by

$$\mathbf{u}_{pwc}(p, \omega) \quad \text{the solution of (2.26)}$$

Since this is the solution of an unconstrained quadratic problem, it can be clearly obtained analytically.

The ideal value of the parameter p is obviously $t_f(X_{pedal})$, namely, the one that is compatible with the transparency requirement in accordance with the above discussion. Unfortunately, this value may lead to a piecewise constant profile:

$$\mathbf{u}_{pwc}(p, \omega)$$

that violates the problem's constraints (2.23).

Based on the above argumentation, the best parameter p is computed by solving the following scalar optimization problem at each instant k,

$$\min_{p} |p - t_f(X_{pedal}(k))| \quad \text{under } A_c \cdot \mathbf{u}(p, \omega(k)) \leq b_c \tag{2.28}$$

Namely, the parameter p (representing the engagement duration) is chosen such that the constraint are satisfied. This can be done by simple scalar dichotomy since by taking sufficiently large value of the engagement duration, the constraints would be satisfied. Typically, the minimum value of the dichotomy operation is taken equal to the ideal value $t_f(X_{pedal})$ in order to enhance this choice in case it leads to an admissible solution in the sense of the constraints (2.23).

Once the scalar optimization problem is solved to yield the optimal parameter:

$$p^{opt}\Big(\omega(k), \nu(k)\Big)$$

that we shortly denoted hereafter by $p^{opt}(k)$ when necessary, the first control in the corresponding control profile:

$$\mathbf{u}_{pwc}(p^{opt}(k), \omega(k))$$

is applied during the sampling period $[k, k+1]$.

At the next decision instant, the new optimal parameter is computed, namely:

$$p^{opt}\Big(\omega(k+1), \nu(k+1)\Big)$$

and the first control in the corresponding optimal control sequence:

$$\mathbf{u}_{pwc}(p^{opt}(k+1), \omega(k+1))$$

is applied during the sampling period $[k+1, k+2]$ etc.

This is precisely the nonlinear model predictive control law.

It is shown later that the corresponding scalar dichotomy can be solved in a fraction of the available computation time while the solution of the original constrained problem (even quadratic with linear constraints) would be beyond the on-board computation capacities.

The implicit assumption according to which the feasibility of the constrained problem is enhanced by increasing the engagement time p is more deeply investigated in appendix (A).

2.6 Conclusion

In this chapter the problem of controlling powertrains equipped with automated manual transmissions by means of a parameterized MPC is investigated. In order to deal with the serial vehicles level of equipment, the proposed strategy uses only measurements which are available in the conventional vehicles. A reduced model is used together with two dedicated observers that are used to recover the unmeasured groups of terms that affect the evolution of the key controlled quantities. The MPC cost function involves reference trajectories that enhance a high level of transparency since they are liked to the driver demands expressed by the acceleration pedal position. The original MPC problem has been re-formulated in order to end up with an optimization problem with scalar decision variable that can be computed by simple dichotomy. The next chapter shows in details the validation of the proposed MPC strategy for AMT-application.

Chapter 3

Application and Validation of AMT Control on a Demo-Car

3.1 Introduction

This chapter illustrates the application and validation of the unified model predictive control strategy presented in the previous chapter. In the first part, in section 3.2 we illustrate the application context and, more particularly, the VEHGAN demo-car, a mild-hybrid vehicle equipped with a rapid prototyping powertrain control system. Then, in section 3.3 we explain how the unified model predictive control strategy is implemented in the integrated powertrain control structure of the demo-car.

The rest of the chapter is dedicated to validation. In section 3.4 the three different environments used for validation are described : simplified simulation, detailed co-simulation and real-time implementation on the demo-car. The following three sections present the specific validation results for each powertrain mode considered : vehicle start-up (section 3.5), gear shifting (section 3.6) and idle mode (section 3.7).

3.2 Application Context

3.2.1 The VEHGAN Project

The unified predictive control presented in the previous chapter has been developed and tested in the framework of VEHGAN[1], a project investigating the benefits of combining, in a small city car (a MCC `smart`), a dedicated downsized engine (660 cm^3) fuelled with compressed natural gas, with the starter-alternator reversible system StARS based on ultra-capacitors, providing mild-hybrid capabilities.

VEHGAN is a joint project involving IFP, Gaz de France, Valeo and INRETS[2], and partially funded by ADEME[3]. The ambition of VEHGAN is to prove that coupling a mild-hybrid architecture to a downsized engine optimized for the use of compressed natural gas (CNG) is an interesting solution to face the environmental challenges of urban transportation.

[1] *VÉhicule Hybride au GAz Naturel*, that is Hybrid Natural Gas Vehicle)
[2] The French National Institute For Transport And Safety Research
[3] The French Environment and Energy Management Agency

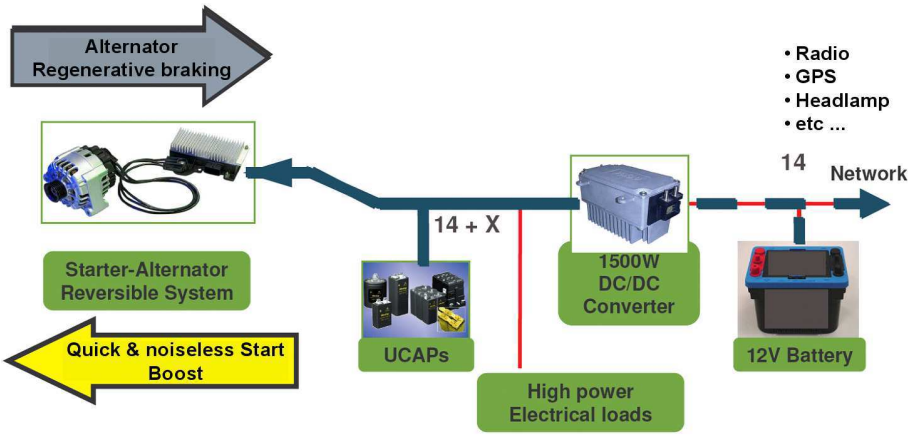

Figure 3.1: Valeo Starter Alternator Reversible System

With several millions of natural gas vehicles (NGV) being used worldwide, natural gas is nowadays considered a viable alternative to petroleum as a transportation fuel. Indeed, natural gas reduces greenhouse gas (GHG) and pollutant emissions, promotes energy diversification, thanks to its abundance on earth, and leads to a high combustion efficiency. As shown by a 2005 study conducted by IFP (Tilagone et al. (2007)), the use of compressed natural gas in a dedicated (mono-fuel) downsized turbo-charged SI engine is particularly attractive for light-duty vehicles in a urban context: a first prototype vehicle based on a MCC `smart` achieved a 27% reduction of CO_2 emissions and reasonably low pollutant levels on the NEDC cycle. However, this study also showed that some CNG characteristics were considerably detrimental to the performance of the demo car. For instance, the production gasoline three-way catalytic converter (TWC), unable to overcome the high stability of methane, put the prototype at disadvantage with respect to pollutant reduction. Moreover, the volumetric efficiency drop, due to natural gas injection, was only partially compensated by the turbocharger: the resulting drivability at low engine speed would probably hinder the acceptance of such a vehicle.

Hence, the rationale behind VEHGAN has been to develop a demo car which takes full advantage of CNG assets, while compensating for its drawbacks. To achieve this goal, several strategies were deployed. First, IFP has worked on engine optimization, increasing the swept volume by 10% and adapting exhaust after-treatment to CNG. After that, the powertrain has been hybridized by adding a small auxiliary power source: a reversible starter-alternator system based on ultra-capacitors. Through the prototype StARS from Valeo shown in Figure 3.1, the resulting mild-hybrid architecture offers some interesting functions such as fast engine restart to implement "stop–and–start", regenerative braking (up to 4kW), torque assist (up to 3kW) and flexible management of on-board consumers. This architecture holds considerable potential for fuel economy, reduction of exhaust emissions and improvement of drivability.

To obtain tight and flexible control of power flows in the powertrain, and take full advantage of the mild-hybrid configuration, IFP has replaced the original engine and automated manual transmission (AMT) control, whose software structure is shown in Figure 3.2, with an integrated powertrain management system, controlling the engine, the transmission, and the starter alternator system.

At the time of writing, the experimental results on the NEDC cycle show that the VEHGAN demo car in "stop–and-start" mode produces CO_2 close to the initial project target of 80 g/km

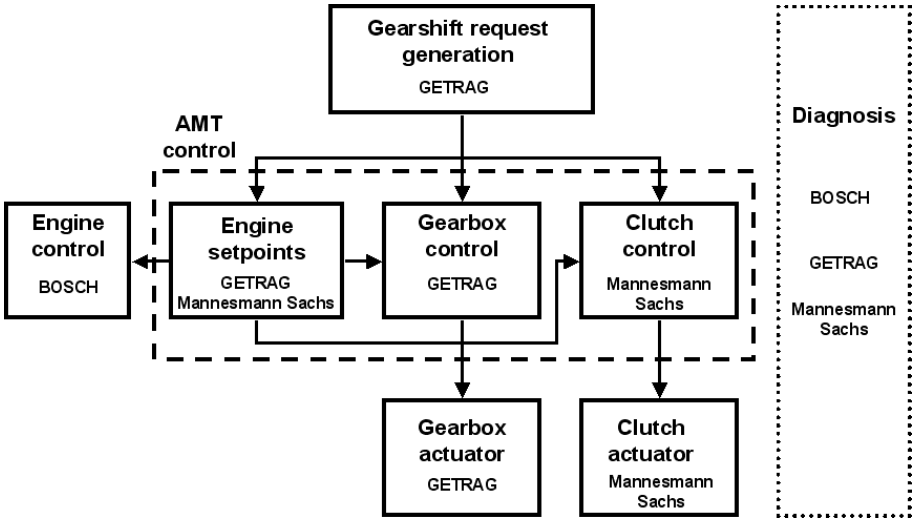

Figure 3.2: Powertrain control software structure in production SMART

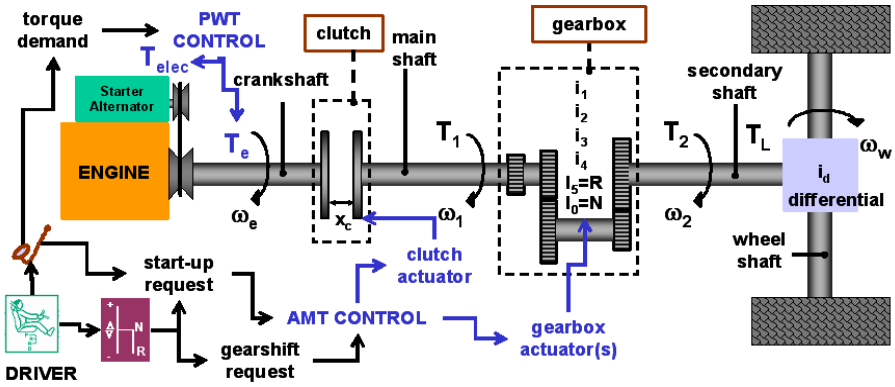

Figure 3.3: Powertrain architecture of VEHGAN

(that is, 32% less than the gasoline version), and pollutant levels well below the Euro 5 limits. Further gains are possible with an appropriate use of the regenerative braking function and of the advanced management of on-board consumers via the StARS. From a drivability point of view, the boost function helps increase the available torque at low engine speed, and the improvement in vehicle acceleration is noticeable to the driver. The performance of current AMT control for vehicle start-up and gearshift maneuvers is satisfactory, but perfectible.

3.2.2 Distinctive Features of the VEHGAN Demo Car

The VEHGAN demo car, whose powertrain architecture is shown in Figure 3.3, is a mild-hybrid vehicle. In a mild-hybrid powertrain, the electric motor can provide small mechanical power to the transmission but not independently from the engine, as opposed to full-hybrid parallel configurations, where the motor and the engine independently providing mechanical power to the same drive shaft. Valeo starter-alternator reversible system (StARS) comprises:

- an electric motor that takes the place on the engine of the conventional starter, driven by a poly-V belt;
- an inverter to manage power flow to and from the electric motor;

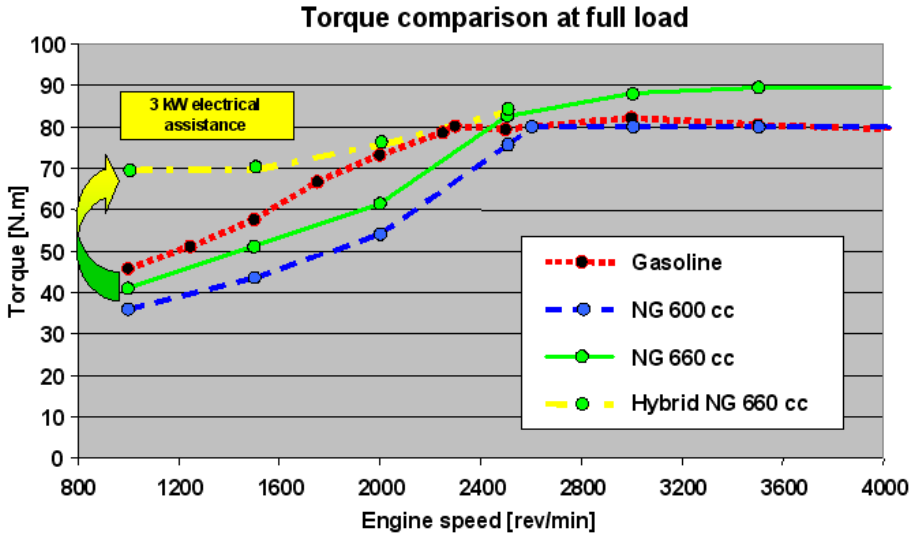

Figure 3.4: Torque increase at low speed using 3kW electrical assistance

- ultra-capacitors with variable voltage (14-24 V) to store power during braking and release it during power assist (boost or start);
- a DC/DC converter to adjust the voltage between networks.

The belt link has been designed for a ratio of 2 to ensure the boost action effectively helps turbo-compressor start-up (at sufficiently low engine speeds). With the nominal motor torque map, the expected torque increase at low engine speed is shown in Figure 3.4. Unfortunately, in the prototype starter-alternator system mounted on the demo car, constraints on maximum induction current prevent continuous control of traction torque. Actually, only regenerative (negative) torque can be controlled in a relatively flexible manner (that is, by specifying a setpoint), while for traction torque, five discrete boost profiles are available plus a special profile for the "stop–and–start" function. This means that the electrical motor torque cannot be considered as a full-fledged high-level actuator to control powertrain dynamics.

The AMT system of the demo car is based, as in standard `smarts`, on electric transmission actuators. The clutch bearing, which permits to press the clutch disk against the flywheel (and to release it) is actuated through a simple DC motor. Contrary to other more complex clutch actuators (hydraulic ones, for instance), a simple PD controller suffices to get good setpoint tracking, with no overshoot and a settling time of 100ms for small changes and of 200ms for steps from fully engaged to fully disengaged position (or vice versa).

`smart` gearbox is also controlled via a DC motor, but with a more complex mechanism. The DC motor rotates a barrel connected to three forks, each of them actuating a synchronizer. As a result, gears are engaged sequentially as the DC motor rotates. A peculiar feature of this system is that, to shift from second to third gear and from fifth to sixth, the gearbox must pass through a sort of "dummy neutral" position. Again, PD control has been used for the DC motor but with a different strategy. In fact, mechanical clearances between the DC motor and the barrel make it difficult to determine an absolute (or relative, between 0 and 100%) set-point value corresponding to the requested gear. An incremental set-point strategy has been adopted, starting from the knowledge of the currently engaged gear. This approach has required a complex finite state machine FSM in the actuator layer of the powertrain control software, but it is totally

transparent for the AMT control strategies, which just need to deal with "high-level" setpoints, such as the requested gear ratio. As to performances, synchronization times are similar to those of the original gearbox control, that is, not very fast (between 350 and 400ms, and twice that when a "dummy neutral" position must be crossed).

The engine is operated similarly to the standard `smart` downsized (600cc or 700cc) gasoline spark-ignition engine, equipped with the GT12 cooled turbocharger produced by Allied Signal Automotive (GARRETT), which allows a maximum torque of 80 Nm from 2000 rev/min to 4500 rev/min (88 Nm in overboost). Beside some mechanical adaptations, the use of natural gas instead of gasoline has required an optimization of exhaust after-treatment, leading to the choice of an appropriate catalyst formulation (to overcome the high stability of methane), and some minor modifications to the standard SI engine control strategies. For the purpose of our thesis, it is only important to recall that the torque produced by the engine can be controlled via "slow" air-path actuators (the air throttle and two wastegate actuators) and, partially, via a "fast" actuator, the spark advance.

As described in (Tona et al. (2007)) and (Tona, Venturi & Tilagone (2008)), the `smart` production engine and transmission electronic control units have been replaced by IFP in-house rapid prototyping powertrain control system, thus making this demonstrator a very flexible testbed for advanced powertrain control strategies.

IFP engine and powertrain control development cycle, shown in Figure 3.5, has covered all the phases of the project, from engine studies to vehicle demonstrator. Within this cycle, engine control design is first carried out using a reference simulation model developed from the available engine characteristics and calibrated with engine bench tests. Coded in AMESim, they can be run in co-simulation with the corresponding control system, coded in Matlab/Simulink. Control and structure algorithms are then iteratively improved using refined versions of the reference simulator. Further tests can be performed using Software-in-the-Loop (SiL) and Hardware-in-the-Loop (HiL) frameworks, based on real-time capable simulators derived from the reference simulator. For demo car applications, the engine simulator developed in the first part of the project is extended to encompass the powertrain to simulate (at least) longitudinal vehicle dynamics, and also declined in different versions from Model-in-the-Loop (MiL) to HiL. This methodology yields meaningful deliverables even in the initial phases of the project, thus allowing fast validation of design choices and reduction of implementation time.

A rapid-prototyping system based on Matlab, Simulink and xPCTarget has been used both for the engine test bench and the vehicle. While engine bench tests were performed with ACEBox, IFP in-house electronic management system, the demonstrator on-board system is based on the GEC system developed by FH Electronics and an industrial micro-PC (Pentium III 1GHZ, RAM 256Mb), and has the structure shown in Figure 3.6. In both cases, control systems validated in co-simulation can be directly "plugged in".

The integrated powertrain control structure described in (Tona, Venturi & Tilagone (2008)) and shown in its Simulink implementation Figure 3.7 has been designed to host the decentralized AMT control strategies presented in (Tona et al. (2007)), that is with a distinct separation, in the intermediate, *functional* layer, between engine and transmission control algorithms. At the supervisor level, it is possible to configure the vehicle in *full-thermal* mode (no StARS functions are used), in *micro-hybrid* mode (only with "stop-and-start") or in mild-hybrid mode, with the regenerative braking and/or boost functions available.

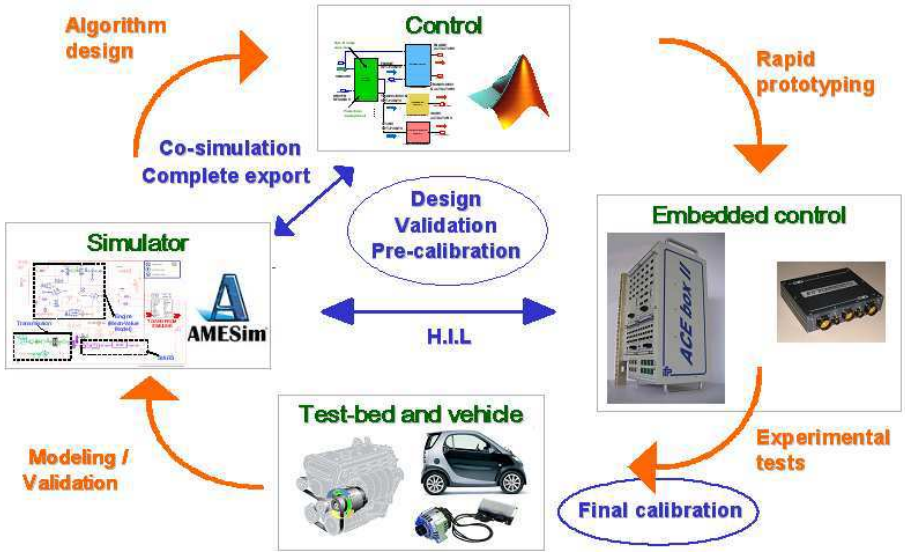

Figure 3.5: Steps and tool-chain for the control development cycle of the VEHGAN demo car

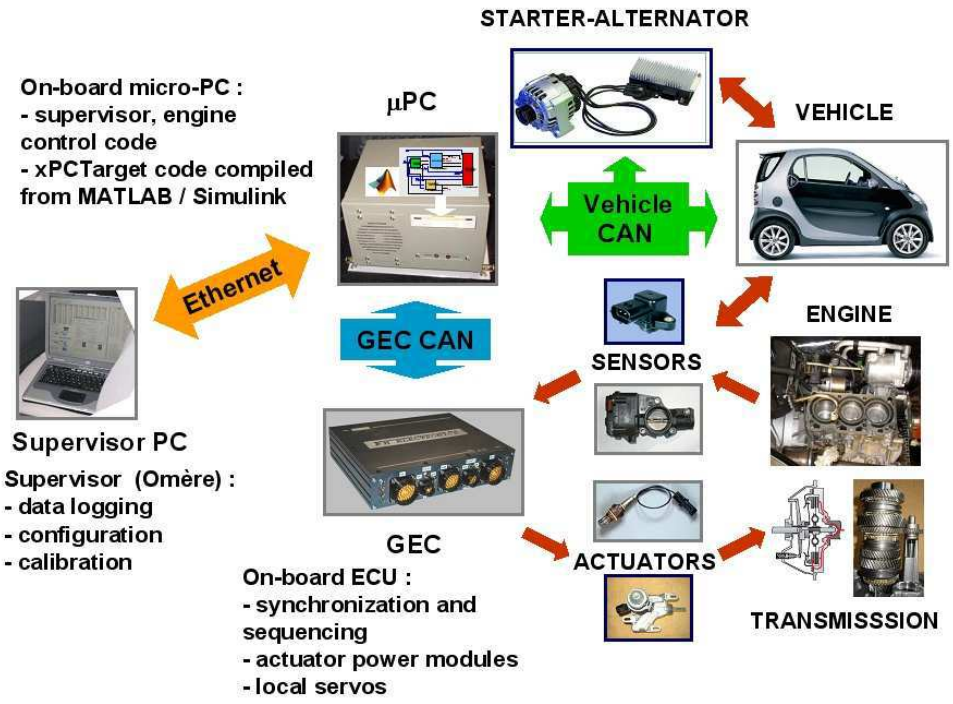

Figure 3.6: VEHGAN on-board rapid prototyping control system

3.3 Implementation of the Unified Predictive Control

The unified model predictive control strategy presented in this thesis has been developed as an alternative to the decentralized PI-based control systems described in (Tona et al. (2007)) and is meant to replace them, should it prove better in terms of performances and ease of calibration.

Its implementation in the integrated powertrain control structure of Figure 3.7 has required some modification to take into account the centralized formulation of the control. More precisely, in the initial software the decentralized PI-based controllers were implemented in the engine and in the transmission control modules (see Figure 3.7). Whereas in the case of the strategy developed in this thesis, the unified approach yields a single controller which has been implemented in the vehicle manager in order to maintain the multivariable structure while complying with the hierarchical torque control.

3.3.1 Control model and controller parameters

The system under consideration can be described by the following simplified powertrain model (already presented in section 1.4):

$$J_e\dot{\omega}_e = \mathbf{T_{comb}} - T_{frict}(\omega_e, .) + T_{elect} - \mathbf{sign}(\omega_{\mathbf{sl}}) \cdot T_c\left(\mathbf{x_c}, .\right) \tag{3.1a}$$

$$\left[J_c + J_{eq}\left(\mathbf{i_g}, i_d\right)\right]\dot{\omega}_c = \mathbf{sign}(\omega_{\mathbf{sl}}) \cdot T_c\left(\mathbf{x_c}, .\right) - \frac{1}{\mathbf{i_g}\ i_d}\left[k_{tw}\,\theta_{cw} + \beta_{tw}\left(\frac{\omega_c}{\mathbf{i_g}\ i_d} - \omega_w\right)\right] \tag{3.1b}$$

$$J_w\dot{\omega}_w = k_{tw}\theta_{cw} + \beta_{tw}\left(\frac{\omega_c}{\mathbf{i_g}\ i_d} - \omega_w\right) - T_L\left(\omega_w, .\right) \tag{3.1c}$$

$$\dot{\theta}_{cw} = \frac{\omega_c}{\mathbf{i_g}\ i_d} - \omega_w \tag{3.1d}$$

where:

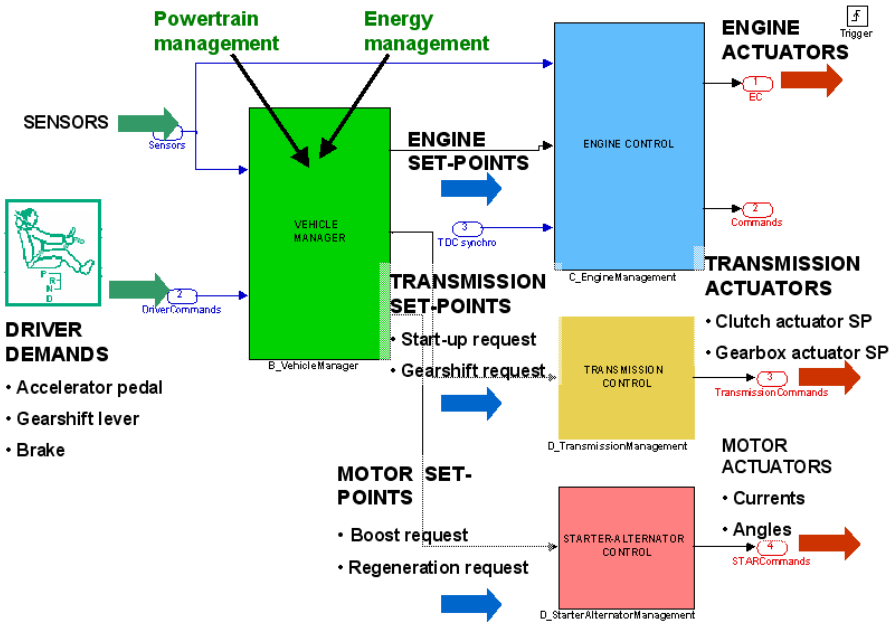

Figure 3.7: Integrated powertrain control for VEHGAN

- ω_e, ω_c and ω_w are the rotating speeds of the engine, the clutch and the vehicle, respectively;
- θ_{cw} is the angular position between the main and the secondary shafts of the gearbox;
- T_{comb} and $T_c(x_c)$ are the engine and the clutch torques respectively;
- i_g is the selected gear ratio, a high level control input defined by the vehicle manager in response to driver requests or forced gearshift conditions;
- T_{elect} is the electric torque which is supposed to be supplied in alternator mode by the StARS.

The parameters of the simplified control model are summarized in table 3.1.

Name	Description	Value	Units
J_e	Engine inertia	0.09	$kg \cdot m^2$
$J_{eq}(i_g, i_d)$	Equivalent inertia	$J_{eq}(i_g, i_d) = J_m + \frac{1}{i_g^2}\left(J_{S_1} + J_{S_2} + \frac{J_t}{i_d^2}\right)$	$kg \cdot m^2$
J_c	Clutch inertia	$J_c + J_{eq} \simeq 0.003$	$kg \cdot m^2$
i_d	Differential ratio	4.92	-
i_g	Gearbox ratios	[3.41 1.95 1.37 1.05 0.85]	-
k_{tw}	Elasticity coefficient	5000	Nm/rad
β_{tw}	Friction coefficient	250	$Nm/(rad/s)$

Table 3.1: Parameters of the assumed powertrain model. With respect to J_c, the dependence of J_{eq} on the gear ratio i_g can be neglected (Glielmo et al. (2006)).

Recall that, as far as control design is concerned, the engine and the clutch speeds are the controlled variables while the engine torque and the transmitted clutch torque setpoints are the manipulated control inputs. A simplified model has been presented in section (2.5) in order to design the AMT control while taking into account the real-time implementation issues. More specifically, the slipping speed ω_{sl} has been chosen as a controlled variable, instead of the mainshaft speed, while two unmeasured quantities δ_e and δ_e have been introduced to cope with non modeled dynamics and inner control loop imperfections. These variables are estimated using dedicated observers. This results in the following simplified model:

$$\dot{\omega}_e = a\, T_{comb} - a\, \underbrace{\left(T_{frict}(\omega_e, .) + T_{elect}\right)}_{\delta_e} - a\, T_c\,(x_c, .) \tag{3.2a}$$

$$\dot{\omega}_{sl} = a\, T_{comb} + a\, \underbrace{\left(-T_{frict}(\omega_e, .) + T_{elect}\right)}_{\delta_e} - (a+b)\, T_c\,(x_c, .) + b\, \underbrace{T_L(.)}_{\delta_c} \tag{3.2b}$$

where: $a = J_e^{-1}$ and $b = [J_c + J_{eq}\,(i_g, i_d)]^{-1}$

The tunable set of parameters includes the observer parameters as well as the MPC related ones. The main parameters are summarized in table (3.2).

3.4 Validation Approach

The development and the validation of the unified model predictive control strategy have been carried out in three different environments:

Name	Description	Value	Units
θ_1	tuning parameter for $\hat{\delta}_e$ estimator	12	-
θ_2	tuning parameter for $\hat{\delta}_c$ estimator	12	-
λ	weighting factor for the *no-lurch* condition	2	-
t_f-map	map: accelerator pedal pos. $\rightarrow$ slipping time duration	$t_f := f(X_{pedal})$	s
x_c-map	map: clutch torque $\rightarrow$ clutch bearing position	$x_c := f(T_c)$	%

Table 3.2: Parameter of the unified MPC control.

- in SIMULINK, simulating the model predictive controller alone on simplified powertrain models;
- within the full powertrain control system (SIMULINK) in co-simulation with detailed powertrain models (AMESIM);
- within the full powertrain control system in real-time (SIMULINK–XPCTARGET) on the VEGHAN demo car.

The first phase of the validation enables to validate the principle and to obtain the nominal performances of our control. The model implemented in Simulink is the reduced-order model (3.2) used for control design to which disturbances are applied to simulate neglected dynamics. Thus, this environment allows to evaluate the nominal performance of the estimators.

The second phase has been carried-out in a co-simulation environment. On the control side, the integrated powertrain control software developed for the VEHGAN project has been used, with the modifications required to implement a centralized (that is, multi-input multi-output) AMT controller. On the powertrain simulator side, in AMESIM, we have both benefited from and contributed to the different versions developed in the framework of VEHGAN.

The reference 0-D high-frequency phenomenological model, built with components of the AMESIM IFP Engine library, can reproduce the dynamic behavior of the complete engine with a timescale of down to 0.1 crankshaft degree. However, the engine-cycle time scale suffices to capture the relevant longitudinal dynamics during start-up and gearshift control, so a mean-value engine model (MVEM) has been used for most co-simulation tests. The gearbox and the clutch are modeled through components belonging to the IFP Drive library and to the Powertrain library, respectively. To represent clutch friction a reset integrator model is used with stiction and Coulomb friction. A look-up table is used to approximate the nonlinear dependency of transmitted clutch torque from clutch bearing position (temperature dependency is neglected). Since the low-level actuators of both clutch and gearbox are PD-controlled DC motors, their dynamic behavior can be represented by simple transfer functions. To simulate StARS, we have developed a special AMESIM library with blocks corresponding to each component. A phenomenological model can be used, with some simplifying assumptions, for the motor-inverter pair, the ultra-capacitor and their low level control system (provided by Valeo). As explained in (Rousseau et al. (2007)), even though the starter-alternator is a permanent magnet motor, the evolution of motor torque and of ultra-capacitor voltage can be predicted using the equations of a separately excited DC motor, a simple RC equivalent circuit for the ultra-capacitor, and a static link between currents and voltages on both sides of the inverter, acting as a control parameter. Finally, vehicle motion is represented via standard IFP drive components. The resulting MVEM simulator is shown in Figure 3.8

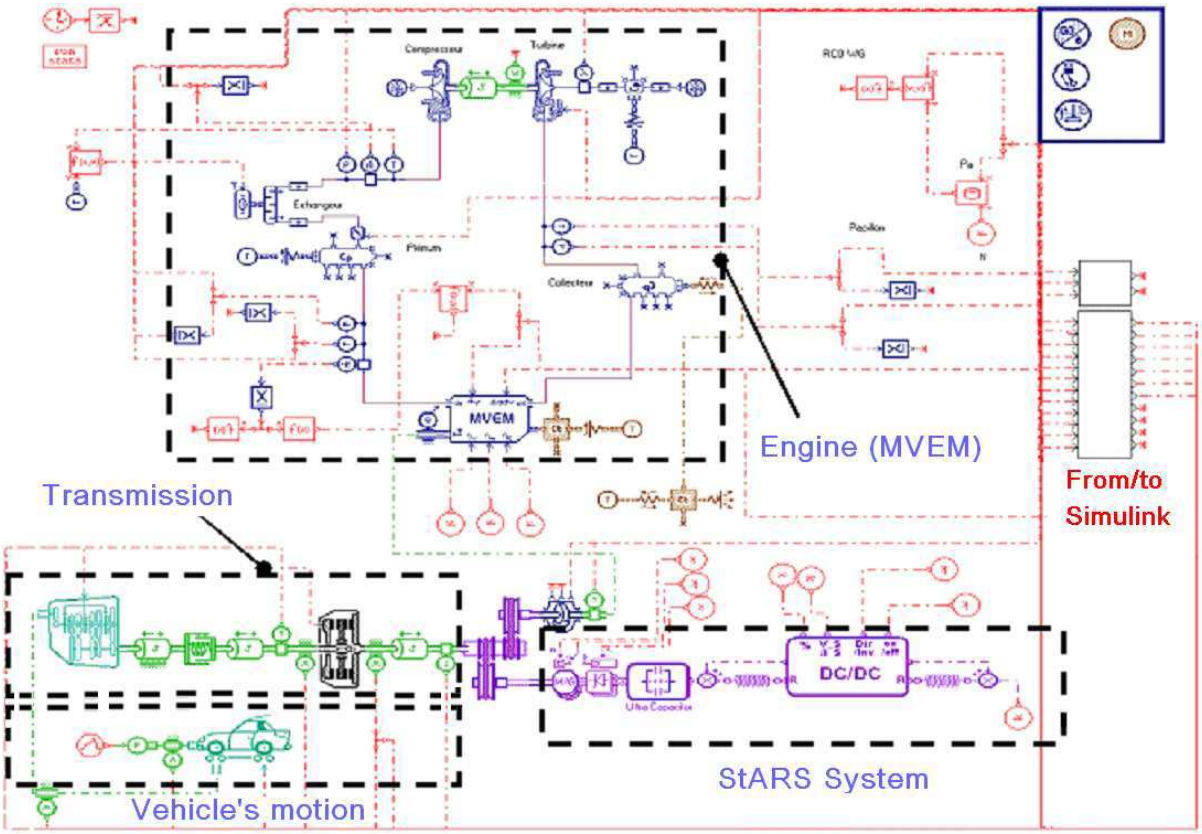

Figure 3.8: AMESim powertrain simulator in the co-simulation framework for the VEHGAN demo car

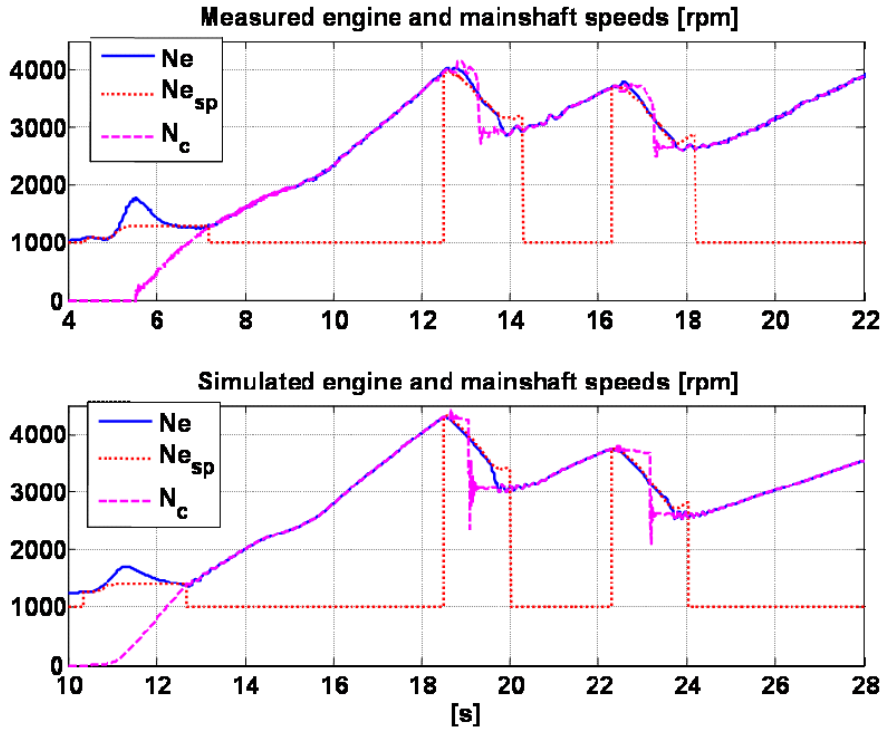

Figure 3.9: Comparison of co-simulation and experimental results for powertrain dynamics

As described in (Tona, Gautier & Amari (2008)) this co-simulation framework has proven realistic enough not only for testing but also for pre-calibration of AMT control systems. The simulated powertrain dynamics results of Figure 3.8, for instance, have been obtained by feeding the co-simulation software with measurements of the relevant driver commands: accelerator pedal, brake pedal, gearshift lever. They are indeed very close to experimental powertrain dynamics results.

The ultimate phase of the validation of the unified model predictive controller has been performed on the real vehicle, with the hardware and software configuration described before (see Figure 3.6). It is meant to compare the performance of our strategy with those of an already implemented AMT control system (the reference control system for the VEHGAN demo car), on one hand, and to show its compatibility with the constraints of embedded control, on the other hand.

In the following section, we present the results obtained on each environment: simplified simulation, co-simulation framework and the real demo-car. First the results on vehicle start-up are discussed, then those on gear shifting. A brief section on the performance of idle-speed control closes the validation discussion.

3.5 Validation of Vehicle Start-up Control

3.5.1 Simulation results

As stated before, a first validation is carried in simulation: both the control system and the nominal reduced-order powertrain model are coded in the SIMULINK environment. On one hand, this approach enables a rapid validation of the control system, based on the simplified prediction model. On the other hand, it makes it easy to assess the effectiveness of the observers in calculating the estimated torques $\hat{\delta}_e$ and $\hat{\delta}_c$, since δ_e and δ_c can be arbitrarily chosen in this simplified simulation environment. The validation of the basic assumptions underlying control design would be more difficult in the co-simulation framework and in real-time on the vehicle.

Among several simulation tests, we have selected two typical cases for presentation, corresponding to a low and high torque demand from the driver, respectively.

In the first test, whose results are shown in Figure 3.10, the driver asks for a slow vehicle start-up by pressing little and gradually the accelerator pedal (see the values of the accelerator pedal position).

In this case, since the torque demand is low, the control can carry out the vehicle start-up without changing the operating point of the engine speed. That is to say, the engine speed is maintained constant to the former idle speed set-point, as shown in Figure 3.10.a. In order to test how the control fulfils the specifications on the control inputs T_e and T_c, hard constraints are specified on T_e and T_c and on their variation rates. Notice that, at the beginning of the start-up, the variation rates $\dot{T}_e$ and $\dot{T}_c$ saturate, and this is reported on the parameter N_f^* [see equation (2.20) where the parameter N_f is used to define the reference trajectory on the slipping speed], which shows a significant increase with a peak of about 50 (see Figure 3.10.b). This saturation on the derivatives is maintained until the engine torque reaches its limit T_e^{Max}. Then, the constraints are progressively relaxed, and the parameter N_f^* reaches the initial desired value N_f^0, at the end of vehicle start-up. Note that in the above discussion, the decision variable N_f is intimately linked to the scalar parameter p that is used in the definition of the parameterized MPC since $p = N_f \cdot \tau$.

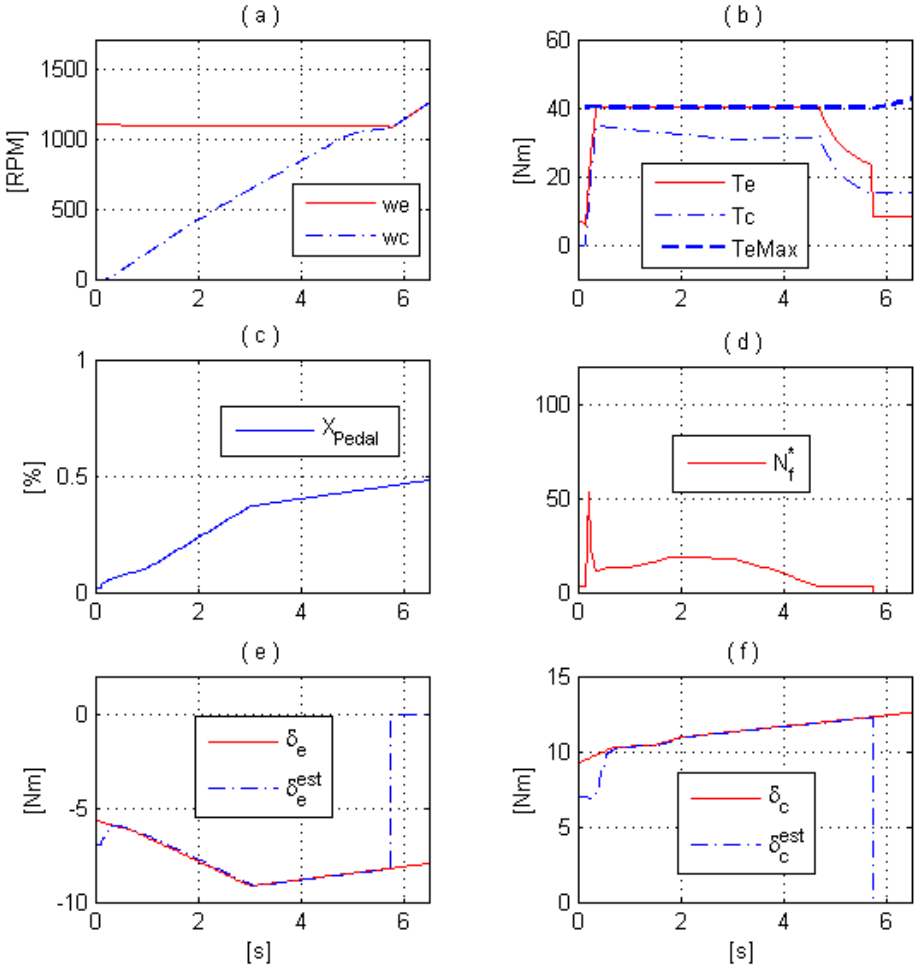

Figure 3.10: Simulation: vehicle start-up in the case of low torque demand. **(a)**: engine and mainshaft speed; **(b)**: control inputs T_e and T_c, $T_c^{max} := T_e^{max}$; **(c)**: accelerator pedal position; **(d)**: parametrization of the control; **(e)**: δ_e estimator; **(f)**: δ_c estimator.

The dynamics of the estimated quantities $\hat{\delta}_e$ and $\hat{\delta}_c$ are represented in Figure 3.10.e and Figure 3.10.f respectively, and compared to δ_e and δ_c, assumed known. During the pedal mode, following the start-up; the observers are turned off, and estimated quantities are set to zero.

The second simulation test concerns a situation where the torque demand is significant and the produced engine torque stays close to its limit (with respect to engine speed) during most of the start-up.

In this case, the control manages to change the engine operating point, allowing a higher production of combustion torque. This feature is introduced through the definition of the engine speed reference trajectory as described in section 2.5.6a. Figure 3.11 shows how the increase of engine speed allows the torque limit to be pushed up, as shown in sub figure (b). The clutch torque is temporarily penalized, with a local decrease around 1 s, before it is allowed to increase again. As shown on Figure 3.10.d., the constraints on the control inputs are handled through the parameter N_f^*, similarly to the previous test, but with higher values this time, which shows that the start-up with higher torque demand is more "difficult" to handle. Concerning the observers,

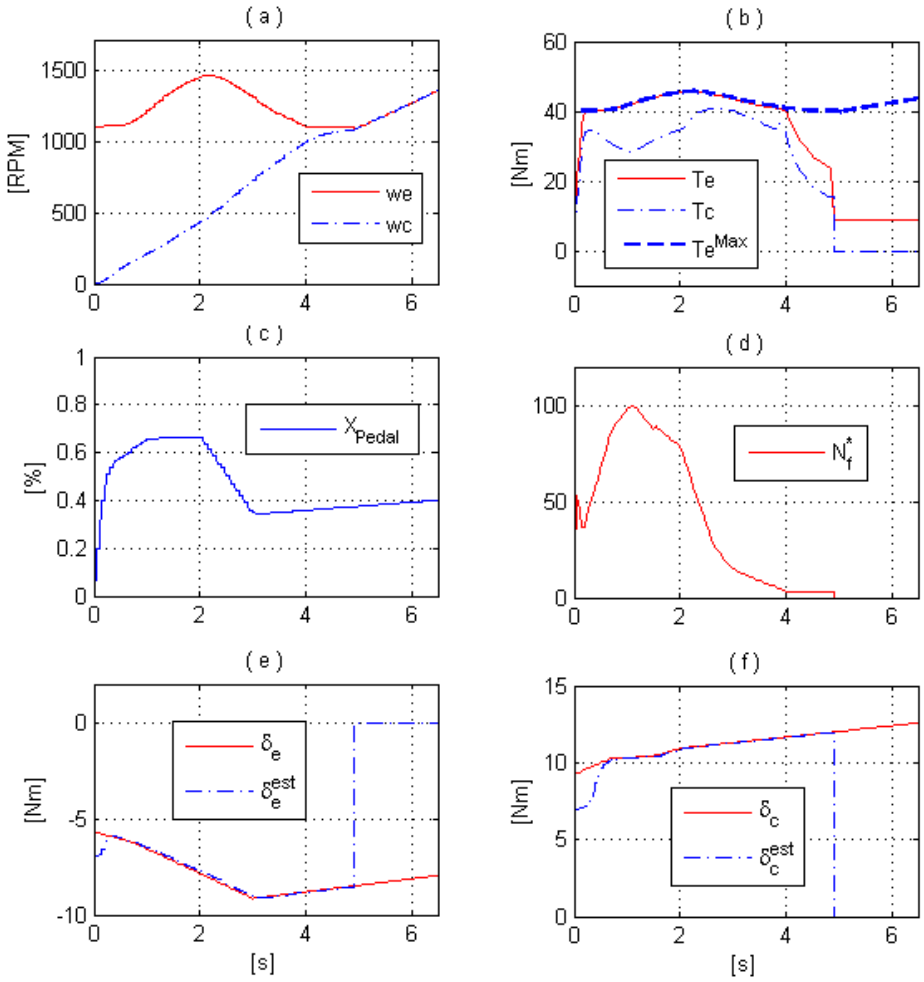

Figure 3.11: Simulation: vehicle start-up in the case of high torque demand. **(a)**: engine and mainshaft speeds; **(b)**: control inputs T_e and T_c, $T_c^{max} := T_e^{max}$; **(c)**: accelerator pedal position; **(d)**: parametrization of the control; **(e)**: δ_e estimator; **(f)**: δ_c estimator.

the same considerations as in the previous case apply.

3.5.2 Co-simulation results

The second phase of the validation of vehicle start-up control is carried out in a co-simulation framework, which includes complex and more accurate models. More specifically, eventual transmission oscillations induced by the control system can be reproduced, so this environment enables to test if the *no-lurch* conditions presented before in section 2.5.3 are respected. The co-simulation environment also includes modeling of the electric components, enabling a further validation of the control when the STARS functions are activated.

Figure 3.12 shows the results of vehicle start-up control in the co-simulation environment. For this test, an additional constraint related to the discontinuity of the applied control input T_e at the terminal instant t_f has been added to the model predictive control law. This constraint tends to impose a continuity on the control input during the transition from the vehicle start-up phase to pedal mode, which could be beneficial to avoid transmission oscillations due to sudden

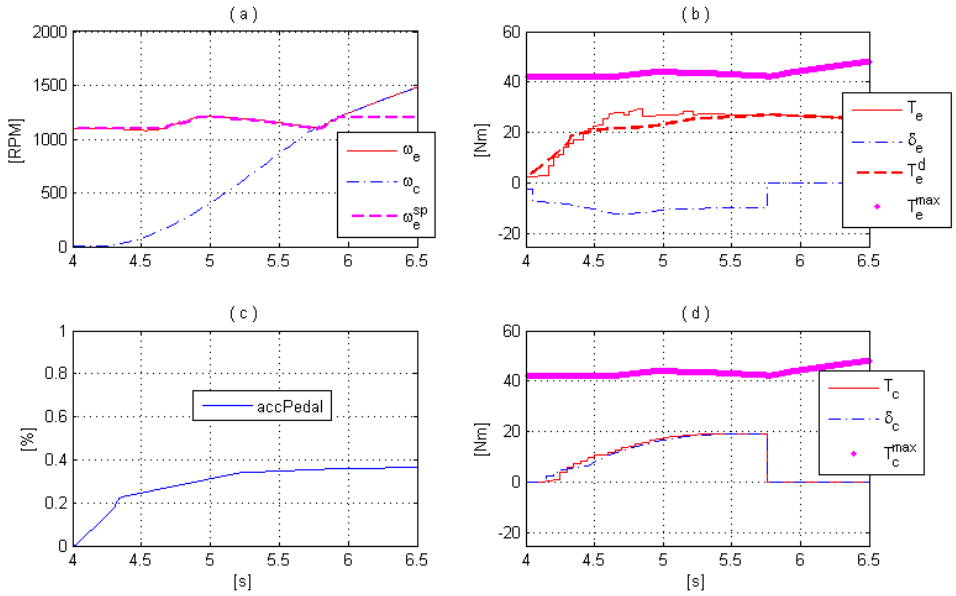

Figure 3.12: Co-simulation Simulink/AMESim : vehicle start-up. **(a)**: engine and mainshaft speeds; **(b)**: control input T_e and its limitations; **(c)**: accelerator pedal position; **(d)**: control input T_c and its limitations.

engine torque variations. As a consequence, the model predictive control should manage to keep the control T_e as close as possible to the open-loop value when the slipping speed is going to zero. Namely:

$$T_e := \begin{cases} T_e^{MPC} & t < t_f \\ T_e^d & t \geq t_f \end{cases}$$

where:

- T_e^{MPC} is the control input of the MPC strategy;
- T_e^d is the open-loop control;
- t_f is final instant where the slipping speed becomes null.

Referring to Figure 3.12.a, where engine speed ω_e and mainshaft speed ω_c are shown, the control achieves a good clutch engagement and no oscillations are induced. Furthermore, the continuity condition, related to the control T_e at the final instant $t_f \simeq 5.75s$, is also respected , as shown on the Figure 3.12.b. However, it must be underlined that, whether this condition is enforced or not, the results do not differ much. As we will see in the following, for the real-time application, we chose not to include this constraint in control design, to avoid increasing the computational load unnecessarily.

As a further validation of vehicle start-up in the co-simulating environment, we can activate the Stars system and let it provides an electric boost torque, by assuming the same accelerator pedal position, as in the previous test (see Figure 3.12). In other words, to simulate one of the demo car operating modes, an electric torque is superimposed to the engine torque to achieve faster start-up and the control must deal with it as an external disturbance. The resulting electric torque, which depends on the chosen boost level, on engine speed and on the ultra-capacitor voltage, is represented in Figure 3.13.e, whereas the engine speed and the ultra-capacitor voltage

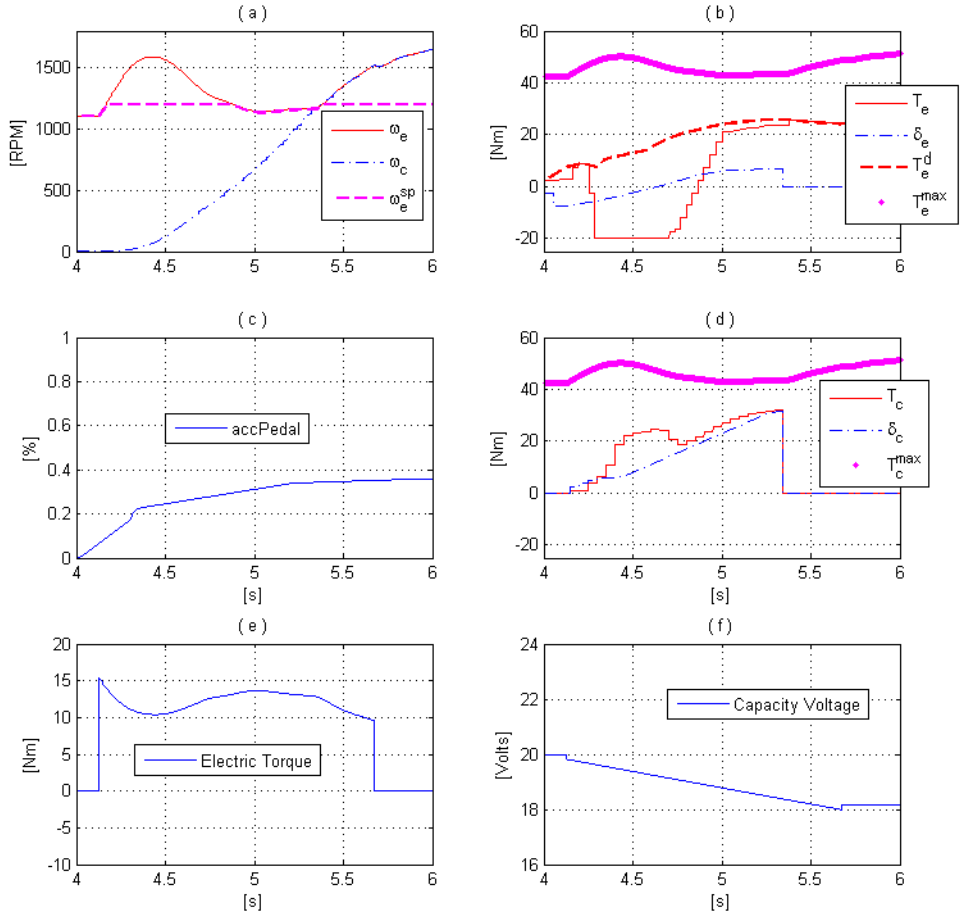

Figure 3.13: Co-simulation Simulink/AMESim : vehicle start-up with electric boost. **(a)**: engine and mainshaft speeds; **(b)**: control input T_e and its limits; **(c)**: accelerator pedal position; **(d)**: control input T_c and its limits; **(e)**: electric torque; **(f)**: ultra-capacitor voltage.

are illustrated on the sub figures (a) and (f), respectively. The motor speed is not shown, as the belt link makes it twice the engine speed. At the beginning of the vehicle start-up, one can notice an important overshoot of the engine speed which is due the high level of the electric torque. In this specific situation, the control reduces the engine torque to its lowest limit, and allows a local increase of the clutch torque, as shown in sub figures (b) and (d) in the time interval `[4.2 4.7]`. As a consequence, the engine speed can be made tracking its reference trajectory rapidly, as reported in sub figure (a). This leads to a relatively fast start-up, as expected. For a comparison, in the previous test in "pure thermal" mode, vehicle start-up ends at `t`$\simeq$`5.8s`, whereas with electrical assistance it ends `t`$\simeq$`5.4s`. Overall, at the end of vehicle start-up phase, the engine speed follows its set-point, the control input T_e is converging to the pedal torque, and there is no induced oscillations on the transmission.

It is worth underlying that the structure of the MPC design makes it easy to incorporate the electrical boost as a control input rather than as a exogenous disturbance. One has only to add this term as a third control variable u_3 and the structure of the control design remains unchanged.

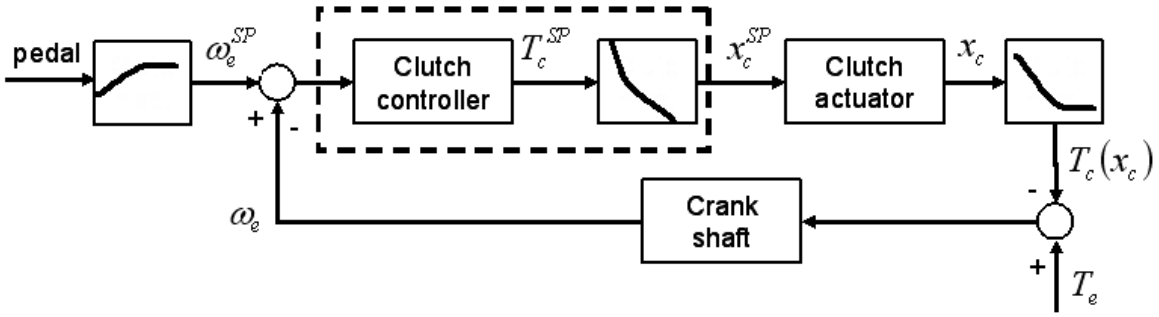

Figure 3.14: PI-based control of the engine speed through clutch position during vehicle start-up.

3.5.3 Experimental Results on the Demo-car

As mentioned before, the experimental results of the proposed unified model predictive control will be evaluated by comparing them to those of the reference control strategies currently implemented on the demo car.

The reference control strategy for vehicle start-up is discussed and experimentally evaluated in Tona et al. (2007). The main idea of this strategy (adapted from Zanasi et al. (2001)) is to let engine torque control respond in open-loop (T_e^d) using the pedal torque map $T_e^d(X_{pedal}, \omega_e)$, whereas the engine speed ω_e is regulated at an appropriate set-point (higher than idle speed) ω_e^{SP} using the clutch actuator (see Figure 3.14). When ω_e exceeds ω_e^{SP}, the clutch starts closing, thus reducing ω_e. When the driver releases the pedal, ω_e drops below ω_e^{SP}, and the clutch automatically reopens. A hybrid supervisor is needed to fully close the clutch after lock-up, otherwise the clutch would indefinitely stay in the lock-up position. Moreover, the nonlinear clutch torque characteristic should be taken into account in the controller (that is, inverted). During clutch closing at start-up, assuming the slipping speed always positive, crankshaft dynamic can be shortly written as:

$$J_e\dot{\omega}_e = T_e^d - T_c \tag{3.3}$$

If clutch controller tracking dynamics is fast enough, after a transient we will have:

$$J_e\dot{\omega}_e \cong 0 \Rightarrow T_c \cong T_e^d \tag{3.4}$$

that is, the torque transmitted by the clutch to the driveline during start-up will be approximately equal to the torque requested by the driver. This gives us a way to act on vehicle acceleration during vehicle start-up, in the same way as engine control normally responds to acceleration pedal requests with the clutch fully engaged. This strategy is very easy to implement and does not require as much calibration time as the standard AMT control system based on look-up tables. However, the generation of appropriate engine speed trajectories to take into account driver torque demand is not straightforward, especially during the initial transient. Notice that equation (3.4) does not hold in general during the initial transient, and as a consequence, engine speed tracking at the beginning of start-up may not be satisfactory.

Figure 3.15 shows a vehicle start-up with the PI-based control. The clutch is smoothly engaged and no oscillations are induced on the transmission. Furthermore, the nature of the strategy guarantees the continuity of the control input T_e during the transition from the start-up

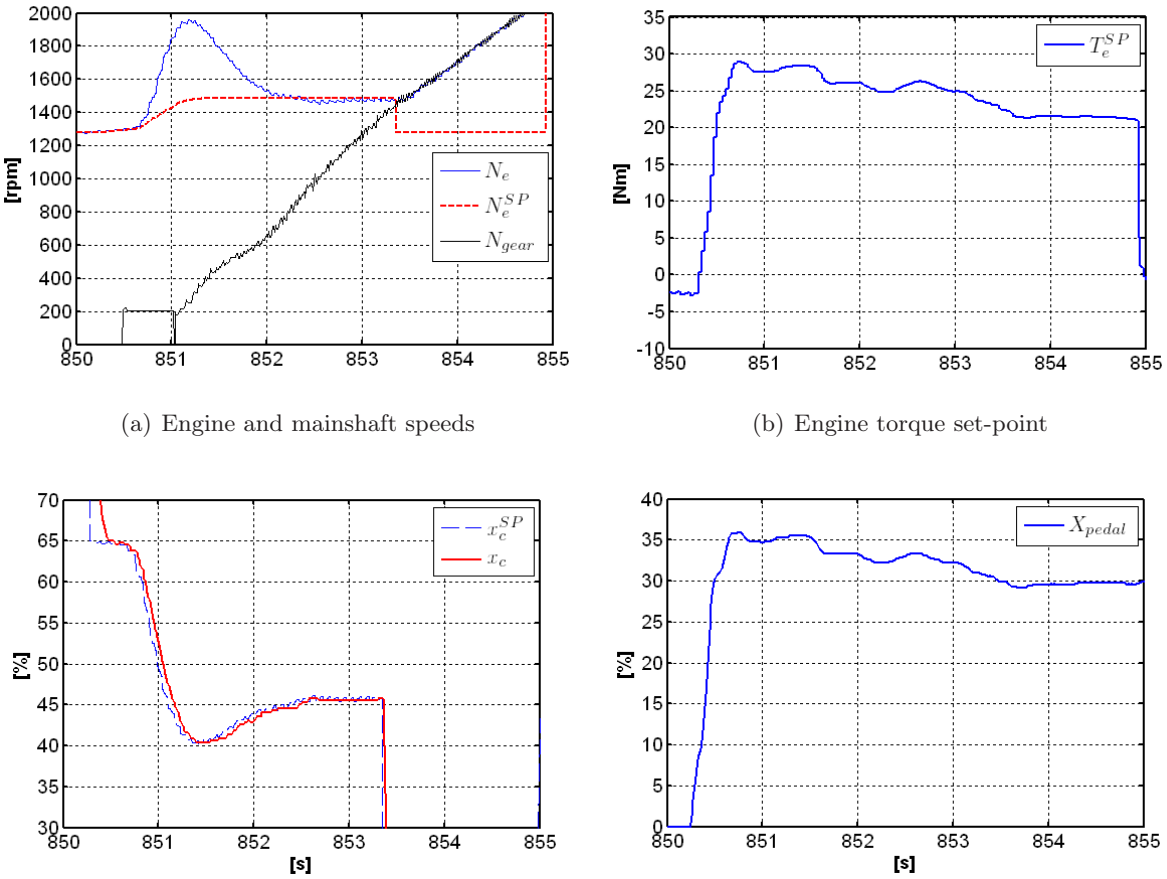

(a) Engine and mainshaft speeds

(b) Engine torque set-point

(c) Clutch bearing position

(d) Accelerator pedal position

Figure 3.15: Vehicle start-up with the PI-based control strategy

phase to the pedal mode (see the instant `t`$\simeq$`853.4s` on the Figure 3.15.b). The time duration of the start-up phase is acceptable ($\simeq$`3s`) but the overshoot of the engine speed is quite large ($\simeq$`500rpm`). This overshoot can be considered as the most significant drawback of this strategy, together with the time required to calibrate the engine trajectory generation. Notice that measurement of clutch speed ω_c ($Ngear$ on the Figure 3.15.a) is not available at low values (<`200rpm`), because of sensor limited sensitivity. This limitation has no effect on the performances of the PI-based strategy, since it does not use clutch speed measurement in the control formulation. Let us underline that the control of the engine speed during idle mode, is achieved through a separate LQ controller.

Contrary to the PI-based approach, the MPC strategy requires measurements of the mainshaft speed or of other transmission rotational speeds that can be related to mainshaft speed (secondary shaft speed or vehicle speed, for instance). An open-loop prediction model is assumed to estimate the mainshaft speed in the range where the sensor does not respond to speed changes ($N_{gear} < 200rpm$).

For a comparative evaluation of the performance the proposed model predictive control during vehicle start-up, three experimental tests are presented.

The first test shows a relatively rapid start-up test, whose results are comparable in engage-

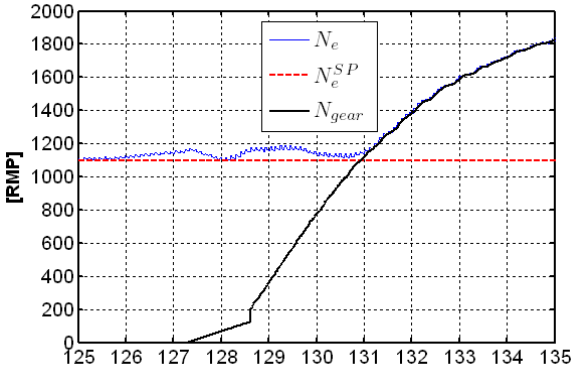

(a) Engine and mainshaft speeds

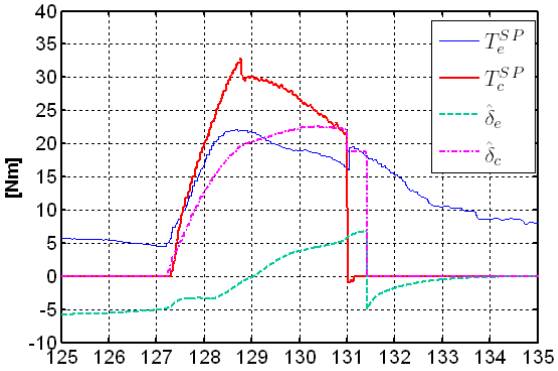

(b) Control inputs T_e & T_c and estimated torques $\hat{\delta}_e$ & $\hat{\delta}_c$

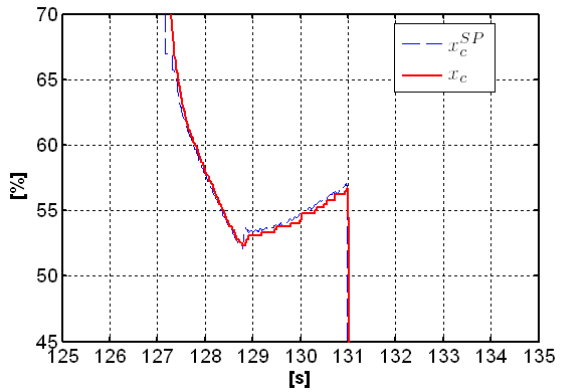

(c) Clutch bearing position

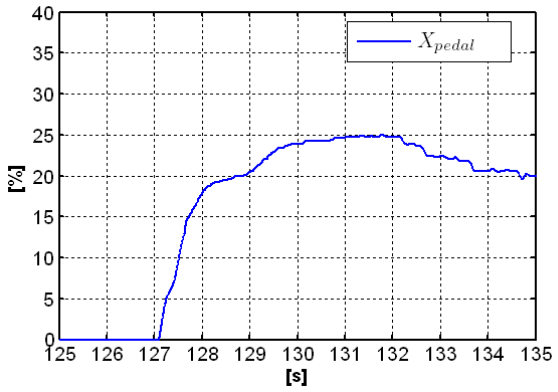

(d) Accelerator pedal position

Figure 3.16: Vehicle start-up with the MPC strategy (faster start-up)

ment time to those of Figure 3.15, obtained with the PI-based approach. As shown in Figure 3.16, the performances of the MPC control are quite good. The overshoot of the engine speed is very limited (`<100rpm`), whereas with the PI-based control it is of approximately `500rpm`. Concerning the fulfilment of the *no-lurch* condition, the MPC control also achieves a smooth clutch engagement since no oscillations are induced on the transmission. It is noteworthy to say that in this case the terminal constraint related to the continuity of the control input T_e at the final instant t_f has been completely relaxed, as it can be noticed from discontinuity of the engine torque at the instant $t = 131s$. Since, it has no sensible effect on real-time performance, this terminal constraint has been completely omitted throughout the experimental tests, in order to reduce the dimension of the control problem.

The second MPC test, whose results are depicted in Figure 3.17, corresponds to a slower vehicle start-up. The comparison with the previous MPC test shows how the accelerator pedal position is used to modulate the duration of clutch slipping and of the overall start-up maneuver. In the first MPC test, this position is approximately `25%` during most of the time, as reported in Figure 3.16.d, and this lets define a slipping phase duration of approximately `4s`. Whereas in the second test, the position of the accelerator pedal is approximately `10%` (see Figure 3.17.d), which causes an increase of the slipping phase duration to approximately `6s`. As in the previous test, there is a discontinuity of the engine torque T_e^{sp} at the terminal instant `t` $\simeq$ `536.7s`, but

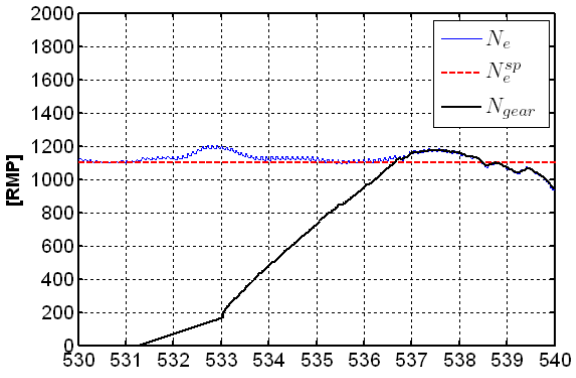

(a) Engine and mainshaft speeds

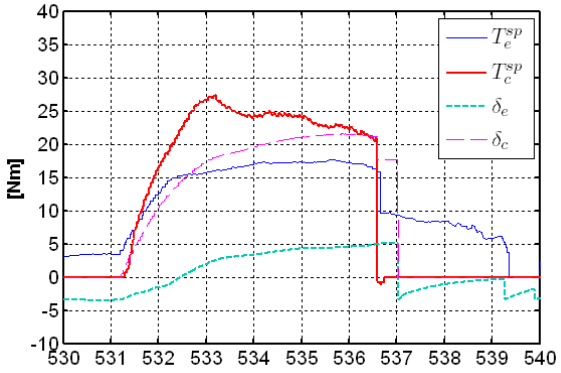

(b) Control inputs T_e & T_c and estimated torques $\hat{\delta}_e$ & $\hat{\delta}_c$

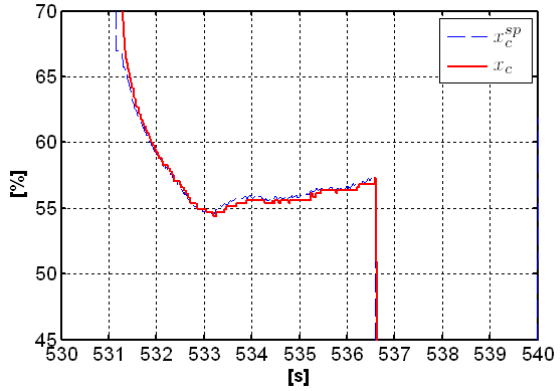

(c) Clutch bearing position

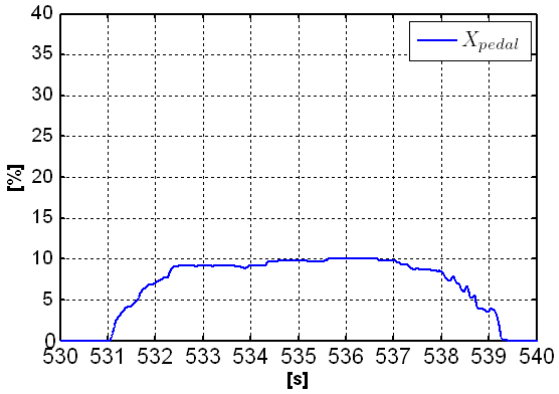

(d) Accelerator pedal position

Figure 3.17: Vehicle start-up with the MPC strategy (slower start-up)

no oscillations are induced in the transmission.

In the third test for MPC validation during vehicle start-up, we impose a rather low limit on the maximum clutch torque T_c^{Max}. More precisely, we suppose that it depends on the upper limit of the maximum engine torque T_e^{Max}, namely:

$$T_c^{Max} = 0.45 \cdot T_e^{Max}(\omega_e)$$

As in the previous tests, the MPC strategy achieves a smooth clutch engagement, while respecting the maximum torque limit of the control input T_c. Figure 3.18.d shows clearly the saturation of clutch torque. We remind that, to handle the constraints the parametrization must compute the optimal value for the parameter $p = N_f \cdot \tau$, by solving online a sequence of unconstrained parameterized problem induced by the dichotomy search for the best p. Figure 3.18.c shows the optimal value N_f^*, that allows to respect the constraints, and the number of iterations needed to get the precision ΔN_f specified for the dichotomy search:

$$|N_f(i+1) - N_f(i)| \leq \Delta N_f$$

where i is the current iteration number.

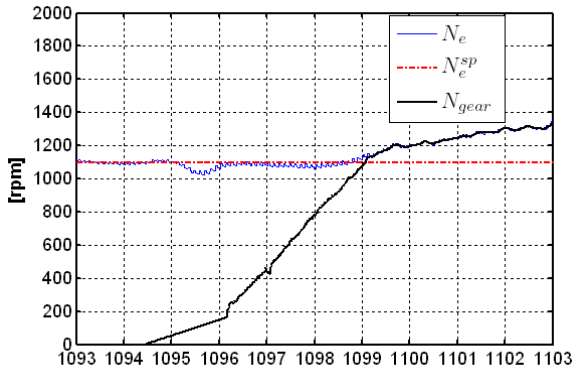

(a) Engine and mainshaft speeds

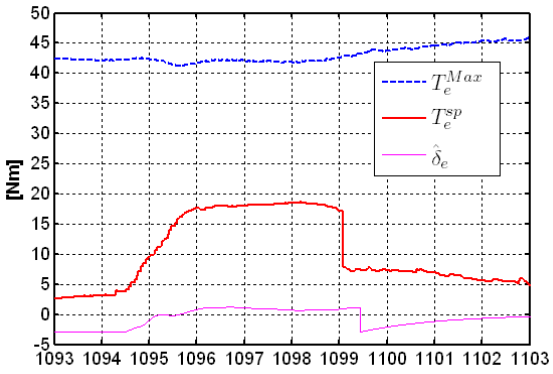

(b) Control inputs T_e and estimated torque $\hat{\delta}_e$

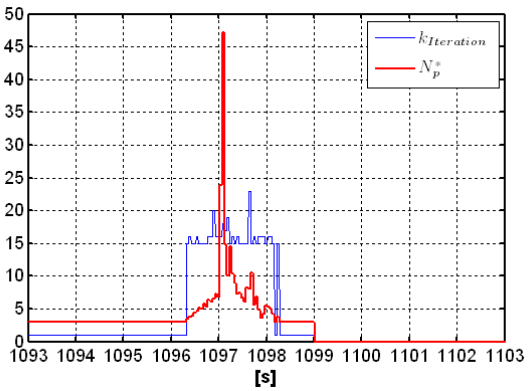

(c) Parameter N_f^* and number of iterations

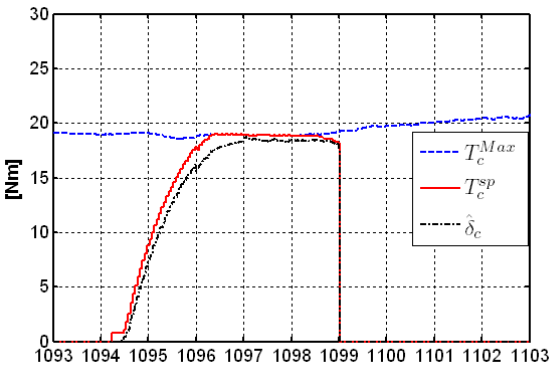

(d) Control input T_c and estimated torque $\hat{\delta}_c$

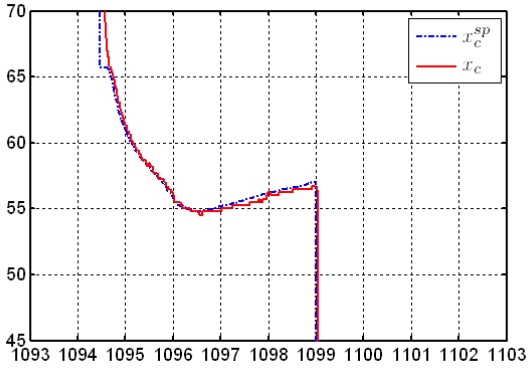

(e) Clutch bearing position (%)

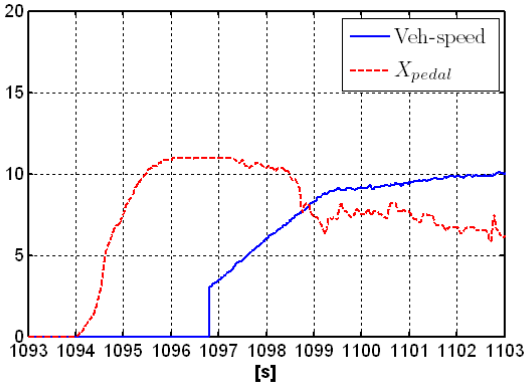

(f) Accelerator pedal (%) and Vehicle speed (km/h)

Figure 3.18: Vehicle start-up with the MPC strategy while testing the saturation of the control input T_c as presented in the quadrant (d).

The number of iterations required to obtain the optimal value of N_f^* depends on the given precision ΔN_f. For the test under investigation, to obtain a precision of 10^{-2} more than 15 iterations are required during actuator saturation, with a peak value of 23 (see Figure 3.18.c).

Finally, Figure 3.19 shows an evaluation of processor computational load due to our algorithm. We remind that the control software is implemented in a fast prototyping environment

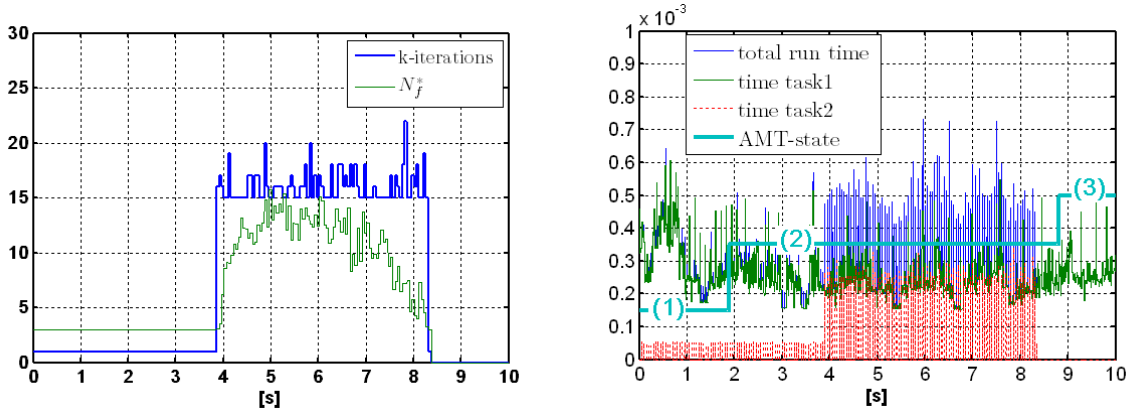

(a) N_f^* Parameter & number of iterations

(b) Computing time & AMT-state

Figure 3.19: MICRO-PC: Pentium III 1GHZ, RAM 256 Mo; The control involves two tasks: main task (task1) and secondary task for the MPC strategy (task2); AMT-state refers to the powertrain modes: (1): idle mode, (2): vehicle start-up, (3): pedal mode.

and runs on an industrial micro-pc, a Pentium III 1GHZ with 256Mb of RAM. The algorithm is parameterized in the same way as for all the experimental tests presented before, with a dichotomy search precision requiring a little more than 20 iterations. The SIMULINK software has been run in a multi-task configuration including two tasks: a secondary task (task2), corresponding to the MPC algorithm, computed every `50ms` and a main task (task1), including the rest of the powertrain control modules, computed every `1ms`. Multi-task mode enables the secondary task to be interrupted if it overruns the main task deadline. The MPC strategy takes approximately `0.05ms` for data initialization and one iteration. Whereas during constraint saturation this time increases to a mean of approximately `0.28ms` (15 iterations) with a maximum of `0.35ms` (21 iterations). As a result, MPC optimization (task2) is never interrupted and there is always enough time to complete MPC computation in one function-call with the deadline being always more than `49.65ms` away.

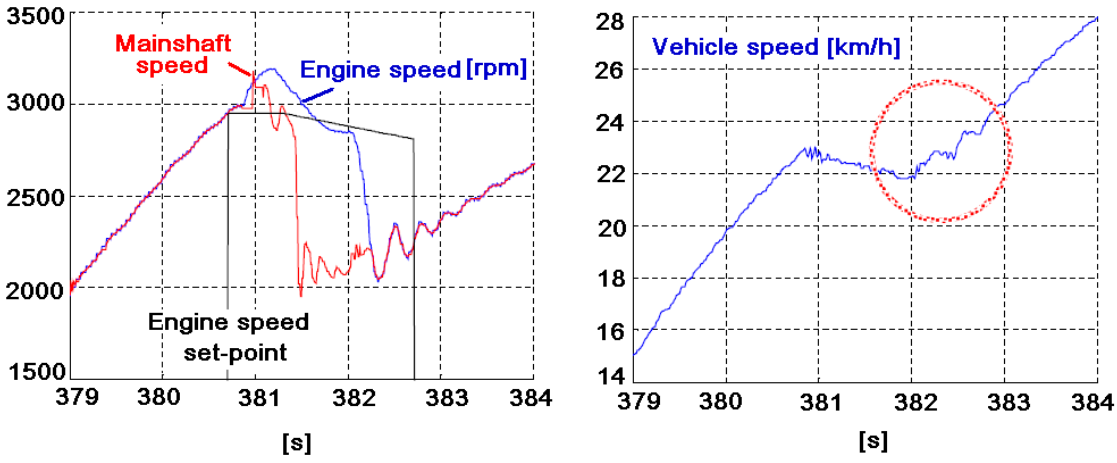

Figure 3.20: Unsatisfactory performance of a ill-calibrated gear shifting control strategy with oscillations induced on the transmission

3.6 Validation of Gear Shifting Control

As for vehicle start-up, AMT gearshift control should ensure a smooth clutch engagement, otherwise oscillations may be induced on the transmission. Figure 3.20 shows typical oscillations that may arise during up-shifting. Those results were obtained during the earliest calibration phase of the PI-based decentralized control strategy which is currently implemented in the demo car. It does not seem relevant for us to present results for gear shifting obtained in SIMULINK on the nominal reduced model: on one hand, the principle of our control strategy has been already validated in section 3.5.1; on the other hand, effective validation of gear shifting control does require the possibility of reproducing transmission oscillations. Thus, we prefer to introduce the validation of gear shifting control, with results obtained within the more accurate co-simulation environment, and to conclude it with the experimental results on the demo-car.

3.6.1 Co-simulation Results

Three tests are presented to illustrate the validation of the MPC strategy in the co-simulation environment. The first test and the second test concern an upshift and a downshift respectively. The third test shows how a possible electric assist can be taken into account during up-shifting, in order to reduce its duration.

As discussed before, the gear shifting phase includes four main sequential sub-states: clutch opening, synchronization, clutch slipping (closing), and clutch (total) closing. The engagement of a new gear during an upshift or a downshift takes place in the synchronization phase, and causes systematically a discontinuity of the mainshaft speed. Figure 3.21 shows an upshift from the first to the second gear. The quadrant (a) shows the controlled dynamics (engine and mainshaft speeds). The quadrants (b) and (d) represent the control inputs (T_e, T_c) and the estimated quantities ($\hat{\delta}_e$, $\hat{\delta}_c$). Whereas, the quadrant (c) resumes the evolution of the sub-states during gear shifting, starting from clutch opening (rising front (1)) to clutch closing (falling front (4)). The synchronization sub-state takes place in the interval (2), which includes the control of the gearbox actuator and the effective engagement of the new gear, whereas the clutch slipping sub-state takes place in the remaining interval (3). During the clutch slipping mode, the MPC

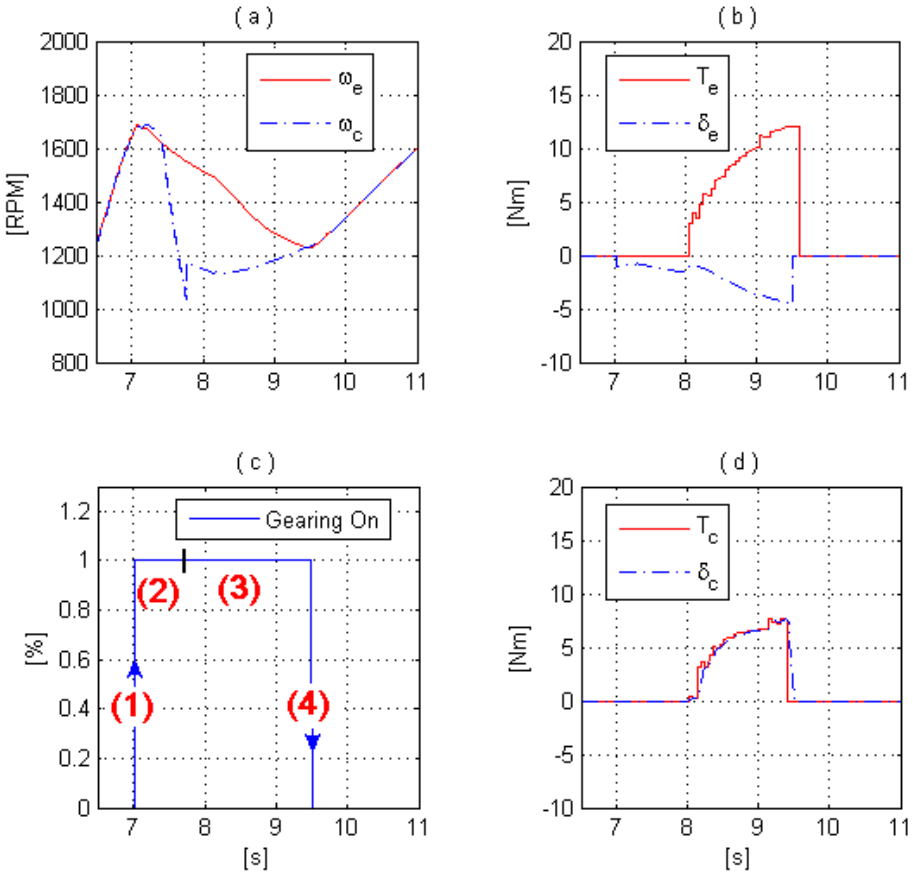

Figure 3.21: CO-SIMULATION: upshift $1 \rightarrow 2$. The sub-states of gear shifting control are: (1) clutch opening, (2) synchronization, (3) clutch slipping (closing), (4) clutch (total) closing.

strategy achieves a smooth clutch engagement and no oscillations are induced in the transmission.

The second CO-SIMULATING test concerns a downshift from the second to the first gear. The corresponding results are reported in Figure 3.22. As for up-shifting, down-shifting also involves the four sequential sub-states recalled before (clutch opening, synchronization, clutch slipping, and clutch total closing), as shown in the quadrant (c). As before, at the end of the downshift, the clutch is completely closed and no oscillations are induced in the transmission. There is however a major difference that is worth underlining, concerning system dynamics: the sign of the slip speed becomes negative when the new gear is engaged (see Figure 3.22.a). The mainshaft dynamics is thus given by the following equation:

$$\left[J_c + J_{eq}\left(i_g, i_d\right)\right]\dot{\omega}_c = -\left|\mathbf{T_c}(\mathbf{x_c}, .)\right| - \frac{1}{i_g\, i_d}\left[k_{tw}\,\theta_{cw} + \beta_{tw}\left(\frac{\omega_c}{i_g\, i_d} - \omega_w\right)\right]. \tag{3.5}$$

which shows how any action on the clutch system would impose a negative clutch torque on the mainshaft, causing an unpleasant deceleration of the vehicle. This deceleration should be avoided unless it is expected by the driver, which is the case when the driver brakes while demanding an upshift. The best that the control can do to avoid it is to maintain the clutch torque to a null value, as shown on the Figure 3.22.a., while using only the engine torque T_e to control the dynamic of the engine shaft. The down-shifting phase in this case is managed similarly to the idle speed mode, in that the control of the mainshaft speed is not needed and is deactivated.

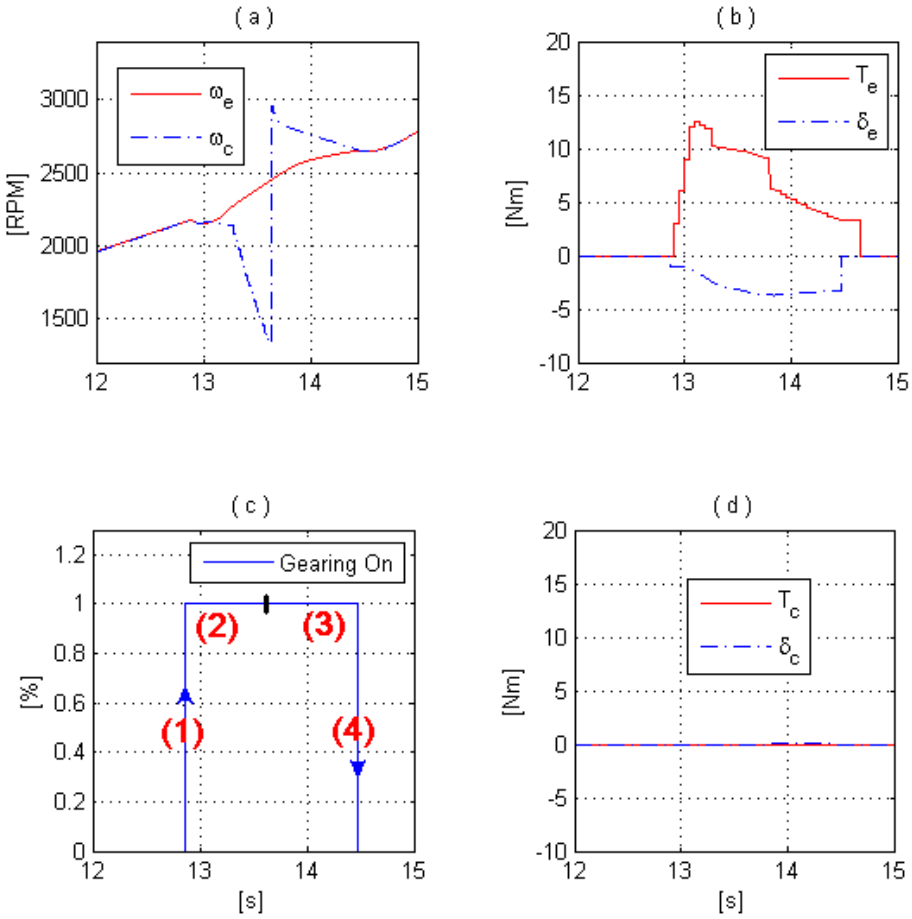

Figure 3.22: Co-simulation: Vehicle down-shifting $2 \rightarrow 1$; During the gear shifting (1) refers to the clutch opening, (2): Synchronization, (3): Clutch slipping, (4): Clutch total closing.

Comparing gearshift durations during up-shifting and down-shifting maneuvers, one can notice that the up-shifting is longer. The main reason is that the control has little or no control possibility to make engine speed decrease during the synchronization phase. Referring to the interval $[7, 8]s$ in Figure 3.21.b, the control T_e is null but the decrease of the engine speed remains relatively slow, since engine speed dynamics in this case are only related to engine internal frictions, that cannot be controlled. This remark is valid for conventional pure-thermal powertrains. But in a parallel hybrid or mild-hybrid electric vehicle, it is possible to use the electric module to impose negative electric torques on the engine shaft, thus enabling the control of engine speed decrease during the synchronization phase.

In the VEHGAN demo car, the StARS system enables electric braking recovery by storing electric power in the ultra-capacitors. To show the potential given by this additional degree of freedom, we have implemented an additional controller which brings the engine speed to its set-point using only the electric torque as a control input. Figure 3.23 shows how electric assist during the synchronization phase enables to reduce considerably the duration of up-shifting. Since engine speed reaches the desired set-point before the end of the synchronization phase (see quadrant (a) of the Figure 3.23), the clutch can be directly closed once the new gear is engaged. Thus, the duration of the gear shifting phase becomes very close to that of the synchronization phase. In quadrant (d), one can remark that the control T_c remains null, as the clutch slipping

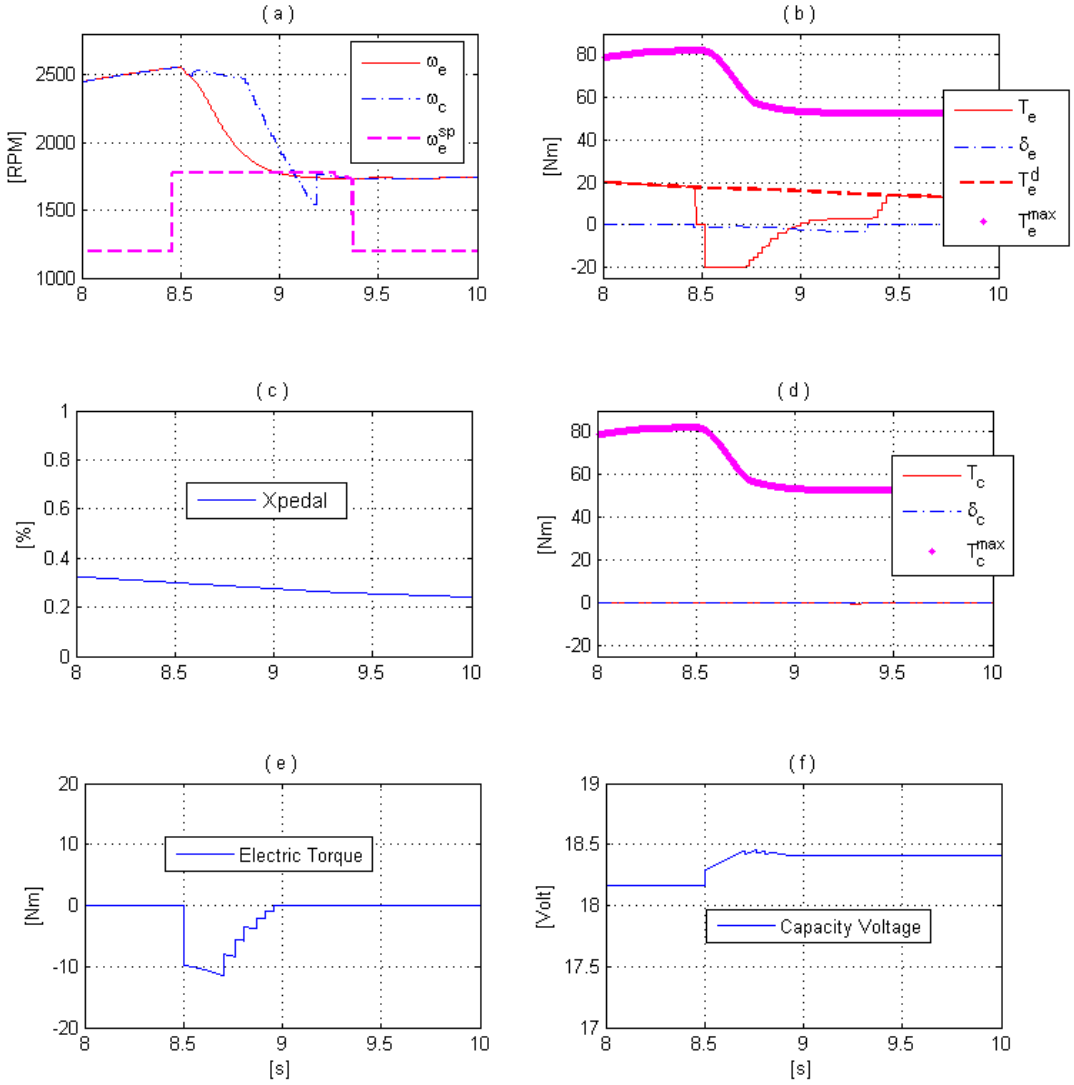

Figure 3.23: Co-simulation: Vehicle up-shifting 1 → 2 using the Reversible Alternator to reduce the duration of the gear shifting, thus it becomes equal to that of the synchronization phase; The duration of the clutch slipping phase is null; In the quadrant (b) the control T_e^d refers to the open loop control (Pedal Torque).

phase is completely skipped. The quadrant (e) and (f) represent the electric torque and the ultra-capacitor voltage, respectively. As in the previous co-simulation tests, the control achieves the gear shifting with no oscillations in the transmission.

3.6.2 Experimental Results

As in the case of vehicle start-up, the experimental results of the unified model predictive control for gear shifting will be evaluated by comparing them to those of the reference control strategy which is currently implemented on the demo car. The latter is the decoupled control system described in (Tona et al. (2007)), and largely inspired by (Glielmo et al. (2006)).

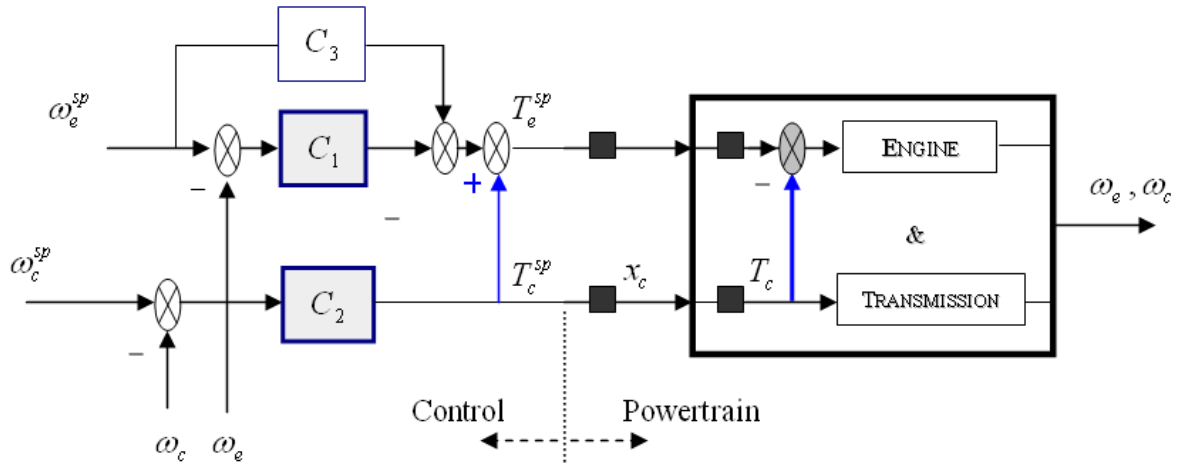

Figure 3.24: Structure of the decoupled control for the powertrain system during gear shifting: C_1 and C_2 are closed-loop controllers (PI), whereas C_3 is a feedforward block to ease engine speed tracking. The perfect decoupling assumes $T_c^{sp} = T_c(x_c, .)$.

Indeed, in the AMT control context, the mainshaft speed dynamics can be considered coupled to the engine speed dynamics via the torque transmitted by the clutch $\mathbf{T_c}(\mathbf{x_c}, .)$. This is clearly shown by the reduced powertrain model, reminded hereafter:

$$J_e \dot{\omega}_e = T_{comb} - T_{frict}(\omega_e, .) + T_{elect} - sign(\omega_{sl}) \cdot \mathbf{T_c}(\mathbf{x_c}, .) \tag{3.6}$$

$$\left[J_c + J_{eq}\left(i_g, i_d\right)\right] \dot{\omega}_c = sign(\omega_{sl}) \cdot \mathbf{T_c}(\mathbf{x_c}, .) - \frac{1}{i_g\, i_d}\left[k_{tw}\, \theta_{cw} + \beta_{tw}\left(\frac{\omega_c}{i_g\, i_d} - \omega_w\right)\right] \tag{3.7}$$

This fact can be advantageously used to design a decentralized control system based on two SISO controllers, as proposed in Glielmo et al. (2006), by adding in feed-forward an estimation of clutch torque or directly the clutch torque setpoint calculated by the mainshaft speed control, to the engine torque setpoint calculated by the engine speed control. The principle is shown in Figure 3.24 where C_1 and C_2 are the two SISO controllers, PI controllers for instance. Once the controlled dynamics are decoupled, each SISO controller may be used to track the desired reference trajectories ω_e^{sp} and ω_c^{sp}. C_3 is a feedforward block to ease engine speed tracking. If the clutch setpoint is directly used in feed-forward, a good decoupling requires that $T_c^{sp} \simeq T_c(x_c, .)$, which is in general not true because of neglected dynamics. It is possible, as suggested in (Glielmo et al. (2006)), to use an estimate of clutch torque for decoupling, based on the inversion of the engine speed equation $J_e \dot{\omega}_e = T_e - T_c(x_c, .)$. But this equation also neglects some important dynamics (those related to engine torque, more particularly) and the dependencies of clutch torque on other parameters such as slip speed or temperature. It is difficult to guarantee an effective decoupling.

Anyway, gear shifting in the VEHGAN demo car is currently controlled through a similar decoupling strategy, which only differs from the one described in (Glielmo et al. (2006)) in few respects. The control loop on mainshaft speed is replaced by the regulation of the absolute value of slip speed, to ensure that the clutch closes in every situation, without relying on the coherence of engine speed and mainshaft speed reference trajectories. Decoupling is based on nominal static clutch torque characteristic, identified experimentally, which can be partially corrected by an on-line observer (of the unknown-input family); before injection, in the engine speed loop, the estimated clutch torque is filtered to compensate (in feed-forward) for neglected engine torque

dynamics. Though these modifications do not guarantee perfect decoupling either, they do help limit interaction between the two loops. The price to pay is a tedious calibration procedure of the different open-loop and closed-loop compensators.

Figure 3.25 shows an experimental upshift ($1 \rightarrow 2$) with the decoupled control strategy. The decoupled control strategy achieves a rather smooth clutch engagement, whose total duration remains reasonable ($\simeq 1.5s$). Consider that, because of gearbox actuator control, the duration of the synchronization phase (effective engagement of the new gear) reaches nearly $1s$, which leaves little margin for further reduction of total upshift duration and it is difficult to be reduced.

After having presented the reference control strategy and its performance, we proceed with the experimental results of the unified model predictive control. We expect an improvement of the control performance, at least because of the truly multivariable nature of our strategy which should enable to handle the coupling in a more effective way.

Figure 3.26 shows an upshift ($1 \rightarrow 2$) using the proposed MPC strategy. With respect to the decoupled approach, the MPC one achieves a very smooth clutch engagement, with no oscillations induced in the transmission, as shown in sub figures (a) and (c), depicting the rotational speeds and the vehicle speed, respectively. Concerning the total duration of the gear shift maneuver, the MPC strategy needs approximately $2s$ to complete the upshift, whereas the decoupled strategy needs approximately `1.5s`. The main reason is that the MPC strategy lets the engine speed attain higher values, during the synchronization, in order to benefit from a slightly longer clutch slipping phase ($\simeq 1s$) to perform the estimation of $\hat{\delta}_e$ and $\hat{\delta}_c$. This does not affect much drivability, since transmission of clutch torque starts to be transmitted right after the synchronization phase is finished, allowing the vehicle speed to be increased again as requested by the driver via the accelerator pedal. Thus, the driver feels the lack of torque only for a duration not much longer than the synchronization phase ($\simeq 1.5s$). This is a major difference with respect to the decoupled control strategy, which does not guarantee that the expected amount of torque is transmitted before the clutch closes completely and the vehicle is in pedal mode again (see Figure 3.25). However, it must be pointed out that, with the current MPC strategy, it would be difficult to reduce the clutch slipping time further, should it be necessary. If the observers do not have enough time to converge, gearshift quality is affected.

Figure 3.27 shows consecutive up-shifting operations ($1 \rightarrow 2 \rightarrow 3$), controlled via the MPC strategy. This control achieves very smooth clutch engagements for all the gearshift. Notice that, as in the previous test, the driver may keep his feet on the accelerator pedal while asking for the gearshift, and this is interpreted as a request to apply a torque to wheels during the gearshift, as in pedal mode. In Figure 3.27.f, the accelerator pedal position is maintained constant during the gearshift $1 \rightarrow 2$, see the interval $[663, 667]s$.

Figure 3.28 shows consecutive down-shifting operations ($3 \rightarrow 2 \rightarrow 1$), controlled via the MPC strategy. As in co-simulation, we can notice how the control T_e makes engine speed track its reference trajectory much more quickly than for upshift control. Since engine speed and mainshaft speeds are very close after synchronization, the clutch slipping phase becomes very short.

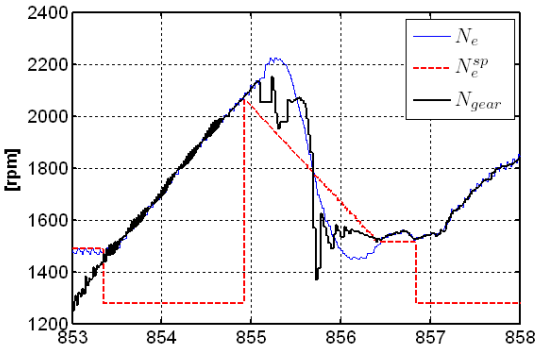

(a) Engine and mainshaft speeds

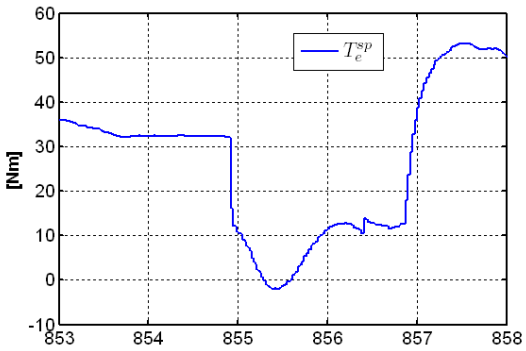

(b) Control inputs T_e

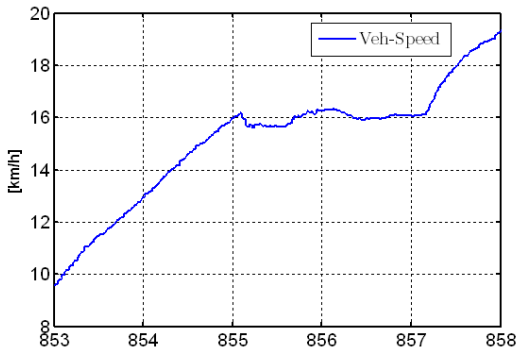

(c) Control inputs T_e

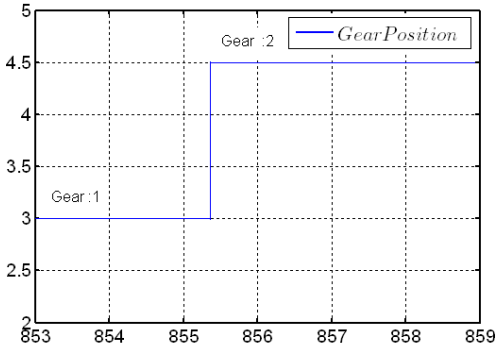

(d) Control inputs T_e

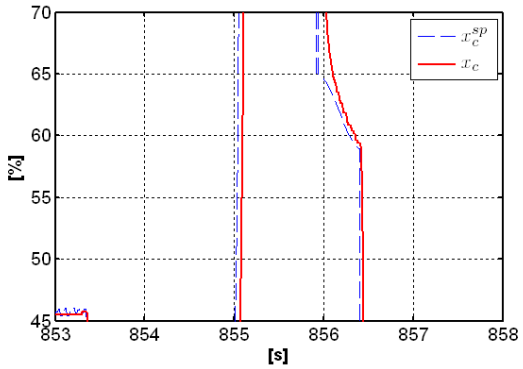

(e) Clutch bearing position

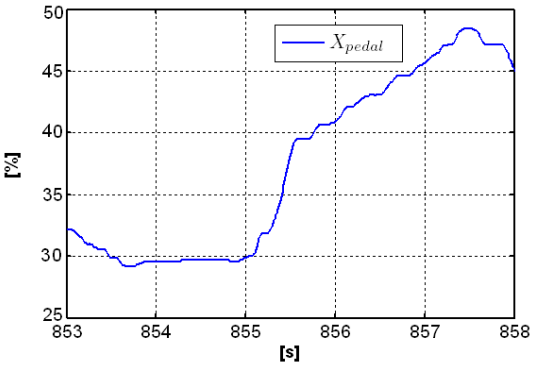

(f) Accelerator pedal position

Figure 3.25: Experimental results for upshift control $1 \rightarrow 2$ using the decoupled control strategy with two PI controllers.

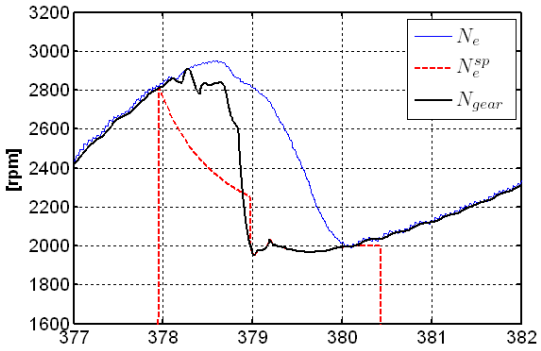

(a) Engine and mainshaft speeds

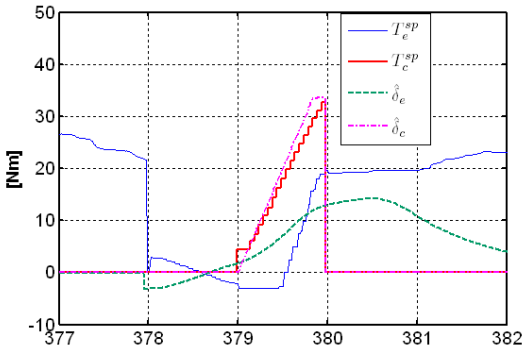

(b) Control inputs and estimated torques

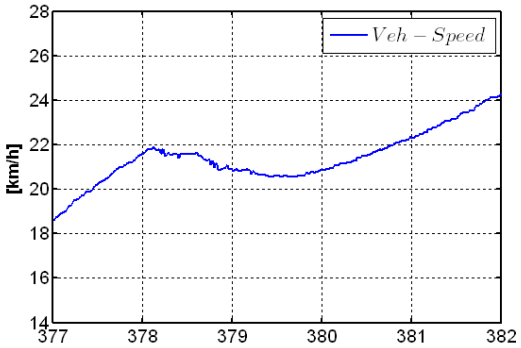

(c) Vehicle speed

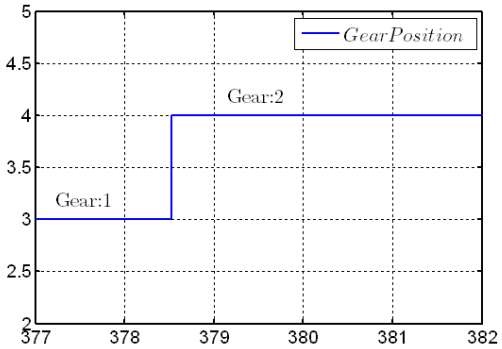

(d) Gear lever position

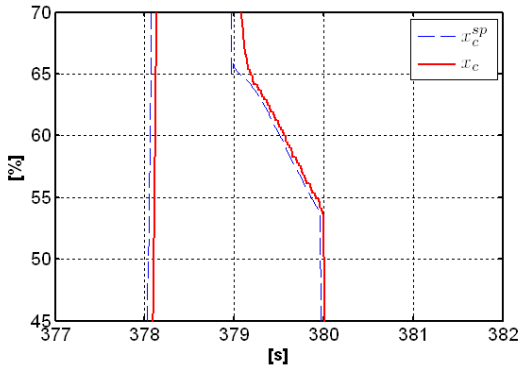

(e) Clutch bearing position

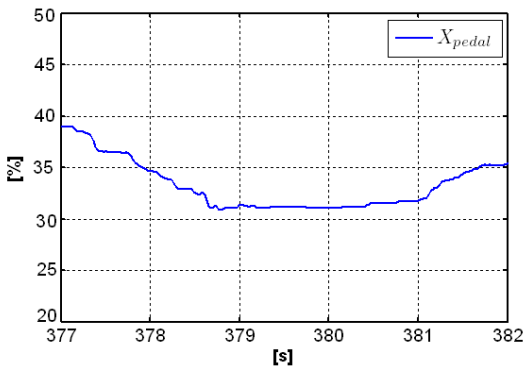

(f) Accelerator pedal position

Figure 3.26: Experimental results for upshift control $1 \rightarrow 2$ using the unified MPC strategy

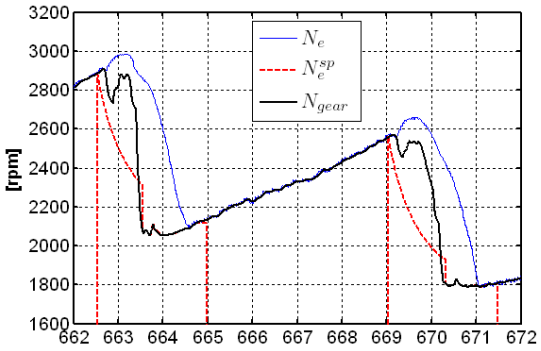

(a) Engine and mainshaft speeds

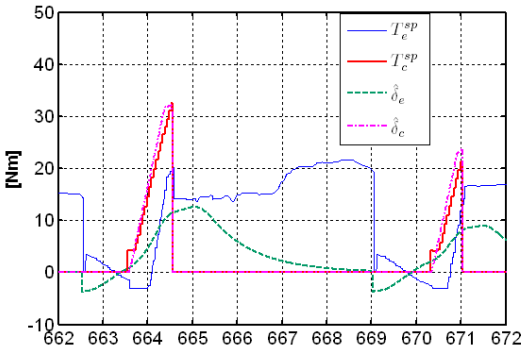

(b) Control inputs and estimated torques

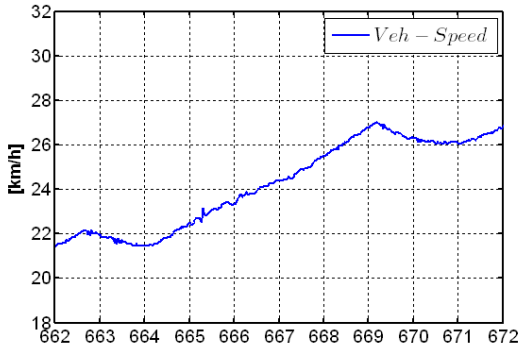

(c) Vehicle speed

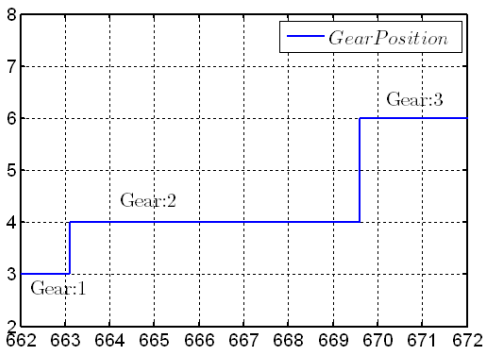

(d) Gear lever position

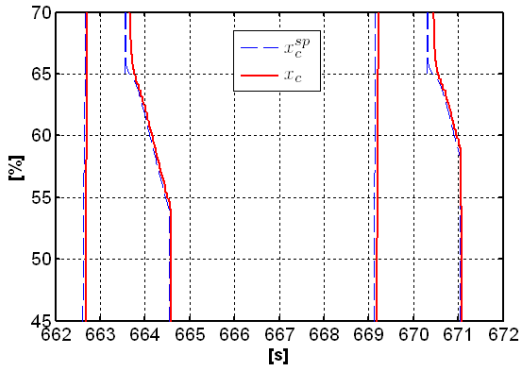

(e) Clutch bearing position

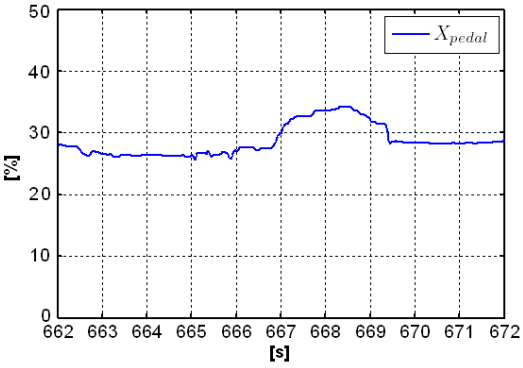

(f) Accelerator pedal position

Figure 3.27: Consecutive upshifts ($1 \rightarrow 2 \rightarrow 3$) using the unified MPC strategy.

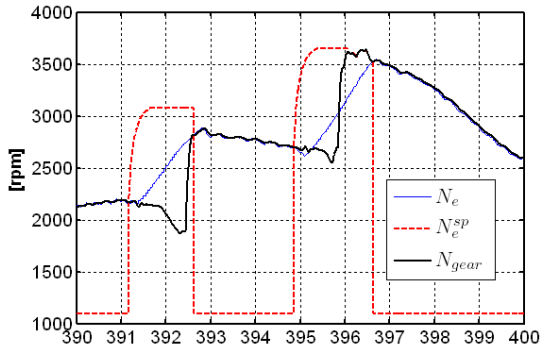

(a) Engine and mainshaft speeds

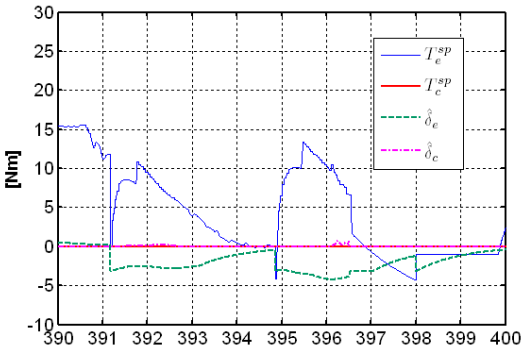

(b) Control inputs and estimated torques

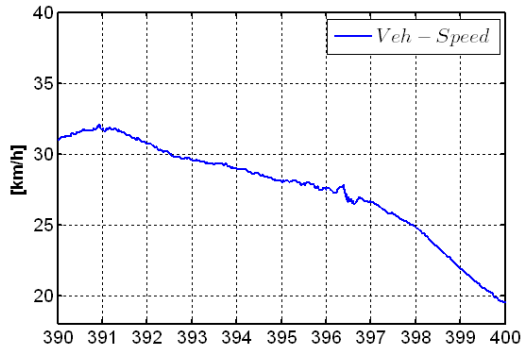

(c) Vehicle speed

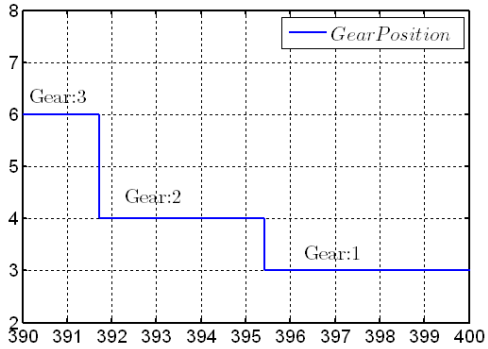

(d) Gear lever position

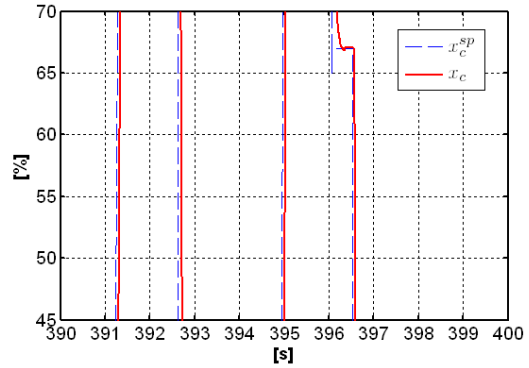

(e) Clutch bearing position

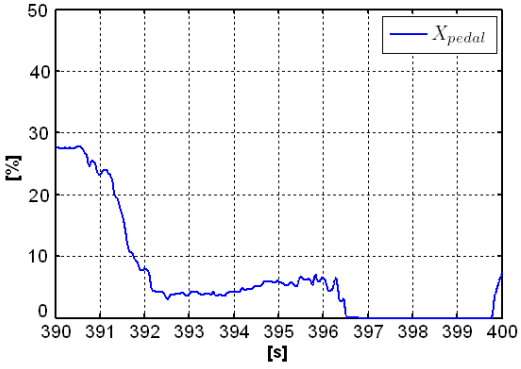

(f) Accelerator pedal position

Figure 3.28: Consecutive downshifts ($3 \rightarrow 2 \rightarrow 1$) using the unified MPC strategy.

3.7 Validation of Idle-Speed Control

Through the previous tests, we have presented the validation of the MPC strategy during vehicle start-up and gear shifting phases. However, before the vehicle start-up takes place, the powertrain control is naturally in the idle mode waiting for vehicle start-up. In this idle mode, the MPC strategy is also turned on to ensuring the regulation of the engine speed to the desired reference trajectory. Recall that, in this phase, the clutch torque is null, and the engine torque should face the internal frictions in the engine and the electric torque to provide power to the auxiliaries (alternator mode). In this mode, the control model is thus:

$$J_e \cdot \dot{\omega}_e = T_{comb}(.) - T_{frict}(\omega_e, .) + T_{elect} \tag{3.8}$$

For this mode, we only show experimental results. In Figure 3.29, a set-point variation is considered. In this test, one can remark that the overshoots and undershoots are very limited, and the control achieves a good regulation at steady state.

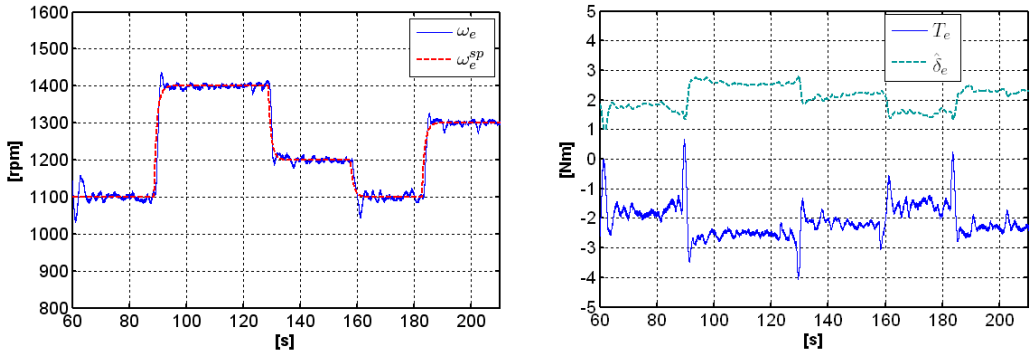

(a) Engine speed and its set-point

(b) Control input and estimated torque

Figure 3.29: Experimental result of the idle speed control, assuming variations of the desired reference trajectories.

It is worth underlying that the control input T_e, represented on Figure 3.29.b is negative because of an overestimation of the engine friction $T_{frict}(\omega_e, .)$, calculated in open-loop as in any standard engine speed controller. Thus, the MPC strategy computes negative values to compensate for the overestimation.

It is also important to recall that our MPC controller does not manipulate the engine torque efficiency set-point (spark advance) directly. In any SI-engine vehicle, this auxiliary control input allows to better respond to sudden load torque variations in the idle-speed control phase, at the expense of a slight fuel consumption increase. In our prototype, however, thanks to the advanced management of auxiliaries via the StARS, the use of engine torque efficiency set-point is, as a matter of fact, unnecessary.

3.8 Conclusion

This chapter has focused on the validation of the unified MPC strategy for AMT control presented in the previous chapter. The strategy has been deployed on a mild-hybrid demo car, equipped with a rapid prototyping powertrain control system. Following a model-based approach to control system design and implementation, the principles and nominal performance of the proposed MPC control have been first validated in a simplified simulation environment. Then, a co-simulation environment has permitted to validate on a detailed powertrain model, the AMT control module, embedded in an integrated powertrain control software, and to pre-calibrate it. Finally, real-time experiments have been carried out on the demo car. The validation has involved all the powertrain modes that can be controlled in closed-loop, idle mode, vehicle start-up, and gear shifting, though the focus has been essentially on AMT maneuvers.

The validation has underlined the main features of the proposed strategy:

- The ability to handle torque saturation constraints by solving on-line a parameterized quadratic problem directly linked to the accelerator pedal position, via a dichotomic search;
- The feasibility of real-time control: within the real-time rapid prototyping framework used to implement an integrated powertrain control system on the demo car, worst-case MPC computation takes less than one hundredth of the control sampling period and is compatible with the execution of the remaining control tasks.
- The viability of design and implementation: a very simple powertrain model is assumed and no additional sensors than those normally available in an AMT powertrain are required, thanks to the use of on-line torque estimators.

The experimental comparison with the decentralized control strategy currently implemented on the demo car, whose features and performances are already more satisfactory than those of usual AMT control systems, has shown the convenience of the unified MPC strategy. While ensuring comparable maneuver durations, the unified model predictive control offers smoother clutch engagement, tighter engine speed control and transparent handling of driver requests with little calibration effort.

A drawback of the proposed strategy is related to the performance of the observers when the desired clutch engagement time is very short. This prevents further optimizations of gear shift control performance, in order to reduce the duration of the manoeuver while keeping a smooth clutch engagement. A possible solution would consist in reducing the impact of uncertainties and neglected dynamics, by improving the accuracy of the powertrain model and more particularly of the clutch torque transmissibility model.

The next chapter is indeed devoted to the development of a phenomenological clutch torque transmissibility model, which can be used in model-based control approaches to improve the drivability of the vehicle. Though it could be beneficial for AMT control also, as suggested before, its rationale in this thesis is to serve driver assistance during vehicle start-up with a manual transmission. In this case, contrary to the AMT context, the driver fully controls the transmission, and from the embedded control point of view, the clutch torque is not a manipulated variable anymore, but a disturbance instead. An accurate model of clutch torque transmissibility is thus of paramount importance.

Part III

Unified Predictive Control for Vehicle Start-Up Assistance

Chapter 4

Clutch Torque Modeling

4.1 Introduction

Characterizing clutch torque during the clutch engagement phase enables to ensure effective control of the powertrain system: when sufficient knowledge is available about it, the right amount of torque can be produced and transmitted in the powertrain components. Information about clutch torque is particularly important in a powertrain control context, since it is the kernel of the drivability problem. In vehicles equipped with automated manual transmissions, the clutch torque is a control input, that can be used for controlling both the engine and the mainshaft speeds. As shown in the previous chapter, accurate knowledge of this control input is desirable but not essential for good control, provided that the control law is designed to overcome the uncertainties. In vehicles equipped with manual transmissions, however, the powertrain control problem becomes more constraining since the clutch torque is only a significant and unknown disturbance that acts on the engine shaft. In this case, any information about the clutch torque would be helpful for controlling engine torque production. This becomes particularly conspicuous, when dealing with manual-transmission vehicles with a *downsized* engine, where control of engine torque production is more constrained than with conventional MT vehicles. During the clutch engagement phases, the engine faces relatively high loads, which may not be compensated fast enough by combustion torque, especially at low engine speeds.

Starting from next chapter, we will study in detail the case of control assistance during start-up for manual-transmission vehicles with *downsized* engines, where the driver fully controls the clutch pedal, whose effect on the powertrain can be considered as a disturbance and corrected by the engine control unit. In this context, we will investigate in the present chapter the characterization of this disturbance and develop a phenomenological clutch model, based on the dynamics of the powertrain system. This phenomenological model can be used for estimation or model-based control to improve the drivability of this kind of vehicles.

This chapter is organized as follows. Since clutch torque transmissibility depends on the friction force that occurs between the clutch disks, section 4.2 gives a brief overview of friction force modeling, starting from the simplest model to more recent and complex ones. Indeed, in automotive applications, the clutch system, mounted between the engine and the gearbox, is designed to be operated as a connecting system that transmits the engine torque to the gearbox. This operating mode motivates us to introduce in section 4.3, a phenomenological model describing how engine torque is transmitted through the clutch to the transmission. The parameters and characteristics of such a model are then identified for two different powertrains, using experimental data coming from two demo cars: the AMT demo car VEHGAN, studied in the previous chapter, and the downsized-engine MT demo car EcoSural, which will be the focus

of chapter 6. Once some nonlinear characteristics are obtained, one can verify the accuracy of the model, as shown in section 4.4. Apart from control applications, which will be investigated in the following chapters, the phenomenological clutch model provides also an alternative way to check the *no-lurch* conditions of the transmission, as explained in section 4.5.

4.2 Overview on Friction Force

Any mechanical contact between two bodies in motion generates a friction force that depends directly on the nature of the surface and the sliding speed between the two bodies. This phenomenon has been studied extensively over the years, thus many models have been proposed to capture the main behavior of motion under friction. Most of these models include a dependency of the friction force according to the slipping speed (Armstrong (1991)). Figure 4.1 shows some profiles of the friction force starting from the simplest one to a more complete and realistic model. The first model illustrated through the sketch (a) assumes that the friction force is constant with respect to the slipping speed. This force is called the *Coulomb* force, and does not provide a realistic representation of the force since there is no dependency on the slipping speed. A better approximation has been suggested by introducing a linear dependency on the velocity that models a viscous friction (see sketch (b)). The latter is still not accurate since the stiction force is not taken into consideration. Thus, a further approximation is done by assuming an initial force needed to move from still (see sketch (c)). This stiction phenomenon is called the *Dahl* effect and is associated to elastoplastic deformations (Dahl (1968)).

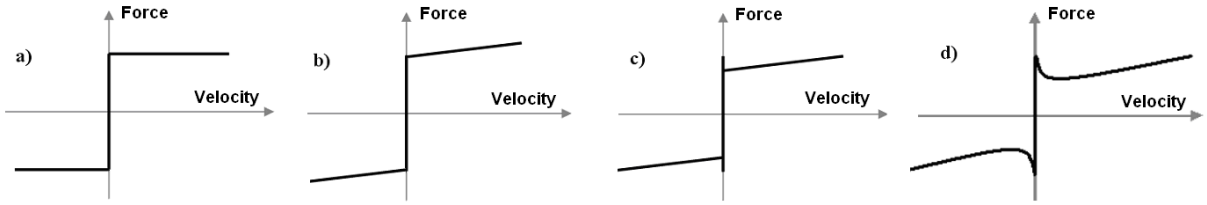

Figure 4.1: Friction force profiles vs velocity (Armstrong (1991)): a) *Coulomb* model; b) "Coulomb + viscous" model; c) "Coulomb + viscous+ stiction " model; d) Complete model with *Stribeck* effect;

A more precise approximation of the friction force can be obtained by introducing the *Stribeck* effect that assumes a parabolic profile of the friction force. This force initially decreases when the velocity increases from zero, until it reaches its minimum. Then it increases to fulfill the dynamic of a viscous friction. The speed corresponding to the minimum value of the force is called the *Stribeck* speed. Sketch (d) shows the corresponding profile of the friction force.

In the following we present a static model which takes in consideration the profiles concerning: the *Coulomb* force, the stiction force and the *Stribeck* effect. Then we present an accurate recent dynamic model which takes also in consideration the *Dahl* effect.

4.2.1 Static Friction Model

In (Bo & Paverlescu (1982)) authors present a static model of the friction force $F(.)$ through an empirical equation which highlights dependency on the *Coulomb* force F_c, the static force F_s, the viscous friction and the *Stribeck* effect. The viscous friction is expressed through a coefficient of friction b_v and velocity. Whereas the *Stribeck* effect is introduced through an exponential term

that depends on the *Stribeck* speed v_s and velocity:

$$F(v) = F_c + b_v|v| + (F_s + F_c) \cdot Exp\left(-\left(\frac{v}{v_s}\right)^{\lambda_v}\right) \tag{4.1}$$

where λ_v and b_v are empirical values, and v is a velocity;

At low speeds, the model can be simplified by linearizing the exponential term. In (Hess & Soom (1990)) authors present a simplification assuming $\lambda_v = 2$:

$$F(v) = F_c + b_v|v| + (F_s + F_c) \cdot \left(1 + \left(\frac{v}{v_s}\right)^2\right)^{-1} \tag{4.2}$$

The friction force expressed through equation (4.1) or (4.2) is useful to express realistically the main dynamic of the force when there is motion ($v > 0$). But the expression is not valid when the velocity is null or very low. This is due to the fact that the *Dahl* effect is neglected.

4.2.2 Dynamic Friction Model

The LuGre model presented in (Canudas De Wit et al. (1993)) includes the *Dahl* effect by assuming a spring displacement which models the asperity deformation under the applied force. The resulting friction force is a linear function of the displacement, up to a critical force at which the break-away occurs:

$$\dot{z} = v - \sigma_0 \frac{|v|}{g(v)} z \tag{4.3a}$$

$$g(v) = F_c + (F_s - F_c) \cdot Exp\left(-\left(\frac{v}{v_s}\right)^2\right) \tag{4.3b}$$

$$F_f = \sigma_0 z + \sigma_1 \dot{z} + b_v v \tag{4.3c}$$

Where:

z: is the internal friction state; σ_0: is the stiffness; σ_1: is the microdamping;

Compared with the *Dahl* model presented in (Dahl (1968)), the LuGre model has a velocity-dependent function $g(v)$ instead of a constant, and there is an additional damping associated to the microdisplacements.

4.3 Clutch Torque Model

In general, clutches are used to join smoothly two inertias rotating at different speeds. Clutching allows for the power to flow from one inertia to another according to the sign of the relative speed (*slip speed*) between the two inertias. In dry clutches, torque transmission is achieved via a friction phenomenon between two surfaces or disks: a high-friction material is added to one surface to maximize the friction coefficient. In automotive applications, clutches are used to connect or disconnect the transmission from the engine. When the clutch is open, no torque is transmitted to the transmission. When the clutch closes with the two surfaces slipping (non zero relative speed) only a fraction of engine torque is transmitted. When the clutch is completely closed, engine torque is fully transmitted to the transmission, unless it exceeds some defined maximum

torque threshold which is a specific characteristic of the clutch, guaranteed by manufacturers in order to protect the transmission from over-torques. In this case, the clutch will slip again to dissipate the excess of power.

① Pressure plat
② Clutch disk
③ Pilot shaft
④ Throw-out bearing
⑤ Pilot pushing

Figure 4.2: Dry clutch

Those different phases can be encountered in typical maneuvers of vehicles equipped with Manual Transmissions (MTs) or Automated Manual Transmissions (AMTs), such as vehicle start-up from standstill and gear shifting. Driver's comfort is directly related to the control of clutch engagement and its coordination with engine torque production. The clutch plays a fundamental role especially during the clutch slipping closing phase, when the throwout bearing position is used to control the transmitted torque. Accurate knowledge of torque transmitted during this phase would be highly desirable in order to improve the performance of strategies controlling start-up or gear shifting in AMT vehicles or assisting the driver during those maneuvers in the case of manual transmissions. Torque sensors are usually too expensive to be integrated in production vehicles, but off-line identification techniques and on-line observers can be used instead to characterize torques produced and transmitted in the powertrain from available measurements such as engine speed and mainshaft speed.

The torque transmitted by the clutch can only be directly controlled via the throwout bearing position, set by an electric or hydro-electric actuator. Indeed, in most control strategies proposed for both AMT control and driver assistance, a (non-linear) static dependency of transmitted torque on the throwout bearing position is assumed (see for instance Glielmo et al. (2004), Dolcini et al. (2005), Tona et al. (2007), Van Der Heijden et al. (2007), Amari et al. (2008). Yet, transmitted torque actually depends on many other factors, such as slip speed and acceleration, wear, temperature and the state of the different springs present in the clutch (diaphragm, flat and torsional springs). Control performance can be considerably affected by these neglected factors, even when an observer is included in the control system. Recently, some authors have proposed more accurate torque transmissibility models for the design of robust control strategies for dry clutch engagement, taking in account actuator dynamics, spring dynamics, and geometry-related modulation of the normal force applied to clutch disks (Lucente et al. (2006) based on Montanari et al. (2002), and Scafati et al. (2008)). It seems difficult, however, to identify the parameters of those more complex models, without the use of test-rigs or other off-board testing facilities.

4.3.1 Usual Clutch Torque Transmissibility Models

To characterize the clutch torque T_c during clutch engagement, it is usually assumed (Lucente et al. (2006)) that a stick-slip friction model (Armstrong et al. (1994)) applies. During the

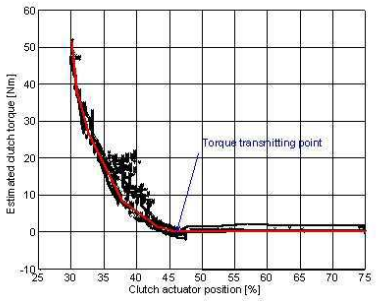

(a) Estimated values and piece-wise linear approximation (from Tona et al. (2007))

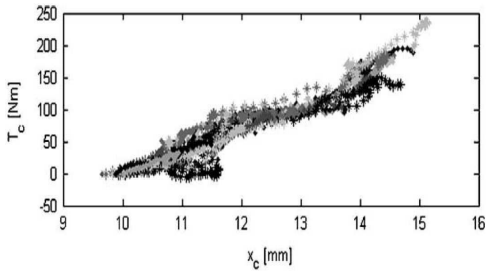

(b) Clutch torque wearing characteristic (from Glielmo et al. (2004))

Figure 4.3: Clutch torque transmissibility curves

slipping phase, T_c is then given by:

$$T_c = \text{sgn}(\omega_{sl}) \cdot T_c^t \left(F_n \left(x_c, \cdot \right), \cdot \right) \tag{4.4}$$

where the amount of transmitted torque T_c^t mainly depends on the normal force applied to the clutch plate $F_n(.)$ which is in turn controlled by the clutch bearing position x_c. In general, this force is not measured directly in vehicles but is reconstructed by using static maps that convert the bearing position into the normal force. Other characterizations can be done by using some measurements available in low level actuators. In hydro-actuation, one can use the pressure of the hydraulic circuit. Whereas in electric actuation one can use motor current.

Neglecting other dependencies, for control design purposes it is often assumed that $T_c^t := T_c^t(x_c)$. In this case, it is possible to estimate a static dependency on x_c (the so-called *clutch transmissibility curve*) by inverting the dynamic of the system and using an observer as explained in (Glielmo et al. (2004)) (*dirty-derivative* observer) or (Tona et al. (2006)) (unknown-input observer). Typical results of such approach are shown in Figure 4.3(a), with experimental data gathered during several vehicle start-ups. The dispersion of estimated values is significant, and can be explained firstly by not having taken into account dependencies on speed, temperature and spring non-linearities in the expression of T_c^t. moreover, as shown in (Glielmo et al. (2004)), over a longer time horizon, clutch wear acts by shifting this curve horizontally (the torque transmitting point changes). Figure 4.3(b) shows the experimental evolution of a clutch torque characteristic under wear. Such an approximate torque transmissibility curve can still be used in feed-forward for control purposes (actuator pre-positioning, decoupling), but it would be desirable to have more accurate estimations.

To improve the characterization of the transmitted torque, the slip friction phenomenon should be analyzed in more detail. Naturally, a static dependency enables to describe the main behavior of the system in steady state. The normal force $F_n(.)$ applied to the clutch disks enables to express the transmitted torque $T_c^t(.)$:

$$T_c^t(.) = \mu \left(. \right) \cdot R_e \cdot F_n(x_c, \cdot) \tag{4.5}$$

where μ is the dynamic friction coefficient and R_e is the equivalent radius of clutch disk, dependent on clutch geometry. If μ is considered constant and F_n dependent only on x_c, we have the same model as (4.4). A more accurate model can be obtained by introducing dependencies on the

operating conditions in each term (for instance, $\mu = \mu(\omega_{sl})$, provided that those dependencies are identifiable with the available experimental facilities.

A generalization of the previous model is presented in (Scafati et al. (2008)):

$$T_c^t = \mu \cdot \tilde{R}_e(r_i(\tilde{F}_n(x_c))) \cdot \tilde{F}_n(x_c) \tag{4.6}$$

where the evolution of the internal radius r_i of the contact surface during engagement is explicitly modeled. A quantity R_μ can be expressed through the friction coefficient and the equivalent radius ($R_\mu = \mu \cdot \tilde{R}_e$). This relation supposes distributions of the friction force and pressure along the contact surface:

$$R_\mu = \frac{\int_0^{2\Pi} \int_{R_1}^{R_2} \quad \tau \cdot \rho^2 \; d\rho d\varphi}{\int_0^{2\Pi} \int_{R_1}^{R_2} \quad \tau \cdot \sigma \; d\rho d\varphi} \tag{4.7}$$

Where:

R_1 et R_2 are internal and external radii of the clutch disk;

τ : is a force distribution along the contact surface;

σ : is a pression distribution;

The relation between the two distributions τ and σ is expressed by:

$$\tau(\rho, \varsigma, F_n) = \mu(\rho\omega_{sl}) \cdot \sigma(\rho, \varsigma, F_n) \tag{4.8}$$

In (Guzzella & Sciarretta (2005)), the authors give an expression of transmitted clutch torque which is based on a clutch maximum torque $T_{c,max}$ and on a normalized clutch bearing position x_c^n $(0 \leq x_c^n \leq 1)$ (see Figure 4.4):

$$T_c^t = T_{c,max}^t(\cdot) \cdot x_c^n \tag{4.9}$$

where

$$T_{c,max}^t = \left[T_b - (T_b - T_a) \cdot \exp\left(-\frac{\omega_{sl}}{|\omega_{sl,0}|} \right) \right]$$

and T_a, T_b and $\omega_{sl,0}$ are parameters determined experimentally, and depending on temperature and wear.

This expression has some analogy with the static friction force presented before in equation (4.2) which takes in consideration the stiction, *Coulomb* friction and the *Stribeck* effect.

If we consider the dynamic friction force expressed through the LuGre model presented before in equation (4.3), one can write a dynamic clutch torque associated to the friction force $F(.)$ (Dolcini (2006)):

$$T_c(F_n, .) = F\left(\sigma_0 z, \sigma_1 \dot{z}, b_v \omega_{sl}\right) \cdot R_m \tag{4.10}$$

4.3.2 A Phenomenological Model for Torque Transmissibility

The purpose is to find a phenomenological model for clutch torque transmissibility during the disk slipping phase that takes into account not only the dependencies on the control variable

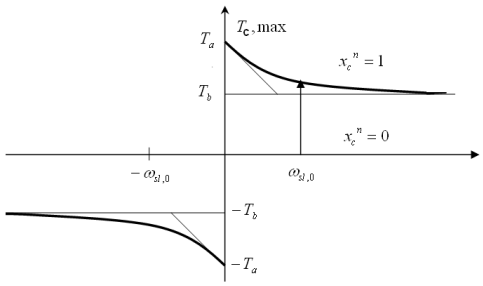

Figure 4.4: Clutch torque transmissibility (Guzzella & Sciarretta (2005))

x_c, the clutch actuator set-point, but also on other available variables characterizing the current operating point, the slip speed ω_{sl} and the engine torque T_e (Amari et al. (2009)):

$$T_c := T_c\left(x_c, \omega_{sl}, T_e\right) \tag{4.11}$$

Roughly, the clutch torque transmissibility is similar to a controlled switch that enables the power flux to get through. Generally, the power goes from the engine to the transmission. However, there is some situations where the engine shaft receives power from the transmission. This happens for instance, when, decelerating or driving downhill. Thus, the clutch torque can be considered as a control input that acts on the vehicle dynamics. Thereafter we remind the dynamic of the powertrain using this control variable:

$$J_e\dot{\omega}_e = T_e - \operatorname{sgn}(\omega_{sl})\ T_c\left(x_c, \cdot\right) \tag{4.12a}$$

$$\left[J_c + J_{eq}\left(i_g, i_d\right)\right]\dot{\omega}_c = \operatorname{sgn}(\omega_{sl})\ T_c\left(x_c, \cdot\right) - \frac{1}{i_g\ i_d}\left[k_{tw}\,\theta_{cw} + \beta_{tw}\left(\frac{\omega_c}{i_g\ i_d} - \omega_w\right)\right] \tag{4.12b}$$

$$J_w\dot{\omega}_w = k_{tw}\theta_{cw} + \beta_{tw}\left(\frac{\omega_c}{i_g\ i_d} - \omega_w\right) - T_L\left(\omega_w\right) \tag{4.12c}$$

$$\dot{\theta}_{cw} = \frac{\omega_c}{i_g\ i_d} - \omega_w \tag{4.12d}$$

In this model the clutch torque is acting directly on the two dynamics $\dot{\omega}_e$ and $\dot{\omega}_c$. For this reason, one can do some simplifications on the model in order to reduce the number of unknown parameters on one hand, and to have a direct dependency between control inputs and measurements on the other hand. An usual simplification is to assume that the transmission is rigid to transfer the load torque to the mainshaft. With this assumption, the dimension of the powertrain model is reduced and the characterization of the clutch torque can becomes easier:

$$J_e\dot{\omega}_e = T_e - \operatorname{sgn}(\omega_{sl})\ T_c\left(x_c, \cdot\right) \tag{4.13a}$$

$$\left[J_c + J_{eq}\left(i_g, i_d\right)\right]\dot{\omega}_c = \operatorname{sgn}(\omega_{sl})\ T_c\left(x_c, \cdot\right) - T_L\left(i_g, i_d\right) \tag{4.13b}$$

This enables us to express the two main dynamics ω_e and ω_c of the powertrain that depend directly on the the control inputs T_e and T_c, and the load torque $T_L(i_g, i_d, .)$. Notice that, in a normal vehicle, T_e and T_c cannot be measured but only estimated. The powertrain control system can only compute set-points T_e^{SP} and T_c^{SP}, that are sent to lower lever open-loop control layers. In the following, we assume that $T_e = T_e^{SP}$ and $T_c = T_c^{SP}$: the proposed model will have to deal with the mismatch.

Basically the clutch engagement enables the powertrain to be moved from an operating point 'A'

defined by $[\omega_e := \omega_e^{idle}, \omega_c := 0]$ to a new point 'B' characterized by $(\omega_c := \omega_e)$. The effort needed for this displacement is operated through the control inputs T_e and $T_c(x_c, .)$. It is very important to control x_c to ensure $T_c(x_c, .) \simeq T_e$ in order to limit the dynamics of ω_e (see equation 4.13a). When the clutch approaches the closed position (powertrain operates at 'B'), conceptually the clutch system can be thought as a closed switch in which the engine net torque is totaly available on the mainshaft. This means that the clutch torque is roughly equal to this engine net torque and explains the motivation of introducing the dependency on T_e. However the dynamic of the mainshaft ($\dot{\omega}_c$, see equation 4.13b) does not depend directly on the control T_e. For this reason it is convenient to rewrite the system dynamics by replacing $\dot{\omega}_c$ with the slip speed $\dot{\omega}_{sl}$:

$$\dot{\omega}_e = J_e^{-1} T_e - \text{sgn}(\omega_{sl})\ J_e^{-1}\ T_c^t\,(x_c, \cdot) \tag{4.14a}$$

$$\dot{\omega}_{sl} = J_e^{-1} T_e - \text{sgn}(\omega_{sl})\ \left[J_e^{-1} + (J_c + J_{eq}\,(i_g, i_d))^{-1}\right]\ T_c\,(x_c, \cdot) + J_e^{-1}\ T_L\,(i_g, i_d) \tag{4.14b}$$

We expect that inserting T_e in the model would have a smoothing effect on the variations of clutch torque transmissibility that are not directly related to x_c and ω_{sl}, since engine torque production is feedback-controlled[1] and tends to compensate these variations in order to obtain the desired vehicle start-up dynamics.

Among several possible structures, experimentally evaluated, we have selected the following:

$$T_c^t\,(x_c, \omega_{sl}, T_e) = T_e \cdot f\,(\omega_{sl}, x_c) \cdot \omega_{sl} \tag{4.15}$$

where $f(\cdot)$ is an unknown function of the position x_c and the slip speed ω_{sl}. The characteristic $f(\cdot)$ is to be estimated experimentally. Figure 4.5[2] illustrate the causality of the proposed model in which N_e and N_c are inputs to the model.

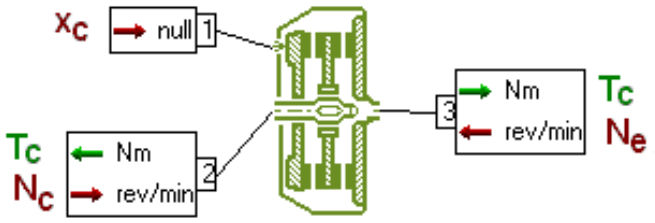

1 : Throwout bearing

2 : Mainshaft

3 : Engine shaft

Figure 4.5: Causality of the clutch torque transmissibility model expressed in a bond-graph formalism. The model calculates torque T_c from inputs x_c, N_e and N_c (where N_e and N_c are respectively the engine speed and the main shaft speed expressed in *rpm*).

By replacing the proposed expression for T_c^t, we have:

$$\dot{\omega}_e = a \cdot T_e - a \cdot \text{sgn}(\omega_{sl})\ \cdot T_e \cdot \omega_{sl} \cdot f(x_c, \omega_{sl}) \tag{4.16a}$$

$$\dot{\omega}_{sl} = a \cdot T_e - (a + b) \cdot \text{sgn}(\omega_{sl}) \cdot T_e \cdot \omega_{sl} \cdot f(x_c, \omega_{sl}) - b \cdot T_L \tag{4.16b}$$

where $a = J_e^{-1}$ and $b = [J_c + J_{eq}\,(i_g, i_d)]^{-1}$.

[1] whether by the AMT control system or the driver

[2] N_e and N_c are respectively the engine speed and the main shaft speed expressed in *rpm*

It is then possible to obtain an estimate of $f(\cdot)$ from equation (4.16a), using experimental data gathered during several different start-up tests and an off-line estimator; namely, a Kalman observer defined as follows:

$$\dot{\hat{X}} = A(T_e, \omega_{sl})\hat{X} + BT_e - S^{-1}C^T(C\hat{X} - y) \tag{4.17a}$$

$$\dot{S} = -\theta S - A(T_e, \omega_{sl})S - SA^T(T_e, \omega_{sl}) + C^T C \tag{4.17b}$$

where:

- $A(T_e, \omega_{sl}) \in \mathbb{R}^{2\times2}$, $B \in \mathbb{R}^{2\times1}$, $C \in \mathbb{R}^{1\times2}$;
- $\hat{X}^T := (\hat{\omega}_e \quad \hat{f}(.))$ is the estimated state and y the measurement;
- $S \in \mathbb{R}^{2\times2}$ a matrix solution of the Riccati differential equation;

The matrix $A(T_e, \omega_{sl})$ and B are updated according to the dynamic (4.16a) to obtain $\hat{f}(\cdot)$. More precisely:

$$A(T_e, \omega_{sl}) = \begin{bmatrix} 0 & -a \cdot sng(\omega_{sl}) \cdot \omega_{sl} \cdot T_e \\ 0 & 0 \end{bmatrix}, \qquad B = \begin{bmatrix} a \\ 0 \end{bmatrix}.$$

During this estimation we should ensure that the variation of the error:

$$\dot{\varepsilon_e}(.) = -S^{-1}C^T(C\hat{X} - y) \tag{4.18}$$

which has the dimension of a torque, is relatively low compared to the engine torque and the transmitted torque. This approach enables us to derive an off-line characteristics that captures the main behavior with respect to clutch actuator x_c.

With a cascaded estimators structure, that is by injecting $\hat{f}(\cdot)$ in equation (4.16b), we can also obtain an estimation of the load torque T_L. This torque depends mainly on wheel rolling friction and road grade (gravitational force).

Remark 4.3.1.
Instead of using cascade estimation, one can supposes an exhaustive characteristic $\hat{g}(\cdot)$ which may include clutch characteristics and load torque. This means we'are looking for one general term that faces the engine torque during clutch engagement. This can be expressed directly through the dynamic of the slip speed $\dot{\omega}_{sl}$ (see equation 4.19b):

$$\dot{\omega}_e = a \cdot T_e - a \cdot \text{sgn}(\omega_{sl}) \ \cdot T_e \cdot \omega_{sl} \cdot \ f(x_c, \omega_{sl}) \tag{4.19a}$$

$$\dot{\omega}_{sl} = a \cdot T_e - (a + b) \cdot \text{sgn}(\omega_{sl}) \cdot T_e \cdot \omega_{sl} \cdot g(x_c, \omega_{sl}) \tag{4.19b}$$

Once $g(\cdot)$ is obtained it's important to go back and express the dependency on the initial characteristic $f(\cdot)$.

Remark 4.3.2.
When the vehicle speed is still nul, the dynamics (4.19a) and (4.19b) are equivalent.

Figure 4.6: Demo cars: VEHGAN `smart` and ECOSural Vel Satis

4.3.3 Experimental characterization

The justification of our modeling approach comes essentially from experimental evidence. The clutch is supposed to act as an actuated switch that transfers a net-engine torque available at the engine shaft to the mainshaft. During this actuating process, the slipping speed moves from an initial value, equal to the actual engine speed, to a zero final value at which the transmission is defined completely closed. For an experimental characterization of this slipping phase we use data that come from two very different prototype vehicles (see figure 4.6) that have been developed by IFP:

- a mild-hybrid city car with a turbo-charged CNG engine, equipped with an automated manual transmission system (VEHGAN project);
- an executive car with a highly-downsized engine, using a turbo-charger and variable valve timing technology, with a manual transmission (ECOSural project).

Moreover, in the former vehicle the clutch is actuated by a simple DC motor, while the latter has a more standard hydraulic actuator. The measurement of this clutch pedal position is available in some commercial vehicles and it can be generalized since those sensors are not expensive. This day, the challenge of improving driver's comfort is very important. As a consequence, those non-expensive solutions are suitable since the final cost of the vehicle remains competitive, including investments on the embedded control.

By applying the estimation approach described in the previous section on data coming from several start-ups on both vehicles, we were able to find a clear dependency of the experimental characteristics $\hat{f}(\cdot)$ on the product of clutch actuator position x_c and slip speed ω_{sl}, that is $\hat{f}(\cdot) = \hat{f}(x_c \cdot \omega_{sl})$. This is shown in Figure 4.7.

If we assume roughly $\hat{\mathbf{g}}(.) \simeq \hat{\mathbf{f}}(.)$, we can write a model which is based only on $\hat{\mathbf{f}}(.)$ and the inputs defined before (see Figure 4.5), namely engine torque set-point T_e, clutch position x_c, engine speed ω_e and mainshaft speed ω_c (or slip speed $\omega_{sl} = \omega_e - \omega_c$):

$$\dot{\omega}_{e,mdl} = a \cdot T_e - a \cdot \mathrm{sgn}(\omega_{sl}) \cdot T_e \cdot \omega_{sl,mdl} \cdot \hat{\mathbf{f}}(x_c \cdot \omega_{sl}) \tag{4.20a}$$

$$\dot{\omega}_{sl,mdl} = a \cdot T_e - (a+b) \cdot \mathrm{sgn}(\omega_{sl}) \cdot T_e \cdot (\omega_{e,mdl} - \omega_c) \cdot \hat{\mathbf{f}}(x_c \cdot \omega_{sl}) \tag{4.20b}$$

The load torque, whose influence is neglected in the previous model (equation 4.20), can be estimated via the cascaded estimators structure introduced before. In this case, we observe a

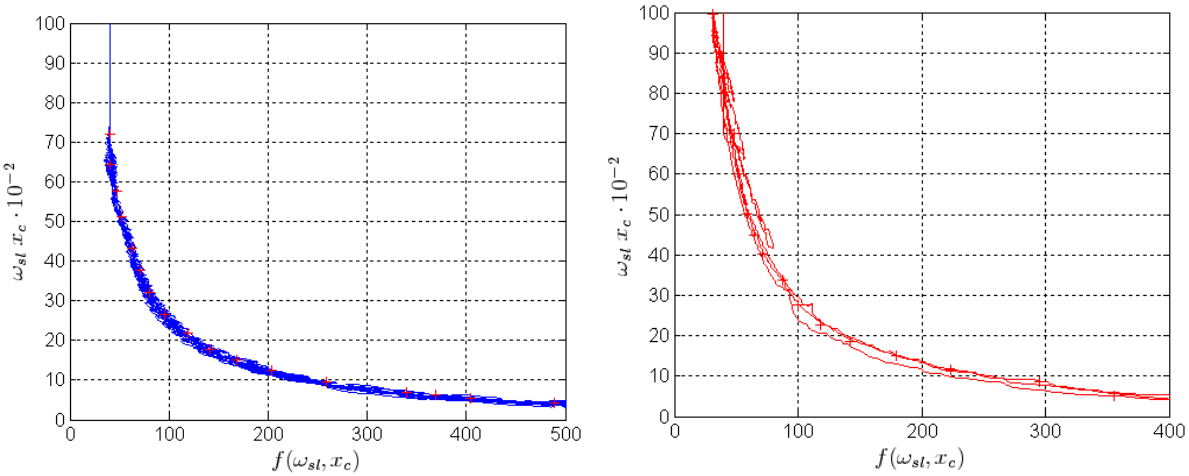

(a) `smart` (b) VelSatis

Figure 4.7: Experimental characterization of $\hat{f}$ over several vehicle start-ups

dependency on the product of engine torque T_e and slip speed ω_{sl}, that is $\hat{T}_L(\cdot) = \hat{T}_L(T_e \cdot \omega_{sl})$. This makes it possible to calculate more accurately the net torque acting on the mainshaft:

$$\dot{\omega}_{e,mdl} = a \cdot T_e - a \cdot \mathrm{sgn}(\omega_{sl}) \cdot T_e \cdot \omega_{sl,mdl_1} \cdot \hat{\mathbf{f}}(x_c \cdot \omega_{sl}) \tag{4.21a}$$

$$\dot{\omega}_{sl,mdl_1} = a \cdot T_e - (a+b) \cdot \mathrm{sgn}(\omega_{sl}) \cdot T_e \cdot (\omega_{e,mdl} - \omega_c) \cdot \hat{\mathbf{f}}(x_c \cdot \omega_{sl}) - b \cdot T_L(T_e \cdot \omega_{sl}) \tag{4.21b}$$

4.4 Validation

To validate the proposed approach, we have tested model (4.20) and its extended version (4.21) on a set of start-up data on both vehicles. Needless to say, the validation set does not include data previously used for identification. Just for convenience of presentation, we present the mainshaft speed ω_c instead of slipping speed ω_{sl}.

Figure 4.8 compares measured and simulated speeds obtained by applying model (4.20) to measured inputs recorded during an AMT-controlled vehicle start-up on the `smart` demo car. The AMT control strategy, based on model predictive control, is described in the previous chapter. Test results show that the model reproduces well start-up dynamics. The improvement with model (4.21), which provides an estimation of stiction torque, is minimal since the latter is small compared to engine torque. Figure 4.9 shows similar results for a faster start-up.

Figures 4.10 and 4.11 compare measured and simulated speeds obtained by applying models (4.20) and (4.21) to measured model inputs recorded during a driver-controlled vehicle start-up on the VelSatis demo car. We notice that, the measure of the mainshaft speed is not available is this demo car. To overtake this limitation, we use the vehicle speed with an appropriate ratio to approximate the mainshaft speed. This approximation doesn't capture some rapid dynamics of the mainshaft. But in general this seems to be sufficient to express the main behavior of the transmission, sine it can be considered as a filtered input.

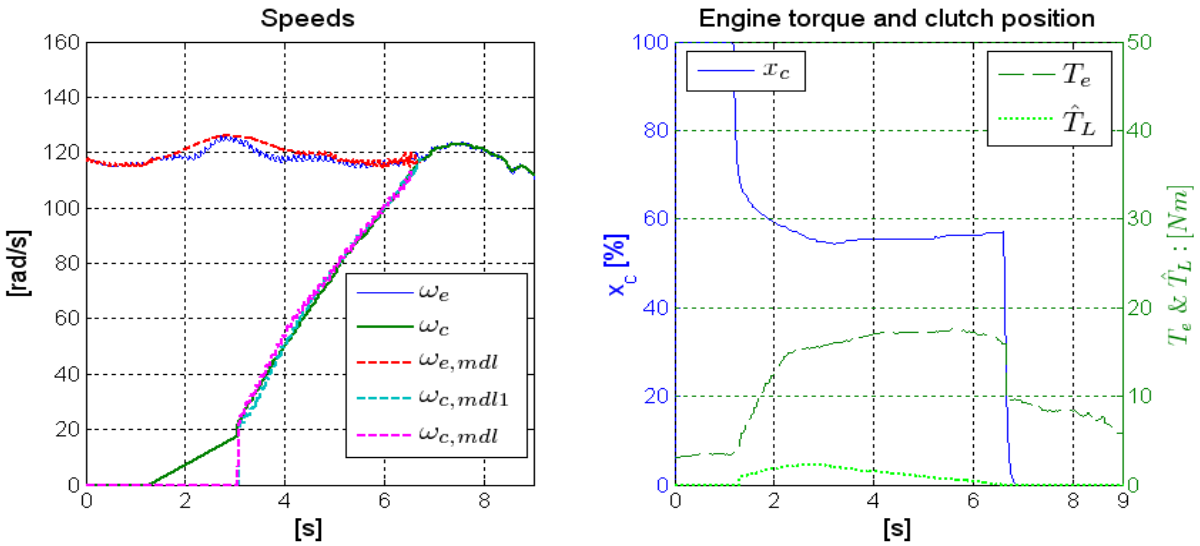

Figure 4.8: Test 1: comparison between measured speeds (with ω_c not available at low values, $< 200rpm$, because of the limited sensitivity of the sensor) and simulated speeds during an AMT-controlled vehicle start-up (`smart`). Slower start-up.

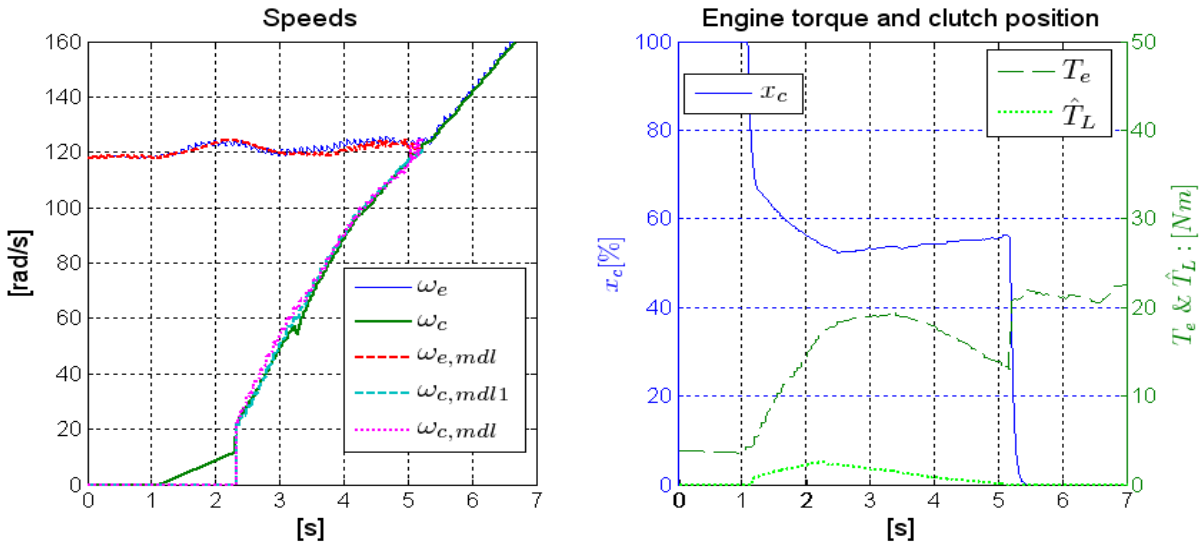

Figure 4.9: Test 2: comparison between measured speeds (with ω_c not available at low values, $< 200rpm$, because of the limited sensitivity of the sensor) and simulated speeds during AMT-controlled vehicle start-up (`smart`). Faster start-up.

Contrarily to the `smart` demo car which is light city car, the `VelSatis` one is a heavy vehicle. As a result, one can tell in advance that the stiction load is relatively important in the heavy vehicles in general, and becomes very important in climbing roads for the same vehicle. In this context we see that the model (4.21) is noticeably more accurate than model (4.20). Indeed, peak estimated load torque is not negligible compared to engine torque set-point. If we refer to the Figure 4.11 for example, the maximum value of the stiction load is approximately 15 $[Nm]$, whereas the net engine torque at this instance is approximately 50 $[Nm]$. This later is defined as a difference between engine torque set-point ($\simeq 70[Nm]$)) and idle torque ($\simeq 20[Nm]$)). As a result, the maximum stiction torque is nearly 30% of the net engine torque. This percentage is

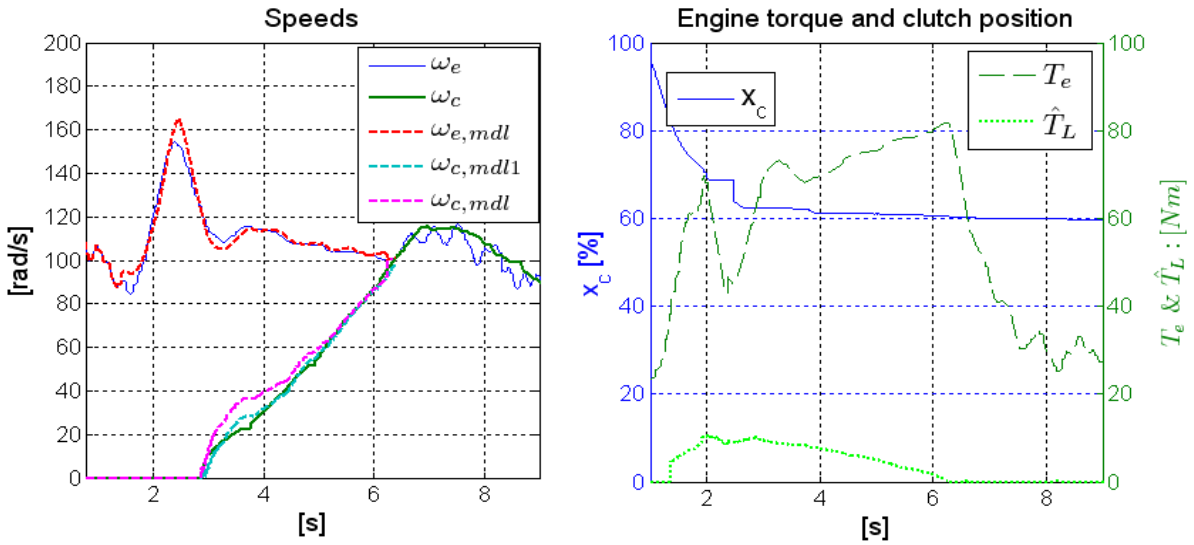

Figure 4.10: Test 3: comparison between measured speeds and simulated speeds during a driver-controlled vehicle start-up (Vel Satis). Slower start-up.

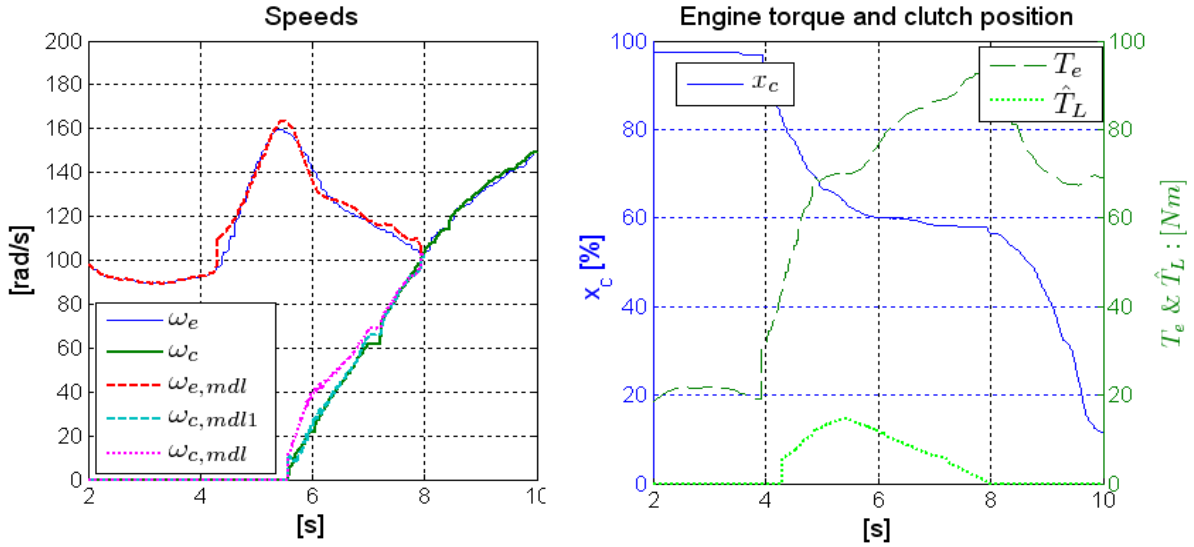

Figure 4.11: Test 4: comparison between measured speeds and simulated speeds during a driver-controlled vehicle start-up (Vel Satis). Faster start-up.

very important, and it affects significantly speeds's dynamic of the supposed model, as presented in Figures 4.10 and 4.11.

During each test, models are applied only inside their validity domain, that is during clutch slipping phase. Concerning stiction torque, the estimation seems to capture well the wheel friction effect which is predominant during start-up.

4.5 Application : *No-lurch* Condition in the Transmission

The model presented in the previous section has been developed to serve the design of new advanced AMT control systems, on one hand, and of control strategies to assist the driver during

manual start-up, on the other hand. We present here another application, in which we show how an accurate estimate of the torque transmitted by the clutch may be useful to better understand the dynamic behavior of the transmission when the clutch locks up.

As shown in (Bemporad et al. (2001)) and (Dolcini et al. (2005)), to avoid oscillations in the transmission at clutch lock-up the driver or the AMT control system must enforce the so called *no-lurch* conditions which defines relations on shaft speeds and their acceleration:

$$\omega_e(t_f) = \omega_c(t_f) = (i_g i_d) \cdot \omega_w(t_f)$$

$$\dot{\omega}_e(t_f) = \dot{\omega}_c(t_f) = (i_g i_d) \cdot \dot{\omega}_w(t_f) = J_v \cdot \left[T_e(t_f) - \frac{T_L(t_f)}{(i_g i_d)^2} \right]$$

where t_f is the lock-up time, and J_v is the equivalent inertia of the vehicle.

Since the condition on accelerations is very difficult to take into account in practice (T_e and $T_L(.)$ are unknown), a set of approximately equivalent conditions, expressed through slip speeds and slip accelerations, can be used instead:

$$\omega_{sl}^{ec}(t_f) = \omega_{sl}^{cw}(t_f) = 0$$

$$\dot{\omega}_{sl}^{ec} \cong \dot{\omega}_{sl}^{cw} \cong 0$$

where

ω_{sl}^{ec}: is the slip speed between engine and clutch

ω_{sl}^{cw}: is the slip speed between clutch and wheels

An alternative way to check the "*No-lurch*" condition of the transmission at lock-up consists of ensuring that the power coming from the engine side equals the power available on the mainshaft side, that is $P_e(t_f) = P_c(t_f)$ or:

$$\omega_e(t_f) \cdot T_e(t_f) = \omega_c(t_f) \cdot T_c(t_f) \tag{4.22}$$

If we refer to equation (4.12) that represents the dynamic of the system, we can express the potential of elastic energy storage in the transmission as:

$$E_{cw} = \frac{1}{2}\, k_{cw}\, \theta_{cw}^2 \tag{4.23}$$

and also through the powers available at the two end of the transmission (see Figure 4.12)

$$E_{cw} = \int (P_c(t) - P_w(t))\, dt \tag{4.24}$$

Assume the clutch has also some springs elasticities in side. And letting k_{ec} be the corresponding stiffness, we can express the elastic energy storage in the clutch using stiffness angle or powers:

$$E_{ec} = \frac{1}{2}\, k_{ec}\, \theta_{ec}^2 \tag{4.25}$$

$$E_{ec} = \int (P_e(t) - P_c(t))\, dt \tag{4.26}$$

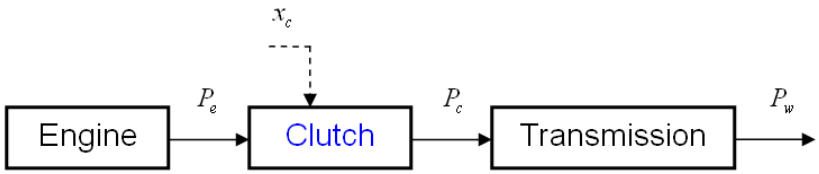

Figure 4.12: Powers flowing in the powertrain system

When the clutch on the verge of being completely closed, any clutch actuation which causes discontinuity on the clutch power generates oscillations on the transmission. In this case, the elastic energies E_{cw} and E_{ec} are not constant since they depend directly on θ_{cw} and θ_{ec} respectively. However, if the control system or the driver achieve clutch engagement respecting the *no-lurch* condition, then $E_{cw}(t_f)$ and $E_{ec}(t_f)$ are constant, and this implies that also θ_{cw} and θ_{ec} are constant. In this case, one can express the *no-lurch* condition through powers at each side of the clutch and of the transmission:

$$P_e(t_f) \simeq P_c(t_f) \tag{4.27}$$
$$P_c(t_f) \simeq P_w(t_f) \tag{4.28}$$

During clutch engagement, oscillations on the transmission are mainly caused by clutch actuation, for this reason it is important to focus on powers available on the clutch disks. Using the previously defined clutch torque transmissibility model to calculate $P_c(t)$ (equation 4.22) , it is possible to study, on experimental data, how the fulfilment of this condition influences the quality of start-up.

Figure 4.13 and Figure 4.14 show the results of this analysis for the AMT demo car (VEHGAN `smart`) and the ECOSural Vel Satis, respectively. For the former, where the AMT control system described before yields very "clean" start-ups, we observe that the power equality condition (4.22) is already attained before t_f, that is before the slip speed becomes null. Moreover, the discontinuity of engine torque after the final instant t_f, does not cause oscillations on the transmission. For the latter, where the start-up is controlled by the driver, it is clearly shown how oscillations do not occur when condition (4.22) is respected (first start-up) and do occur when it is not (second start-up).

4.6 Conclusion

We have presented a phenomenological clutch model which characterizes the transmissibility of the engine torque to the mainshaft during the clutch engagement phase. The proposed model is based on the identification of a nonlinear characteristic that relates the transmissibility of engine torque to the mainshaft to the clutch actuator position and the difference between the rotational speeds of the pressure plate and clutch disk (slip speed). The inclusion of engine torque set-point in the model helps smoothing the effect of neglected dependencies on torque

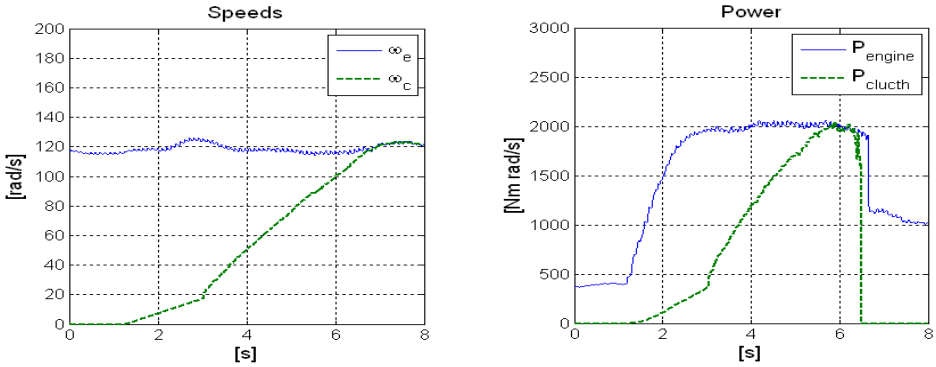

(a) Test 01

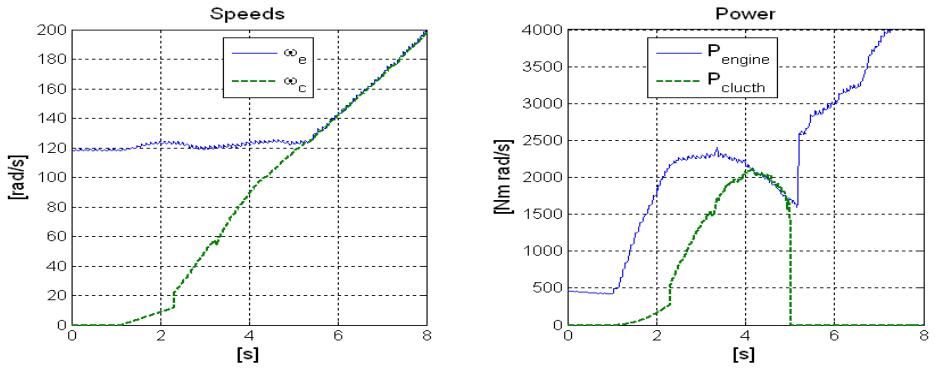

(b) Test 02

Figure 4.13: *No-lurch* analysis of the automated manual transmission (`smart` demo car), by reporting speeds (left) and powers (right) available on the engine shaft and the mainshaft.

transmissibility and yields a non-linear characteristic with very low dispersion. An empirical estimation of load torque during start-up, dependent on slip speed and engine torque set-point, completes the model and improves its accuracy.

The model has been identified and validated on two prototype vehicles with very different features: a small city car with an electrically-actuated automated manual transmission and a big executive car with a hydraulic-actuated manual transmission. This diversity suggests some degree of genericity of the model in a clutch control context.

An application example is given to show the usefulness of the model: an alternative analysis, based on power computation, of the conditions that have to be respected to avoid oscillations at clutch engagement.

In the next chapter, the model introduced above, will be used in a control context to assist the driver during vehicle start-up with a manual-transmission vehicle. More particularly, a nonlinear model predictive control (NMPC) law will be developed based on the phenomenological clutch model.

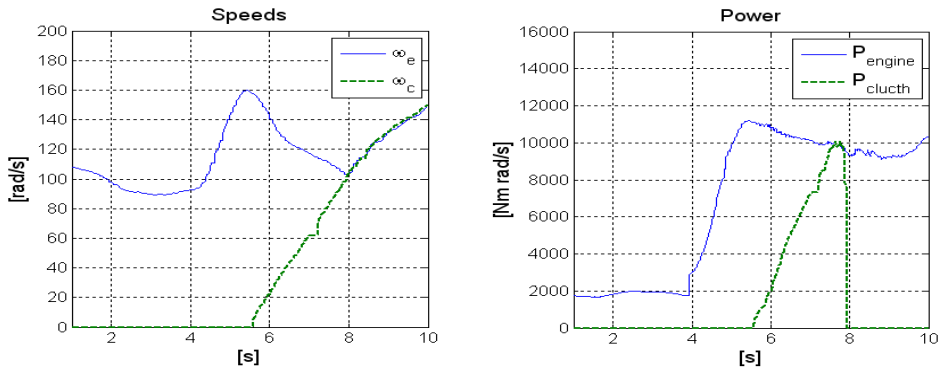

(a) Test 01

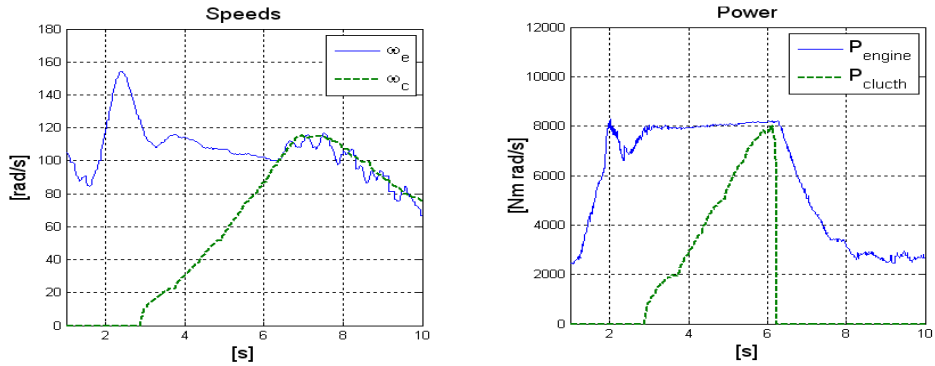

(b) Test 02

Figure 4.14: *No-lurch* analysis of the manual transmission (Vel Satis demo car), by reporting speeds (left) and powers (right) available on the engine shaft and the mainshaft.

Chapter 5

Control Assistance During Vehicle Start-Up

5.1 Introduction

In most cases, the drivability of vehicles equipped with manual transmission relies entirely on driver skills. In particular, during the vehicle start-up phase, the driver has to control both the engine torque production through the accelerator pedal position and its transmission through the clutch pedal (and hence the clutch bearing) position. The resulting comfort depends on the driver ability to perform these two tasks simultaneously. This objective becomes even more difficult to achieve in downsized vehicles since the engine is always facing relatively high loads with little power available at low speed. In this context, some enhanced control strategies may be implemented in order to meet an acceptable comfort level assuming that some corrections on the inputs that come from driver can be made. More clearly, the embedded control strategies can modify the torque demand expressed through the accelerator pedal, or the clutch pedal, in specific applications including some by-passing mechanism, at software or hardware level. In this context, some forms of driving assistance may be developed in order to help the driver during critical powertrain maneuvers.

This chapter is organized as follows. Section 5.2 introduces the downsizing concept in the case of internal combustion engines (ICE) together with some turbocharging techniques which enable to increase the power of the engine. In section 5.3, the context of the application is first described, the manipulated control variables are then introduced, and finally a conventional control structure is presented. The phenomenological clutch model, which enables to characterize the transmissibility of the engine torque through the clutch system is recalled in section 5.4. Finally, the integration of this model in a unified model predictive control framework is described in section 5.5.

5.2 Engine Downsizing

Engine downsizing consists in decreasing engine displacement, in order to reduce internal friction and pumping losses, and improve combustion efficiency. Since this leads to significant reductions of fuel consumption, this technology has been widely adopted in mass production. To recover the power lost with the reduction of volumetric capacity, downsizing is usually coupled to a form of supercharging in order to increase the density of air entering the engine. Turbochargers, which compress the gas at the engine intake using a fraction of the exhaust gas energy, otherwise lost, are the most interesting components from the thermal efficiency point of view. On the

other hand, with respect to other technologies, it is difficult to make a turbocharger deliver boost smoothly: at low engine speeds, acceleration is limited by the little energy available in the exhaust gas (engendering the so-called turbo lag), while, after the turbine starts spinning, pressure surges caused by the rapid increase in power may affect drivability or even safety.

Turbocharging is often coupled with one or more advanced engine technology, such as *variable valve timing* (VVT), exhaust gas recirculation (EGR), and direct injection (DI). Thanks to these solutions the pollutant emissions are also considerably reduced. Nevertheless, as environmental constraints become tighter and tighter, new solutions are continually being researched (see for instance Lake et al. (2004), in which authors discuss five alternative turbocharging approaches for direct injection gasoline engines).

In the downsized vehicle, the driving assistance does not depend on the downsizing concept: it deals with the high level control layer (torque demand), whereas the downsizing concept and its control concern the low level actuator layer (realization of the torque demand).

5.3 Hybrid Control of the MT-Powertrain System

5.3.1 Framework

In automotive applications, it is well known that the vehicle start-up phase is critical since the friction forces in the clutch disks are very important. This is due to the fact that the vehicle starts from still which renders the component that represents the static torque predominant. In this context, the information about the load and/or the clutch torques would be helpful for controlling the engine torque production in order to deliver the transmitted torque through the clutch. Furthermore, in the downsized vehicles, the information about the resistance torques is very important since the operating points of the downsized engine differ from those of the conventional engines.

In common vehicles equipped with manual transmissions, the driver acts both on the accelerator and clutch pedals to move the vehicle. Conceptually, the clutch actuation is directly applied to the clutch bearing system, which enables to transmit the engine torque. As for the accelerator pedal position, it is indirectly related to the engine torque production through the embedded control strategies and few low level actuators, as shown in Figure 5.1.

In this architecture, it is possible to identify three common layers:

- a high level controller (master controller) which represents the driver who controls all the components of the transmission (clutch, gearbox and brakes) and delivers some set-points to the embedded control of the lower layers;
- a secondary controller which ensures nominal operating conditions of the powertrain relative to the internal combustion and the electric modules;
- a low level of actuators having the lowest authority in the powertrain system since they are designed to track the set-points that come from the higher layers.

5.3.2 Manipulated and Control Variables

When considering the MT-powertrain system depicted in Figure 5.1, drivability can be enhanced by replacing the conventional open-loop control (torque demand) by an appropriate engine torque control which is designed to achieve a smooth start-up of the vehicle and suitable dynamic of

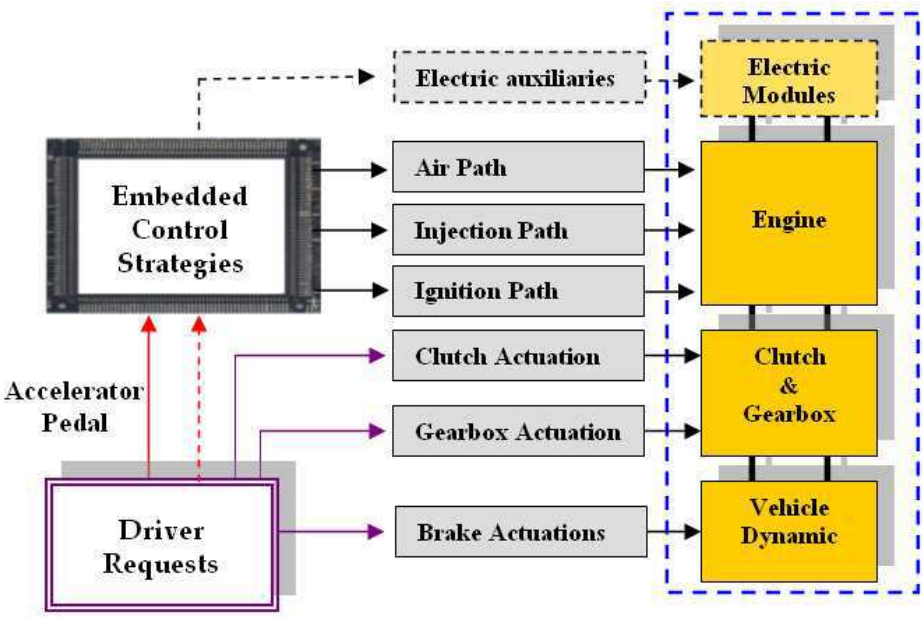

Figure 5.1: Control architecture on powertrain equipped with manual transmission.

the engine speed. Recall that, the torque demand T_e^d is computed through a static map (pedal torque) according to the accelerator pedal position X_{pedal} and engine speed ω_e, namely:

$$T_e^d := f(X_{pedal}, \omega_e) \tag{5.1}$$

In the context of start-up assistance, a specific closed-loop control can be implemented to assist the driver during the vehicle start-up manoeuvre. For example, the idle speed controller can be extended to the start-up phase by computing the appropriate engine torque which replaces or corrects the open-loop control value T_e^d.

As mentioned in section 1.4, the engine torque production is directly linked to the quantity of air injected in the engine at each cycle, as a consequence of the pressure attained in the manifold or the air flowing through the throttle valve. In principle, the engine combustion torque should be equal to the engine torque set-point T_e^{sp} generated at each cycle, by assuming the engine torque efficiency, noted by $\eta_{T_e}^{sp}$, at its optimal value, namely $\eta_{T_e}^{sp} = 1$. In general, this assumption is valid when the accelerator pedal is pushed. Nevertheless, during the idle mode or in some enhanced control approaches, the engine torque efficiency can be used as a control input in order to achieve short settling time.

During the start-up assistance, we consider in our formulation that the engine torque efficiency is a low level control input by opposition to the desired engine torque T_e^{sp} that is assumed to be a high level set-point (see Figure 5.2). This enables to use the same MPC controller regardless of the fact that the accelerator pedal is pushed or not. This means that the MPC strategy and the driver have the same decision variable since the MPC strategy computes the torque set-point T_e^{sp} while the driver suggests the desired torque T_e^d.

In the low level module depicted in Figure 5.2, the engine torque is converted into an air torque, whereas the engine torque efficiency is selected according to the accelerator pedal position, namely:

$$\eta_{T_e}^{sp} := \begin{cases} \mathcal{K}_\eta(\omega_e, \omega_e^{sp}, .) & \texttt{if} \quad X_{pedal} = 0 \\ 1 & \texttt{if} \quad X_{pedal} > 0 \end{cases} \tag{5.2}$$

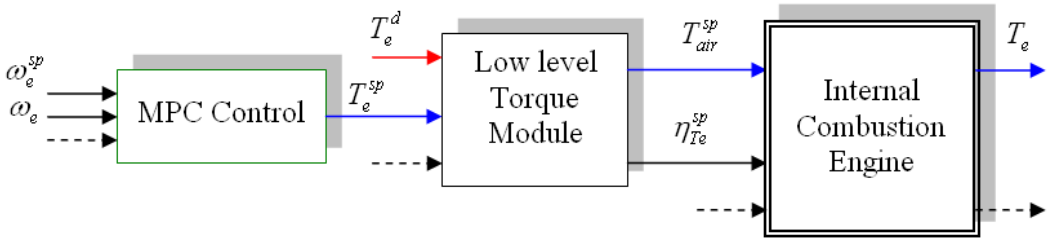

Figure 5.2: Hierarchical configuration of the model predictive control in the torque-based structure.

where: $\mathcal{K}_\eta(.)$ is a closed-loop controller that performs the engine speed tracking (see section 5.5.3 for more details).

5.3.3 Dual Start-up Assistance Through Clutch Actuator

In parallel to the vehicle start-up assistance which assumes the engine torque as a control input, one can mention a dual approach which assumes the clutch bearing position as a control input rather than the engine torque. This approach in proposed in (Dolcini et al. (2005)), and it needs an additional mechanical device that by-passes the driver actuation on the clutch pedal, enabling to get the operating mode of the automated manual transmission. Due to the computational time of the control, the assistance is only applied during a short horizon ($t < 0.6s$) before the end of the vehicle start-up phase. More precisely, the vehicle start-up begins with an open loop mode, like in the conventional manual transmission, whereas at the end of the start-up phase, the clutch actuation switches to closed-loop mode in order to guarantee a smooth clutch engagement (*no-lurch* condition). The proposed approach computes only the clutch bearing position, while assuming the engine torque as a known disturbance that comes from the engine control unit (ECU). Notice that, the proposed control assistance is suitable to be implemented in the transmission control unit (TCU).

In the IFP-control application however, the closed-loop relies on the computation of the engine torque, whereas the driver controls totally the clutch pedal. This scheme is detailed in the next section.

5.3.4 Torque-based Structure and Feedforward Application

As mentioned before, conventional control for start-up assistance in vehicles equipped with manual transmission is generally operated in an open-loop mode by using some predefined static maps related to the torque demand and potential disturbances. Figure 5.3 shows a possible torque-based structure that can be considered during the start-up phase. This control structure assumes mainly two maps: The first map $f_1(.)$ is referred to as the pedal map which gives the pedal torque related to the driver demand expressed through the accelerator pedal position while taking into account the engine operating point ω_e. The second map $f_2(.)$ gives the available information about the clutch torque given the clutch bearing position x_c. Additionally, other disturbances can be considered like the internal frictions in the engine system and the electric torques due to the electric auxiliaries.

Recall that, in manual transmissions, the driving comfort depends on the driver experiences since he is the master controller. Thus, he should find a suitable synchronization between the

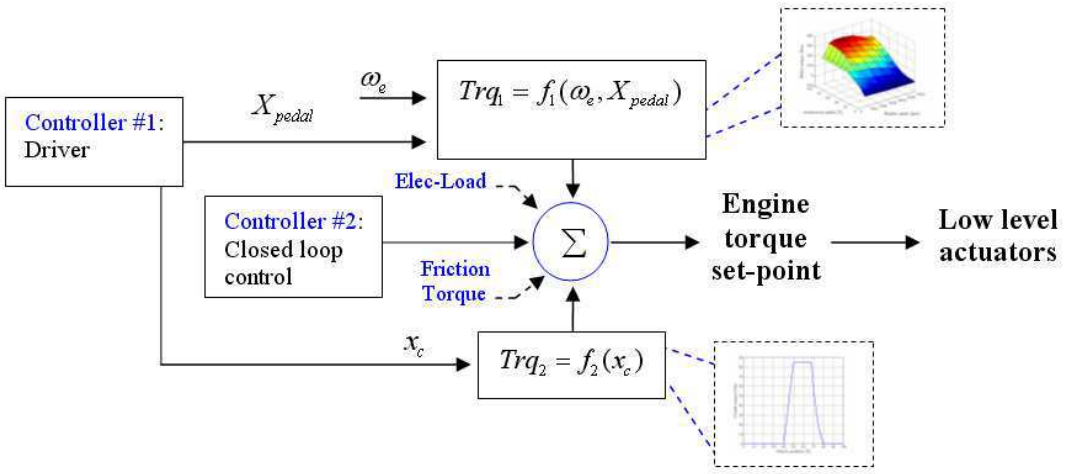

Figure 5.3: Typical torque-based structure for vehicle start-up assistance in vehicles equipped with manual transmission.

accelerator pedal position leading to the torque T_{rq_1} (see Figure 5.3), and the clutch pedal x_c which induces the disturbance torque T_{rq_2}. The idea of the control scheme is to discharge the driver from the tedious synchronization task, by implementing an advanced control strategy that acts on the engine dynamic. In this case, the driver may *feel that he is a good driver* since the control interferes and correct his potential bad actions.

5.4 Phenomenological Clutch Model for Start-up Assistance

In order to guarantee a good vehicle start-up assistance, it is convenient to have a precise information about the clutch torque, since this torque is an important disturbance which may cause important oscillations in the transmission and may even induce engine stall. In section 4.3 we have proposed a phenomenological clutch model during the vehicle start-up phase. This model involves the engine torque set-point, the clutch slipping speed, and a nonlinear function that can be experimentally identified as it has been shown in the previous chapter. In particular, the dependence on the clutch bearing position is expressed through the nonlinear function. Hereafter, we recall the dynamic of the powertrain system using the proposed clutch model:

$$\dot{\omega}_e = a \cdot T_e - a \cdot \text{sgn}(\omega_{sl}) \cdot T_e \cdot \omega_{sl} \cdot f(x_c, \omega_{sl}) \tag{5.3}$$

$$\dot{\omega}_c = b \cdot \text{sgn}(\omega_{sl}) \cdot T_e \cdot \omega_{sl} \cdot f(x_c, \omega_{sl}) - b \cdot T_{load}(i_g i_d, .) \tag{5.4}$$

where:

- $a = J_e^{-1}$ is the inverse of the engine inertia; $b = [J_c + J_{eq} i_g, i_d]^{-1}$ is the inverse of the equivalent inertia of the mainshaft;
- ω_e, ω_c are the rotating speeds of the engine and the mainshaft, respectively;
- ω_{sl} is the slipping speed;
- $f(.)$ is the nonlinear characteristic, which depends on the clutch bearing position and slipping speed;
- T_{load} is an equivalent load torque on the mainshaft that depends on the gearbox ratio $i_g i_d$.

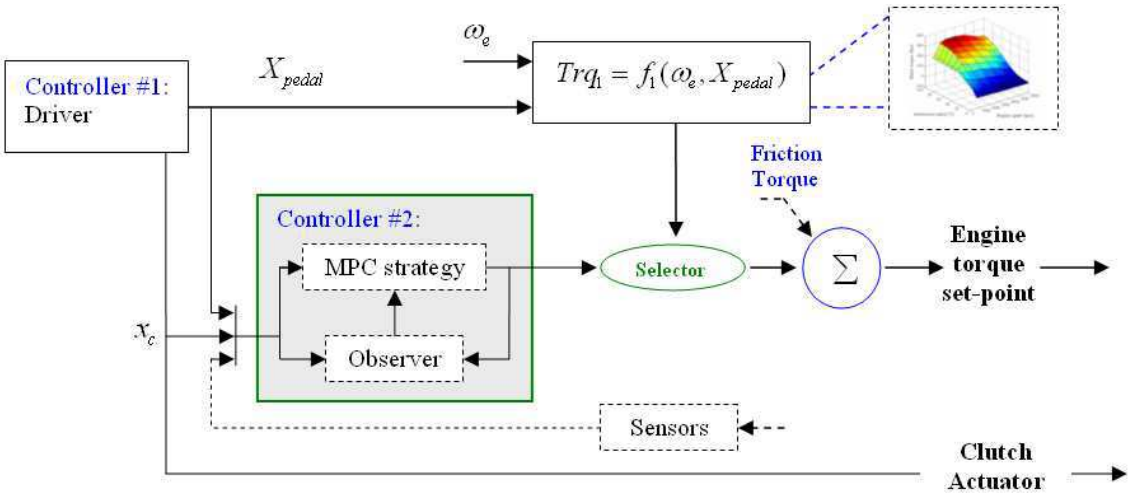

Figure 5.4: Structure of the proposed model predictive control for driving assistance in powertrains equipped with manual transmissions; the strategy includes the idle speed control, the vehicle start-up, and the coasting mode.

Note that equations (5.3) and (5.4) describe powertrain dynamics for both manual or automated manual transmission systems. For AMT-powertrains, the embedded control strategies can act on both dynamics, whereas in the MT-powertrains only the first dynamics can be controlled. The second dynamics is imposed by driver though the clutch pedal.

5.5 Unified MPC Strategy for MT-Powertrain

In the unified control approach, the formulation involves three operating phases which are: the idle speed control, the vehicle start-up, and the coasting of the vehicle. During these phases, the MPC strategy has to ensure the regulation and/or the tracking of the engine speed around a specified reference trajectory and this, using only the engine torque as a control input. To keep close to the conventional structure, a selector is used that can switch between the closed loop-control (MPC) and the open-loop control (pedal torque) as shown in Figure 5.4. Roughly, this selector module applies the pedal torque whenever it is larger than the MPC control. This enables one to maintain some sensitivity on the accelerator pedal if the driver demand is very important. Notice that, in the proposed control structure, the internal friction in the engine are compensated for in a feedforward mode in order to limit the complexity of the MPC control on one hand, and to remain close to the conventional control, on the other hand.

5.5.1 Control Specifications

5.5.1a Control Inputs and Their Limitations

In the proposed model predictive control strategy, the unique control input is the engine torque set-point. The constraints on the control input are similar to those described earlier, namely:

$$T_e \in [T_e^{min}, T_e^{max}(\omega_e)] \tag{5.5}$$
$$\dot{T}_e \in [\dot{T}_e^{min}, \dot{T}_e^{max}] \tag{5.6}$$

where:

- T_e^{max} and T_e^{min} are the upper and the lower bounds on the engine torque, respectively;

- $\dot{T}_e^{min}$ and $\dot{T}_e^{max}$ are the bounds on the variation rate of the engine torque.

Adopting the same notation as the one used in the preceding chapters, namely, denoting by $\tilde{u}$ the sequence of future control inputs over a prediction horizon of length N, one can write the above constraints in the following condensed form:

$$A_c\tilde{u}(k) \leq B_c \tag{5.7}$$

with a straightforward expressions for the constant matrices $A_c \in \mathbb{R}^{4N\times N}$; $B_c \in \mathbb{R}^{4N\times 1}$.

5.5.1b Fuel-Consumption and Limited Engine Torque

Recall that the purpose of the clutch actuation during the vehicle start-up is to steer the main-shaft speed (or vehicle speed) to the engine speed. This has to be done while respecting the control specifications and constraints. Among the specifications, the minimization of the fuel consumption which depends on the applied engine torque. During vehicle start-up, the natural way of achieving minimum fuel consumption is to limit the set-point variation of the engine speed. However, as it has been described for the AMT problem, it is important to allow for relatively high values of the engine speed whenever the needed engine torque goes close to its upper limit. Such situations arise under high loads or rapid vehicle start-up.

5.5.1c No-lurch Condition

The problem of maintaining the *no-lurch* condition for vehicles equipped with manual transmission is much more critical than it is for the vehicles equipped with automated manual transmission. This is because, contrary to MT-applications where the diver controls the clutch engagement through a direct actuation of the clutch pedal; in AMT-applications the embedded control strategies have a total control on the dynamic of the powertrain. As a result, the quality of the clutch engagement depends only on the embedded control.

In MT-applications however, it is possible to ensure smooth clutch engagements provided that the variations of the clutch actuation are very limited close to the terminal instant t_f where the transmission is closing, namely:

$$\dot{x}_c(t_f) \simeq 0 \tag{5.8}$$

this condition is not difficult to meet since it holds in the common situations of vehicle start-up. It is noteworthy to mention that, any total closing of the clutch actuator before the terminal instant t_f, will systematically generate oscillations in the transmission regardless of the control assistance algorithm being used.

5.5.2 Engine Speed Reference Trajectories

5.5.2a Reference Trajectories During Idle Mode

The definition of reference trajectory for the engine speed during the idle mode is quite straightforward, since only constant values are generally assumed. This desired constant trajectory is maintained as low as possible, while taking into account the residual induced vibrations in the engine compartment. These oscillations are very important at very low speeds.

However, during the first cool ignition of the engine, the reference trajectory is maintained at relatively high values in order to get rapidly close to the warm/nominal conditions in terms of the engine temperature. In this case, the engine speed set-point may be defined as follows:

$$\omega_e^{ref} := \omega_e^0 + \triangle\omega_e(T_{cool}) \tag{5.9}$$

where ω_e^0 is a constant value, and T_{cool} is the cooling temperature of the engine. Note that the term $\triangle\omega_e(T_{cool})$ becomes null whenever the engine is going to its nominal temperature.

5.5.2b Reference Trajectories During Vehicle Start-up

The rationale behind the definition of the reference trajectory of the engine speed follows the same principles as those used for the AMT control problem studied in section 2.5.6a. This roughly consists in maintaining the set-point of the idle mode during the vehicle start-up phase when the engine torque production is nominal, and to change the engine operating point whenever the needed engine torque is above this nominal value. Moreover, additional specifications may be taken into consideration to address the specific case of manual transmissions. More precisely, the driver actions on the clutch pedal are *unpredictable* and particularly significant during the first instants of the vehicle start-up around the clutch torque transmitting point. Therefore, one can assume a systematic step variation of the engine speed whenever the clutch bearing gets near to the contacting point. This step variation enables the engine *no-kill condition* to be satisfied during the first instants of vehicle start-up. Consequently, equation (5.9) may be extended using the following expression:

$$\omega_e^{ref} := \omega_e^0 + \triangle\omega_e(T_{cool}) + \triangle\omega_e(T_e^{max}) + \triangle\omega_e(x_c, x_{c0}) \tag{5.10}$$

where:

- $\triangle\omega_e(T_e^{max})$ is a variation related to the limitation of the engine torque production. These situations arise under high loads or rapid vehicle start-up. Figure (5.5.a) shows a typical curve of the engine torque limitation as a function of the engine speed. For example, if the engine speed is regulated at `600rpm`, the maximum torque that can be obtained through the fuel combustion is physically limited to `100Nm`. Thus, if the torque demand goes beyond this limit, the control should change the engine operating point to get more combustion torque at relatively high values of the engine speed. Note that the engine maximum torque normally decreases beyond some engine speed threshold (p.ex. `4000rpm`).
- and $\triangle\omega_e(x_c, x_{c0})$ is a variation related to the *unpredictability* of the clutch bearing position around the clutch contacting point x_{c0}. Thus for computing the term $\triangle\omega_e(x_c, x_{c0})$ we have assumed the map which is presented on the Figure (5.5.b).

Note that, the term $\triangle\omega_e(T_e^{max})$ vanishes when the control T_e is far from the maximum limit T_e^{max} while the term $\triangle\omega_e(x_c, x_{c0})$ is only significant near the clutch contact point.

5.5.2c Reference Trajectories During Coasting Mode

During the vehicle start-up phase, the dynamic of the vehicle is totally controlled by the driver through the clutch pedal. In this phase the derivative of the mainshaft speed is largely positive ($\dot{\omega}_c \gg 0$). However, if coasting mode follows start-up (that is, the driver does not press the accelerator pedal), the derivative becomes very small. Therefore, one can write:

$$\dot{\omega}_c \gg 0; \quad \texttt{if} \quad t \ll t_f \tag{5.11}$$

$$\dot{\omega}_c \simeq 0; \quad \texttt{if} \quad t \simeq t_f \tag{5.12}$$

where t_f is the terminal instant at which the slipping speed becomes null.

A sudden transition between the two limit cases would lead to an important deceleration, and

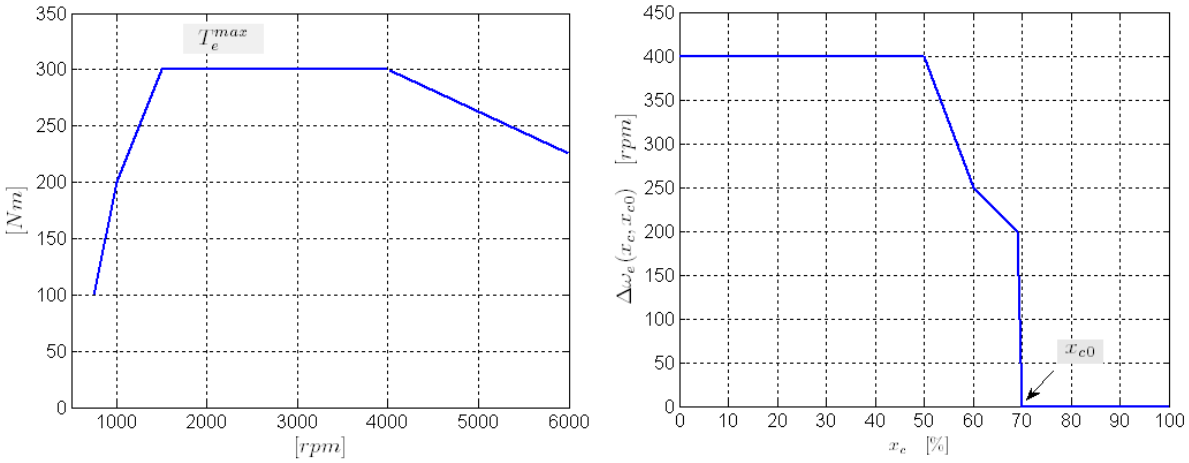

(a) Engine maximum torque production

(b) $\triangle\omega_e(x_c, x_{c0})$ vs the clutch bearing position

Figure 5.5: Typical maps for generating the trajectory of the engine speed.

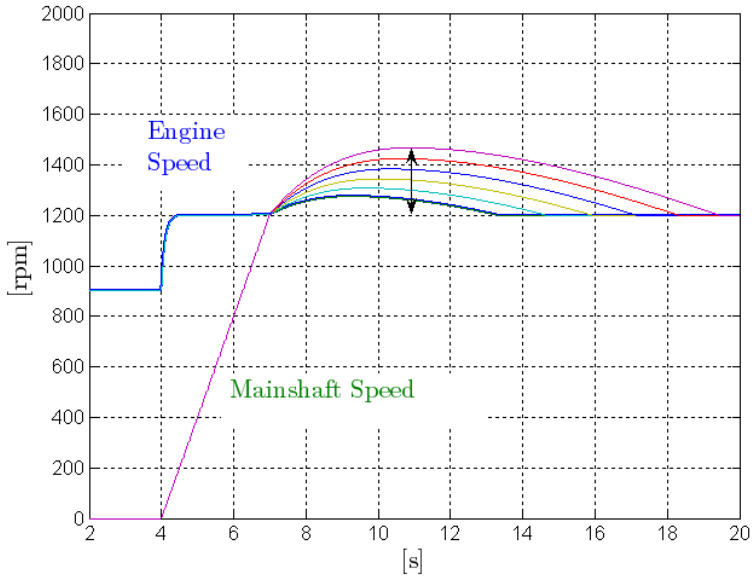

Figure 5.6: Decelerating profiles for the engine speed during the coasting mode.

this may affect considerably the driving comfort. Consequently, reasonable reference trajectories may be the ones depicted in Figure (5.6).
The computation of the desired trajectories assumes some relation between the derivative $\dot{\omega}_c(t_f)$ at the final instant t_f, and the internal frictions T_{frict} in the engine during the coasting mode. The corresponding term is noted by $\triangle\omega_e(\dot{\omega}_c(t_f), T_{frict})$, and is used to extend the previous equation (5.10) leading to the following expression for ω_e^{ref}:

$$\omega_e^{ref} := \omega_e^0 + \triangle\omega_e(T_{cool}) + \triangle\omega_e(T_e^{max}) + \triangle\omega_e(x_c, x_{c0}) + \triangle\omega_e(\dot{\omega}_c(t_f), T_{frict}) \tag{5.13}$$

5.5.3 Control Structure During Idle Mode

As discussed above, the control of the engine speed is vulnerable during the idle mode, since the amplitudes of the disturbances are comparable or larger than the applied engine torque. Therefore, an offset on the engine torque efficiency is used to guarantee a rapid transient on the engine torque realization. In the nominal operating condition during which the engine speed is equal to its reference set-point, the engine torque efficiency $\eta_{T_e}^{sp}$ should be lower than its optimal value, namely:

$$\eta_{T_e}^{sp} \leq 1.0 \tag{5.14}$$

Because of the lack of an accurate model linking the dynamic of the engine speed to the engine torque set-point and its efficiency (the two control inputs), the control architecture assumes two separate controllers. The first one computes the engine torque set-point using the proposed MPC design and ensures tracking. The second controller, computes the torque efficiency so as to assist the MPC controller for regulation purposes. As shown in Figure 5.2, the MPC controller is assumed to be a high level controller, whereas the torque efficiency set-point is manipulated at a lower control level.

During the idle mode, the following model is used in the MPC formulation:

$$\dot{\omega}_e \quad = \quad a \cdot T_e^{SP} + a \cdot \hat{\delta}_e \tag{5.15}$$

where $\hat{\delta}_e$ is an estimated torque that gathers the effects of all the imperfections of the above model similarly to the scheme that has been used for the AMT control problem described previously chapter.

5.5.4 Vehicle Start-up Assistance

Recall that, the design of MPC control for AMT-powertrains involved a sort of *transparency* requirement w.r.t to the driver demand by linking the definition of the reference trajectories to the accelerator pedal position. This approach cannot be applied to MT-powertrains since the driver imposes the dynamic of the vehicle through the clutch pedal. In this case, only the engine speed is controllable by the embedded controller. The resulting control problem is roughly similar to the idle mode control, since the clutch torque T_c is a disturbance and the control has the only engine torque set-point as degree of freedom. Therefore, one can extend the idle speed model (5.15) to the clutch engagement phase by using:

$$\dot{\omega}_e \quad = \quad a \cdot T_e - a \cdot q \cdot T_c(x_c, .) + a \cdot \hat{\delta}_e \tag{5.16}$$

where $q \in \{0, 1\}$ is a Boolean related to activation/deactivation of the start-up phase.

5.5.5 Coasting Mode

During the driving assistance, the coasting mode is also important since the driver may achieve a vehicle start-up with only the clutch pedal actuation. In this case, the embedded control should ensure the vehicle start-up and vehicle's coasting once the start-up phase is achieved. Furthermore, the coasting mode involves also the situations where the accelerator pedal position is low during the start-up phase, and remains also low during the coasting phase. In this case, the pedal torque which depends on the accelerator pedal is never applied to the low level actuators. Thereby, the embedded control ensures totally the driving of the vehicle like the previous case where the accelerator pedal position is null. Finally, one can mention the activation of the

coasting mode that follows the pedal mode when the driver releases totally the accelerator pedal while keeping the transmission completely closed.

Concerning the powertrain model during the coasting mode, it is similar to the idle mode model except that the transmission is completely closed and the amplitudes of the load torque, involved in the term $\hat{\delta}_e$, are very important.

5.5.6 Proposed NMPC Design for Driving Assistance

5.5.6a Control Structure

In this section, the Model Predictive Control design is explained. One major feature is the use of the phenomenological clutch model developed in the previous chapter in a model predictive control framework for vehicle start-up assistance. The implementation of this control strategy is investigated through the use of the Constrained Parameterized Approach (CPA), which enables real-time implementation while handling the problem constraints and nonlinearities in the process model.

Recall that NMPC formulation needs the definition of a dynamic model of the system that can be written as follows:

$$x(k+1) = f(x(k), u(k)) \tag{5.17}$$

where $x \in \mathbb{R}^n$, $u \in \mathbb{R}^m$ are the state and the input respectively. In the remainder of this section, the notation $x(k)$ denotes the value of the state vector at the sampling instant k.

Recall that predictive control is obtained by applying at each instant k the first action $u(k)$ of the optimal sequence of actions

$$\mathbf{u}(k) = \big(u^T(k), u^T(k+1), \ldots, u^T(k+N-1)\big) \in \mathbb{R}^{Nm}$$

that minimizes some cost function. The latter expresses the control objective over a prediction horizon of length N, that is to say, over the time interval $[k\tau, (k+N)\tau]$. In what follows, a preliminary cost function is denoted by:

$$\Omega(x(k), \mathbf{u}(k), \mathbf{r}(k), \nu(k)) \tag{5.18}$$

where

- $x(k)$ is the current state at instant k;
- $\mathbf{r}(k)$ is some set of desired trajectories that may be defined on the regulated variables. Here, the reference trajectory concerns the engine speed $\omega_e^{ref}(\cdot)$;
- ν is an exogenous input vector that describes some key quantities of the context at instant k that may influence the definition of the cost function. In our case, this vector is given by:

$$\nu := \begin{pmatrix} \hat{\delta}_e \\ x_c \\ X_{pedal} \end{pmatrix} \in \mathbb{R} \times \mathbb{R} \times \mathbb{R}. \tag{5.19}$$

This cost function is to be minimized in the decision variable $\mathbf{u}(k) \in \mathcal{U}(k) \subset \mathbb{R}^{Nm}$ unless a low dimensional parametrization is adopted as introduced in section 1.6. Note also that the minimization has to be performed over the admissible set $\mathcal{U}(k)$ of decision variables. This is

defined through a set of operational constraints that have to be respected in closed-loop. The constrained set $\mathcal{U}(k)$ gathers all the limitations that are partially described by (5.5)-(5.6). Note that the admissible set $\mathcal{U}(k)$ can be implicitly state-dependent through the time index k. This is due to the fact that the engine maximum torque depends on the engine operating point (engine speed).

In the present context of vehicle start-up assistance, the manipulated variable is the set-point of the engine torque $u := T_e^{sp}$. Ideally, in the absence of real-time implementation constraint, the decision variable at sampling instant k would be the piece-wise constant profile of the decision variable over the prediction horizon $[k, k+N_p]$, namely:

$$\mathbf{u}(k) = \big(u^T(k), \ldots, u^T(k+N_p-1)\big)^T \in \mathbb{R}^{N_p} \tag{5.20}$$

Taking into account the value of the exogenous vector $\nu(k)$ [see (5.19)] which involves the estimated torque $\hat{\delta}_e$ and two known inputs X_{pedal} and x_c as well as the reference trajectory, one can write the predictive control formulation using the following constrained optimization problem:

$$\underset{\mathbf{u}}{min}\ \Omega(x(k), \mathbf{u}(k), \mathbf{r}(k), \nu(k)) \quad \texttt{under} \quad A_c\mathbf{u} \leq B_c \tag{5.21}$$

where

$$\Omega(x(k), \mathbf{u}(k), \mathbf{r}(k), \nu(k)) := \sum_{i=1}^{N_p} \Big\| \Big(\omega_e(k+i) - \omega_e^{ref}(k+i, x_c(k), X_{pedal}(k))\Big) \Big\|_Q^2 \tag{5.22}$$

in which $\omega_e(k+i)$ is the solution of the control model starting from the initial condition $\omega_e(k)$ under the control profile defined by $\mathbf{u}$ and using the estimation $\hat{\delta}_e(k)$ contained in the context vector $\nu(k)$ while the reference trajectory $\omega_e^{ref}(\cdot)$ is defined as described above for the given positions $x_c(k)$ and $X_{pedal}(k)$ (see equation (5.13)).

5.5.6b Control Parametrization

Solving on-line the constrained quadratic problem (5.21) would be certainly beyond the on-board computation facility when considering the sampling time of the targeted application. This is the reason why a sub-optimal formulation is proposed hereafter to meet the real-time implementation requirements. In order to do this, let us first rewrite the engine speed dynamic equation using the clutch torque model derived in the preceding chapter:

$$\dot{\omega}_e = a \cdot T_e - a \cdot \mathrm{sgn}(\omega_{sl}) \ \cdot T_e \cdot \omega_{sl} \cdot \ f(x_c, \omega_{sl}) \tag{5.23}$$

Note that in the forthcoming discussion, for the sake of simplicity, the control input is supposed to be given by T_e while it is rigorously the engine torque set-point T_e^{SP} that plays this role. The same mechanism that has been used for the AMT problem can be used here by introducing the uncertainty term δ_e that is then reconstructed by a dedicated dynamic observer.

The equation (5.23) can be reformulated using the notation $u = T_e$ as follows:

$$\dot{\omega}_e = a \cdot u_1 + \big[\alpha(\omega_{sl}, x_c)\big] \cdot u_1 \tag{5.24}$$

Contrary to the structure of the system model for the AMT problem where a linear time invariant system has been derived, here, the model clearly shows nonlinearities that have to be overcome for real-time implementation to be made possible. This is done using a priori assumptions on the future trajectories of the nonlinearity related terms ω_{sl} and x_c. Namely, at each instant k, the following assumptions are used to construct the prediction over the prediction horizon $[k\tau, (k+N)\tau]$:

- a convergence profile is assumed on $\omega_{sl}(k+i)$ for $i \in \{1, \ldots, N\}$ that is compatible with the current value $\omega_{sl}(k)$ and a standard settling time for the clutch closing. This leads to a given predicted trajectory that is referred to hereafter by:

$$\omega_{sl}^{pred}(k+i|k)$$

- The same feature is assumed concerning the behavior of the clutch pedal position x_c leading to the predicted trajectory:

$$x_c^{pred}(k+i|k)$$

Based on these prediction models, one can write an approximation of the quadratic cost on the tracking error (between the predicted engine speed ω_e and the reference trajectory on the engine speed ω_e^{ref} discussed earlier in this chapter) that takes the following form:

$$\left\| \left[A_1\right] \cdot \mathbf{u}(k) + \left[A_2(\omega_e(k), \nu(k))\right] \cdot \mathbf{u}(k) - B(\omega_e(k), \nu(k)) \right\|^2 \tag{5.25}$$

where $\nu(k)$ is the context vector mentioned above [see equation (5.19)] that is used to compute the reference trajectory on the engine speed and which also contains the current value of the clutch bearing position $x_c(k)$. Note that $A_1 \in \mathbb{R}^{N \times N}$ is a constant matrix while $A_2 \in \mathbb{R}^{N \times N}$ and $B \in \mathbb{R}^N$ are time varying matrix and vector respectively.

Unfortunately, here again, this cost function would be heavy to handle since the quadratic term related matrix would be state dependent and hence would have to be computed at each decision instant. More precisely, the pseudo-inverse of this matrix cannot be computed off-line once for all for on-line use. In order to overcome this drawback, the cost function (5.25) is first rewritten in the following equivalent form:

$$\left\| \left[A_1\right] \cdot \mathbf{u}(k) + B_1(\mathbf{u}(k), \omega_e(k), \nu(k)) \right\|^2 \tag{5.26}$$

where the following notation is introduced:

$$B_1(\mathbf{u}(k), \omega_e(k), \nu(k)) := \left[A_2(\omega_e(k), \nu(k))\right] \cdot \mathbf{u}(k) - B(\omega_e(k), \nu(k)) \tag{5.27}$$

This last form suggests the following definition of a parameterized unconstrained quadratic cost function in the decision variable $\mathbf{u}$ that is defined at each decision instant k according to:

$$\begin{aligned} &\Omega^{unc}(\mathbf{u}, p, x(k), \nu(k), \mathbf{u}(k-1)) := \\ &\left\| \left[A_1\right] \cdot \mathbf{u} + B_1(\mathbf{u}(k-1), \omega_e(k), \nu(k)) \right\|^2 + p \cdot \|\mathbf{u} - \mathbf{u}(k-1)\|^2 \end{aligned} \tag{5.28}$$

where

$$p \in [0, \infty]$$

is a scalar parameter.

The rationale behind the definition (5.28) lies in the following facts:

- By using the previously computed sequence $\mathbf{u}(k-1)$ as an argument for B_1 in the definition of the current cost function, the only remaining term that involves the unknown sequence $\mathbf{u}$ is $A_1\mathbf{u}$ which leads to a constant matrix in the quadratic term. As mentioned above, this drastically simplify the on line implementation at the price of a slight modification of the cost function.

- For $p = 0$, the cost function (5.28) is a slight modification of the original cost (5.26) due to $\mathbf{u}(k)$ being replaced by the preceding sequence $\mathbf{u}(k-1)$ as an argument of B_1.

- When $p \to \infty$, the optimal solution satisfies the constraints provided that the preceding solution $\mathbf{u}(k-1)$ satisfies these constraints which always hold by choosing a suitable initialization.

Therefore, the Model Predictive Control strategy is defined by the following scalar optimization problem in the decision variable p:

$$\begin{aligned} &p^{opt}(\omega_e(k), \nu(k), \mathbf{u}(k-1)) := \\ &\arg\min\Big\{p \in [0, p_{max}] \quad \text{such that} \quad A_c \mathbf{u}_{pwc}(p,k) \leq B_c\Big\} \end{aligned} \tag{5.29}$$

where

$$\mathbf{u}_{pwc}(p,k) \quad \text{is the unconstrained minimum of (5.28)}$$

while p_{max} is a sufficiently high upper bound for all initial conditions of interest. Remember that the computation of the unconstrained minimum of (5.28) can be performed very easily since the quadratic term related matrix $A_1^T A_1$ is constant. Therefore, its pseudo inverse can be computed off-line once for all. Only the term B_1 has to be updated by the current values of its arguments.

The optimization of the parameter p can be done by simple scalar dichotomy since, by taking a sufficiently large value, the constraints would be satisfied. Once the scalar optimization problem is solved to yield the optimal parameter:

$$p^{opt}(\omega_e(k), \nu(k), \mathbf{u}(k-1))$$

the first control in the corresponding control profile:

$$\mathbf{u}_{pwc}(p^{opt}(k), k)$$

is applied during the sampling period $[k, k+1]$.

At the next decision instant, the new optimal parameter is computed, namely:

$$p^{opt}(\omega_e(k+1), \nu(k+1), \mathbf{u}(k))$$

and the first control in the corresponding optimal control sequence:

$$\mathbf{u}_{pwc}(p^{opt}(k+1), k+1)$$

is applied during the sampling period $[k+1, k+2]$ etc.

This is precisely the nonlinear model predictive control law.

Remark 5.5.1. Another option that can be used to define the parameterized cost function (5.28) that proved efficient during the design related simulations is based on the following definition:

$$\begin{aligned} &\Omega^{unc}(\mathbf{u}, p, x(k), \nu(k), \mathbf{u}(k\text{-}1)) := \\ &\Big\| \big[A_1\big] \cdot \mathbf{u} + (1-p) \cdot \big(B_1(\mathbf{u}(k\text{-}1), \omega_e(k), \nu(k))\big) + p \cdot \big(B_1(\mathbf{u}(k\text{-}2), \omega_e(k\text{-}1), \nu(k\text{-}1), p(k\text{-}1))\big)\Big\|^2 \end{aligned} \tag{5.30}$$

where $p \in [0,1]$. Note that when $p = 0$, the same cost function is obtained while the value $p = 1$ leads to the previous cost function.

5.6 Conclusion

In this chapter a model predictive control design has been proposed for start-up assistance for vehicles equipped with a manual transmission. The proposed approach covers idle speed control, vehicle start-up, and vehicle coasting. During the vehicle start-up phase, the model predictive control strategy uses the phenomenological clutch model developed in chapter 4 to perform precise prediction of the system behavior over the prediction horizon.

The problem of real-time implementation of the proposed MPC strategy is addressed thanks to some suitable simplifications and a specific parametrization. This results in a simple scalar optimization problem that can be solved by dichotomy in which, each cost function evaluation involves a matrix product. Moreover, the proposed control uses measurements which are commonly available in mass-production vehicles, except the clutch bearing position sensor which may be absent in some vehicles. The relatively low cost of the sensor and the benefits of start-up assistance might motivate the adoption of such a sensor. An adaptation of the control strategy using the clutch pedal position instead, could be also considered.

The next chapter presents a validation of the proposed unified MPC control in a highly-downsized vehicle equipped with a manual transmission. In this application, start-up assistance is very important since the downsized engine operates in a more severe context than that of conventional vehicles.

Chapter 6

Application and Validation of Clutch Torque Modeling and Vehicle Start-Up Assistance on a MT Demo-Car

6.1 Introduction

This chapter illustrates the application and validation of the contributions developed in the previous two chapters. In chapter 5, a model predictive control design has been proposed for start-up assistance in vehicles equipped with a manual transmission. The aim of start-up assistance is to improve driving comfort, in a context where the driver controls directly the transmission. Depending on the driver's actions on the accelerator and clutch pedals, start-up assistance is usually activated during engine idle control mode and handles the transition to pedal mode or coasting mode. The only degree of freedom left to the embedded control system is to modify the engine torque setpoint of the current engine control mode in order to compensate the driver's actions on the clutch pedal, which can be seen as a disturbance. During the vehicle start-up phase, the model predictive control strategy uses the phenomenological clutch torque transmissibility model developed in chapter 4 to perform precise predictions of the system behavior over the prediction horizon.

In the first part of the chapter, we present the application context and, more particularly, the EcoSural demo-car, a manual transmission vehicle equipped with a highly-downsized turbocharged engine (section 6.2). Then we explain in detail what a start-up assistance controller is supposed to do and how it interacts with the standard engine control modes. We also describe the control and co-simulation layout used for validation.

The rest of the chapter is devoted to validation. In section 6.3, we make the first steps to validate the clutch torque transmissibility model itself. To that purpose, a simplified version of the model is used in feed-forward in a standard idle speed controller to replace the simple clutch torque characteristics that are usually adopted in this context. This provides a basic form of start-up assistance, which can be further improved by introducing an *ad-hoc* assistance controller start-up, also using the simplified phenomenological clutch model. The second part of the validation, in section 6.4), concerns more specifically the full-fledged start-up assistance based on the nonlinear model predictive control strategy proposed in chapter 5. The performances of this strategy are illustrated by simulation results.

6.2 Application Context

6.2.1 The Ecosural Demo Car

The development of the clutch torque transmissibility model and of the nonlinear model predictive control strategy presented respectively in chapters 4 and 5, finds and interesting application framework in the VELSATIS ECOSURAL demo car. Resulting from a project conducted in partnership with Faurecia Système d'Echappement and Honeywell Turbo Technologies and with the contribution of Renault, the Velsatis Ecosural is a prototype sedan car equipped with a highly-downsized SI engine (Le Solliec et al. (2006), Le Solliec et al. (2007)).

Figure 6.1: The VELSATIS ECOSURAL demo car.

The downsizing concept implies a reduction of engine displacement and compensation by turbo charging and other technologies (such as variable valve timing). This makes it possible to reduce the fuel consumption and CO_2 emissions. For this demonstrator, IFP has developed a 1.8-liter turbo charged gasoline engine with direct injection in homogeneous combustion mode. The resulting performance is equivalent to that of a 3-liter engine: 340 Nm at 1500 rpm and 147 kW at 5500 rpm. In the resulting demo car, the fuel consumption is reduced by up to 20% and the pollutant emissions comply with the Euro 5 European standard. This vehicle integrates demonstration of this concept with a *full-path* IFP engine control, making the most of the technology potential. In particular, advanced engine control strategies are needed to make full use of the twin variable camshaft timing (VCT) technology implemented on the engine, and improve its performances:

- control of residual burnt gases at low load to minimize fuel consumption and pollutant emissions;
- control of air scavenging at high load to avoid knock and to improve combustion efficiency (reducing residual burned gases and in-cylinder temperatures);
- reduction of turbo-lag duration during transients by increasing mass flow rate through the turbine.

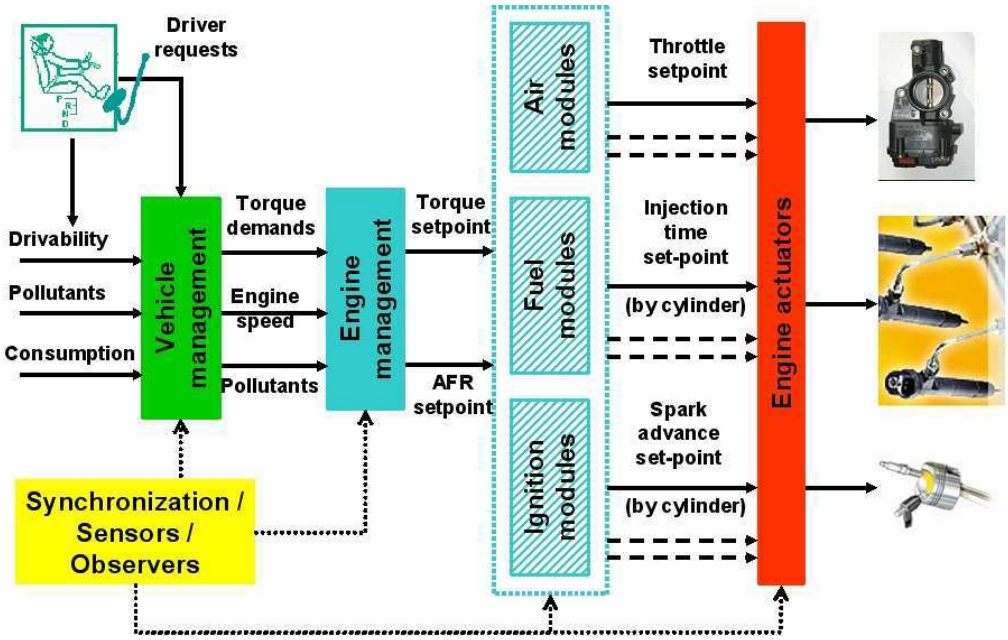

Figure 6.2: Hierarchical torque-based control structure of the EcoSural engine management system (manual-transmission powertrain equipped with a spark-ignition engine)

The last item is particularly relevant for our application context: despite the improvements brought by advanced control strategies, it is still difficult to make a highly-downsized engine produce high torque outputs, fast, at low speeds. With a vehicle weighing nearly 2 tons, drivability at start-up is clearly affected, and deserves specific attention.

As for the VEHGAN demo car, a rapid-prototyping system based on MATLAB, SIMULINK and xPCTARGET has been used both for the engine test bench and the vehicle. In the first version of the demonstrator, the on-board system was based on an industrial prototyping micro-PC (Pentium III 1GHZ, RAM 256Mb) and on the GEC system developed by FH Electronics. The latter has then been replaced by a more flexible ECU designed at IFP. The engine management system, coded in Simulink adopts the standard torque-based control structure first mentioned in section 1.3 and shown again in Figure 6.2 for convenience.

The demo car has been developed using the same steps and tool-chain as for the control development cycle adopted for the VEHGAN project:

- first, engine control design is carried out using a reference simulation model;
- control and structure algorithms are then iteratively improved using refined versions of the reference simulator;
- further tests are performed within Software-in-the-Loop (SiL) and Hardware-in-the-Loop (HiL) frameworks, based on real-time capable simulators derived from the reference simulator;
- engine control software validated in co-simulation is directly "plugged in" on the on-board system of the demonstrator, tested and re-calibrated where needed.

6.2.2 The Start-up Assistance Context

Figure (6.3) represents the two main scenarios which are to be considered for vehicle start-up assistance. In the first scenario, the driver acts on both the accelerator pedal and the clutch pedal. Whereas, in the second scenario, the driver releases only the clutch pedal to move the vehicle from still.

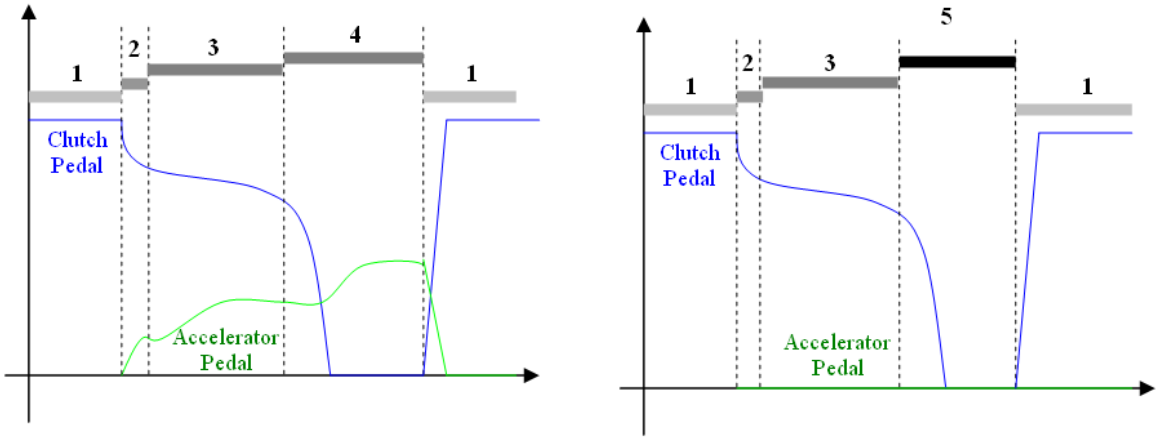

(a) Vehicle start-up → Pedal mode

(b) Vehicle start-up → Coasting mode

Figure 6.3: Operating modes of a manual transmission vehicle related to start-up. (1): Engine idle mode - transmission open; (2): Vehicle stand-by with clutch go-to-slipping; (3): Vehicle start-up (clutch closing); (4): Pedal mode (clutch closed); (5): Coasting mode (idle mode with transmission closed).

The interval (1) corresponds to the engine idle mode, with the transmission completely opened. In both scenarios, vehicle start-up is preceded by a stand-by phase (2) where a gear is engaged, the driver starts releasing the clutch pedal and the clutch is the go-to-slipping phase where the disks are still not in contact. When the disks are at the torque transmitting point, the vehicle start-up phase (3) begins. In this mode, if the driver accelerates, the assistance controller computes the engine torque that guarantees a "suitable" start-up of the vehicle (more particularly, engine stall must be avoided), compares it with the pedal torque (open-loop torque) requested by the diver and correct it if it is necessary. Thus, it should bring the powertrain to the normal pedal mode (4) without hitches. Instead, if the driver closes the clutch without using the accelerator pedal, the assistance controller has to bring (smoothly) the powertrain from the engine idle mode with the transmission open to the idle mode with the transmission closed (5), and the vehicle moving at minimum speed.

In normal vehicles, with standard engine control, the second scenario is generally dealt by the idle-speed controller via a feed-forward compensation of the resistant torque applied by the clutch (and eventually a modification of the idle speed set-point). The first scenario is dealt with in a similar way, but in pedal mode. Provided that the compensation torque can be delivered quickly enough, and that the driver does not release the clutch too fast, those strategies are generally effective enough, even when the estimation of clutch torque is coarse. But this is not the case for a heavy vehicle with a highly-downsized engine, where a full-fledged start-up assistance is needed.

6.2.3 Control and Co-Simulation Layout

The standard IFP *full path* engine control, with some modifications in the *engine torque manager* (see Figure 6.4), is the starting point of the validation and of the implementation.

Concerning the validation of the improvements to the basic start-up assistance, the modifications affect essentially the idle speed control block. For the rest part of the validation, a special control block overrides the operations of the standard idle speed and pedal modes during vehicle start-up, and implements the full-fledged start-up assistance.

Before and in parallel to the experimental test, a co-simulation environment has been used for test and validation. On the control side, it includes the same engine management system introduced before. Similarly to the case of AMT control for the VEHGAN demo car, since the engine-cycle time scale suffices to capture the relevant longitudinal dynamics during start-up, most validation tests have been carried out in a framework centered on a mean-value engine model (MVEM) coded in AMESIM with blocks from the IFP Engine library and a relatively simple powertrain and vehicle chassis (with blocks from the IFP Drive and the Powertrain library). The resulting AMESim sketch is shown in Figure (6.5).

To test the limits of the start-up assistance controller, we have considered different scenarios requiring specific modulations of the vehicle load torque and specific actions on the clutch. Figure 6.6 shows the parts of the co-simulation framework dedicated to this validation.

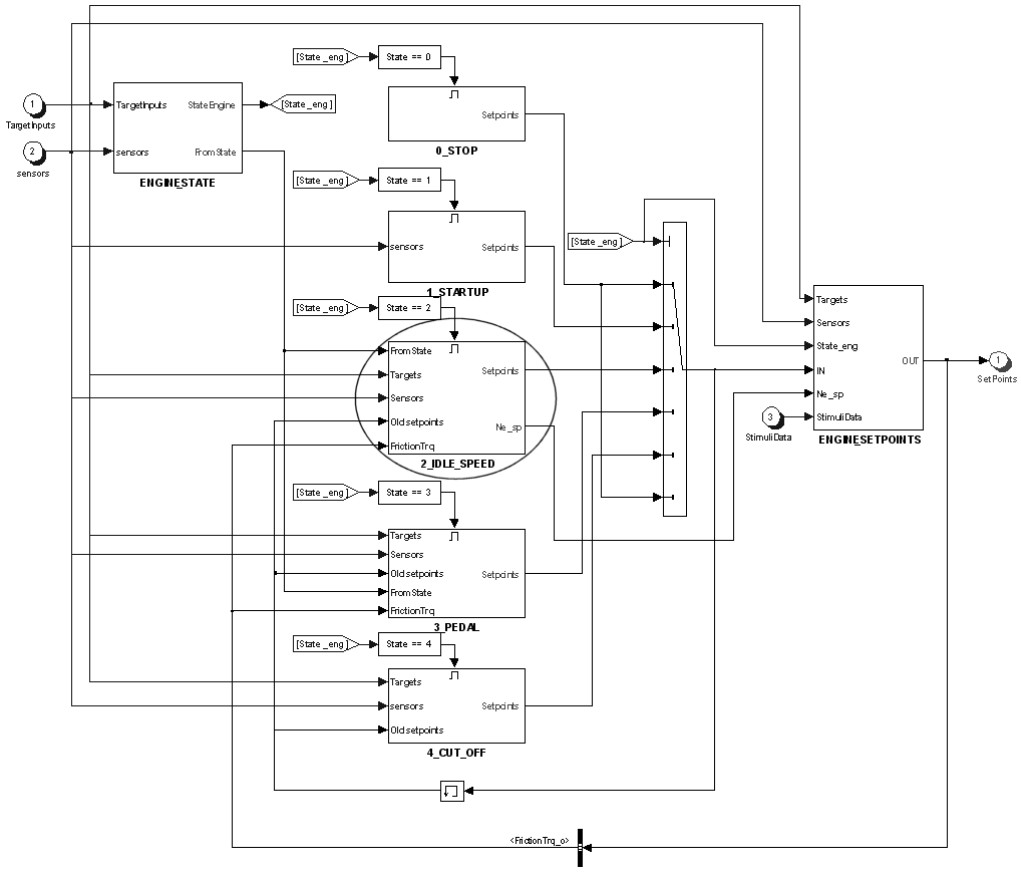

Figure 6.4: Engine torque manager in the standard IFP *full path* engine control

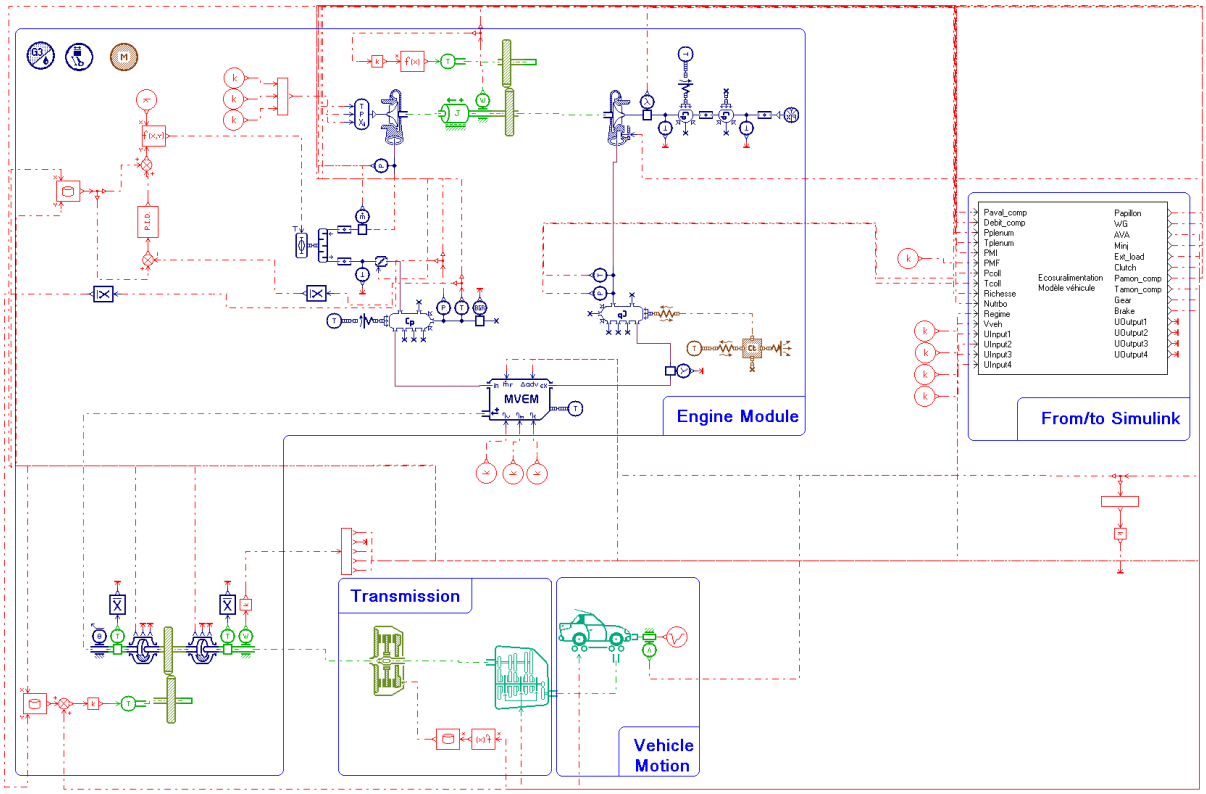

Figure 6.5: VelSatis co-simulating framework: the engine module involves a turbocharged mean value engine model (MVEM); the transmission includes a dry clutch and a manual gearbox.

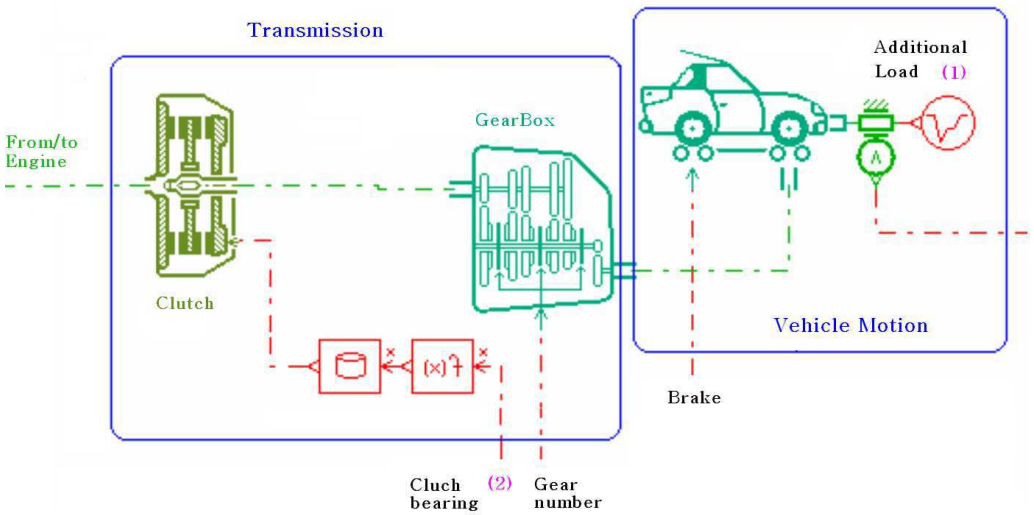

Figure 6.6: Co-simulation framework: (1) Additional variations of the load torque; (2) Different actuations on the clutch actuator.

6.3 From Basic to Full-Fledged Start-up Assistance

6.3.1 Usual Clutch Torque Characteristics vs. Phenomenological Model

As recalled before, during the start-up phase of a vehicle with a manual transmission, the clutch actuation imposes a significant negative torque on the engine shaft. The driver should compensate this torque himself/herself, but his/her action may be insufficient or even null, as it is the case when he/she releases the clutch pedal only and expects the vehicle move slowly from stand-still.

Standard engine control systems usually deal with this case by adding a feed-forward compensation to the controller active during this kind of start-up, namely the idle speed controller. A similar compensation can be applied in pedal mode, if the action on the accelerator pedal is insufficient.

In both cases, the feed-forward compensation is based on simple clutch torque transmissibility characteristics, identified experimentally (see Figure 6.7) or built from information gathered from the clutch manufacturer. These characteristics generally assume that the transmitted torque depends only from the clutch bearing position, namely:

$$T_c := h(x_c) \tag{6.1}$$

where $h(.)$ is the nonlinear clutch characteristic vs. the clutch bearing position x_c. All the other dependencies are neglected.

This is precisely the case for the standard engine control software embedded in the EcoSural prototype, whose clutch torque transmissibility curve is shown in Figure (6.8). Notice that the shape of the curve is "physical" only fror clutch bearing positions comprised between 100% (clutch completely open) and 72%. The rest of the shape is motivated by an attempt to avoid that the feed-forward torque stay added indefinitely to the engine torque set-point when the clutch is completely closed (and a degree of freedom is lost in the powertrain model).

A first step towards the improvement of start-up assistance consists in replacing the usual clutch torque transmissibility curves, by the phenomenological model we have proposed in chapter (4) for the vehicle start-up phase, which ensures accurate characterization of the clutch torque.

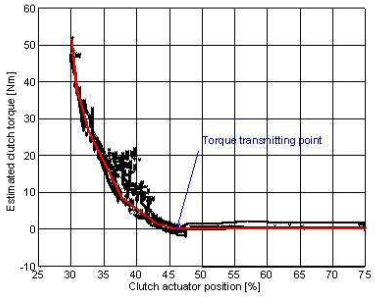

(a) Estimated values and piece-wise linear approximation (from Tona et al. (2007)) used in the SMART demo-car

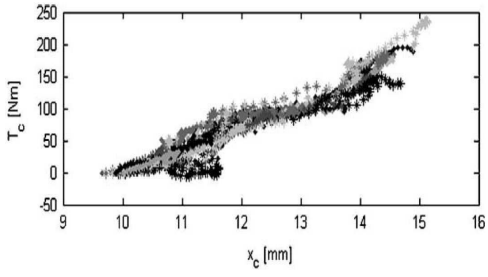

(b) Clutch torque wearing characteristic (from Glielmo et al. (2004))

Figure 6.7: Experimentally identified clutch torque transmissibility curves

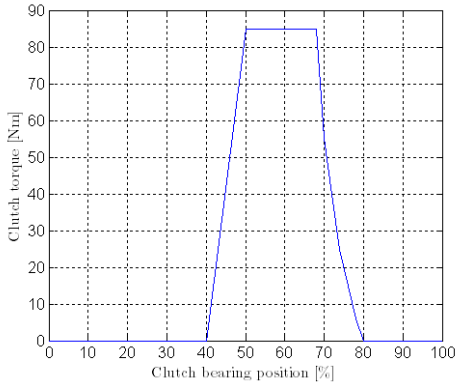

Figure 6.8: Clutch torque transmissibility curve used in the EcoSural demo-car

In this model, the clutch torque is assumed to depend on the engine torque set-point T_e, the slipping speed ω_{sl}, and a nonlinear characteristic $f(.)$, namely:

$$T_c := T_e \cdot \omega_{sl} \cdot f(\omega_{sl}, x_c) \tag{6.2}$$

The non linear function $f(.)$ depends on the clutch bearing position x_c and on the slipping speed ω_{sl}. An experimental identification of this nonlinear characteristic for the EcoSural demo car is represented on the Figure (6.9).

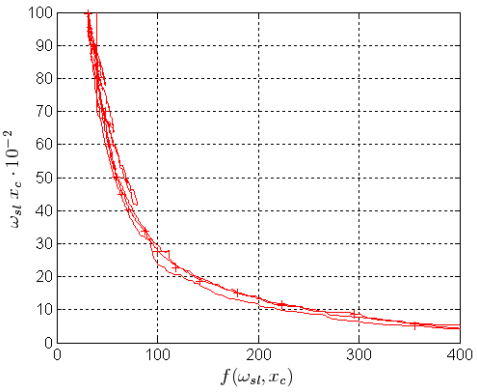

Figure 6.9: Experimental characterization of function $f(.)$ for the EcoSural demo car

Based on the phenomenological clutch model, a feed-forward term can be obtained by assuming a nominal value for engine torque during the vehicle start-up phase, corresponding to a constant value of load torque during start-up. This approximation allows to define a *nominal* phenomenological clutch model, namely:

$$T_c^n = T_e^n \cdot \omega_{sl} \cdot f(x_c, \omega_{sl}) \tag{6.3}$$

where: T_e^n is a constant nominal value.

This nominal clutch torque T_c^n can be used directly in the feed forward compensation by replacing the former assistance term

$$T_c = h(x_c)$$

in the standard idle-speed (and pedal-mode) controller. In the next section a comparison is made between the two approaches.

6.3.2 Improvement of Basic Start-up Assistance

In the configuration under scrutiny, idle-speed control is carried out by a standard Linear Quadratic (LQ) controller which computes both the engine torque set-point and the engine torque efficiency set-point. Once the driver acts the clutch pedal, an assistance torque is summed to the computed engine torque set-point in order to reject the clutch disturbance. More accurate information about the torque transmitted by the clutch (than available with the usual clutch torque models) facilitates the task of the closed-loop control and ensures better performances. This is shown in Figure 6.10 which compares two vehicle start-ups, obtained with similar driver actions on the clutch: sub-figure 6.10(a) is obtained through the usual clutch characteristic $T_c = h(x_c)$, whereas sub-figure 6.10(b) is obtained using the characteristic issued from the nominal phenomenological model of equation (6.3). The idle-speed controller using the nominal clutch model ensures relatively good regulation of the engine speed, with respect to an action on the clutch that is not handled well in the former case.

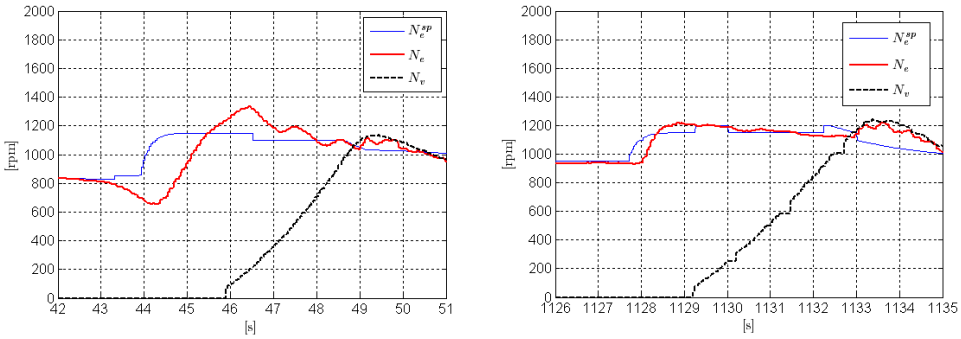

(a) Initial clutch characteristic (b) Nominal clutch characteristic

Figure 6.10: Driving assistance using a standard idle-speed controller; (a) refers to the first test which is obtained using the initial clutch characteristic; (b) represents the second test with the nominal phenomenological clutch characteristic.

6.3.3 Towards a Full-Fledged Start-up Assistance

In the previous section, we have shown that using a simplified version of the phenomenological clutch model in feed-forward, in a standard idle-speed controller, has improved its performance. However, that controller is specifically designed and calibrated for idle mode operations and not for start-up assistance. Before implementing of the full-fledged start-up assistance controller described in chapter 5, we have designed and tested a simpler linear controller. This controller is a linear MPC whose control model is the following :

$$\dot{\omega}_e = J_e^{-1} \cdot T_e - q \cdot J_e^{-1} \cdot T_c^n(.) + J_e^{-1} \cdot \hat{\delta}_e \tag{6.4}$$

where:

- T_e is the control input;
- T_c^n is the nominal clutch torque;
- $q \in \{0, 1\}$ is a boolean which goes to 1 during the start-up phase;
- $\hat{\delta}_e$ gathers uncertainties and model mismatches.

The generation of engine speed reference trajectories in order to ensure a proper start-up is carried out as explained in section 5.5.2 for the full-fledged NMPC assistance controller. If the driver uses the clutch pedal only, the torque T_e computed by the assistance controller is directly applied to the engine, otherwise it is compared with the torque T_e^d requested by the driver via the accelerator pedal, and $max(\ T_e,\ T_e^d\ )$ is applied.

Notice that, in the control model, we have assumed a clutch torque computed via the nominal phenomenological model, which neglects the dependency on the applied engine torque. Since the latter is not constant during start-up, we expect a relatively large variation of the term $\hat{\delta}_e$.

Figure 6.11 shows the results of an experimental test of vehicle start-up assistance, obtained using the aforementioned linear model predictive control. In this test, the driver releases the clutch pedal with no action on the accelerator pedal, as shown on the quadrant (c). On the EcoSural demo car the torque transmitting point of the clutch is approximately 80%, which yields a vehicle start-up phase starting at $t \simeq 54s$.

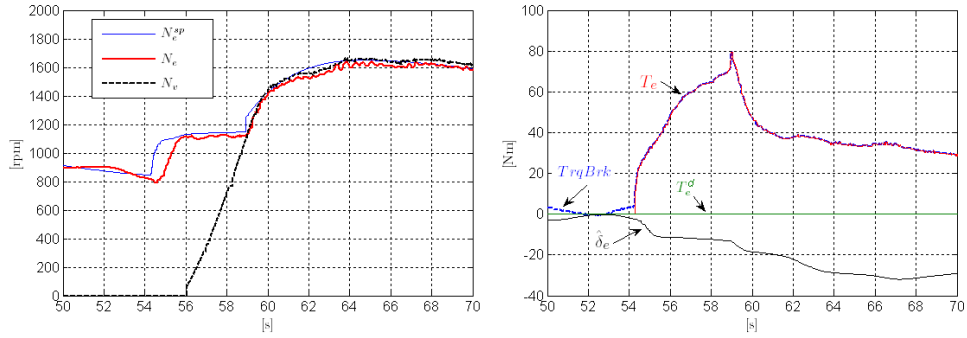

(a) Speeds (b) Torques

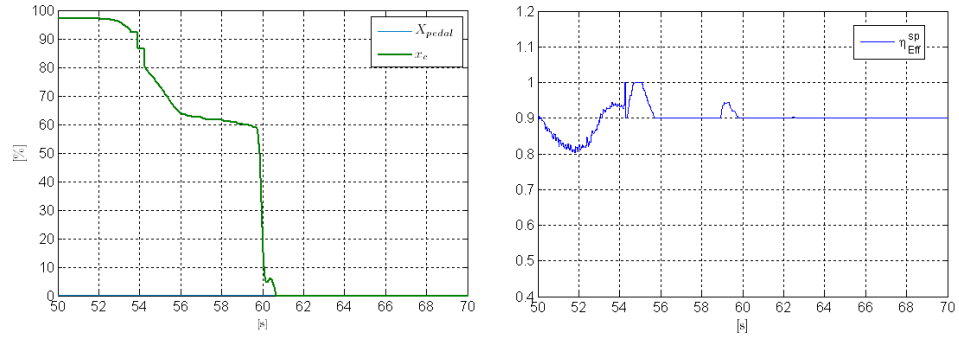

(c) Accelerator and clutch pedals (d) Engine torque efficiency

Figure 6.11: Validation of start-up assistance via a simple MPC controller using the nominal phenomenological torque of clutch torque. The driver acts only the clutch pedal to start the vehicle, as shown in the quadrant (c).

The performances of the proposed control are good, without any induced oscillations in the transmission, and with good engine speed tracking to the trajectory specified by the controller during vehicle start-up and vehicle coasting. As expected, there is a large variation of $\hat{\delta}_e$ (of nearly $12Nm$ during start-up phase), represented on the quadrant (b), which captures uncertainties and missing dynamics in the clutch torque. Finally, in quadrant (d) one can remark that the engine torque efficiency, during the activation of the MPC strategy, is limited since the regulation and tracking errors are also limited.

Other experimental tests show that, when $\hat{\delta}_e$ is larger or varies faster, a degradation of performance occurs. This happens for instance for uphill start-ups.

6.4 Start-up Assistance through Unified NMPC

So far, we have shown that the phenomenological clutch model, in his approximated form, where the dependency on engine torque is reduced to a value corresponding to a nominal load torque, can be profitably used to improve the performance of basic assistance, via feed-forward compensation in a standard idle-speed controller, or to design a simple linear assistance controller, whose performance has been proven acceptable in a set of experimental tests, provided that uncertainties in clutch torque estimation are not too large. The latter condition is not always ensured: typically, during uphill or downhill start-ups, information about the clutch torque used in the control is not accurate.

To make the most of the the phenomenological clutch model proposed in chapter 4, we have to resort to nonlinear control approaches, and more particularly, to the unified nonlinear model predictive control which has been investigated previously in chapter 5. Let us recall that its design is based on the following powertrain control model is rewritten shortly by:

$$\dot{\omega}_e \quad = \quad J_e^{-1} \cdot T_e - q \cdot J_e^{-1} \cdot T_c\big(x_c, T_e, \omega_{sl}, .\big) + J_e^{-1} \cdot \hat{\delta}_e \tag{6.5}$$

where:

- T_e is the control input;
- T_c is the clutch torque given by the phenomenological model;
- $q \in \{0, 1\}$ is a boolean which goes to 1 during the start-up phase;
- $\hat{\delta}_e$ gathers uncertainties and model mismatches.

The resulting controller can cover all the phases involved in vehicle start-up, idle-speed control at stand-still and idle-speed control with the transmission closed and the vehicle running (coasting). In the former, $\hat{\delta}_e$ should capture the uncertainties of the internal friction model used in feed-forward, by standard engine control: if that model is accurate, $\hat{\delta}_e \simeq 0$. In the latter, $\hat{\delta}_e$ should capture the load torque acting on the vehicle.

During the start-up phase, we expect that $\hat{\delta}_e$ remains close to $\hat{\delta}_e(t_0)$, its value at the end of the idle speed phase.

The validation of the proposed nonlinear model predictive control has been carried out in the co-simulation environment introduced before in section (6.2). Two different set of validation scenarios are considered : against variations of vehicle load torque and against different driver actions on clutch pedal.

Unfortunately, no experimental results are available for this controller, since at the time of writing, the embedded control system of the EcoSural demo car has undergone a major hardware and software revamping.

6.4.1 Validation against Variations of Load Torque

In the following we will test the performance of the proposed unified nonlinear predictive control during the idle, vehicle start-up, and coasting mode, for different profiles of resistant torque applied to the vehicle, in order to simulate start-ups of increasing difficulty.

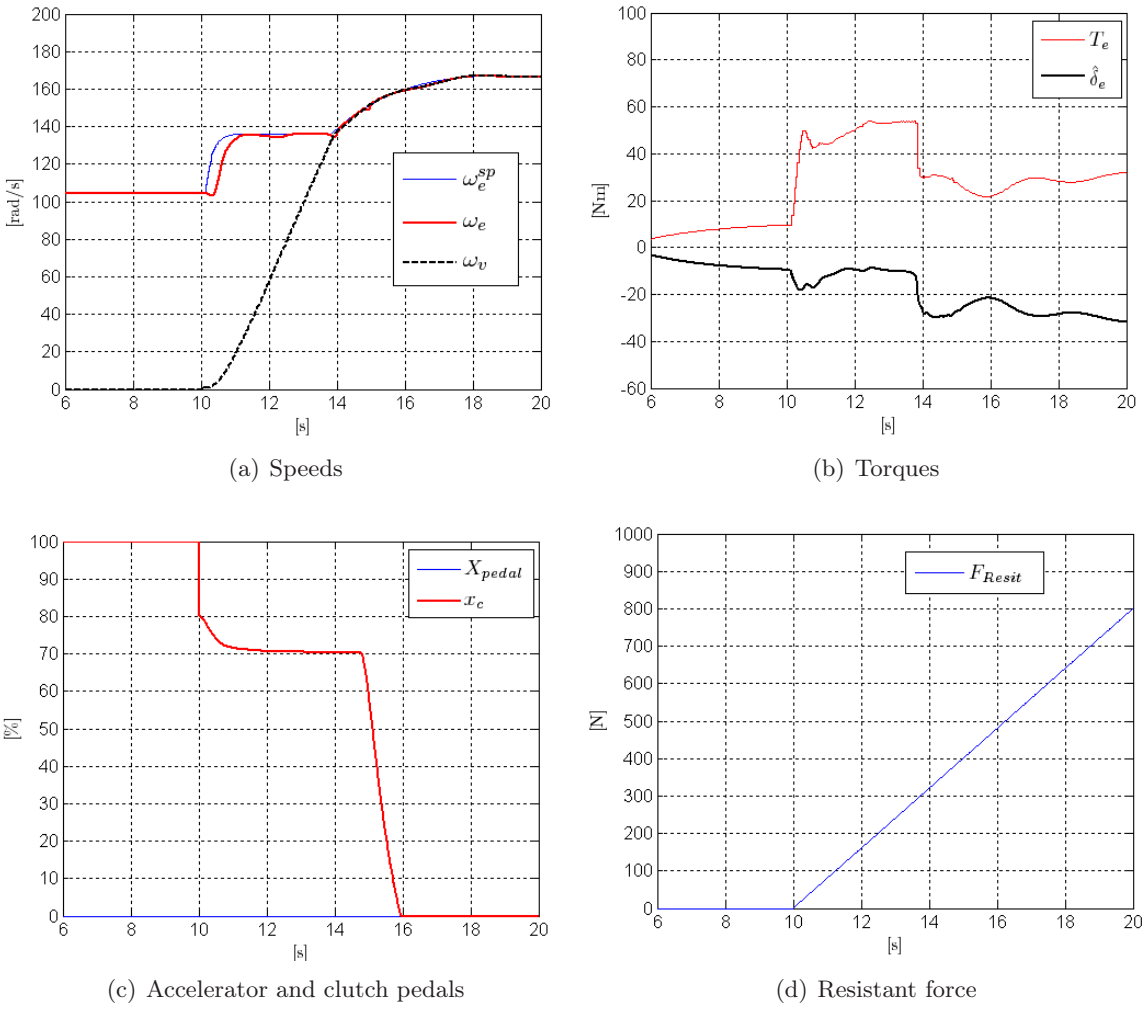

(a) Speeds

(b) Torques

(c) Accelerator and clutch pedals

(d) Resistant force

Figure 6.12: Validation of the unified NMPC strategy during the idle, vehicle start-up, and coasting modes

Figure 6.12 shows the results of the first validation test. Along the idle mode, the control ensures a good regulation of the engine speed along the desired reference trajectory. At the instant $10s$ the driver releases the clutch pedal to move the vehicle from still with no action on the accelerator pedal. The clutch torque transmitting point, where the engine torque starts to be transmitted to the mainshaft, is approximately at 80% of the clutch bearing position. Once the vehicle starts moving, an additional ramp-like resistant force is applied to the front of the vehicle. During the start-up phase, the control ensures again a good regulation of the engine speed (see quadrant (a) of Figure 6.12). Quadrant (b) of Figure 6.12 shows that, as expected, the variation of the estimated torque $\hat{\delta}_e$ remains limited and proves the accuracy of the phenomenological clutch model in this situation. When the vehicle start-up is achieved, at $t = 14s$, the control moves to the coasting mode and the NMPC strategy ensures again good tracking of the engine speed.

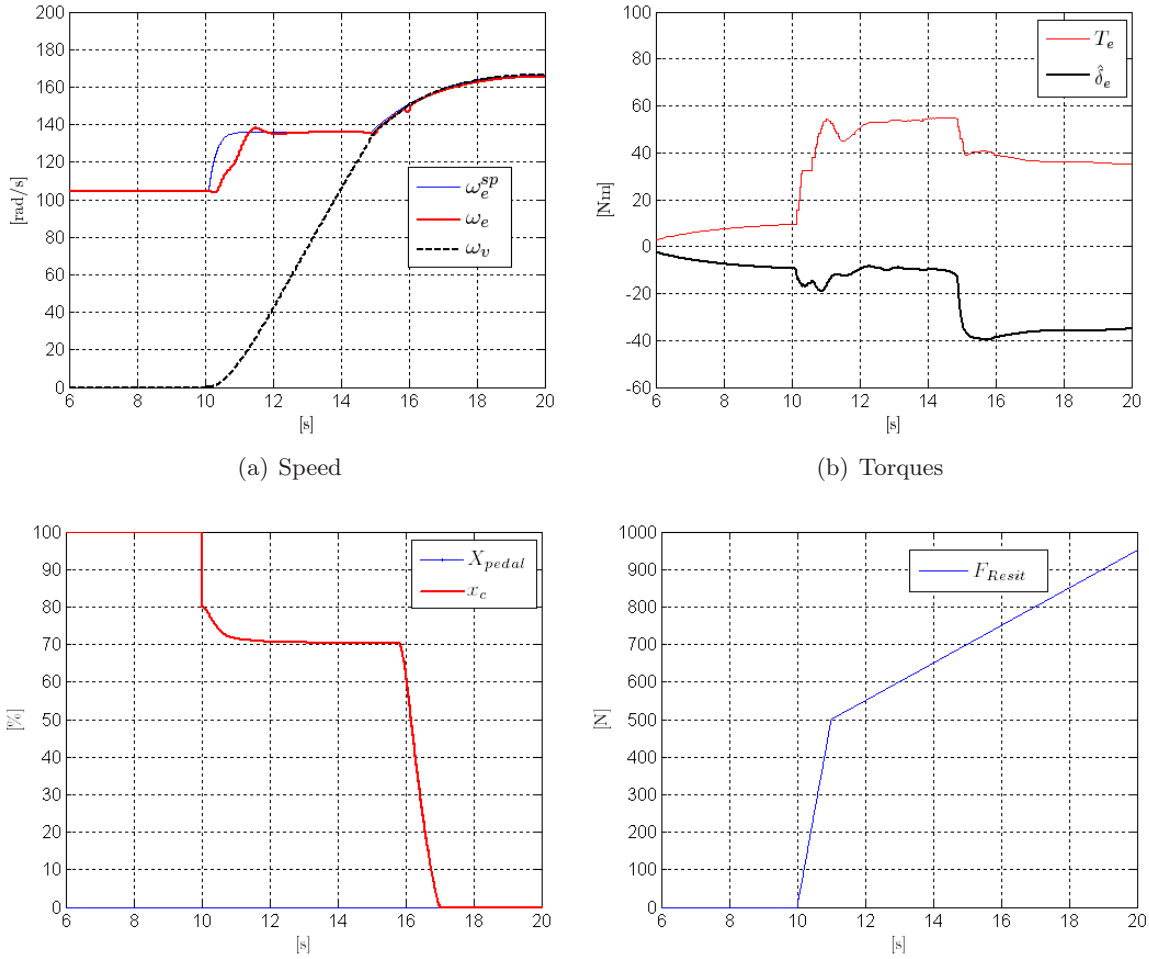

(a) Speed

(b) Torques

(c) Accelerator and clutch pedals

(d) Resistant force

Figure 6.13: Validation of the unified NMPC strategy assuming a larger resistant force. Start-up duration is increased to $\simeq$ 5s.

A second validation test is presented in Figure 6.13. This time a more severe resistant force is applied during the vehicle motion, while keeping the same start-up clutch pedal profile used in the previous test. The increase of the resistant force affects the duration of the start-up phase. In the previous test the time duration is approximately $4s$, whereas in the actual test it nears $5s$. Concerning the control performance, the NMPC strategy ensures a good regulation and tracking of the engine speed, except for a very limited overshoot at the beginning of the vehicle start-up phase. Like the previous test, the variation of the estimated torque $\hat{\delta}_e$ remains very limited during the start-up phase.

A third validation test has been designed by assuming a very large resistant force acting on the vehicle, as represented on the quadrant (d) of Figure 6.14. In this case the vehicle start-up is close $6s$, compared to the first test and the second test whose durations were $4s$ and $5s$, respectively. Concerning control performance, there are no major differences with respect to the second test. Again, the variation of the estimated torque $\hat{\delta}_e$ during vehicle start-up is very limited, thus indicating that the assumed control model, including the phenomenological clutch model, is quite accurate in this situation.

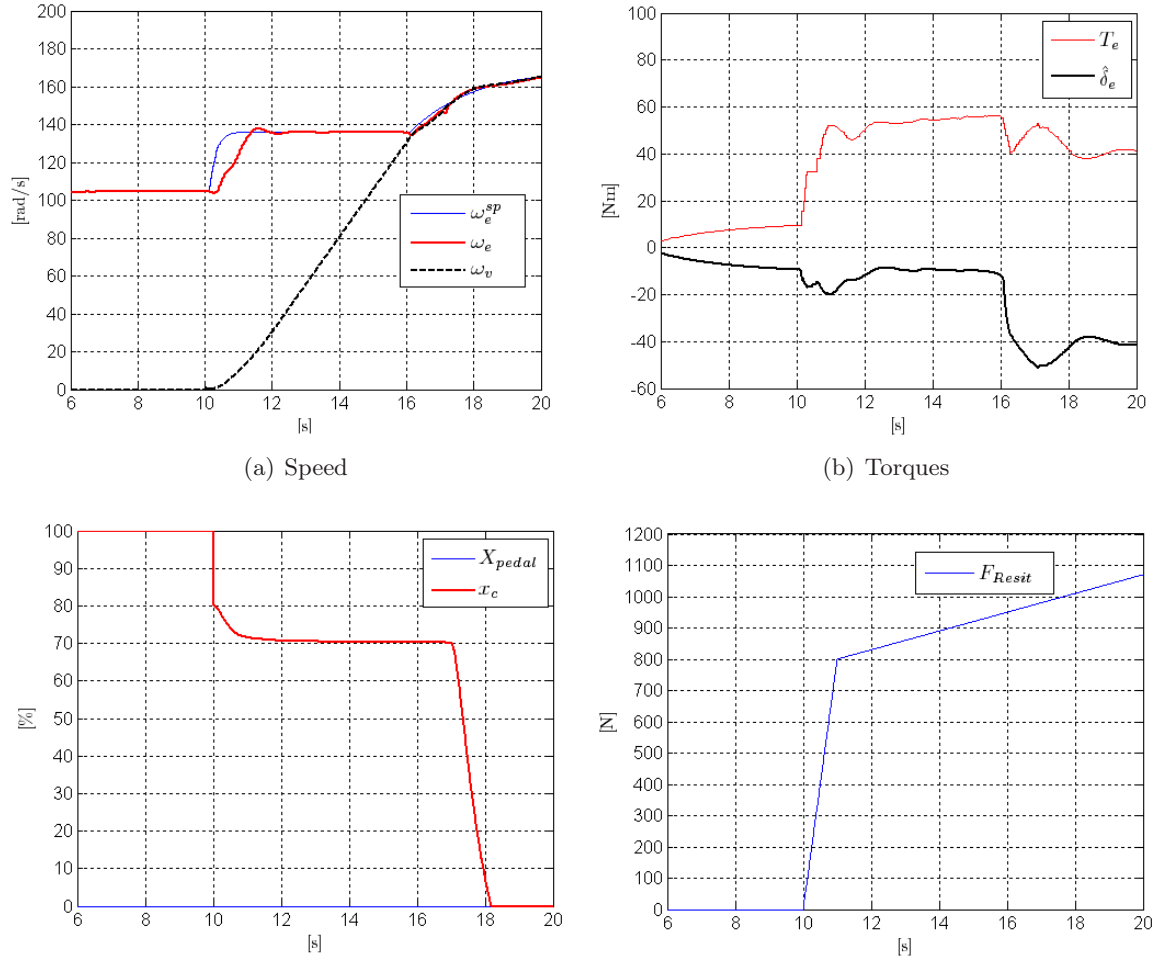

(a) Speed

(b) Torques

(c) Pedals

(d) Resistant force

Figure 6.14: Validation of the unified NMPC strategy assuming a very large resistant force; the vehicle start-up duration is increased to 6s.

6.4.2 Validation against Actions on the Clutch Pedal

The scenarios presented in this section are meant to validate the NMPC performance against different actions of the driver on the clutch pedal. Generally speaking, fast releasing of the pedal imposes rapid vehicle start-up whereas slow releasing imposes slow vehicle start-up. Figure 6.15 resumes the results of three tests of vehicle start-up obtained with three different clutch pedal profiles.

The first test, shown on quadrant (a) can be considered as a nominal case, in which the vehicle start-up duration is approximately $4s$. In the second test, shown on quadrant (b), the clutch is released relatively fast, thus reducing the start-up duration down to $3s$. In the third test, shown on the quadrant (c), the releasing is very fast, thus yielding a duration of $2s$.

Notice that for a fixed load torque, the amplitudes of the applied engine torque are inversely proportional to the vehicle start-up duration. More precisely, when the duration is small, the control applies significant torques to achieve the vehicle start-up. In the our tests, the durations

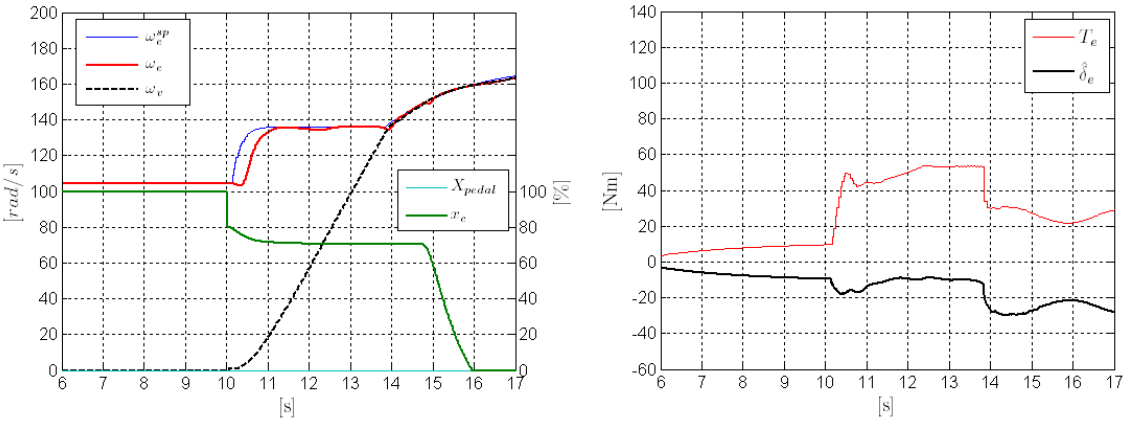

(a) Nominal vehicle start-up

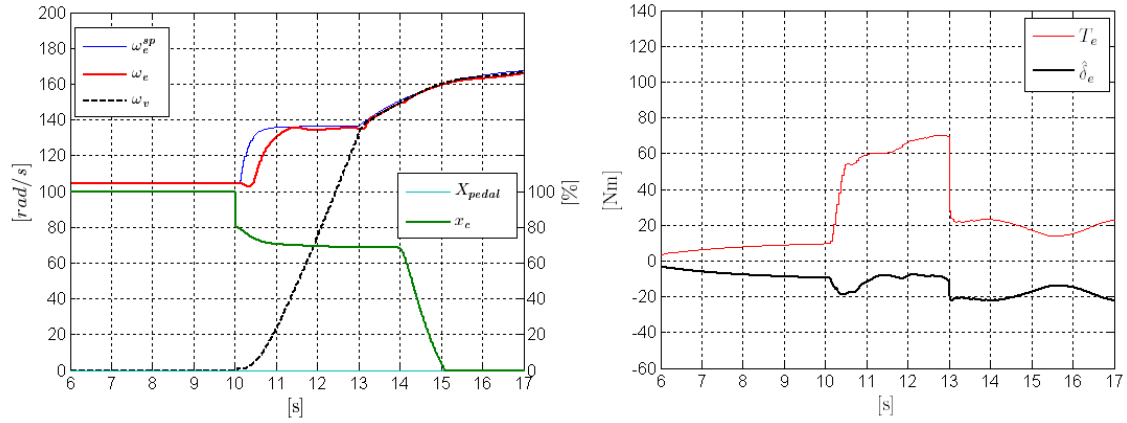

(b) Relatively rapid vehicle start-up

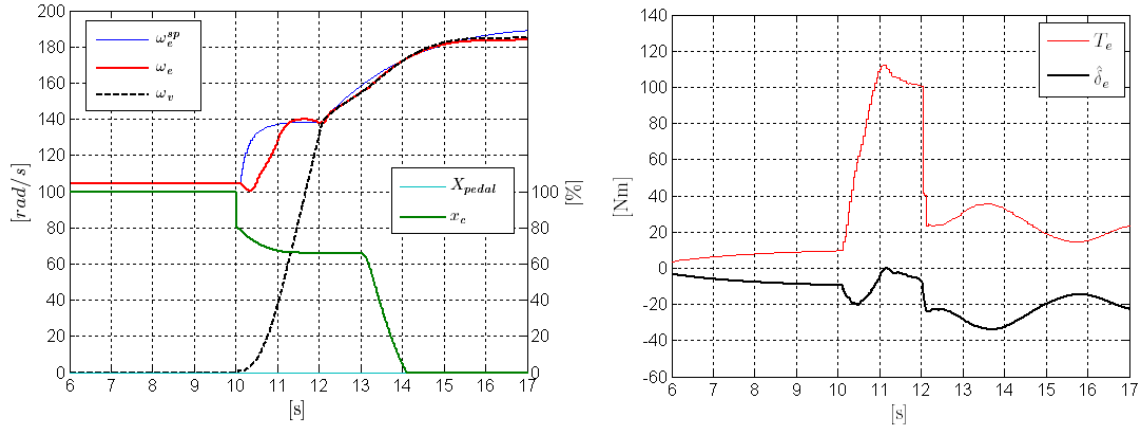

(c) Rapid vehicle start-up

Figure 6.15: NMPC validation for different clutch pedal profiles.

are $4, 3, 2$ [s], whereas the nominal values of the engine torques are $50, 70, 110$ [Nm], respectively. Notice also that the clutch profiles for start-up are realistic since they have been designed based on common experimental profiles, resembling that of figure 6.11. Nonetheless, it must be underlined that on a real vehicle, nothing prevents the driver from releasing the clutch abruptly. In this case, it would be impossible for any controller manipulating only the engine torque to compensate the sudden increase in resistant torque.

Regarding the overall control performance for these tests, the proposed nonlinear predictive control achieves good regulation and tracking of the engine speed, on the one hand, with limited variations of the estimated torque $\hat{\delta}_e$ during the clutch engagement phase, on the other hand.

6.4.3 Validation against Actions on Both Clutch and Accelerator Pedals

As explained before, if the driver accelerates in addition to releasing the clutch pedal, the task of the assistance controller is to compute the engine torque that guarantees a "suitable" start-up of the vehicle (more particularly, engine stall must be avoided), to compare it with the pedal torque (open-loop torque) requested by the diver and correct it if it is necessary.

We do not wish to dwell much on start-up assistance in this context, since we reckon that our contribution stands out more clearly and can be better assessed in the case where there is no driver action on the accelerator pedal. Still, it is important to provide elements of validation of our solution in this case, since it represents a relevant facet of the original problem we wanted to solve.

There are several practical issues that arise when dealing with this case. For instance, calibration engineers require that the driver be free of increasing engine speed as he/she likes to "feel the power" of the engine. Thus, it may happen that the driver tries to start up the vehicle with an insufficient torque demand, then accelerates a lot before decelerating too much just before clutch lock-up. In such a situation, the assistance controller should first compensate the inadequate torque demand, then hand control over to the driver, than compensate again. The management of the transitions is complex and not every situation can be dealt with satisfactorily.

In our implementation, in order to ensure a bumpless transfer from closed-loop control (by assistance controller) to manual control (by the driver) and back, we "freeze" the assistance controller during the manual control phases, but keep updating its observer all along the start-up. This enables to handle most situations correctly.

Figure 6.16 show a simulation test considering simultaneous action on the accelerator and clutch pedals. At the beginning of the start-up, the assistance controller compensates the driver's torque demand T_e^d (up to $20Nm$ are added to it), then each time T_e^d exceeds the torque T_e computed by the assistance controller, the latter is "frozen", while its observer keeps running. When the control is handed over to the driver, there is nothing that prevents the engine speed from overshooting (since this is indeed what the driver wants). But when driver's torque demand becomes too low to ensure a smooth clutch lock-up, the assistance controller intervenes again, in a rather seamless way.

Of course, situations where the driver acts on the pedal in an inconsiderate manner, cannot be handled so smoothly. But our simulation tests show that our solution helps in most of the cases.

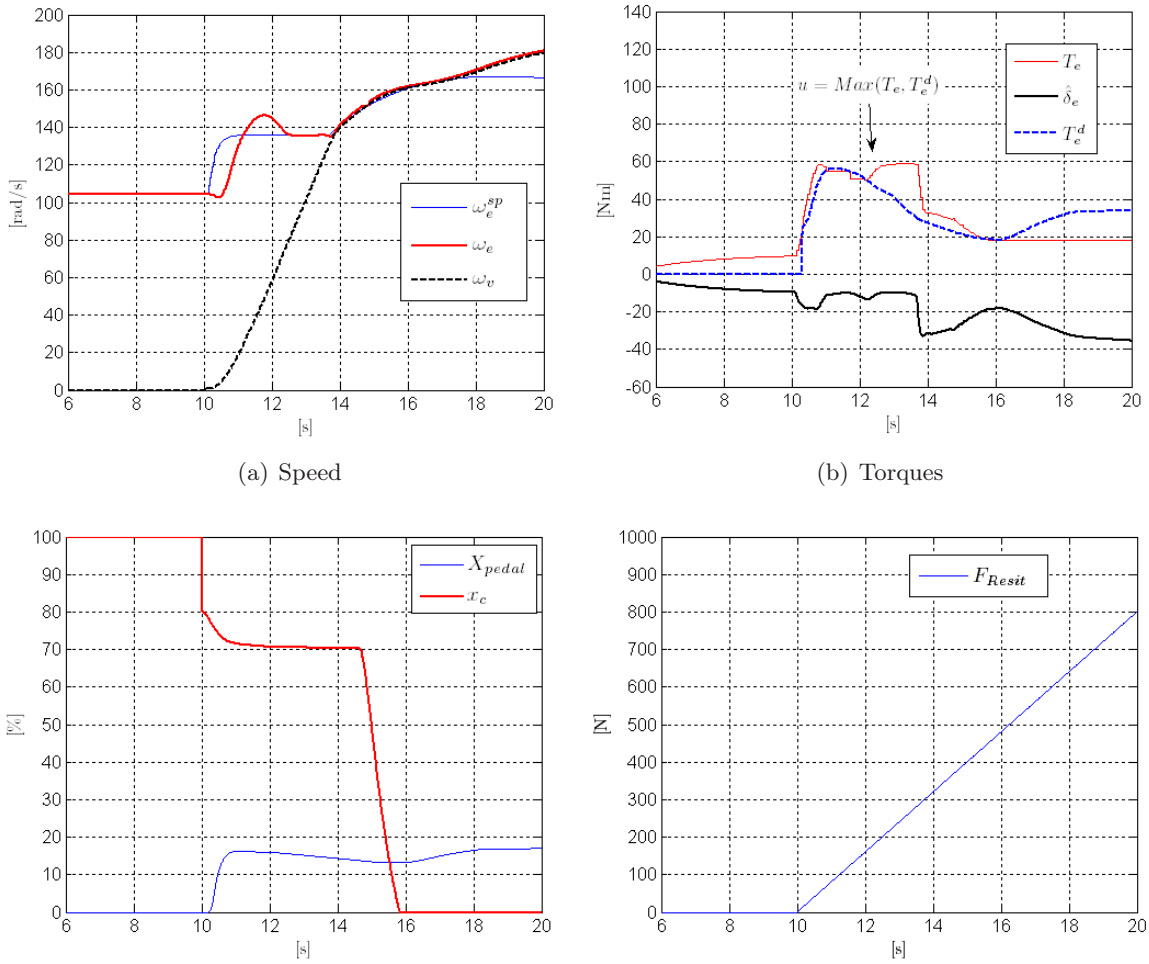

(a) Speed

(b) Torques

(c) Pedals

(d) Resistant force

Figure 6.16: NMPC validation for actions on both the accelerator pedal and the clutch pedal.

6.5 Conclusion

We have shown how the phenomenological clutch torque transmissibility model developed in chapter 4 and the nonlinear model predictive control strategy designed in 5 can be profitably used to solve the start-up assistance problem for a manual transmission vehicle equipped with a highly-downsized turbo-charged engine (section 6.2)

The first set of validation tests, performed experimentally, on the Eco-Sural demo car have indicated that even a simplified version of the phenomenological clutch model can be beneficial to the quality of start-up, whether a basic assistance strategy or a specifically designed one is chosen.

However those solution are unnecessarily limited. The use of the complete phenomenological clutch torque transmissibility model in the nonlinear model predictive control strategy, allows to reduce the bias on the estimated disturbance torque seen by the controller, thus improving its overall robustness. Let us recall, once again, that only the use of a nonlinear control design allows to take full advantage of the phenomenological clutch model.

We have mostly focused on situations where there is no driver's action on the accelerator pedal, since the contributions of the start-up controller are clearer and easier to explain.

Conclusions and Perspectives

With the increase in complexity of mechatronic systems used in modern vehicles, control systems play nowadays a fundamental role in the automotive world. In response to ever more stringent environmental, fuel economy and performance demands, car manufacturers keep designing new engine and powertrain concepts. Control engineers must, in turn, provide solutions to help mastering the resulting complexity.

Viable solutions are those that deal appropriately with the design and implementation issues involved in the automotive control context:

- hybrid operating modes, with mixed discrete-time and continuous-time dynamics;
- constrained manipulated variables;
- scarcity of available sensors;
- integration in standard, distributed, control architectures;
- computational and memory storage limitations;
- ease of calibration.

We bore these considerations in mind when we addressed the two drivability-related powertrain control problems which are the focus of this thesis:

- control of a mild-hybrid powertrain with an automated manual transmission;
- driver assistance for vehicle start-up with a powertrain composed of a manual transmission and a highly downsized gasoline engine.

Though those problems are different, we have studied them in a common framework where, with respect to vehicle longitudinal dynamics, the driver acts as master controller either providing references to a slave controller, the embedded AMT control strategies, or applying commands directly to the transmission. We have developed a structured control approach, based on a single controller which interacts directly with the driving and chosen to solve these two problems in the framework of Model Predictive Control. To meet the tight real-time requirements of automotive control, we have resorted to the Control Parametrization Approach.

As long as control architecture is concerned, we consider that the contribution of our Ph.D. work is twofold:

1. The definition of a unified design scheme based on a simplified model. The simplification extensively uses dynamic observer in order to recover the unmeasured/unmodelled quantities such as the load torque, the imperfection of the controlled engine torque loop as well as the clutch torque. A large part of the success of the control implementation directly results from the above simplification.

2. The implementation of iterative schemes enabling the solution of the underlying constrained quadratic problem to be obtained by solving a sequence of quadratic unconstrained problems. Without such an iterative scheme, the model predictive control strategy cannot be applied in real-time.

In the proposed architecture, the problem-related specifications, such as transparency and smoothness of the clutch closing, are taken into account through the definition of the references trajectories on the engine speed and the slip speed. The receding-horizon principle enables these reference trajectories to be periodically updated in accordance with the driver action on the pedal(s).

Experiences on the prototypes showed the efficiency of the proposed strategy since the computation of the feedback takes only a small fraction of the overall computation tasks. One nice feature of the proposed solution lies in the relatively small storage memory when compared to off-line piecewise affine solution. Moreover, the proposed strategy can be easily extended to potentially different context (new actuator, new exogenous signals, etc.) while it is known that off-line computed solution have to be entirely re-designed (with rapidly increasing complexity) when the definition of the problem changes, even slightly.

We have shown that to solve the vehicle start-up problem, where the embedded control strategies can only correct driver actions to improve drivability, a more precise knowledge of the torque transmitted by the clutch is needed. To that purpose, we have developed an original phenomenological clutch model, based only on available on-board measurements, which has been used to design a NMPC control law for the start-up assistance.

Contrary to the AMT control case, addressed in the first part of the thesis, the developments for the start-up assistance have not been thoroughly validated. Indeed, an extensive experimental validation of NMPC on the prototype car would be the more natural follow-up to this work. Additionally, it would be interesting to evaluate the benefits of using the phenomenological clutch torque for AMT control design, in view of an improvement of performance during gear shifting.

Appendix

Appendix A

Parametrization Feasibility of the AMT-Control Problem

Recall of the AMT Control Formulation

As presented before in the chapter 2, the parametrization of the AMT-control problem involves solving unconstrained parameterized control problem, which is rewritten shortly hereafter:

$$\min_{\mathbf{u}} \Omega^{unc}(\mathbf{u}, \omega(k), \nu(k), p) \tag{A.1}$$

in which

$$\Omega^{unc}(\mathbf{u}, \omega(k), \nu(k), p) := \sum_{i=1}^{N_p} \left\| \begin{pmatrix} \omega_{sl}(k+i) - \omega_{sl}^{ref}(k+i, p)) \\ \omega_e(k+i) - \omega_e^{ref}(k+i, X_{pedal}(k)) \end{pmatrix} \right\|_Q^2 \tag{A.2}$$

where the parameter p a given engagement duration.

The intuition behind the parametrization is that by taking p sufficiently large, the constraints

$$A_c \ \mathbf{u}(p) \leq B_c$$

can be fulfilled.

The defined cost function is assumed to be quadratic in the control $\mathbf{u}$, as noted hereafter:

$$\Omega^{unc}(\mathbf{u}, \omega(k), \nu(k), p) := \mathbf{u}^T \ H(J_e, J_{cw}(i_g i_d)) \ \mathbf{u} - 2 \left[W(\omega(k), \nu(k), p) \right] \ \mathbf{u} \tag{A.3}$$

where the matrices $H(.)$ and $W(.)$ are to be obtained through the simulation of the powertrain model over the predicting horizon N_p.

More precisely, the powertrain model can be written by:

$$A_p(J_e, J_{cw}(ig, id)) \ \mathbf{u} = S_p(\omega(k+i), \nu(k+i), p) \tag{A.4}$$

and the matrices $H(.)$ and $S_p(.)$ can be obtained as follows:

$$H := A_p^T A_p \in \mathbb{R}^{2N_p \times 2N_p}$$

$$W := S_p^T A_p \in \mathbb{R}^{1 \times 2N_p}$$

The aim of the numerical investigation is to check the existence of any potential candidates $\mathbf{u}(p)$ that can be applied to the system while respecting the given constraints.

Numerical Investigation of the Parameterized Solutions

As presented before, the cost function is assumed to be quadratic in the control $\mathbf{u}$. Thus, the optimal parameterized solutions can be obtained by simple derivation of the cost function $\Omega^{unc}(.)$. Obviously, the first potential candidate is that obtained for:

$$p := t_f$$

for which the given constraints $A_c\ \mathbf{u}(p) \leq B_c$ may be respected or not.

In the case where the given constraints are respected, the control sequence $\mathbf{u}(t_f)$ is approved and then its first components u_1 and u_2 are applied to the process. Otherwise, the optimization is turned-on for finding the appropriate value of the parameter p that respects the constraints. Recall that, u_1 and u_2 are refereeing to the engine and clutch torques, respectively.

During the optimization, we assume relatively high values of the parameter p enabling to penalize the variation of the slipping speed which limits the control inputs. More precisely, the desired reference trajectory $\omega_{sl}^{sp}(k+i)$ goes to measured slippig speed $\omega_{sl}(k)$ whenever the parameter p is sufficiently large.

In the case limit, that corresponds to the min-max saturation of the control inputs, the parametrization enables to limit the derivative of the slipping speed and this lets getting a control input $\mathbf{u}(k)$ nearest or equal the previous control sequence $\mathbf{u}(k-1)$.

To show the existence of any solutions, a numerical investigation is carried out by drawing a feasibility grid related to the estimated torques $\hat{\delta}_e$ and $\hat{\delta}_c$, where:

$$(\hat{\delta}_e, \hat{\delta}_c) \in (\mathbb{R}, \mathbb{R}^+)$$

The input $\hat{\delta}_c$ is assumed to be in $\mathbb{R}^+$, since the term $-\hat{\delta}_c$ is supposed to include the load torque which represents negative values.

Concerning the upper and the lowest limitations of the control inputs T_e and T_c, the following arbitrary domain $(\mathcal{D}_u)$ is assumed:

$$\begin{array}{lll} T_e^{Max} = +50\,\texttt{[Nm]} & ; & T_c^{Max} = 50\,\texttt{[Nm]} \\ T_e^{Min} = -10\,\texttt{[Nm]} & ; & T_c^{Min} = 0\ \texttt{[Nm]} \end{array}$$

It is noticeable to remind that the lowest limit of the engine torque is assumed to be negative, since the internal frictions in the engine are compensated through a feedforward module, and they can be overestimated.

Let us consider $(\mathcal{D}_\delta)$ a bi-dimensional domain related to the exogenous inputs δ_e and δ_c. The existence of any control candidates are to be checked numerically through the verification of the following condition:

$$\forall(\delta_e, \delta_c) \in (\mathcal{D}_\delta) \subset \mathbb{R}^2; \quad \exists\ \mathbf{u}(p) \in (\mathcal{D}_u) \quad : \quad A_c\ \mathbf{u}(p) \leq B_c \tag{A.5}$$

As stated before, relatively high value of the parameter p enables to penalize the derivative of the slipping speed $\dot{\omega}_{sl}(t_f, X_{pedal})$ and maintains eventually the previous control. Figure A.1 represents a grids of a feasible '*' and unfeasible 'o' regions of the control in the domain $(\mathcal{D}_\delta)$. The quadrant (a) represents the initial grid before the vehicle start-up, in which the pedal position

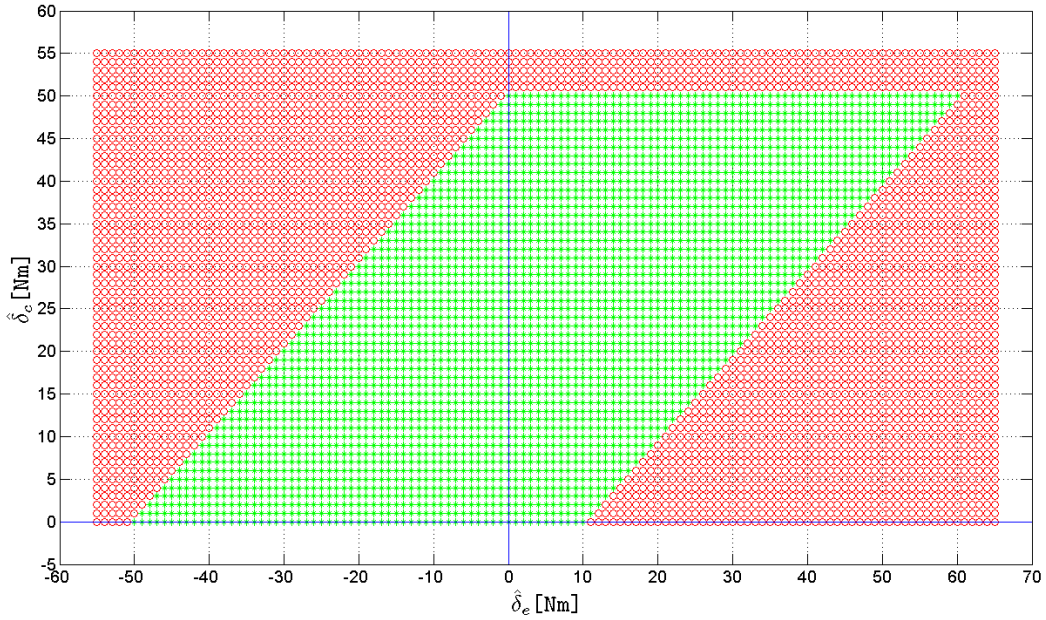

(a) Initial grid assuming large values for the parameter t_f

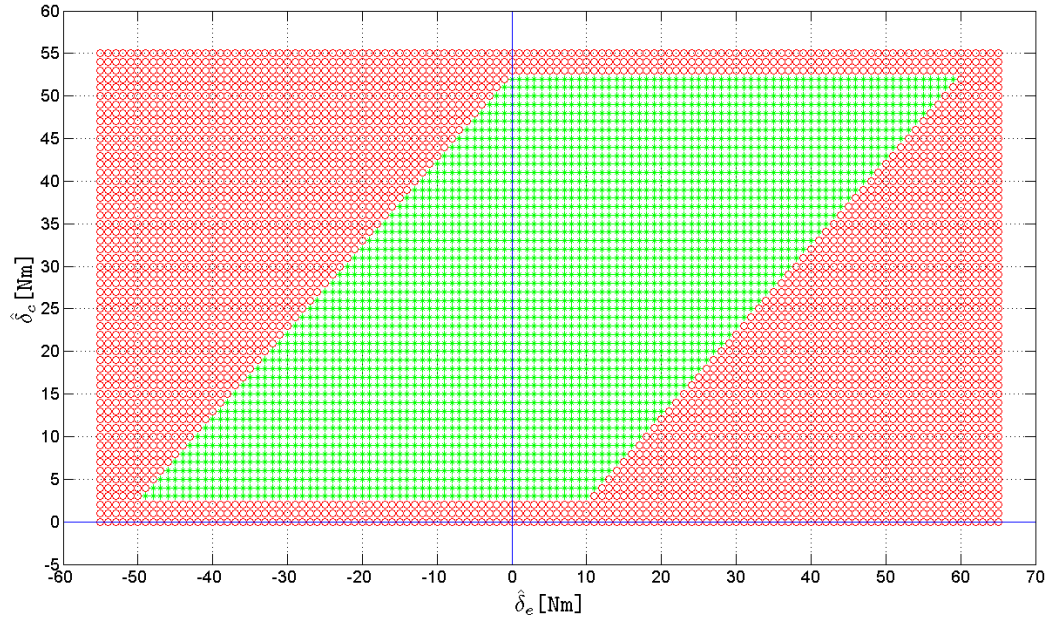

(b) Evolution of the grid vs the diminution of the parameter t_f

Figure A.1: Feasible subsets related to the existence of the solution vs the inputs $(\hat{\delta}_e, \hat{\delta}_c) \in (\mathbb{R}, \mathbb{R}^+)$ and the parameter p; The symbol '*' (green color) denotes the feasible area of the control, whereas 'o' (red color) refers to the unfeasible area.

is null and its slipping time duration is infinity. In this case, the powertrain system is in the idle mode, and the control model is supposed to be operated on the axle:

$$\hat{\delta}_c = 0,$$

in which the control $u_2 = 0$.

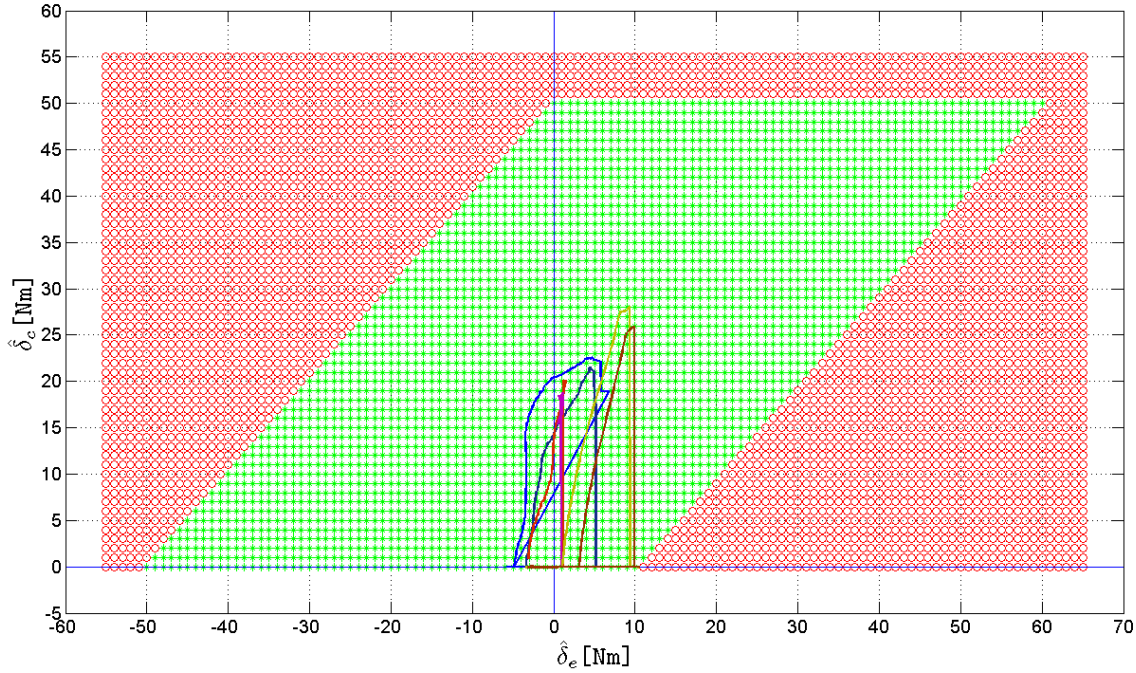

Figure A.2: Experimental trajectories of the estimated torques $(\hat{\delta}_e, \hat{\delta}_c)$ during many phases (six) of clutch engagement; these phases include both of start-up and gear shifting; One can remark that the trajectories remain largely in the feasible domain '*' (green color).

Let us assume an arbitrary value of the accelerator pedal, $X_{pedal} = 20\%$, which defines the torque demand. The feasible subset related to this demand is represented on the Figure A.1.b. One can remark that the actual subset (b) is just a sliding-up of the former subset, which is represented on the quadrant (a). The amount of the displacement is directly proportional to the accelerator pedal position.

The variation of the accelerator pedal position implies variations of the control inputs. In the Figure A.1, sliding down of the feasible subset (b) enables to respect the constraints related the variation rate since the parameter p enables to modulate of the derivative of the slipping speed, as explain before. Thus, the parametrization enables to compute a trade-offs between the previous optimal control $\mathbf{u}(k-1)$ and the actual pedal position $X_{pedal}(k)$.

Nominal Evolutions of $\hat{\delta}_e$ & $\hat{\delta}_c$ During the Clutch Engagement

As presented on the Figure A.1, it seems that the feasibility of the control depends on the accelerator pedal position and on the evolution of the inputs $\hat{\delta}_e$ and $\hat{\delta}_c$ during the clutch engagement. Recall that the estimated torque $\hat{\delta}_e$ is related to the imperfection of the assumed control model, and its variation is generally limited during the clutch engagement. Whereas, the variation of $\hat{\delta}_c$ is larger, since it includes the load torque. Thereby, we expect that the operating trajectories $(\hat{\delta}_e, \hat{\delta}_c)$ remain nearest the axle $\hat{\delta}_e = 0$, otherwise the accuracy of the assumed control model can be considered bad.

For checking that the estimated quantities $(\hat{\delta}_e, \hat{\delta}_c)$ remain in $(\mathcal{D}_\delta)$, many experimental trajectories are represented on the Figure A.2. This application concerns the SMART demo-car, in

which the engine maximum torque T_e^{Max} is approximately `50[Nm]` at the idle point. On the Figure A.2 six tests of clutch engagement are presented, including both of vehicle start-up and gear shifting. In these tests, one can remark that the trajectories start from zero, and they remain on the neighborhood of the axle:

$$\hat{\delta}_e = 0.$$

This means that, the assumed control model is quiet accurate. In general, the operating trajectories $(\hat{\delta}_e, \hat{\delta}_c)$ have the tendency to go the middle of the former subset $(\mathcal{D}_\delta)$, and this is not constraining for the parametrization. Once the clutch engagements are achieved, the estimation of $\hat{\delta}_c$ is set to zero, and this explains the discontinuity of the trajectories.

Bibliography

Abou, B., Chamaillard, Y., Corde, G., Gissinger, G., Higelin, P., Le Fort-Piat, N. & MalVille, J. (2002), Contrôle-commande de la voiture, *in* 'Hermès science Publications', Paris.

Alamir, M. (2001), 'Nonlinear receding horizon sub-optimal guidance law for minimum interception time problem', *Control Engineering Practice* **9**(1), 107–116.

Alamir, M. (2006), *Stabilization of Nonlinear System Using Receding-Horizon Control Schemes: A parametrized approach for Fast Systems*, Lecture Notes in Control and Information Science, Springer, London, ISBN 1-84628-470-8.

Alamir, M. (2008), *Assessement and future direction in NMPC*, Lecture Notes in Control and Information scienses, Springer, chapter A Framework for Monitoring Control Updating Period in Real-Time NMPC.

Alamir, M. & Marchand, N. (2003), 'Constrained minimum-time-oriented feedback control for the stabilization of nonholonomic systems in chained form', *Journal Optimization Theory with Applications* **118**(2), 229–244.

Amari, R., Alamir, M. & Tona, P. (2008), Unified mpc strategy for idle speed control, vehicle start-up and gearing applied to an automated manual transmission amts, *in* '17th IFAC World Congress', Seoul, Korea.

Amari, R., Tona, P. & Alamir, M. (2009), A phenomenological model for torque transmissibility during dry clutch engagement, *in* 'IEEE Multi Conference on Systems and Control, MCSC'2009', Saint Petersburg, Russia.

Antoniotti, M., Balluchi, A., Benvenuti, L., Ferrari, A., Flora, R., Nesci, W., Pinello, C., Rossi, C., A., S.-V., Serra, G. & Tabaro, M. (1998), A top-down constraint-driven methodology for powertrain control systems, *in* 'Global Powertrain Congress 1998', Detroit, USA.

Armstrong, B. H. (1991), Control of machines with friction, *in* 'The Kluwer international series in engeneering and computer science. Robotics', Vol. 30, p 1083-1138.

Armstrong, H., Dupond, B. & Canudas De Wit, C. (1994), A survey of analysis tools and compensation methods for control of machines with friction, *in* 'Vol. 30, p 1083-1138'.

Bemporad, A., Borrelli, F., Glielmo, L. & Vasca, F. (2001), Hybrid control of dry clutch engagement, *in* 'European Control Conference', Porto, Portugal.

Bemporad, A., Morari, M., Dua, V. & Pistikopoulos, E. N. (2002), 'The explicit linear quadratic regulator for constrained systems', *Automatica* **38**, 3–20.

Bo, L. C. & Paverlescu, D. (1982), The friction-speed relation and its influence on the critical velocity of stick-slip motion, *in* 'Wear 82', pp. 277–289.

Borrelli, F., Bemporad, A. & Morari, M. (2003), 'A geometric algorithm for multiparametric linear programming', *Journal of Optimization Theory and Applications* **110**, 515–540.

Cameron, T. M., McCombs, T., Tersigni, S. & Jao, T.-C. (2005), Flash temperature in clutches, *in* 'SAE Technical Paper Series', USA.

Canudas De Wit, C., Holsson, H., Astrom, K. & Lischinsky, P. (1993), Dynamics friction models and control design, *in* 'IEEE, American Control Confrence,ACC, pp.1920-1926', San Francisco.

Dahl, P. (1968), A solid friction model, *in* 'The Aerospace Corporation, TOR-158(3107-18)', El Segundo, California.

Diehl, M., Bock, H. G. & Schlöder, J. P. (2005), 'A real-time iteration scheme for nonlinear optimization in optimal feedback control', *Siam Journal on Control and Optimization* **43**, 1714–1736.

Dolcini, P. (2006), Contribution to the clutch comfort, *in* 'PhD Thesis, INPG - Institute of Technology's Engineers', Grenoble.

Dolcini, P., Canudas de Wit, C. & Bechart, H. (2005), Improved optimal control of dry clutch engagement, *in* '16th IFAC World Congress', Prague, Czech Republic.

Dolcini, P. J., Canudas de Wit, C. & Bechart, H. (2007), 'Observer-based optimal control of dry clutch engagement', *Oil & Gas Science Technology-Revue de l'Institut Français du Pétrole* **62**(4), 615–621.

Falcone, P., Borrelli, F., Tseng, H. E., Asgari, J. & Hrovat, D. (2008), 'Linear time varying model predictive control and its application to active steering systems: Stability analysis and experimental validation', *International Journal of Robust and Nonlinear Control* **18**(8), 862–975.

Ferreau, H. J., Bock, H. G. & Diehl, M. (2006), An online active set strategy for fast parametric quadratic programming in mpc applications, *in* 'Proceedings of the IFAc Workshop on Nonlinear Model Predictive Control For Fast Systems', Grenoble.

Ferreau, H. J., Ortner, P., Langthaler, P., del Re, L. & Diehl, M. (2007), 'Predictive control of a real-world diesel engine using an extended online active set strategy', *Annual Reviews in Control* **31**, 293–301.

Ferriera, C. H. & Leal, M. A. (2006), Gear shift strategies analysis of the automatic transmission in comparison with double clutch transmission, *in* 'SAE Technical Paper Series', Word Congress,Sao Paulo, Brasil.

Florencio, D. G., Reis Assis, E. & Cesar Henrique, F. A. (2004), The manual transmission automated -gearshift quality comparison to a similar manual transmission, *in* 'SAE Technical Paper Series', Word Congress,Sao Paulo, Brasil.

Garofalo, F., Glielmo, L., Iannelli, L. & Vasca, F. (2001), Smooth engagement for automotive dry clutch, *in* '40th IEEE Conference on Decision and Control', Orlando, Florida, USA.

Garofalo, F., L., G., Iannelli, L. & Vasca, F. (2002), Optimal tracking for automotive dry clutch engagement, *in* 'IFAC 15th Triennial Word Congress', Barcelona, Spain.

Gianluca, L., Marcello, M. & Carlo, R. (2006), Modelling of an automated manual transmission system, *in* 'Science Direct mechatronics 17 (2007), 73-91, Copyright © 2006 Elsevier Ltd', Elsevier Ltd.

Glielmo, L., Iannelli, L., Vacca, V. & Vasca, F. (2004), Speed control for automated manual transmission with dry clutch, *in* '43th IEEE Conference on Decision and Control', Atlantis, Paradise Island, Bahamas.

Glielmo, L., Iannelli, L., Vacca, V. & Vasca, F. (2006), 'Grearshift control for automated manual transmission', *IEEE/ASME Transactions on Mechatronics* **11**(1), 17–26.

Glielmo, L. & Vasca, F. (2000), Optimal control of dry clutch engagement, *in* 'Transmission and Driveline Symposium, SAE 2000 World Congress', Detroit, Michigan, USA.

Guzzella, L. & Sciarretta, A. (2005), Vehicle propulsion systems, introduction to modeling and optimization, *in* 'Springer', .

Hess, D. & Soom, A. (1990), Friction at a lubrificated line contact operating at osillating sliding velocities, *in* 'Journal of Trigology,Vol 112 n°1, P147-152)', .

James, D. & Narasimhamurthi, N. (2006), Plant identification and design of optimal clutch engagement controller, *in* 'SAE Technical Paper Series', Michigan, USA.

Keerthi, S. S. & Gilbert, E. G. (1988), 'ptimal infinite horizon feedback laws for general class of constrained discrete time systems. stability and moving horizon approximations', *Optimization Theory and Applications* **57**, 265–273.

Lake, T., Stokes, J., Murphy, R., Osborne, R. & Schamel, A. (2004), Turbocharging concepts for downsized di gasoline engines - possibilities and limits in production- type vehicles, *in* 'SAE Technical Paper Series, (SP-1832)', Detroit, Michigan.

Le Solliec, G., Le Berr, F., Corde, G. & Colin, G. (2007), Downsized SI-Engine control: A torque-based design from simulation to vehicle, *in* 'SAE World Congress', Detroit, Michigan.

Le Solliec, G., Le Berr, F., Corde, G. & Colin, G.and Chamaillard, Y. (2006), Engine control of a downsized spark ignited engine: from simulation to vehicle, *in* 'New Trends in Automotive Powertrain Control and Modelling', Rueil–Malmaison, Paris.

Livshiz, M., Kao, M. & Anthony, W. (2004), Validation and calibration process of powertrain model for engine torque control developement, *in* 'SAE Technical Paper Series, Electric Engine Control (SP-1822)', Detroit, Michigan.

Lucente, G., Montanari, M., Rossi, C. & Tilli, A. (2006), Modeling of an automated manual tranmission system, *in* 'Elsevier, Mechatronics', Elsevier.

Matias, L., Burghard, V., Eric, E. & Rolland, N. (2001), The automated shift transmission (ast) - possibilities and limits in production- type vehicles, *in* 'SAE Technical Paper Series, Transmision and Drive Systems Symposium (SP-1598)', Detroit, Michigan.

Mayne, D. Q., Rawlings, J. B., Rao, C. V. & Scokaert, P. O. (2000), 'Constrained model predictive control: Stability and optimality'.

Montanari, M., Ronchi, F., Rossi, C. & Tilli, A. (2002), Performance evaluation of a hybraulic clutch control system, *in* 'IFAC 15th Triennial Word Congress', Barcelona, Spain.

Morselli, R., Zanasi, R. & Visconti, A. (2002), Generation of acceleration profiles for smooth gear shift operations, *in* 'IEEE 2002 28th Annual Conference of the Industrial Electronics Society, IECON 02', Vol. 2, Sevilla, Spain, pp. 1681– 1686.

Ohtsuka, T. (2004), 'A continuation/gmres method for fast computation of nonlinear receding-horizon control', *Automatica* **40**, 563–574.

Rousseau, G., Sinoquet, D. & Sciarretta, A. (2007), Real-time control strategies for hybrid vehicles issued from optimization algorithms, *in* 'Proceedings of Hybridfahrzeuge and Energiemanagement'.

Scafati, M. T., Vasca, F., Innelli, L. & Senatore, A. (2008), Modeling torque transmissibility for automotive dry clutch engagement, *in* 'American Control Conference, ACC 2008', Seattle, WA.

Serrarense, A., Dassen, M. & Steinbuch, M. (2004), Simulation and control of an automotive dry clutch, *in* 'IEEE Catalog Number: 04CH37538–T.p. verso ISBN 0-7803-8335-4', ACC, Boston, Massachusetts.

Streib, H.-M. & Leonhard, R. (1992), Hierarchical control strategy for powertrain functions, *in* 'SAE Technical Paper Series, 24th FISITA Congress', United Kingdom.

Tilagone, R., Venturi, S. & Monnier, G. (2007), Natural gas: An environmentally friendly fuel for urban vehicles: The smart demonstrator approach, *in* 'SAE Technical Paper Series', number 2007-01-0286, Detroit, Michigan, U.S.A.

Tona, P., Gautier, P. & Amari, R. (2008), Modeling and control of a mild-hybrid city car with a downsized turbo-charged CNG engine, *in* 'Proceedings of Advanced Vehicle Control Symposium AVEC 2008'.

Tona, P., Moulin, P., Venturi, S. & Tilagone, R. (2007), AMT control for a mild-hybrid urban vehicle with a downsized turbo-charged CNG engine, *in* 'SAE Technical Paper Series', number 2007-01-0286, Detroit, Michigan, U.S.A.

Tona, P., Moulin, P., Venturi, S., Tilagone, R. & Gautier, P. (2006), Towards integrated powertrain control for a mild-hybrid urban vehicle with a downsized turbo-charged CNG engine, *in* 'New Trends in Automotive Powertrain Control and Modelling', Rueil–Malmaison, Paris.

Tona, P., Venturi, S. & Tilagone, R. (2008), Integrated powertrain control for a mild-hybrid urban vehicle with a downsized turbo-charged CNG engine, *in* 'SAE Technical Paper Series', number 2008-01-0081, Detroit, Michigan, U.S.A.

Van Der Heijden, A. C., Serrarens, A. F. A., Camlibel, M. K. & Nijmeijer, H. (2007), 'Hybrid optimal control of dry clutch engagement', *International Journal of Control* .

Wagner, G. (2001), Application of transmission systems for different driveline configurations in passenger cars, *in* 'SAE Technical Paper Series', USA.

Wheals, J. C., Crewe, C., Ramsbottom, M., Rook, S. & Westby, M. (2002), Automated manual transmission - a european survey and proposed quality shift metrics, *in* 'SAE Technical Paper Series', Word Congress, Detroit, Michigan, USA.

Zanasi, R., Visconti, A., Sandoni, G. & Morselli, R. (2001), Dynamic modeling and control of a car transmission system, *in* 'IEEE/ASME International Conference on Advanced Intelligent Mechatronics', Vol. 1, Como, Italy, pp. 416 – 421.